Degree Project in Chemical Science and Engineering
Second cycle 30 credits

Spent Nuclear Fuel under Repository Conditions

Update and Expansion of Database and Development of Machine Learning Models

MARIA ABADA

Stockholm, Sverige 2022

Author
Maria Abada abada@kth.se
Division of Applied Physical Chemistry, Department of Chemistry
KTH Royal Institute of Technology

Project Location
Barcelona, Spain
Amphos 21

Examiner
Mats Jonsson matsj@kth.se
Division of Applied Physical Chemistry

Supervisors
David Garcia david.garcia@amphos21.com
Olga Riba olga.riba@amphos21.com
Darío Perez dario.perez@amphos21.com
ChemRad group
Amphos 21

Abstract

Spent nuclear fuel (SNF) is highly radioactive and therefore needs to be stored in deep geological repositories for thousands of years before it can be safely returned to nature. Due to the long storage times, performance assessments (PA) of the deep geological repositories are made. During PA dissolution experiments of SNF are made to evaluate the consequences of groundwater leaking into the fuel canister in case of barrier failure. These experiments are both expensive and time consuming, which is why computational models that can predict SNF dissolution behaviour are desirable.

This thesis focuses on gathering available experimental data of dissolution experiments to update and expand a database. Using the database, the dissolution behaviour of each radionuclide (RN) has been evaluated and compared to previous knowledge from existing literature. While it was difficult to be conclusive on the behaviour of elements where a limited amount of data was available, the dissolution behaviours found of different radionuclides in this thesis not only correspond to previous studies but also provide a tool to manage and compare SNF leaching data from different starting materials, irradiation history and leaching conditions. Moreover, the compilation of such a large amount of experimental data made it possible to understand where future experimental efforts should be focused, i.e. there is a lack of data during reducing conditions.

In addition, machine learning models using Artificial Neural Network (ANN), Random Forest (RF) and XGBoost algorithms were developed and run using the database after which the performances were evaluated. The performances of each algorithm were compared to get an understanding of which model performed best, but also to understand whether these kinds of models are suitable tools for SNF dissolution behaviour predictions. The best performing model, with training and test R^2 scores close to 1, was the XGBoost model. Although XGBoost, had a high performance, it was concluded that more experimental data is needed before machine learning models can be used in real situations.

Sammanfattning

Förbrukat kärnbränsle är mycket radioaktivt och behöver därför lagras i djupa geologiska förvar i tusentals år innan det säkert kan återföras till naturen. På grund av de långa lagringsperioderna görs säkerhetsanalyser av de djupa geologiska förvaren. Under säkerthetsanalyserna görs upplösningsexperiment på förbrukat kärnsbränsle för att utvärdera konsekvenserna av att grundvatten läcker in i bränslet vid barriärbrott. Dessa experiment är både dyra och tidskrävande, varför beräkningsmodeller som kan förutsäga förburkat kärnbränsles upplösningsbeteende är önskvärda.

Denna avhandling fokuserar på att samla in tillgängliga experimentella data från upplösningsexperiment för att uppdatera och utöka en databas. Med hjälp av databasen har upplösningsbeteendet för varje radionuklid utvärderats och jämförts med tidigare kunskap från befintlig litteratur. Även om det var svårt att vara avgörande om beteendet hos element där en begränsad mängd data fanns tillgänglig, motsvarar de upplösningsbeteenden som hittats för olika radionuklider i denna avhandling inte bara tidigare studier utan ger också ett verktyg för att hantera och jämföra förbrukat kärnbränsles upplösningsdata från olika utgångsmaterial, bestrålningshistorik och betingeleser under upplösning. Dessutom gjorde sammanställningen av en så stor mängd experimentella data det möjligt att förstå var framtida experimentella ansträngningar bör fokuseras, exempelvis finns det en brist på data under reducerande förhållanden.

Dessutom utvecklades och kördes maskininlärningsmodeller med hjälp av Artificial Neural Network (ANN), Random Forest (RF) och XGBoost-algoritmer med hjälp av databasen, varefter prestandan utvärderades. Prestanda för varje algoritm jämfördes för att få en förståelse för vilken modell som presterade bäst, men också för att förstå om dessa typer av modeller är lämpliga verktyg för att förutspå förbrukat kärnbränsles upplösningsbeteende. Den bäst presterande modellen, med träning och test R^2 resultat nära 1, var XGBoost-modellen. Även om XGBoost hade en hög prestanda, drogs slutsatsen att mer experimentell data behövs innan maskininlärningsmodeller kan användas i verkliga situationer.

Acknowledgements

This thesis marks the end of a five-year degree program in Chemical Engineering at KTH, Royal Institute of Technology, Sweden. The degree project has been written within the Master of Chemical Engineering for Energy and Environment, at the school of Engineering Sciences in Chemistry, Biotechnology and Health and was conducted during the spring semester of 2022 in collaboration with Amphos21 in Barcelona.

First and foremost, I would like to thank my supervisors from Amphos21 - Olga Riba, Darío Perez, and David Garcia - for all the help, guidance, and support throughout this thesis work. I would also like to thank my professor, Mats Jonsson, for helping me find this thesis project as well as the help and guidance throughout the thesis and Amphos21 for this opportunity and for receiving me so warmly.

Lastly, I would like to thank my family and loved ones for the support not only during this project, but throughout these five years. I would not have been the same person I am today without you.

Key words
Spent nuclear fuel, SNF dissolution, SNF corrosion, ML model, dissolution predictions, ANN, RF, XGBoost

Abbreviations

ANN - Artificial Neural Network
BU - Burn-up
FIAP - Fraction of inventory in aqueous phase
HBS - High burn-up structure
IRF - Instant release fraction
LWR - Light water reactor
ML - Machine learning
RF - Random Forest
SNF - Spent nuclear fuel

Table of Contents

1 Introduction

Ongoing international efforts are in place, e.g. the Paris agreement, to decrease the use of fossil fuels due to decreasing reserves and environmental effects of its use. This increases the importance and use of fossil free energy sources such as hydro, wind, sun, and nuclear fuel. Nuclear fuel, having a high energy density and producing minimal amounts of greenhouse gases [1], becomes an integral part of this transition from fossil fuels. Spent nuclear fuel (SNF), however, is highly radioactive and classified as a high-level waste, therefore SNF needs 100 000 – 1000 000 years of safe storage in deep geological repositories before it can be returned to nature in a safe manner. To evaluate the long-term safety of these repositories, performance assessments (PA) are made where, among other scenarios, the possibility of groundwater leaking into the fuel due to engineered barrier system (canister, bentonite buffer, cement) and host rock failure is assessed. When SNF comes into contact with groundwater it will start to dissolve and the mobility of the radionuclides (RNs) that it contains will increase. Apart from dissolution, corrosion of SNF due to the oxidants produced during water radiolysis caused by the ionizing radiation emitted by the SNF might also occur and increase RN mobility [2].

The amount of radionuclides released in SNF dissolution is evaluated experimentally during PA, which is a costly as well as time consuming part of the process. To reduce the time and cost of a PA it is desirable to have a reliable model that is able to predict the SNF behaviour during dissolution [4]. Another aspect that is worth mentioning is the age of the fuel during these experiments. The ground water comes into contact with the fuel after 1000-10 000 years [5], but there are no SNFs this old, causing dissolution experiments to not be fully representative of SNF dissolution behaviour during repository conditions. The dissolution behaviour of SNF depends on a variety of characteristics like irradiation history of the fuel, microstructure of the pellet, the chemical state of the radionuclides, redox conditions, and solution composition. The interrelation of all these parameters makes dissolution of the different radionuclides in the SNF difficult to predict [4]. Machine learning (ML) is a tool that is being explored to do predictions on this complex system, while considering a variety of the parameters earlier mentioned in correlation to time. However, in order to train a machine learning model to make as accurate predictions as possible, a large amount of data is needed [6]. Meaning that machine learning models would in short-term require many costly experiments, but the ambition is that in long-term machine learning models will reduce or cease the need for these experiments.

In this work a pre-existing database of SNF dissolution, first developed during the EURATOM project FIRST Nuclides, is expanded, and further developed. The expansion of the database is done using experimental data from available published studies and company reports, dating back to 1993, as well as the EURATOM project reports from the FIRST Nuclides [4] and DisCo [7] projects. Apart from the release of different radionuclides during dissolution, the database also contains fuel history, sample characteristics, solution characteristics, and atmospheric conditions. Compiling all this data in the same place and format facilitates finding general correlations between the different radionuclides' behaviours and atmospheric conditions, solution composition, sampled region etc. in relation to matrix dissolution. This

makes the database a tool of great value for i) comparing the behaviour of the different fission products, ii) determining the relation between the release of each fission product and microstructure of the SNF pellet iii) getting and understanding of what type of experimental data is lacking in order to determine where future experimental efforts should lie that can be used to learn more about SNF and the behaviours of the radionuclide it contains.

A second step of this work is to evaluate machine learning as a prediction tool for SNF dissolution. This is done by using the database to train Artificial Neural Network models, a Random Forest model as well as an XGBoost model and evaluating their performances.

1.1 Objectives

The main objective of this thesis is to expand and develop a pre-existing spent nuclear fuel database containing fuel history, sample characteristics, solution characteristics and measured release of radionuclides during dissolution. Throughout the development of the database its consistency and exhaustivity should be thoroughly checked by evaluating outlier datapoints and double-checking values as well as typing errors. Using the database as a basis further objectives are analysing the dissolution behaviour of spent nuclear fuel and evaluate the machine learning algorithms Artificial Neural Network and Random Forest as tools to predict it.

The questions to be answered in the end of this report are:

- How are different radionuclides released during spent nuclear fuel leaching process in relation to matrix dissolution?
- Are Artificial Neural Network and Random Forest suitable tools for predictions of spent nuclear fuel dissolution behaviour?

2 Background

To understand the work of this thesis prior knowledge of the principles of nuclear power, spent nuclear fuel, prior projects about spent nuclear fuel dissolution and machine learning models are necessary. This section will explain these principles to enable understanding of the following sections.

2.1 The Nuclear Fuel Cycle: An Overview

Nuclear fuel consists of a fuel matrix most commonly consisting of UO_2 enriched with 2-4% of the isotope ^{235}U (UOX fuel) or ^{239}Pu (MOX fuel) which is shaped into cylindrical pellets. These pellets are then stacked into fuel rods where they are encapsulated by a cladding, commonly made from zircaloy, and the rods are what nuclear reactors are loaded with. Nuclear power production is based on nuclear fission which is the uneven cleavage of an atom nucleus and can be summarised as follows:

$$^{235}U + n \rightarrow FP + Xn$$

where n is a neutron, FP are the fission products and X is the amount of new neutrons released [8].

Nuclear fuel is irradiated with neutrons which are consumed by fissile components, usually ^{235}U or ^{239}Pu. On average 2.5 new neutrons are released per neutron consumed, these new neutrons can then be consumed by another fissile component and hence, a chain reaction commences. In conventional reactors there are several passive and active control mechanisms in place to control the chain reaction so that for each fission only one neutron is used for further reaction. This is to control the heat produced so that it does not overload the system and make the reaction violent [8]. Around 80% of the energy released during the fission reaction is kinetic energy in the fission fragments (FP + Xn) which is transformed into heat through collisions with other atoms. Direct collisions of atoms cause the atoms to move from their lattice position in the fuel, which in turn affects neighbouring atoms leading to displacement cascades. While most atoms return to their normal lattice position, some microstructural defects remain. Apart from the defects caused by irradiation, microcracking also occurs as a result of thermal stress [9]. The microstructural defects of the fuel include the accumulation of fission products in void spaces of the fuel: fuel-cladding gap, fractures, bubbles, and grain boundaries. This redistribution depends on irradiation characteristics such as burn-up[1] (BU), linear power density and irradiation history [10]. In addition, a microstructural defect that has been observed in the outer rim of spent nuclear fuel pellets with a BU higher than 40 GWd/t_{HM} is the high burn-up structure (HBS). This structure is present in a very thin region of the fuel pellet - a few micrometres of the total ~9.6-9.7 mm diameter - and can have 2-3 times higher BU than the

[1] Burn-up (BU) is a common way to express the energy extracted from nuclear fuel and it uses the unit gigawatt day per tonne heavy metal (GWd/tHM), where 1 GWd/tHM = 86400 GJ and corresponds to the fission of approximately 1.05 kg ^{235}U [8].

fuel average. The HBS is characterised by its extended defects, fission gas redistribution and decreased grain size. Fission gases that have travelled from the fuel matrix are concentrated in closed pores in the HBS, which has an increased porosity with reported fractions exceeding 20%. Moreover, the grain size within the HBS is decreased to ~0.1-0.3 μm, approximately 100 times smaller than the original grain size of ~10 μm. The occurrence of HBS is mainly associated with BU and irradiation temperature [9].

The composition of spent nuclear fuel depends on a variety of factors such as type of fuel, design of the fuel rods, position in reactor, and cooling time after removal from the reactor. Due to these deciding factors, the elemental inventory of spent fuels from different types of reactors and with varying irradiation history differ from each other as well as between batches from the same reactor. In general, however, spent fuel contains fission products, trans-uranium elements and actinides [8]. Kleykamp et al. [11] groups together the fission products according to their chemical state:

1. Fission gases and volatile fission products: Kr, Xe, Br, I
2. Fission products forming metallic precipitates: Mo, Tc, Ru, Rh, Pd, Ag, Pd, In, Sn, Se, Te
3. Fission products forming oxide precipitates: Rb, Cs, Ba, Zr, Nb, Mo, Te
4. Fission products dissolved as oxides in fuel: Sr, Zr, Nb, Y, La, Pr, Ce, Nd, Pm, Sm

While Johnson and McGinnes [12] describes the location of different radionuclides in the fuel rod:

1. Found in fuel-cladding gap: C, I, Cs, Se, Sn, H.
2. Found in grain boundaries: C, I, Cs, Se, Tc, Sn, Pd, H
3. Found in matrix: Actinides and 98% of fission products.
4. Cladding: C, Cl, Ni, Zr, Nb

Figure 2.1 illustrates the microstructure of a spent fuel pellet cross section together with the expected location of the different fission products, where FG refers to gaseous fission products and FGGB refers to gaseous fission products in the grain boundaries. In this illustration micro and macro structural defects on the fuel rod caused by irradiation are also shown with images on a micro scale of the fuel grains.

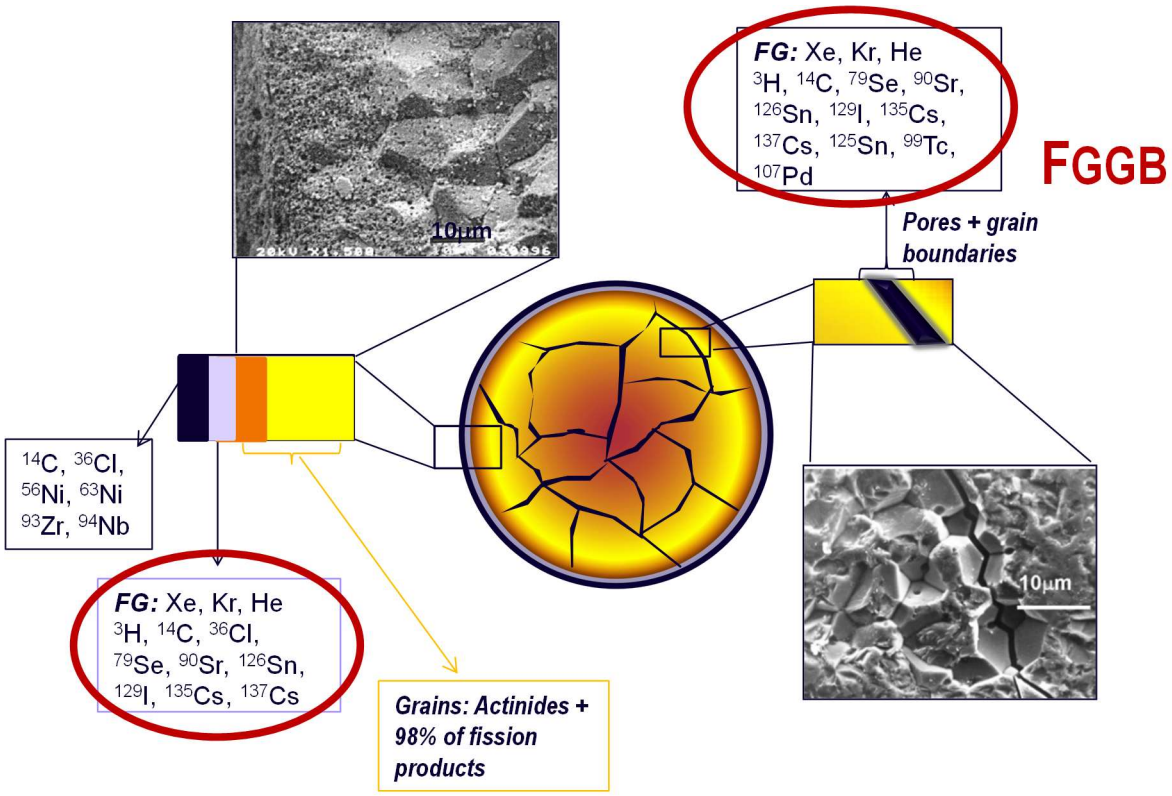

Figure 2.1 Illustration of spent nuclear fuel with expected locations of fission products indicated. FG stands for Fission Gas, while FGGB stands for Fission Gas in Grain Boundary.

Fission products and transuranic elements produced during the use of the nuclear fuel lower the fuel's efficiency and therefore the fuel is periodically replaced. Once removed from the reactor, the spent nuclear fuel is first stored at the reactor site for a minimum of 6 months [2]. This first storage of spent nuclear fuel is a wet storage, pool of water, which provides the spent fuel with the necessary cooling. Once out of the pool, the spent fuel is stored in temporary (individual or centralised) storage facilities awaiting final management in a deep geological repository [3]. This is needed to decrease the radioactive heat of the spent fuel. Once the spent nuclear fuel has cooled enough to facilitate safe handling and transport it is transported to the final storage, a deep geological repository [2].

There are several deep repository designs with diverse engineering. In principle, the deep repositories consist of tunnels, also called galleries, at a depth of 500-1000 m below the surface in deep bedrocks. The spent nuclear fuel is firstly placed into metal canisters which in turn are placed in the galleries. In the deep repositories, the environment is reducing which is beneficial since most of the concerned radionuclide have low solubility in reducing conditions. Several countries also plan to use bentonite clay in future repositories as a buffer between the bedrock and the canister. Bentonite clay expands when it sorbs water, due to its low porosity and permeability it acts as a second barrier between the spent nuclear fuel and water [2].

Spent nuclear fuel is stored in the deep geological repositories for 1000-10 000 years. During this time ground water might leak into the fuel canister, due to the degradation of the materials

in the different layers of the repository, causing the radionuclides to dissolve. Two modes of radionuclide dissolution have been distinguished [5]:

1. The first mode is called the instant release fraction (IRF) and refers to the elements that are first released when water meets the fuel. This IRF does not include the fraction of elements released on a long term from the fuel matrix and the release rate of IRF radionuclides is independent of the dissolution kinetics of the fuel matrix. So, the release of the IRF depends on the contact area of the fuel rod that the water has access to, the micro and macro structure of the fuel rod and the migration of the radionuclide within the rod.
2. The second mode refers to the slow dissolution of radionuclides and is dependent on the ambience of which the fuel is in contact with. The oxidation of the fuel matrix caused by the surrounding air and the chemical or radiolytic dissolution caused by the fuel being in contact with water all affect this second dissolution mode.

Radionuclide release depends on the redox conditions and composition of the solution as well as the radionuclides own chemical state, solubility, and distribution within the fuel. The dissolution of the fraction of radionuclides that have migrated into the void spaces of the fuel - fuel-cladding gap, grain boundary, fractures, and bubbles - are independent of the fuel matrix. These radionuclides will dissolve in the aqueous phase in a time interval of days to months, this fraction is called the IRF. On the other hand, radionuclides embedded in the fuel matrix (actinides and other fission products) will not migrate into the aqueous phase independently of the matrix dissolution as the fuel matrix acts as a barrier for this large fraction of radionuclides [10]. Dissolution of both matrix and IRF have been shown to be slower under reducing or anoxic conditions in comparison to under oxic conditions [4].

2.2 Previous Projects

In the past, several EU projects have focused on learning more about the dissolution behaviour of spent nuclear fuel. Two of these EU projects, FIRST Nuclides and DisCo which can be found at www.firstnuclides.eu and www.disco-h2020.eu respectively, have been extensively used in this work and will therefore be summarised below.

2.2.1 FIRST NUCLIDES

FIRST Nuclides is a 3-year project that started in 2012 and was commissioned by the European Commission and was a part of the EURATOM FP7 collaborative project. A consortium of 10 European beneficiaries implemented the FIRST Nuclides as a project, however there was also a group of 13 organisations who contributed to the project without funding and an *End-User group* of 6 regulatory organisations who made sure that the waste management organisations' and regulators' interests were reflected in the work [4].

The objective of the project was to get a better understanding of how spent UOX fuel with high burn-up behaves in deep geological repositories in case of container breaching. For this purpose, several experiments were carried out on fuel samples from both BWRs and PWRs, as

well as samples of varying BUs and investigations on the dissolution of instant release fractions (IRF) as well as of the matrix were conducted. Efforts were also made to determine the composition and quantity of fission gases in spent nuclear fuel as well as the diffusion mechanisms in the fuel. In addition, a state-of-the-art (SoA) database was developed containing both basic information concerning the areas of the project and a compilation of experimental results [4].

Conclusions of the project include that IRF is a highly contributing factor to peak releases after breaching of containers [4].

2.2.2 DisCo

DisCo is another collaborative project funded by the European Commission and is also a part of the EURATOM. This project started in 2017 and went on for 4.5 years [7].

As more modern and unconventional nuclear fuels are being used, there is a need to know if dopants in the fuel matrix affect the dissolution rate of spent nuclear fuel in a repository environment, DisCo was launched to investigate this question. During the project, the dissolution of spent nuclear fuel containing Cr, Cr+Al and Gd as well as MOX and UOX fuels were experimentally investigated. Furthermore, the project also focused on developing computational models to further study the dissolution [7].

2.3 Machine Learning Techniques

Machine learning (ML) is based on human learning. According to Chandramouli et al. [6] the process can be divided as follows: Input data, Abstraction and Generalisation. The machine, like humans, learns through experience, or an informational basis, which in the case of the machine is the input data. For humans it is easier to learn using a conceptual map, categorising information instead of memorising it. In the case of the machine this is the pre-processing or re-representation of raw data using a model. The machine is trained by using the input data to fit the model, meaning that the constants in the model are determined using input data. Abstraction is the process of re-representing the data and training the model. Generalisation is the decision-making framework of the machine, it is based on the abstraction, and it is the part where the machine makes decisions on unknown sets of data, the test data which is a randomly chosen subset of the input data. During generalisation, problems may arise while trying to make precise decisions since the model is trained using a finite set of data. The problems that might arise are:

1. The trained model is too aligned with the training data and hence yields a false trend or
2. The test data contains characteristics that the training data does not.

To avoid these problems, the approach of approximate decision making, comparable to human intuition, is used [6].

Machine learning can be categorised into:

1. Supervised training

2. Unsupervised training and
3. Reinforcement training.

Supervised training is when the machine predicts the category or value of unknown objects based on prior knowledge. Unsupervised training is when the machine finds a pattern in the data, while during reinforcement training the machine learns to act on its own to classify data [6]. For the purposes of this study, the unsupervised and reinforcement training will not be used and hence not be further explained.

Supervised training can be used to predict the categorical or numerical variables. When categorical variables are to be predicted, this is called classification and when numerical variables are to be predicted this is called regression. Supervised training is dependent on its training data. Training data of inadequate quality will yield predictions of poor precision. Furthermore, machine learning models require a large amount of training data to be effectively used and yield good quality predictions. Partially since the impact of a bad set of data is larger in a small pool of data than in a large one [6]. This work focuses on predicting real-numerical values and therefore the following sections will explain different regression models for ML.

2.3.1 Artificial Neural Network

The Artificial Neural Network model (ANN), also known as neural network, is a supervised learning model used for prediction. It is a model of the biological neural network and simulates its functions. ANN consists of nodes, also known as neurons, which receive and transmit information, signals x_i. The three main components of an artificial neuron are: the synapses, the summation junction, and the activation function. Each neuron has a set of synapses i, which each have a weight, w_i. The summation junction is an adder of the weighted input signals as expressed in eq. 2.1, while the activation function transforms the summation junction into an output signal only when the input signal exceeds the specific threshold of the function. The activation function output depends on the summation junction and is expressed in eq. 2.2. There are several different activation functions that can be used in an ANN [6]. Figure 2.2 illustrates the structure of an artificial neuron.

$$y_{sum} = \sum_{i=1}^{n} w_i \cdot x_i \tag{2.1}$$

$$y_{out} = f(y_{sum}) \tag{2.2}$$

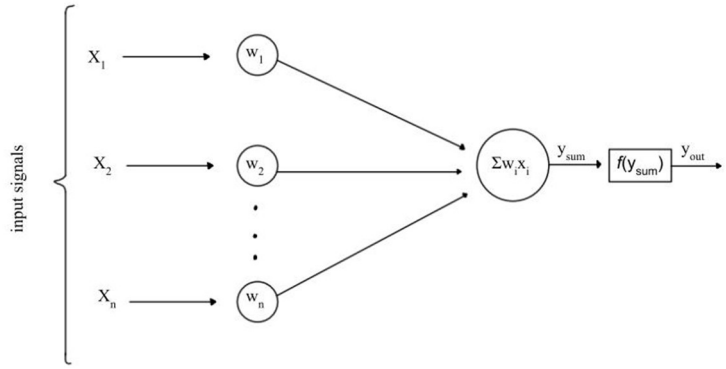

Figure 2.2 Illustration of an artificial neuron with all its main components.

An ANN consists of a large number of neurons that are interconnected, the connection between the neurons transmits signals from one neuron to another. The neurons in the ANN make up layers of three different kinds: input layer, hidden layer, and output layer. The input layer is the first layer that the signals go through, its number of neurons corresponds to the number of features in the data set. A hidden layer is an intermediate layer of neurons placed in between the input and output layers, its amount of neurons is chosen by the user and influences the model's performance. ANN performance is improved with an increasing number of hidden layer neurons, however, too many hidden layer neurons can also result in an overfitting and increases the computational work as well as cost. Finally, the output layer is the last layer, its number of neurons corresponds to the number of possible outcomes since this layer generates the output of the model [6].

As can be seen from eq. 2.1 and 2.2, the final output of the model is dependent on the weight of the neuron interconnections. This weight is determined by the algorithm through iterations. Firstly, the user sets an arbitrary start value for the weight and an error threshold, the error, which in this case is the difference between the resulting output and the expected output. Later, by modifying the weight after each iteration until the error has reached the threshold, the algorithm determines the final weights [6].

Neurons in each layer can be connected in different ways and have different directional flow, i.e. the signals can be sent in different directions. The number of layers and their directional flow make up the architecture of an ANN, the neurons can be connected in different ways depending on this architecture [6]. Below, explanations of a few of the most common architectures, can be found.

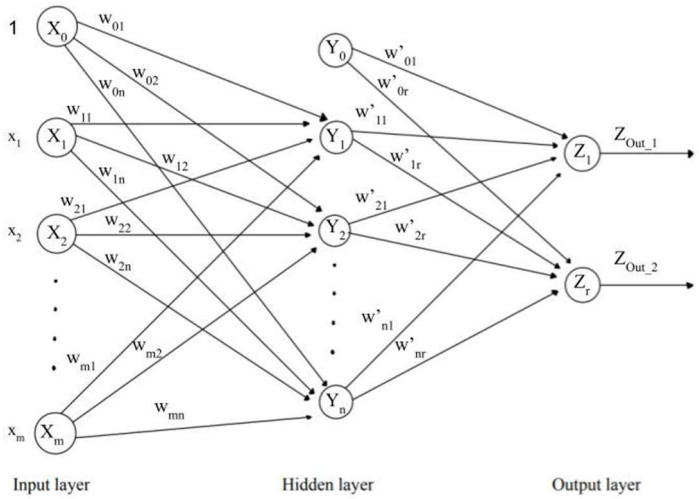

Figure 2.4 Illustration of a recurrent neural network.

Another common ANN implementation is the backpropagation algorithm which is applicable on multi-layer feedforward networks. It is an efficient method for determining connection weights which continuously, through iterations known as epochs, adjusts the connection weights. In the epochs' forward phase the signals flow forward as normal, however, in its backward phase the resulting output is compared to the expected output. If the error is larger than the set limit, the error is propagated backwards to the input layer and the weights of the connections is adjusted accordingly until the error is within the limit. The technique used to adjust the weights is called gradient descent, it identifies the extent of the weight change needed to minimize the squared error through the partial derivatives of the activation function [6].

Another addable feature of the ANN algorithm is the dropout layer and dropout rate. A dropout layer randomly chooses a subset of nodes to deactivate in each layer of the ANN architecture. The number of deactivated nodes is determined by the dropout rate, which is set by the user. A dropout rate of for example 0.2 deactivates 20% of the nodes in each layer. For the backpropagation architecture dropout entails that one set of randomly selected nodes are deactivated during forward and backward propagation and a new subset of nodes is deactivated for each iteration until the weights of the connections have been set. However, dropout is only applied during the training phase of the algorithm, when the test data is run all nodes are activated. The purpose of a dropout layer is to lower the risk of overfitting. Overfitting easily becomes an issue when a network with a wide variety of features is trained. The network finds patterns that are present in the training data leading to a failure of generalization. Dropout allows the training process to be based on several different network architectures since a new subset of input and features are run each iteration until the weights are set [13].

2.3.2 Random Forest

Random forest (RF) is a supervised machine learning algorithm which can be used both for classification and regression problems. It has shown high performance in situations with a larger number of variables than number of observations and can be applied to large scale

problems [14]. For the purpose of this thesis only RF regression analysis was used and therefore, the focus of the further explanation will be on RF regression.

To better understand the RF model, first a background in Decision Tree regression is required. Decision trees can be used both as classifiers and regressors, in both cases a decision tree consists of decision nodes and leaf nodes. Decision nodes contain conditions according to which the dataset is split, the datapoints that fulfil the condition of the decision node fall into the leaf node and decide the class or value of that lead node. A tree starts with one decision node which splits into a leaf node and another decision node, this split goes on until there are two pure leaf nodes left. The data is fed into the root decision node, the points that fulfil the condition of the node fall into the leaf node and their class or value is the class or value of that leaf node. The points that do not fulfil the condition of the decision node go on to the next decision node where the same process is repeated until all points have been classified or given a numeric value [6]. Figure 2.4 shows an illustration of a decision tree.

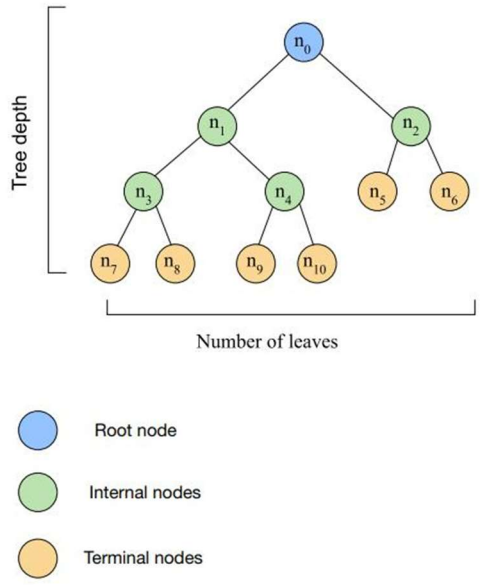

Figure 2.4 Illustration of decision tree.

The machine learning aspect of decision trees is the determination of the optimal way of splitting the dataset, in other words the determination of the decision nodes' conditions. Each decision node's condition is determined one at a time without back tracking, meaning that each split is dependent on the previous split, but previous conditions are not adjusted. The final goal is to have pure leaf nodes. The determination of decision node conditions is different for classifier and regressor trees. For regressor trees, the purity of leaf nodes is evaluated through variance reduction. Using eq. 2.3 with y as the desired output, the variance of each node is calculated, while the variance reduction is calculated using eq. 2.4. The purity of a node increases with a decreasing variance reduction [15].

$$Var = \frac{1}{n}\sum_{i=1}^{n}(y_i - \bar{y})^2 \quad (2.3)$$

$$Var\ red = Var(parent) - \sum Var(child_i) \quad (2.4)$$

Where the parent is the decision node in question and the children are the two following nodes.

In the end, a leaf node in a tree regressor can contain more than one value. When a new datapoint with an unknown y-value is put through the tree, it gets the mean value of the y-values in the node it ends up in [15].

The RF algorithm uses multiple random decision trees. Each tree has its own subset of data that has been randomly sampled from the original training data. These random subsets can contain the same dataset multiple times as each time a dataset is chosen for a subset, it is put back to the original training data pool and can be chosen again. The random sampling makes the algorithm less sensitive to the original training data. Similarly, each tree has a random feature selection, meaning that no tree considers all given features from the original dataset, but rather a few of them that have been randomly chosen. Random feature selection further reduces the correlation between the trees allowing the decision trees to be more diverse. Each tree is trained independently of the other and yields different output. Now when a new datapoint is passed through the model for prediction, it goes through each one of the trees, receiving a predicted output each time. The final prediction is the average of the predictions of all trees [15]. Figure 2.5 shows a visual representation of a random forest.

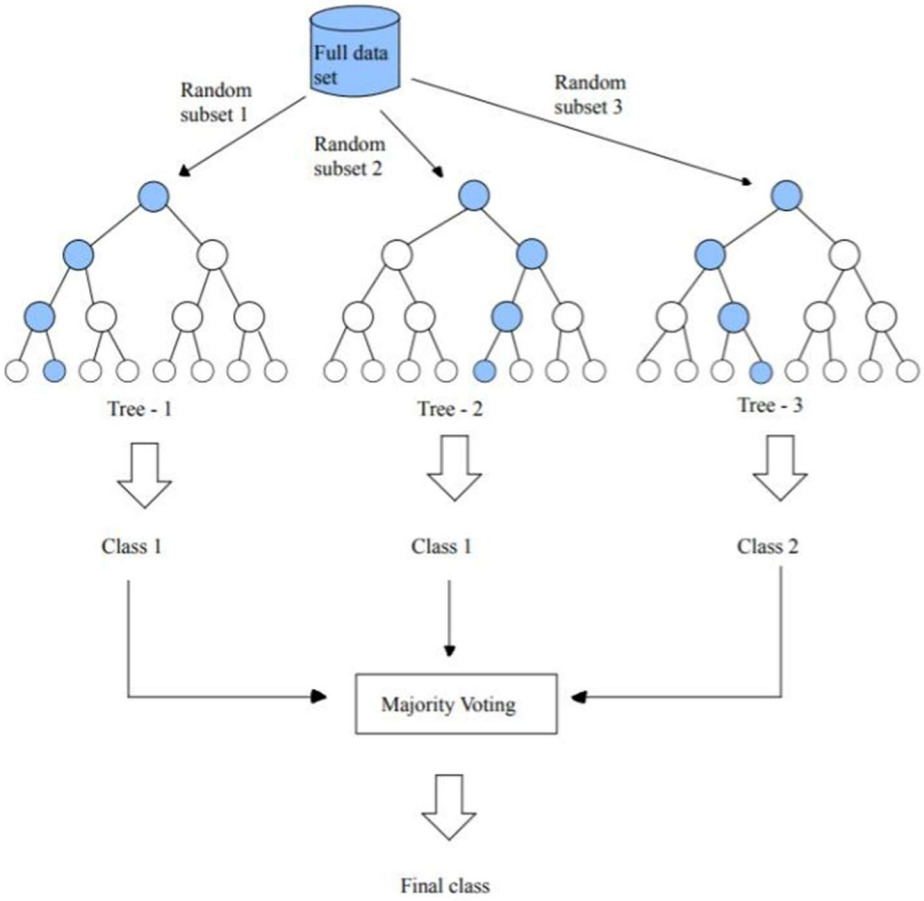

Figure 2.5 Visual representation of RF.

Extreme gradient boosted trees (XGBoost) is another algorithm similar to the RF concept. XGBoost also uses decision trees, however, as opposed to RF XGBoost uses gradient descent and regularization to increase performance while avoiding overfitting. The algorithm considers weak learners, meaning trees which yield predictions with high errors, to improve performance. Gradient descent allows the algorithm to find the loss function minima using the second order gradient. Regularization is used to increase the bias while training the data in order to gain a minimized variance for later predictions. This means that the regression is fitting the training data less, while the errors for later predictions are decreased [18].

3 Methodology

The work of this thesis can be divided into two main areas: 1. the expansion and refinement of the pre-existing database and 2. the machine learning modelling using Artificial Neural Network and Random Forest algorithms. In the two following sections, the methodology of the two areas is explained in detail.

3.1 Updating and Expanding the Database

The database is an update and expansion of the initial SoA database that was created during the FIRST Nuclides project [4]. It is a compilation of corrosion and dissolution studies performed on spent nuclear fuel, meaning that results from corrosion experiments on unirradiated fuel have not been included. In the SoA database the units used to document the elemental release during spent fuel dissolution are FIAP% and IRF where FIAP% considers the initial inventory of the spent fuel and IRF shows the concentration of the element as a percentage of the total measured IRF. In this updated version, the desired metric is FIAP%, hence studies where FIAP% has not been given or is possible to calculate from given data have not been included.

Revised literature

The largest amount of data in the database was taken from the Scientific and Technical Contributions of the EURATOM Collaborative Projects FIRST-Nuclides and DisCo, the deliverables of which were found at www.firstnuclides.eu and www.disco-h2020.eu respectively. Some of the experiments conducted in the projects had not been finalized before the end of the projects, hence, the data presented in the deliverables was not complete. For FIRST-Nuclides experiments, a more complete presentation of data could be found in papers published later. For DisCo experiments, extended data was obtained through personal communication with the authors. Table 3.1 shows which studies from the projects that were complemented with data from studies later published or data given by authors.

Table 3.1 The table shows which studies from the European projects, included in the database, that were complemented with data from studies later published or data given by authors.

Corresponding Author of Study	Later published	Personal Communication	FN[a] continuation	DisCo continuation
Martinez et al.	Yes (2017)	No	Yes	No
Roth et al.	Yes (2019)	No	Yes	No
Serrano-Purroy et al.	No	Yes	No	Yes
Herm et al.	No	Yes	No	Yes
Clarens et al.	No	Yes	No	Yes
Barreiro-Fidalgo et al.	No	Yes	No	Yes

[a]FN - Abbreviation for FIRST-Nuclides

While data was collected from the deliverables of the mentioned European projects, the studies referred to in the Scientific and Technical contributions were studied and evaluated. When these studies presented relevant data, they were added to the database. In addition, an effort was made to find studies from the open literature, for this purpose the search engines Scopus and Google Scholar were used. During the search, the relevant keywords were "SNF," "spent nuclear fuel," "leaching" and "corrosion". From the open literature, only studies that had been peer-reviewed and published were deemed credible and suitable for use in the database. When reviewing studies from the open literature some of the studies that came up were earlier or later published versions of EURATOM project experiments, in other cases different studies presented data from the same experiment. In order to not repeat the same dataset multiple times in the database, the data presented in studies from the open literature was compared to its corresponding study in the EURATOM projects. Characteristics of studies that were compared were: Irradiation history and characteristics of fuel used in experiment, experimental set-up, sample characteristics and results of leaching. If the same data was presented in both cases, then the results from the project deliverables were kept, if the study from the open literature presented more or less data than its corresponding study from the projects, then the study containing more datasets was used.

Selected data for radionuclide migration

Cumulative fraction of inventory in aqueous phase in percentage (FIAPc %) was the chosen unit for data to be used in the machine learning model. Non-cumulative FIAP % is calculated as described in eq. 3.1.

$$FIAP\% = \frac{C_i \cdot V_{solution} \cdot M_i}{m_{sample} \cdot H_i} \cdot 100 \qquad \text{eq. 3.1}$$

Where C_i is the concentration (M) of element *i* in the solution, $V_{solution}$ is the volume (dm^3) of the solution, M_i is the molar weight (g/mol) of element *i*, m_{sample} is the mass (g) of the sample and H_i is the fractional inventory (g i/g fuel) of element *i*. To obtain FIAPc %, the cumulative

concentration of an element *i* ($C_{c,\,i}$) is needed or the non-cumulative FIAP % can be added as shown in eq. 3.2.

$$FIAP_c\% = \sum_{k=1}^{n} FIAP_k\% \qquad \text{eq. 3.2}$$

Depending on the study, the results of the leaching/corrosion experiments were presented in different ways. The radionuclide releases were presented as: release fraction (FIAP), cumulative release fraction (FIAPc), cumulative FIAP% and cumulative concentration. In order to make use of available data the radionuclide releases were converted into $FIAP_c$ % using eq. 3.1 and 3.2 whenever sufficient information (concentration, solution volume, sample mass and fuel inventory) was available. In most cases the isotope of element *i* was not specified for concentration and inventory. In these cases, the average molar weight of the element was used in the calculations.

Apart from radionuclide release data, fuel properties, irradiation history of the fuel sample, information about the sample, experimental atmosphere and solution composition were also of interest and collected whenever possible.

Data collection

Excel was used to build the database. At times authors presented the obtained data in tables, in these cases the values were used as given or converted to the appropriate unit and used. At other times, authors presented the obtained data through graphs. To collect data from graphs the software tool Graph Grabber 2.0.2 by Quintessa [16] was used.

Data evaluation

Scatterplots were made using Python where each element's FIAP% was plotted against FIAP(U)% to compare radionuclide release to matrix corrosion. As there, in some cases, is data available for different isotopes of the same element, a common plot was made per element where all isotopes' releases were included. The release of isotopes was differentiated using markers, an example of this can be seen in Figure 3.1 where the circles represent Eu (not specified), and the triangles represent ^{153}Eu. In addition, the plots were categorized by different parameters, in the case of Figure 3.1 the plot has been categorized by sample type.

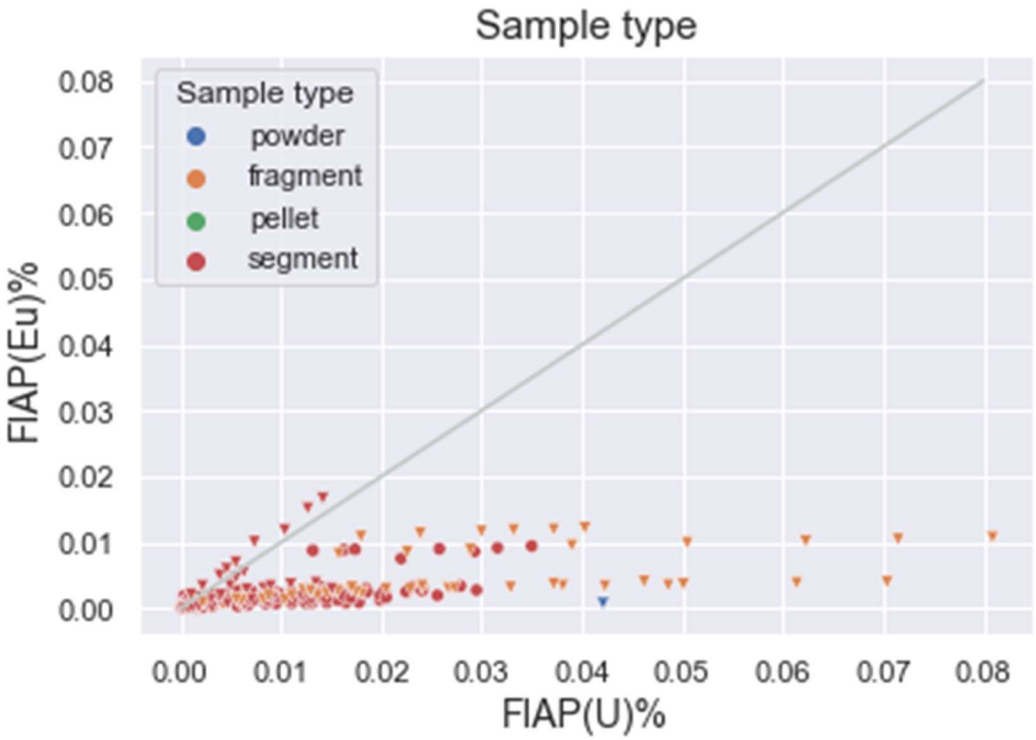

Figure 3.1 Scatterplot of FIAP(Eu)% against FIAP(U)%, categorized by sample type where circles represent unspecified Eu and triangles represent the isotope ^{153}Eu.

3.2 Machine Learning Models

In the scope of this thesis the machine learning models that have been used are Artificial Neural Network (ANN), Random Forest (RF) and XGBoost. The database, which is the learning and testing basis for the models, has a large amount of data features (36 features) and a large amount of missing values. Therefore, the models used need to be able to handle the amount of input features chosen while also minimizing the effect of the missing values. In this regard, ANN, RF and XGBoost were deemed most suitable due to their ability to handle large amounts of input data, in this case the features, as well as their randomized processes of handling the data. For ANN the randomized process referred to is the dropout layer and for RF as well as XGBoost the training data selection as well as the random feature selection during training.

The main libraries used to run and define the models are TensorFlow and Keras respectively. TensorFlow is a widely used open-source end-to-end platform for machine learning models. Keras, which is a high-level Python library for deep learning, is commonly used on top of TensorFlow to define models [17].

The desired output data, meaning desired predictions, of the algorithms was the FIAP% of each radionuclide. From the literature it is known that the dissolution of radionuclides is dependent on irradiation history, chemical state of the radionuclides, redox conditions, and solution composition. Therefore, the parameters chosen as input features for the models were: Reactor type, BU, pH, U-secondary phase, and cumulative time. Furthermore, during the evaluation of

radionuclide behaviour, seen in section 4.2, it was evident that sample type, sampled region and presence of cladding affected the release of radionuclide, hence these features were also chosen as input features. In the beginning of the modelling stage, it was established that the models needed an input feature which would change with the cumulative time, and which could be correlated to the release of other radionuclides. Therefore, FIAP(U)% was also used as an input feature while keeping in mind that this entails that for the models to be usable in the future, the FIAP(U)% of a spent nuclear fuel needs to be known. Also worth mentioning is that using FIAP(U)% as an input feature causes the model to look past datasets where FIAP(U)% is missing, since not all studies document the release of U this means that not all fission products or datasets are considered by the model. The output data, and because of that also the training and test data, was chosen as the unspecified isotopes of each element. As C, Se and Pd were only documented as specific isotopes, there are therefore no predictions made for these elements.

The database was imported to the models and when running the training of the models, they each produced summarized data reports containing, among other information, an overview of dataset statistics and variable types as well as interactions between all input data in the form of graphs. These data reports were used to check the database for errors such as typing errors by analysing the information and looking for outsider values. When the database had been revised of typos and errors, the predictions were run.

3.2.1 Artificial Neural Network

The backpropagation algorithm was used due to its ability to adjust the weights of the connections between the nodes in relation to the error. To find the best possible configuration of the model, 10 different architectures were tested using a trial-and-error approach. During the testing of the models, the batch sizes, epochs, and optimizer were also changed manually to find the parameter configuration which yielded the lowest error, the metric used to measure errors was mean square errors. Worth mentioning is that a try was made to use the Optuna optimizer on the ANN algorithm to eliminate the need of manual tuning of parameters, however, this try was unsuccessful. The Optuna optimizer is an automated framework which can be used in python to find the optimal parameters for models and can be run in parallel allowing several architectures to run at once [19].

3.2.2 Random Forest

Two types of RF algorithms were used, a conventional RF algorithm as well as an XGBoost algorithm combined with an Optuna optimizer. For the conventional RF algorithm, different parameters were changed manually, while the Optuna optimizer chose the parameters for the algorithm automatically.

3.2.3 Commonalities

Imputation of missing FIAP% values was necessary for the models to run. All models were tested with imputing zeros as well as column mean values, meaning the mean FIAP% per element.

During the evaluation of these models, the R^2 score of the models' training and test phases were considered as well as their learning curves. Learning curves refer to graphs like the one shown in Figure 3.2 where the curves represent the evolution of the error between prediction and true value. Training loss refers to error evolution during the model training, while validation loss refers to the error evolution during model testing. In this case, the metric used to calculate the error is the mean squared error described by eq. 3.2. R^2 score is calculated as explained in eq 3.1, where y_i is the true value, $\hat{y}_i$ is the predicted value and $\bar{y}_i$ is the mean value of the true values. The R^2 score explains how well the model fits data, where a score of 1 entails a 100% fit and a negative value entails that the mean value for each output is a better fit than the predictions made [20]. To further investigate the model performance per element, training-validation reports were generated where the true values and their corresponding predictions for both training and test data were documented. These reports were also used to create prediction/true value plots to be used as visual illustrations of the model performance and the graphs were evaluated using R^2. The difference between R^2 score and R^2 is that R^2 score considers the models multiple dimensions (in this case 20 dimensions) while R^2 does not.

Figure 3.2 Example of a learning curve for machine learning models.

$$R^2 = 1 - \frac{\Sigma(y_i - \hat{y}_i)^2}{\Sigma(y_i - \bar{y}_i)^2} \quad (3.1)$$

$$mse = \frac{1}{n}\sum_{i=1}^{n}(y_i - \bar{y}_i)^2 \quad (3.2)$$

4 Results & Discussion

In this section the final database will briefly be presented, and an evaluation of the general correlations obtained from it will be given. In addition, the machine learning models used will be evaluated.

4.1 Spent Fuel Dissolution Database

The final database contains 800 datapoints and is a summary of experimental data from 21 different studies and a total of 94 different experiments, the findings of which were published during the years 1993-2021. The information available in the database can be divided into 6 categories: fuel characteristics, irradiation history, sample characteristics, atmospheric conditions, solution composition and radionuclide release as a function of time. Each category and parameters that it includes have been listed in table 4.1.

Table 4.1 Listing of each category and their respective parameters that are present in the database. The first column lists the categories while the rows list each category's parameters.

Sample characteristics	Sample type	Cladding	Cladding specification	Sample size	Region sampled	Surface area	Position in rod
Fuel characteristics	Fuel type	U^{235} enrichment	Pu^{239} enrichment	Reactor type	Burn-up	Fuel power	
Radionuclide release	Type of data	Origin of data	Cumulative time	U secondary phase	FIAPc(X)%	FGR%	
Atmospheric conditions	Atmosphere	Atmospheric composition	pH	Temperature			
Solution composition	Solution composition	Concentrations of various ions	Solid present (e.g. Ti)				
Irradiation history	Irradiation cycles	Irradiation time	Cooling time				

Due to the variety of studies and the difference in time between them (conducted over a period of 3 decades), the experimental conditions as well as sample preparation differed between studies and not all studies provide the same information. Additionally, analysing tools, like ICP-MS, have limiting thresholds that need to be met for the tool to yield a reading. Hence, there are empty cells in the database due to unprovided data or unmeasurable data. Furthermore, the number of elements considered in each study also differs, entailing more datapoints for certain elements and less for others. Ag, Cd, Te, Pm and Sm are examples of elements whose release have only been measured in 1 out of the 21 studies.

Having all these different parameters present in the same place and format made it possible to compare the release of different radionuclides with the matrix dissolution through scatterplots using Python, ex. plot FIAP(Tc)% against FIAP(U)%. Simultaneously having access to sample characteristics, atmospheric conditions and solution composition in the same database made it possible to investigate correlations based on these parameters. Examples of possible correlations can be seen in Figure 4.1 and 4.2 below.

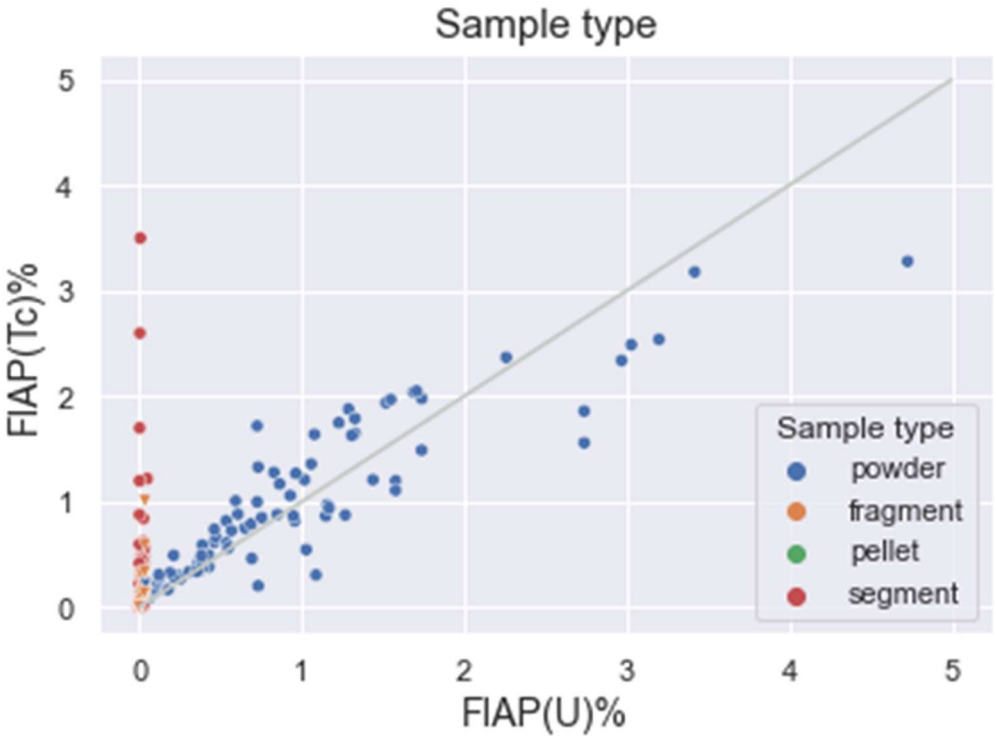

Figure 4.1 Scatterplot of FIAP(Tc)% and FIAP(U)% where the different colors of the plotted points represent the sample type of the datapoint and the grey line is a straight y = x line.

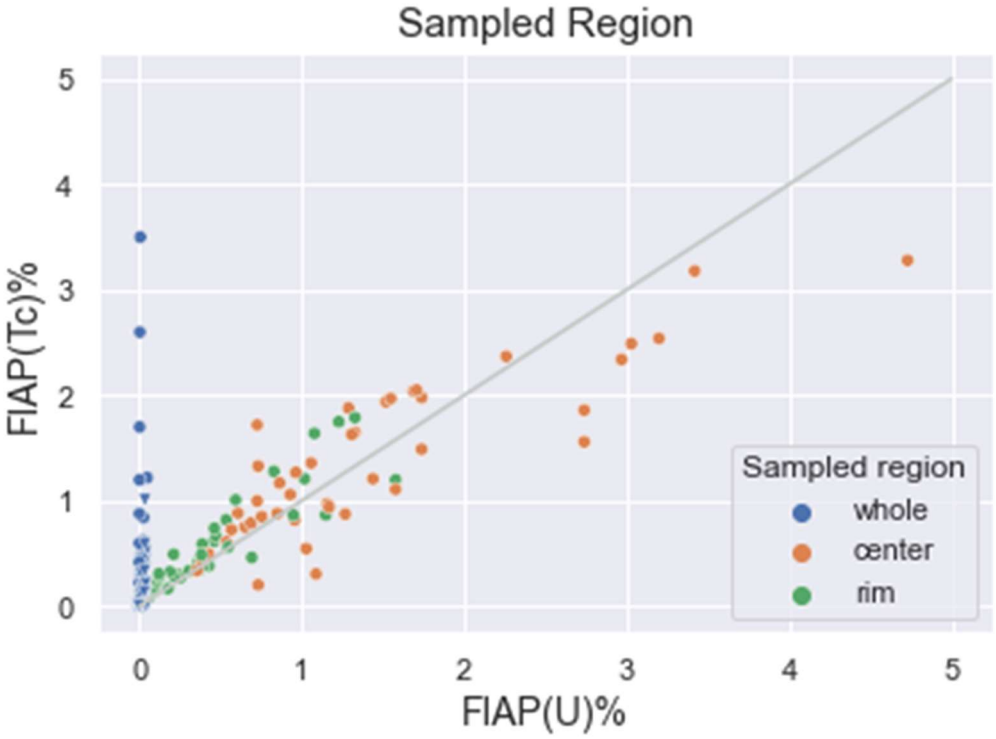

Figure 4.2 Scatterplot of FIAP(Tc)% and FIAP(U)% where the different colors of the plotted points represent the sampled region of the datapoint and the grey line is a straight y = x line.

Since it was desirable to gain a better understanding of how different parameters influence the radionuclide release, this was checked using the plots for each study. However, it showed to be difficult to generalize on the behaviour of elements per parameter. For instance, Figure 4.3 shows the release of Cs vs the release of U considering BU which does not seem to show any BU dependent trend.

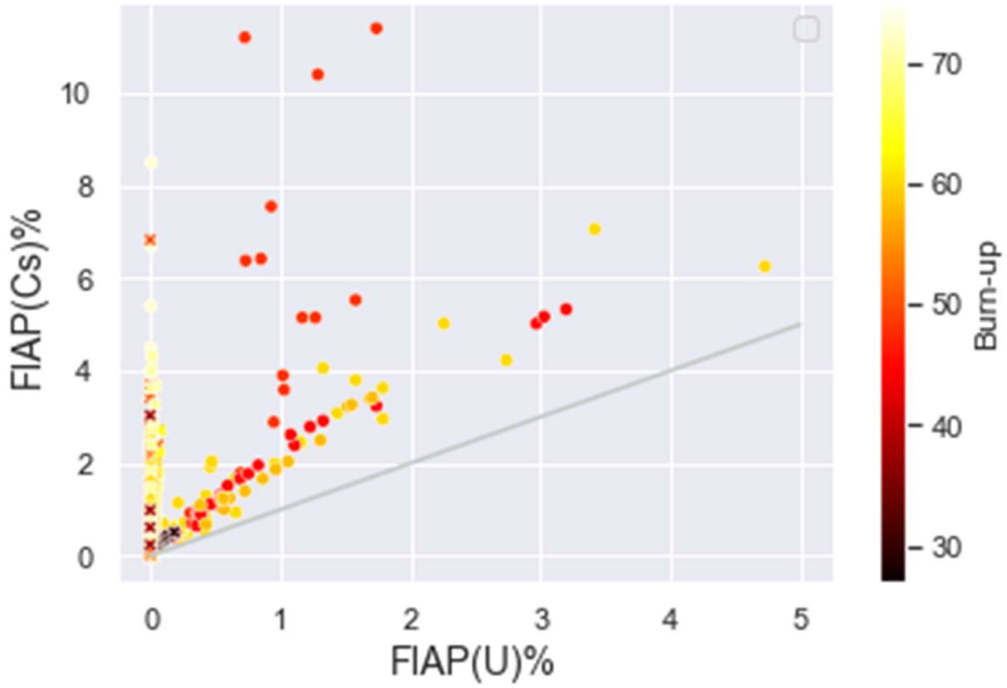

Figure 4.3 Scatterplot of FIAP(Cs)% and FIAP(U)% where the different colors of the plotted points represent BU of the datapoint and the grey line is a straight y = x line. Circles represent unspecified Cs, triangles represent ^{133}Cs, squares represent ^{134}Cs, diamonds represent ^{135}Cs and crosses represents ^{137}Cs.

4.2 Evaluation of Radionuclides Using Database

As explained in the section above, the database made it possible to create scatterplots and evaluate correlations between radionuclide and U release in relation to varying parameters. While evaluating behavioural trends of each element it was possible to group the elements based on these trends. Four main groups were found:

1. Group 1: elements showing U dependent release
2. Group 2: elements showing low release independently of U
3. Group 3: elements showing high release independently of U
4. Group 4: elements exhibiting particular behaviour.

Each group contains subgroups where the behaviours have been further specified. In the following section these groupings as well as the evaluations the groupings are based on will be presented and explained.

4.2.1 Elements Showing U Dependent Release: Group 1

Elements showing U dependent release are elements whose release follow a correlation with the release of U. This group of elements can be divided into 3 subcategories based on exhibited behaviour on the scatterplots:

a) Elements whose release show a 1:1 correlation with U: Np, Y, Sr
b) Elements whose release mainly show a 1:1 correlation with U, but also show some data with lower release than U: Pu, Am, Cm, Nd, La, Zr
c) Elements whose release are partly correlated with the U release, but also exhibit a trend indicative of being more resistant to dissolve than U: Eu, Ce, Pr, Pm, Sm

4.2.1.1 Group 1a: Np, Y, Sr

Figure 4.4 shows how the elements of **group 1a** behave, appendix A.1 contains the remaining scatterplots of these elements.

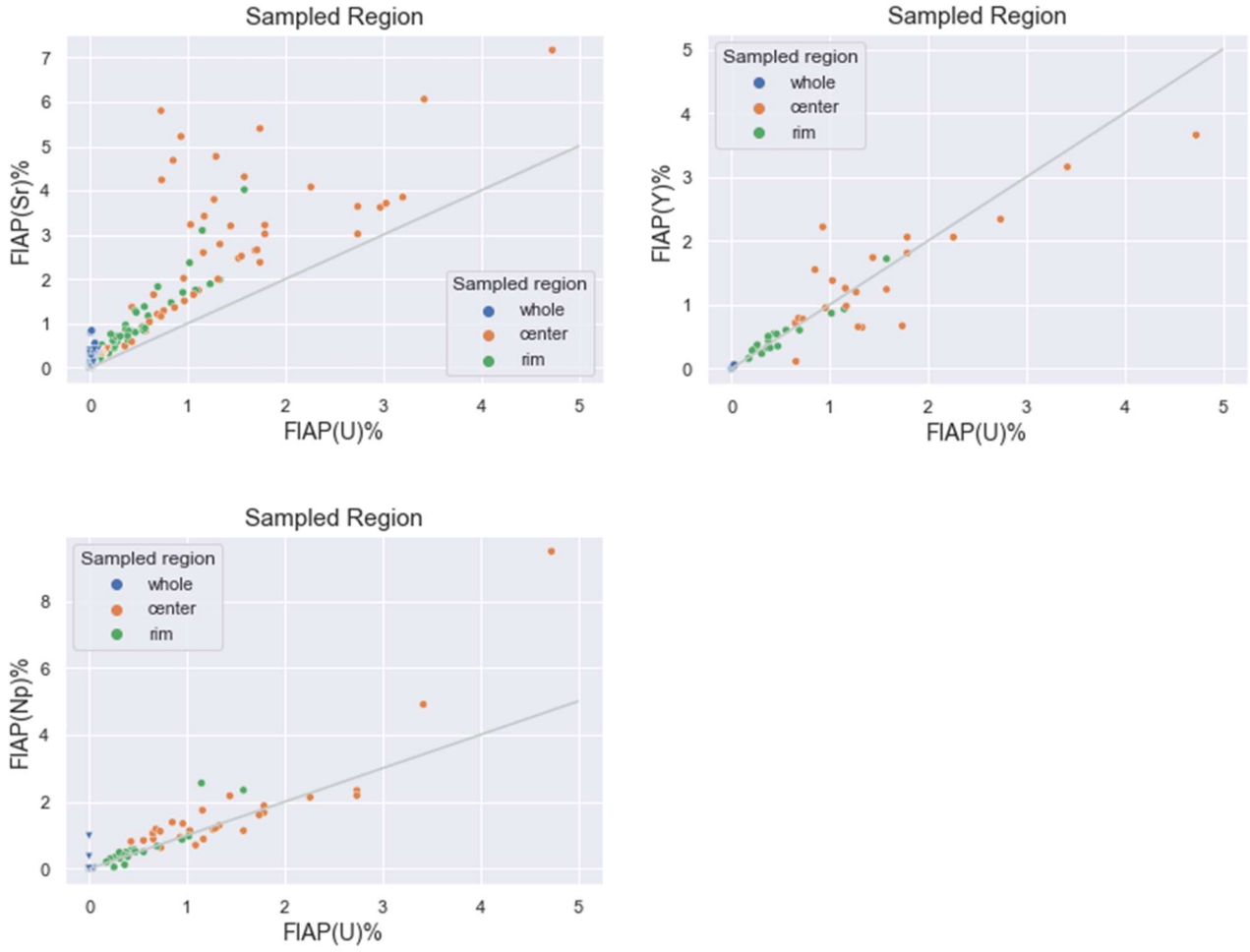

Figure 4.4 Scatterplots of group 1a radionuclide releases in relation to U release, where points have been categorized by colour depending on sampled region and the grey line is a straight y = x line. a) Sr release correlated to U, b) Y release correlated to U, c) Np release correlated to U.

From Figure 4.4 a), b) and c) it is evident that the general trends of the radionuclide releases follow the grey line, which is a straight y = x line, meaning that the radionuclide releases follow

the release trend of U. This indicates that the release of radionuclide in group 1a are dependent on the matrix corrosion and hence are embedded in the fuel matrix. Furthermore, since the datapoints lay on the grey line, a similar ease of release of the radionuclide and U is indicated, except for Sr. In Figure 4.4 a) can be seen that the general trend of Sr is parallel to but slightly above the grey line, indicating that Sr has U dependent release yet is dissolved more easily. Additionally, from Figure 4.4 a) and c) outliers with high Sr and Nd releases respectively are visible. These points all originate from the same study where it is brought up that U is forming a secondary phase [22], which would explain the outliers. It is further evident from Figure 4.4 that the higher content of these elements is in the center of the fuel pellet, further supporting that these elements are embedded in the fuel matrix.

4.2.1.2 Group 1b: Pu, Am, Cm, Nd, La, Zr

The behaviour of **group 1b** is shown in Figure 4.5 including Pu, Am and Cm, and in Figure 4.6 including Nd, La and Zr. The datapoints again have been categorized by the sampled region and the grey line is a straight y = x line. These elements also follow the grey line, however, not to the same extent as group 1a. At first glance it is evident that this group of elements are released with the matrix corrosion and to some extent have a similar ease of release as U due to the linearity of the elements' behaviour. In appendix A.2 the remaining scatterplots of the elements in group 1b can be found.

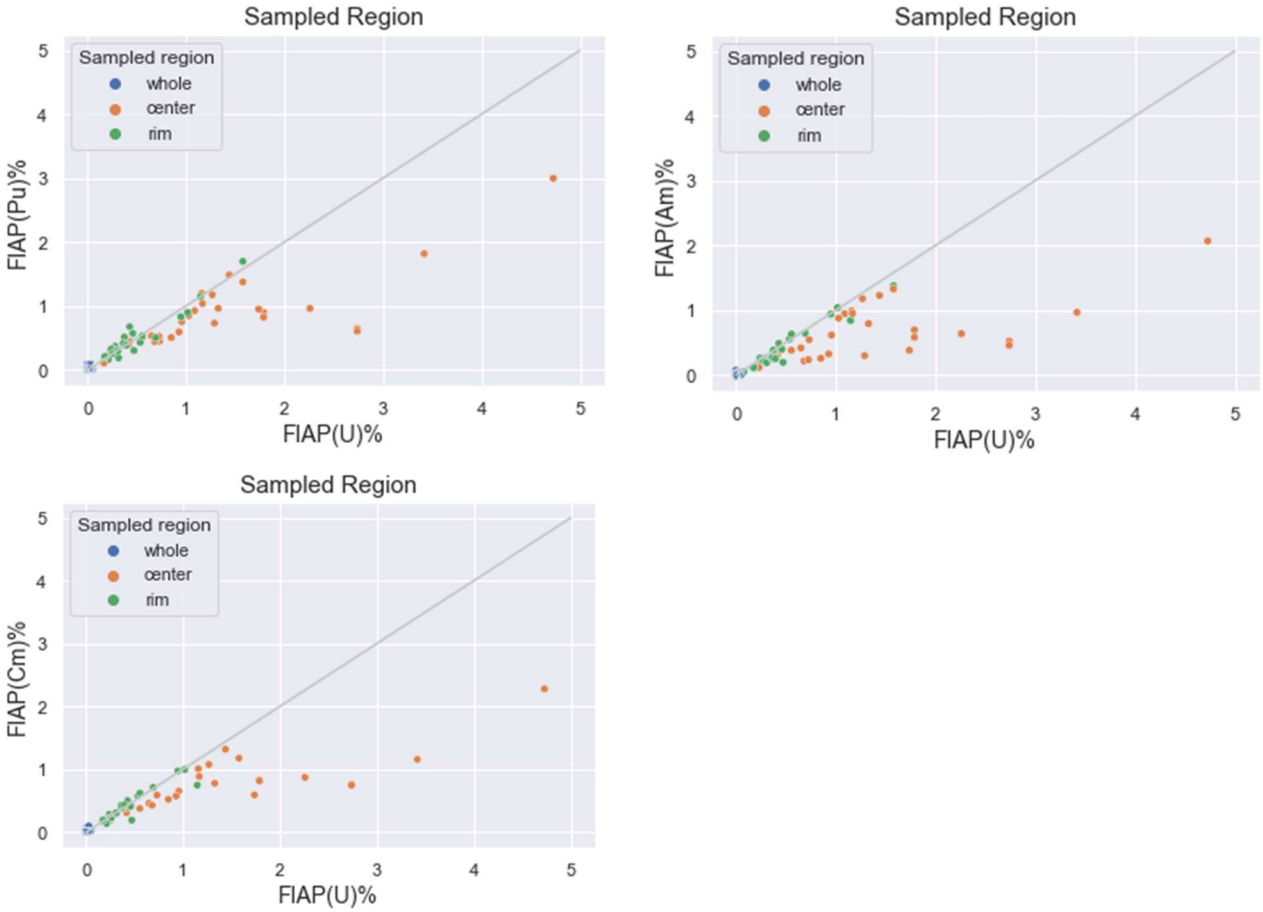

Figure 4.5 Scatterplots of group 1b radionuclide releases in relation to U release, where points have been categorized by colour depending on sampled region and the grey line is a straight y = x line. a) Pu release correlated to U, b) Am release correlated to U, c) Cm release correlated to U.

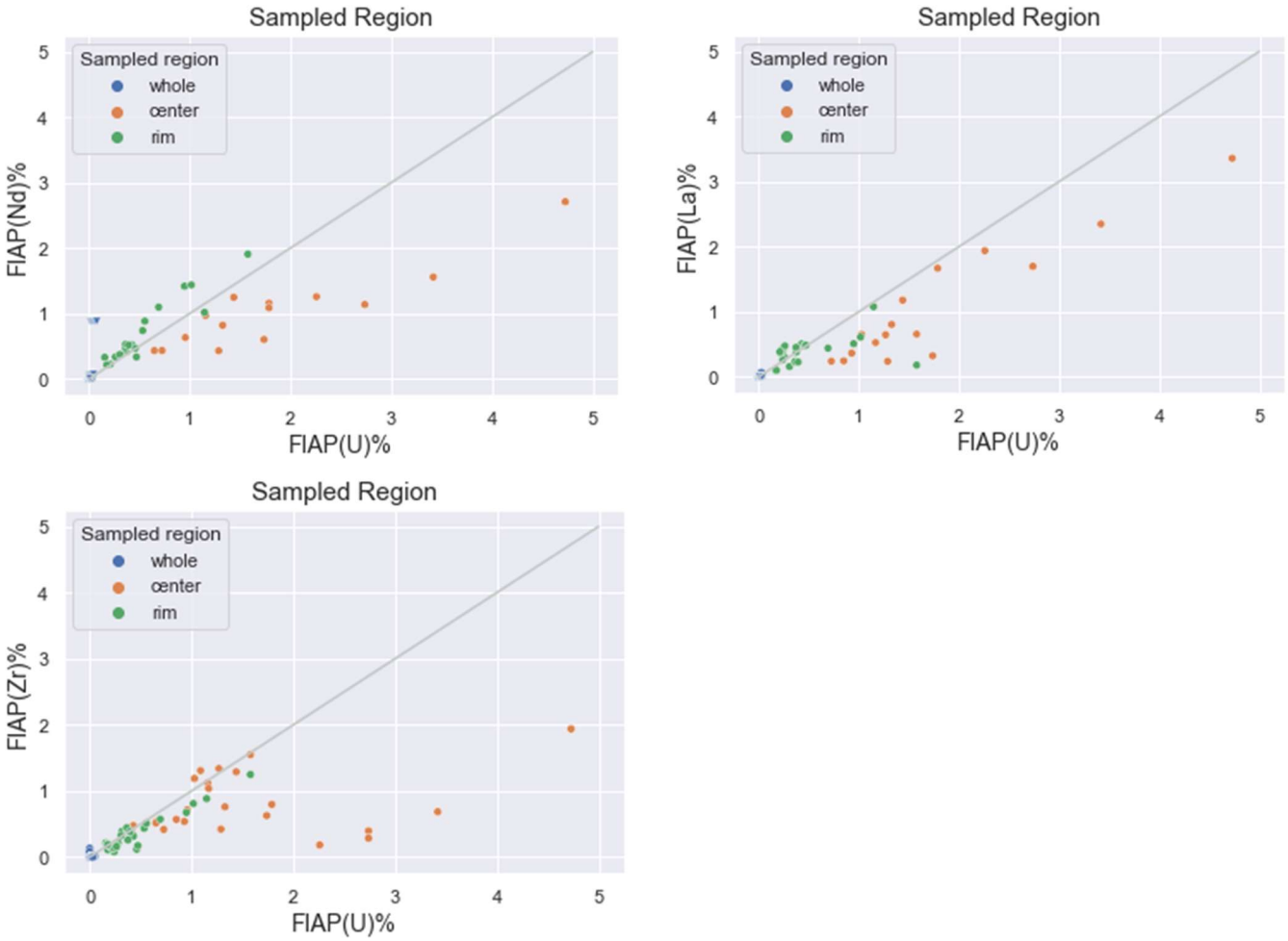

Figure 4.6 Scatterplots of group 1b radionuclide releases in relation to U release, where points have been categorized by colour depending on sampled region and the grey line is a straight y = x line. a) Nd release correlated to U, b) La release correlated to U, c) Zr release correlated to U.

The main difference between group 1a and 1b is the outlier trend below the grey line which shows the 1:1 release of each fission product with respect to U. These outlier trends could be explained by the formation of secondary phases, as identified in Gonzalez-Robles (2011) [22], decreasing the measurable concentration of the different radionuclides in the solution. Gonzalez-Robles (2011), determined through solubility calculations the formation of: NpO_2(am,hyd), $Pu(OH)_4$(am), $AmOHCO_3$(s), $CmOHCO_3$(s), $Zr(OH)_4$(am), $La_2(CO_3)_3$ and $NdOHCO_3$ limiting the solubility of Np, Pu, Am, Cm, Zr, La and Nd, respectively.

4.2.1.3 Group 1c: Eu, Ce, Pr, Pm, Sm

Elements in **group 1c** are shown in Figure 4.7 including Ce, Pr and Eu and in Figure 4.8 including Pm and Sm. Overall, these elements have a low release, which can be seen by the scale of the y-axis, indicating that these elements have low solubility. These elements generally show two different trends: some data of radionuclide release seem to correlate almost 1:1 with U but the majority of data indicate lower release than U.

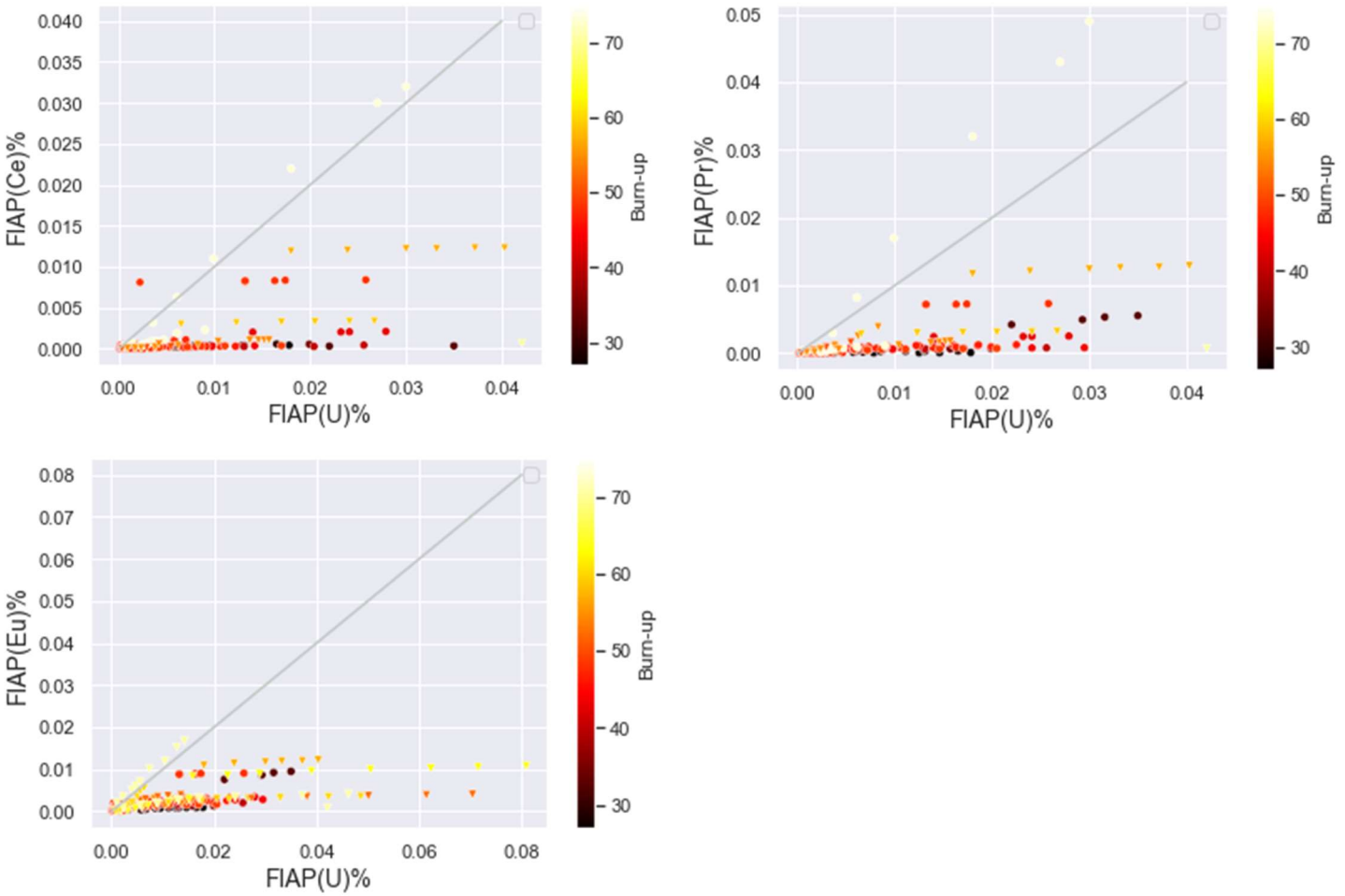

Figure 4.7 Scatterplots of a) Ce, b) Pr and c) Eu release in relation to U release, where points have been categorized by colour depending on BU and the grey line is a straight y = x line.

For Eu, Ce and Pr, seen in Figure 4.7, there is a dataset that shows dependence with U (white points). For these three elements the linear dependent release with U seems to occur at BU ≥ 70 GWd/t_{HM}. For Eu, this dataset is from Roth et al. [21] and the linearity is attributed to segment type samples with the same material and under the same leaching conditions, the correlation with U it is not seen in the case of fragment type samples.

For Ce and Pr, the datasets showing correlation with U are from Clarens et al. [7] and this behaviour is attributed to leaching with bicarbonate (BIC) water, as the same material being leached with young cement water with calcium (YCWCa) does not show dependency with U release (see Figure 4.8). The same behaviour is observed for Pm and Sm, which were only documented by Clarens et al. [7] in the DisCo project and hence have a limited set of data to be evaluated. The compositions of the leaching solutions used in Clarens et al. [7] can be found in table 4.2.

Table 4.2 Solution compositions of leaching solutions used in Clarens et al. [7].

Solution	pH	Na^+ (mmol/L)	Ca^{2+} (mmol/L)	Cl^- (mmol/L)	SiO_3^{2-} (mmol/L)	CO_3^{2-} (mmol/L)	OH^- (mmol/L)
YCWCa	13.4	$5.0 \cdot 10^2$	$9.8 \cdot 10^{-1}$	-	$2.0 \cdot 10^2$	$2.5 \cdot 10^0$	$2.5 \cdot 10^2$
BIC	7.4	$2.0 \cdot 10^1$	-	$1.9 \cdot 10^1$	-	$1.0 \cdot 10^0$	$2.5 \cdot 10^{-7}$

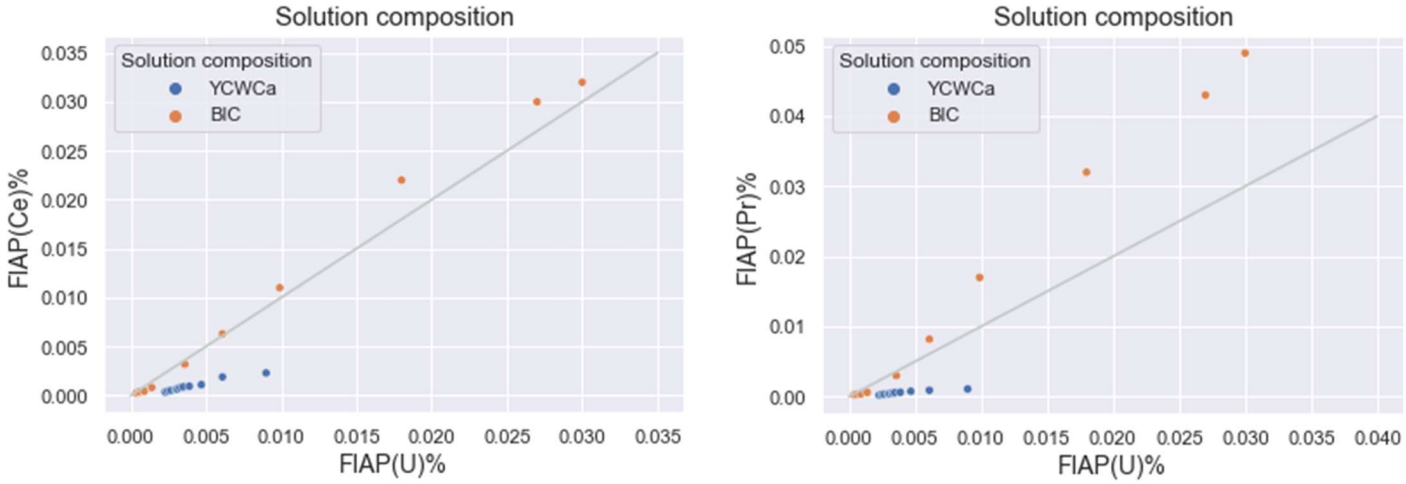

Figure 4.8 Scatterplots of a) Ce and b) Pr release in relation to U release from Clarens et al. [7], where points have been categorized by colour depending on solution composition and the grey line is a straight y = x line.

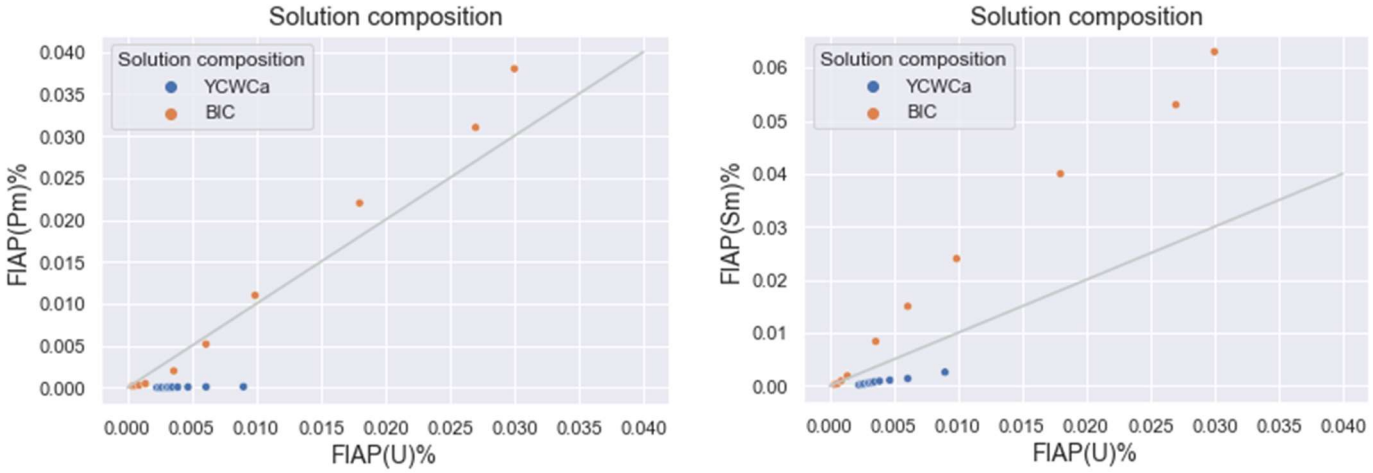

Figure 4.9 Scatterplots of a) Pm and b) Sm release in relation to U release, where points have been categorized by colour depending on solution composition and the grey line is a straight y = x line.

As discussed in [7] the YCWCa solution with high pH containing calcium and silicon showed an inhibition in the dissolution of U compared to the BIC solution experiment. This indicates that calcium with silicon might form a protective layer on the surface and hence prevent dissolution of the matrix.

4.2.2 Elements Being Released Independently of Matrix Corrosion: Group 2

Elements in group 2 show trends of low radionuclide release with increasing U release indicating insolubility of radionuclides. From the available data this group can further be divided into subgroups:

a) Elements showing different behaviour depending on solution composition: Pd, Ag
b) Elements showing consistently lower release than U: Rh, Ru

4.2.2.1 Group 2a: Pd and Ag

The elements of **group 2a** are shown in Figure 4.10 below.

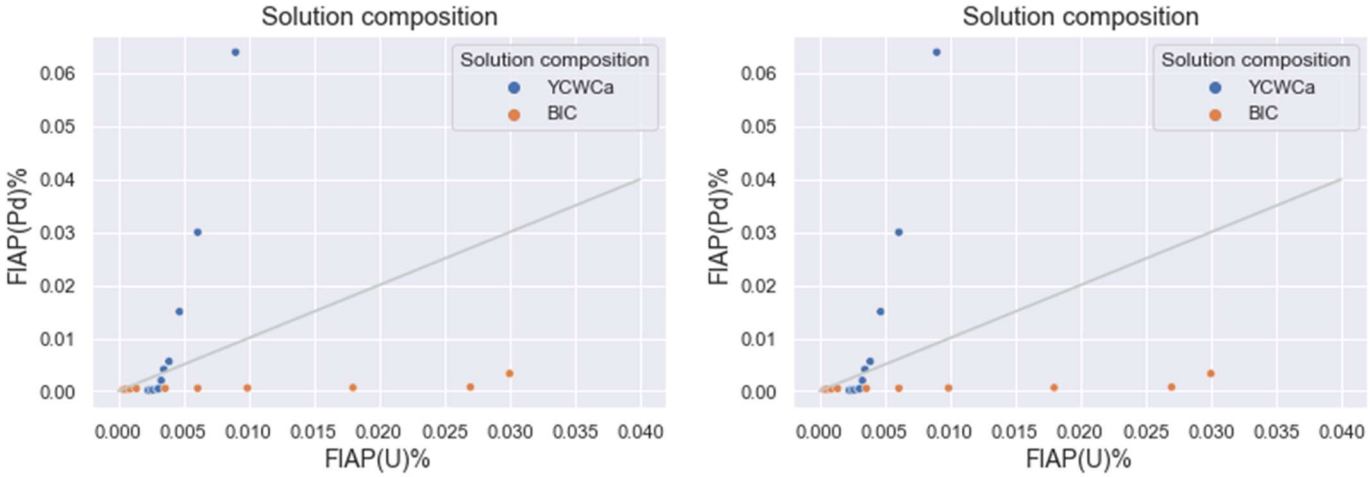

Figure 4.10 Scatterplots of a) Pd and b) Ag release in relation to U release, where points have been categorized by colour depending on solution composition and the grey line is a straight y = x line.

Both Pd and Ag have a limited set of datapoints which come from the same study (Clarens et al. [7]) from the DisCo project making it difficult to generalize their behaviour. From Figure 4.10 it is overall evident that these elements show two behavioural trends depending on the solution composition: one below the grey line (BIC solution) and one above the grey line (YCWCa solution) with a steeper slope than 1. These trends indicate that the release of Pd and Ag is independent of the U release and the existence of the steeper trends is indicative of the fission product being located in the void spaces of the fuel rod. Considering the BIC solution trends it is evident that the ease of release of these fission products is decreased in this solution. Further investigations are needed to be able to draw certain conclusions, however from what can be seen from the available data these elements seem to be present in the void spaces in the fuel rod and present themselves as metallic precipitates whose ease of release depend on the solution composition. The remaining plots for Pd and Ag can be found in appendix A.4.

4.2.2.2 Group 2b: Ru and Rh

The behaviour of group 2b is shown in Figure 4.11, the remaining plots of Ru and Rh can be found in appendix A.5. From Figure 4.11 it is evident that regardless of sampled region, the release of group 2b elements is constantly lower than the release of U indicating that these fission products have reached a plateau concentration. This could be explained by the fission products having a low inventory in the spent fuel or that they are present as insoluble metallic precipitates in the solution.

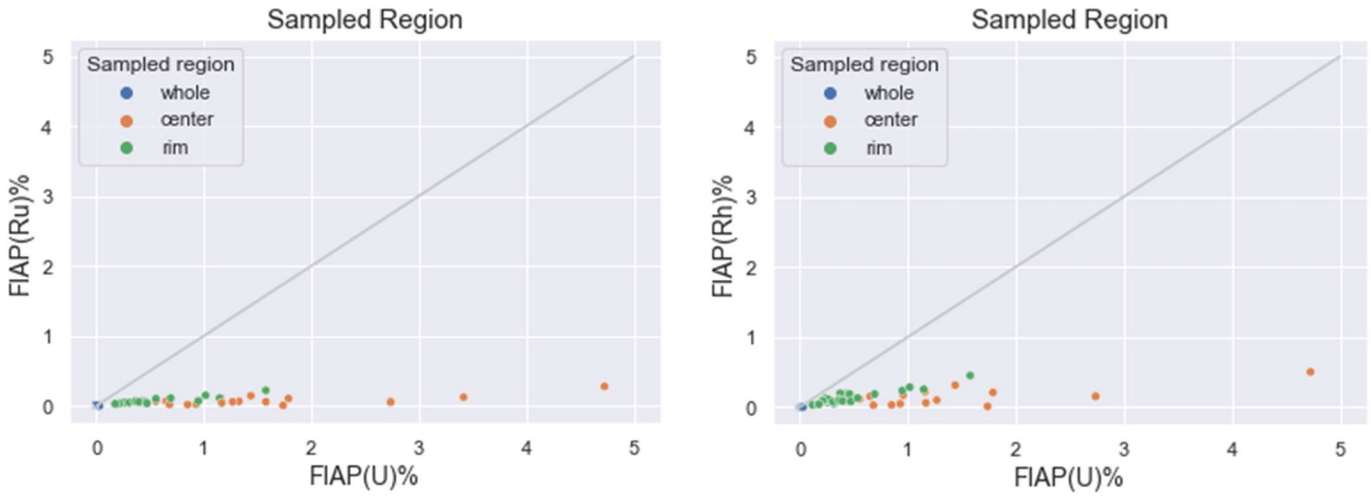

Figure 4.11 Scatterplots of group 2b radionuclide releases in relation to U release, where points have been categorized by colour depending on sampled region and the grey line is a straight y = x line. a) Ru release correlated to U, b) Rh release correlated to U.

4.2.3 Elements Showing High Release Independently of U Release: Group 3

The elements in group 3 all show a trend of high radionuclide release in relation to U release and can be divided into 2 subgroups:

a) Elements showing evidence of being part of IRF (I, Ba, Cd, Te)
b) Elements showing evidence of being part of IRF and fuel matrix (Cs, Mo, Rb, Tc)

4.2.3.1 Group 3a: I, Ba, Cd, Te

Group 3a element behaviour is shown in Figure 4.12, the remaining plots for the elements of this group can be found in appendix A.6. The main behaviour of group 3a which shows evidence of the elements belonging to the IRF is the high radionuclide release in relation to U release. Low U release indicates low matrix dissolution, if the radionuclide then has a high release, this indicates that the radionuclide is present in spaces that are more easily penetrated by the solution, i.e. open spaces. These open spaces can be the fuel-cladding gap, fractures, bubbles and grain boundaries. From Figure 4.12 it is evident that both cladded and non-cladded samples exhibit high I and Ba release with low U release. This suggests that these elements are present in both fuel-cladding gap as well as in the grain boundaries.

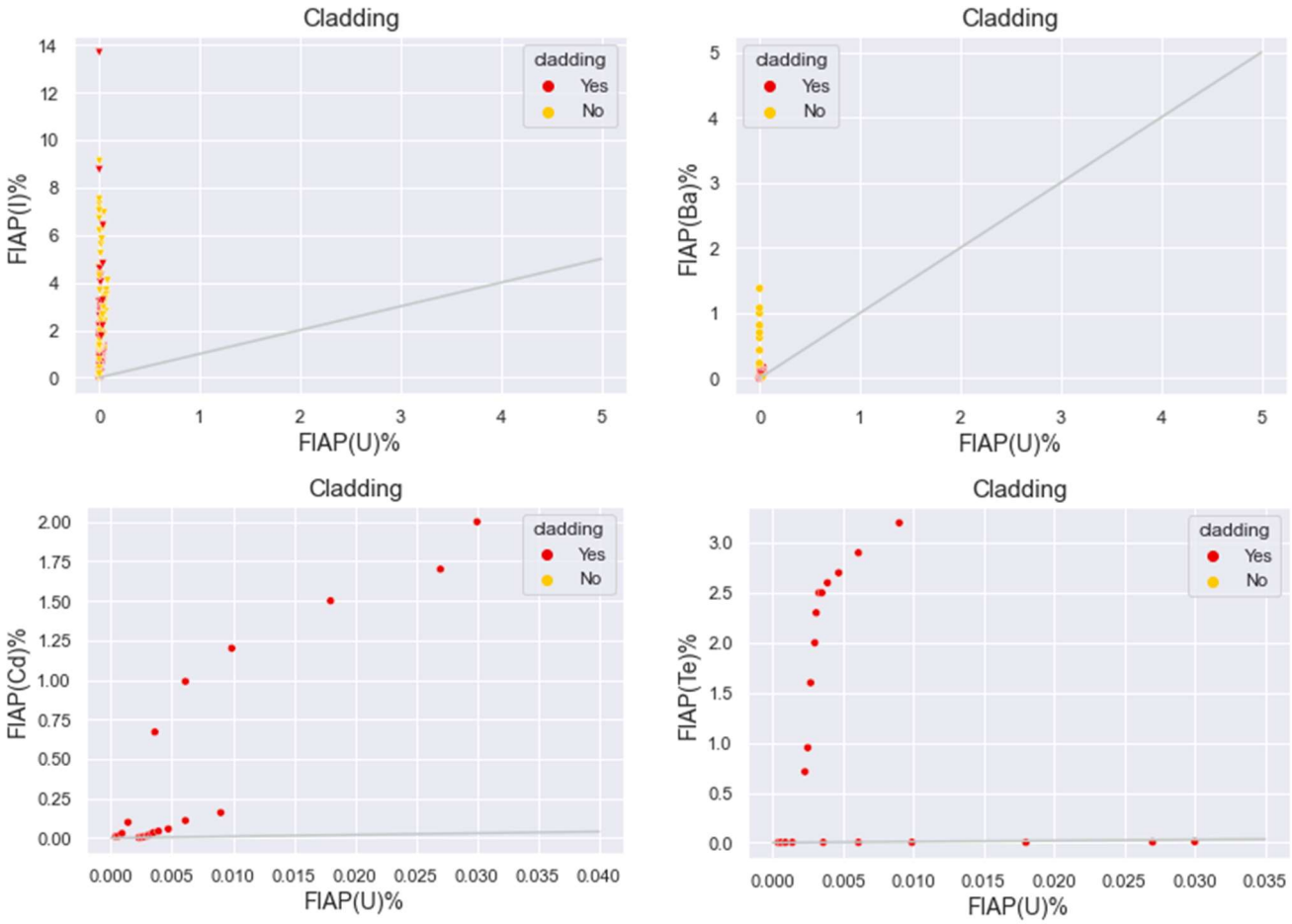

Figure 4.12 Scatterplot of group 3a radionuclide release in relation to U release, where points have been categorized by colour depending on presence of cladding and the grey line is a straight y = x line. a) I release correlated to U, b) Ba release correlated to U, c) Cd release correlated to U, d) Te release correlated to U.

Although Cd and Te show similar behaviour as I and Ba, only a few datapoints from the same study (Clarens et al. [7]) are available for these elements. To be able to generalize the behaviour of Cd and Te more data is needed, like the case of subgroup 2a. However, from Figure 4.13, it is evident that regardless of whether the leaching solution is BIC or YCWCa, these elements show release independent of and higher than or in line with the U release. The release of Cd is probably limited by the presence of calcium with silicon forming a protective layer on the surface (Clarens et al. [7]). However, the release of Te shows a similar behaviour as Pd and Ag except that the release of Te is two orders of magnitude higher than U, indicating to be part of the IRF.

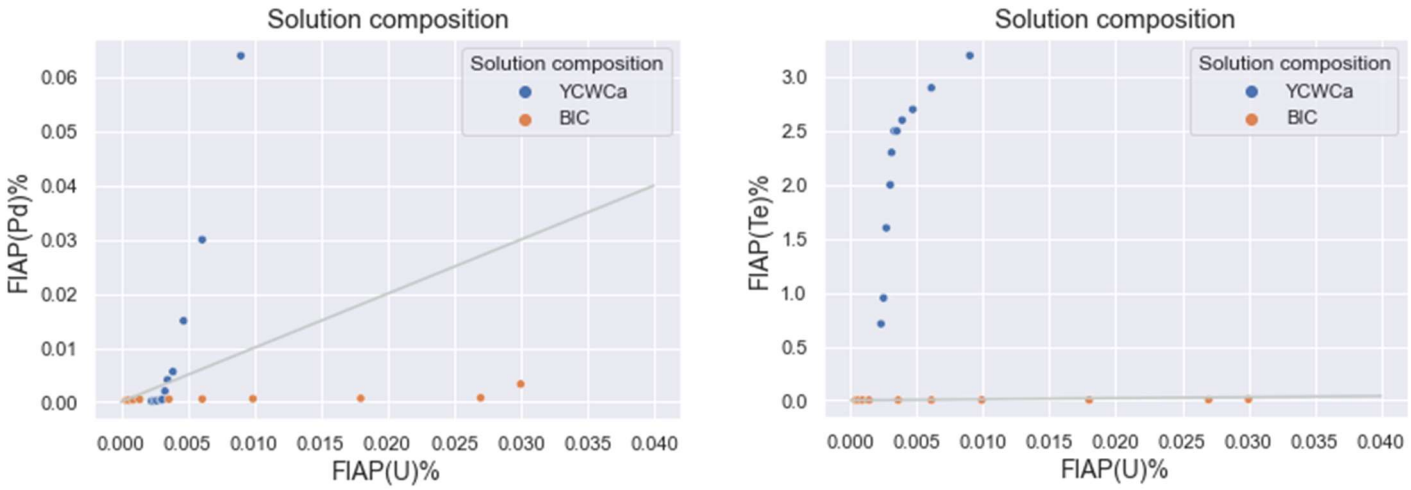

Figure 4.13 Scatterplots of a) Cd and b) Te release in relation to U release, where points have been categorized by colour depending on the solution composition and the grey line is a straight y = x line.

4.3.2.2 Group 3b: Cs, Mo, Rb, Tc

Plots of the elements in group 3b are shown in Figure 4.14 and 4.15, and the remaining plots for elements can be found in appendix A.7. The elements of group 3b show two clear behavioural trends: one with high radionuclide release while U release is low and one where the radionuclide release follows the grey line. Following the reasoning of group 3a and group 1a, these trends suggest that the elements of group 3b are present in the IRF and that they are also embedded in the fuel matrix. While the U dependent trend of Tc, Figure 4.14 a), seems to follow the 1:1 release with respect to U, it is evident from Figure 4.14 b), c) and d) that the U dependent releases of Cs, Mo and Rb are above the grey line. This could be attributed to differing ease of release of the elements compared U. Furthermore, distinctive outlier points with high low U release and high radionuclide release can be seen for powdered samples of Rb and Cs. These points come from the same study, Gonzalez-Robles et al. [22] and could be attributed, as earlier mentioned, to the formation of U secondary phases.

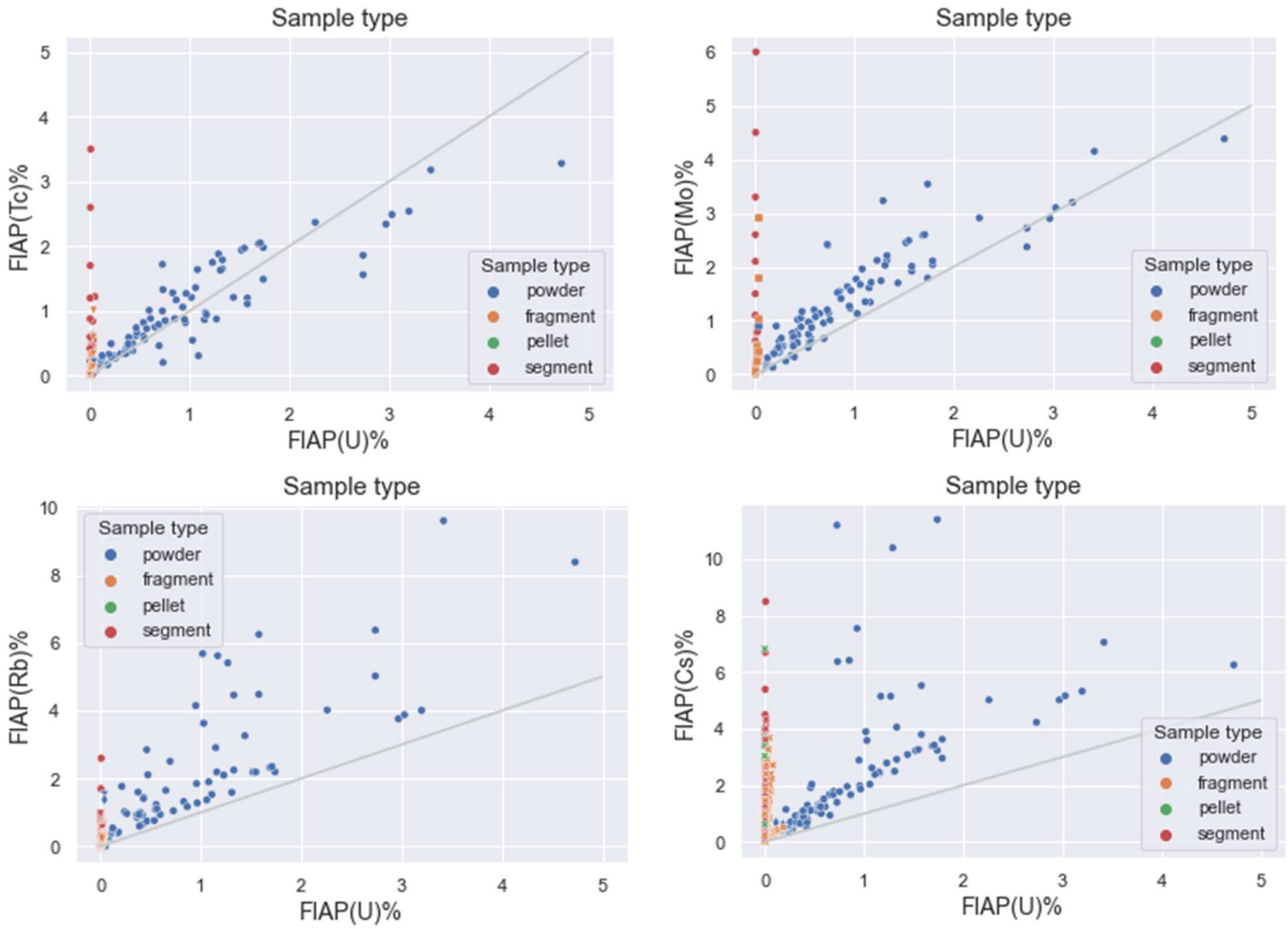

Figure 4.14 Scatterplot of group 3b radionuclide release in relation to U release, where points have been categorized by colour depending on sample type and the grey line is a straight y = x line. a) Tc release correlated to U, b) Mo release correlated to U, c) Rb release correlated to U, d) Cs release correlated to U.

Looking at Figure 4.14 and 4.15 it can be seen that cladded samples are either segment or fragment type samples. Keeping the cladding on a sample and having larger size should leave cladding-fuel gap, grain boundaries, fractures etc., the void spaces, more intact than for powdered non-cladded samples. Since the void spaces are more intact in these segment or fragment cladded samples, the radionuclides they contain which are part of IRF are also still present to a greater extent than for powdered non-cladded samples. This is strengthened by the higher release of radionuclides as compared to U release for red points in Figure 4.15.

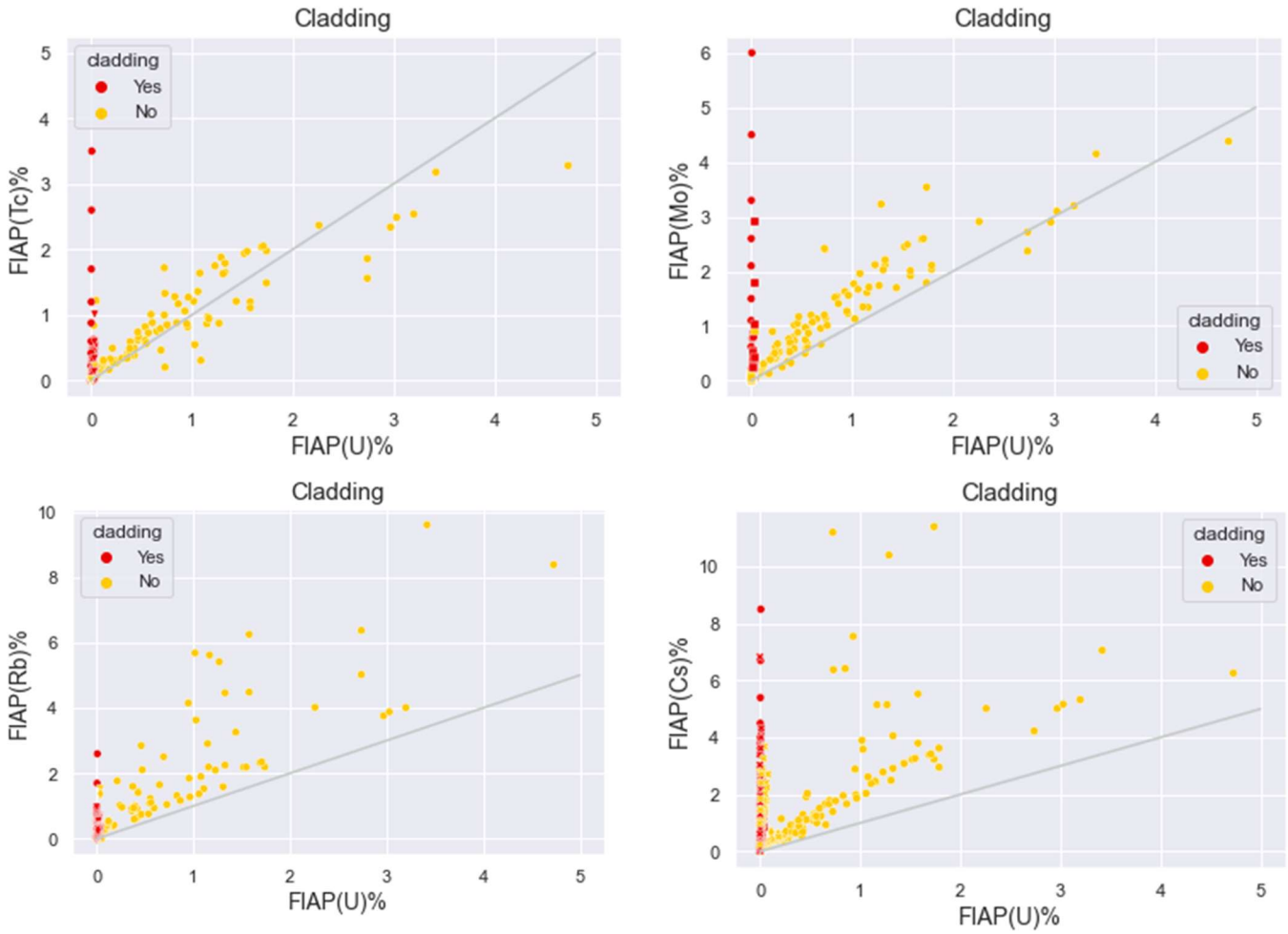

Figure 4.15 Scatterplot of group 3b radionuclide release in relation to U release, where points have been categorized by colour depending on presence of cladding and the grey line is a straight y = x line. a) Tc release correlated to U, b) Mo release correlated to U, c) Rb release correlated to U, d) Cs release correlated to U.

4.2.4 Elements Showing Particular Behaviour: Group 4: Se and C

Elements of group 4 (Se, C) show particular behaviour and cannot be grouped with other elements. Both elements have been considered in one study each and hence do not have many datapoints available. Therefore, it is difficult to generalize their behaviours.

From Figure 4.16 it is evident that all considered isotopes of Se seem to follow 2 different trends, one of faster release and one of slower release. From the remaining plots of Se in appendix A.8 it can be seen that most parameters are the same for these two trends. The BU of the faster trend is slightly higher, by 2 GWd/t_{HM} according to the database, however, the most evident difference between the samples is the type of fuel. Further investigations would be needed to verify whether the sample size or type of fuel is the reason behind the difference in release of Se as well as to investigate the reproducibility of these trends.

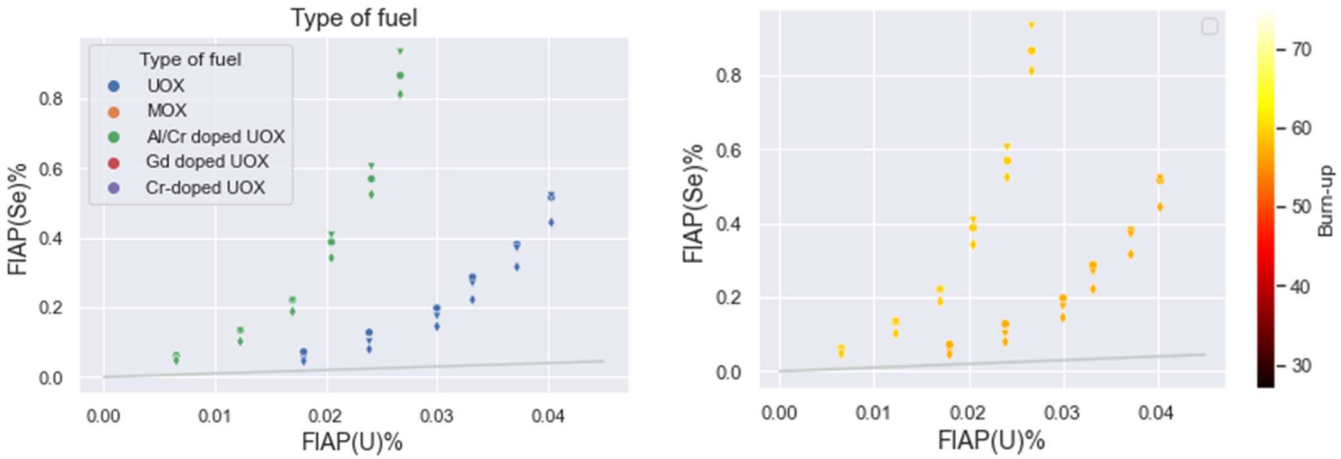

Figure 4.16 Scatterplot of Se release in relation to U release, where points have been categorized by colour depending on the type of fuel. Circles represent unspecified ^{79}Se, triangles represent ^{80}Se and diamonds represent ^{82}Se.

From Figure 4.17 and 4.18 it is evident that the release of C is both low and unpredictable as the point do not follow any apparent trend. What can be said is that C seems to be released independently of U.

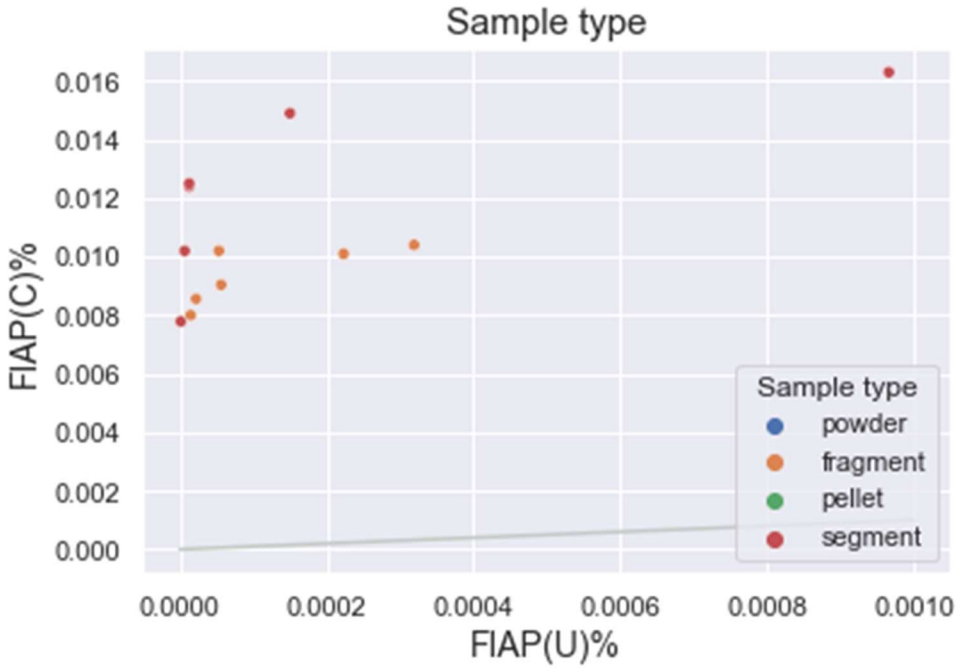

Figure 4.16 Scatterplot of C release in relation to U release, where points have been categorized by colour depending on the sample type.

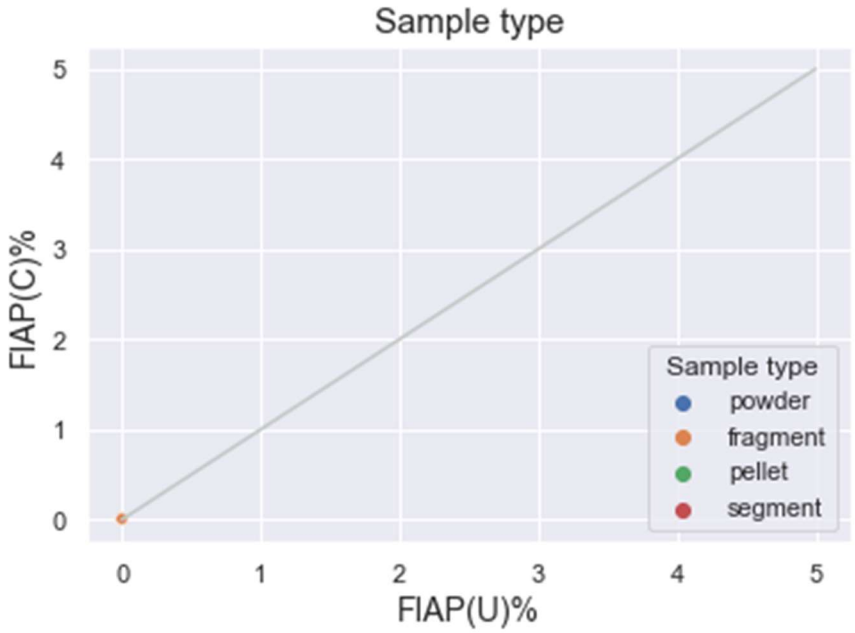

Figure 4.17 Scatterplot of C release in relation to U release, where points have been categorized by colour depending on the sample type.

4.2.5 Chemistry and Behaviour of Grouped Elements

Figure 4.18 shows a periodic table where the elements have been marked in colour based on the previously explained groups. As can be seen group 1a) – 1c) elements all show evidence of being embedded in the fuel matrix where the main differences are their chemical solid form within the fuel. Group 1a) elements exhibit release trends strongly correlated to the release of U, indicating that these fission products are dissolved similarly to U. Group 1b) elements show a similar behaviour, however, they also show a tendency to form secondary phases lowering their detectability. Group 1c) elements show a release similar to U at BU > 70 GWd/t_{HM}, but low releases at BU < 70 GWd/t_{HM}. Considering knowledge from previous studies, Kleykamp et al. [11], these low releases could be attributed to lower solubility of the elements due to the oxides they have formed within the fuel matrix.

Group 2 elements all show evidence of being present in the fuel as insoluble metal precipitates, having low solubility. The main difference between group 2a) and group 2b) elements is the type and amount of data available. Group 2a) elements have a limited amount of data as they are only measured by Clarens et al. [7], what can be seen is that these elements show evidence of being part of the IRF but present themselves as metallic precipitates. Group 2b) elements on the other hand show no evidence of where in the fuel rod they are present.

The elements of group 3 all show evidence of being part of the IRF. The main difference between group 3a) and 3b) is that group 3b) elements exhibit evidence of being embedded in the fuel matrix as well.

Group 4 contains the elements with peculiar behaviour. What both Se and C have in common is the low amount of available data, making it hard to draw certain conclusions on their

behaviour. From what can be seen Se tends to be released faster in Al/Cr doped fuel compared to regular fuel. For C the available data does not show any clear trends, but it seems that C release is independent of U release.

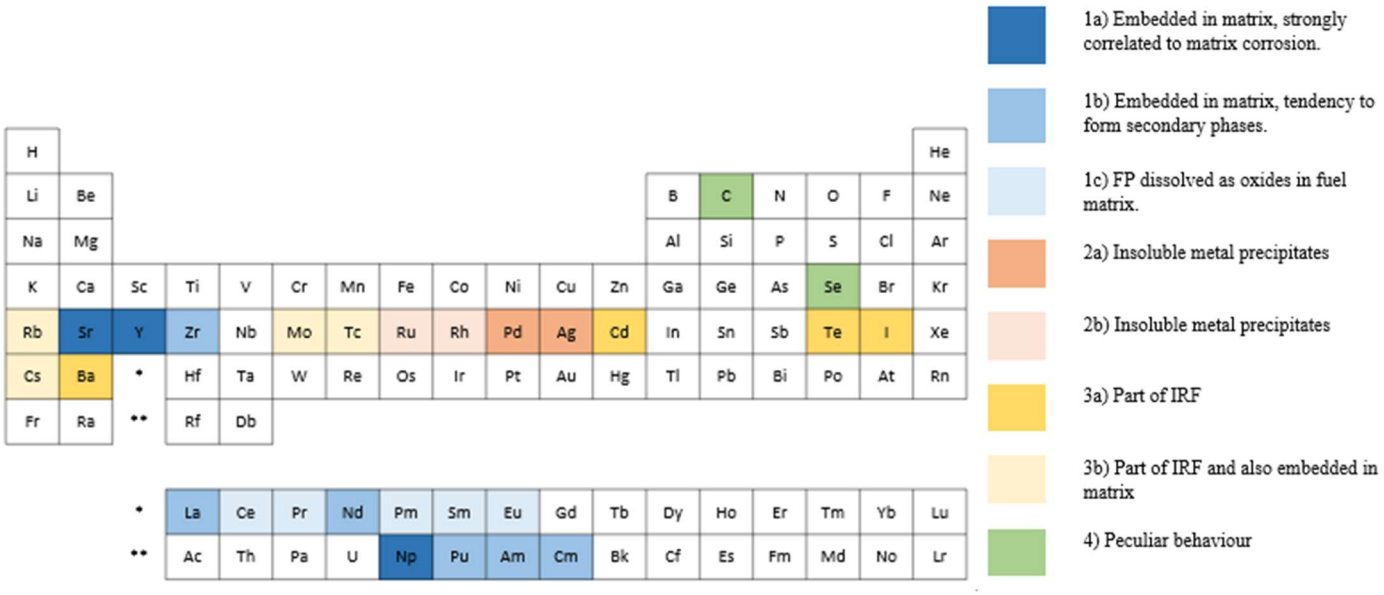

Figure 4.18 Periodic table illustrating the groupings and subgroupings concluded from evaluation.

4.3 Machine Learning for Predictions

As earlier explained, section 3.2, multiple Artificial Neural Network (ANN) and Random Forest (RF) models were built, trained, and evaluated. Since the purpose of this thesis is to investigate the potential of machine learning models for prediction of radionuclide release, only the models with best performance of each algorithm will be presented in this section.

Out of the ANN models, the one with highest performance consists of one hidden layer with 23 nodes and a dropout rate of 0.4. On the other hand, the best performing RF model is the XGBoost model. From the R^2 scores in table 4.3 it is clear XGBoost is outperforming ANN.

Table 4.3 Summary of global R^2 score for best performing models

	Global training R^2 Score	**Global test R^2 Score**
ANN	0.4205	0.314832
XGBoost	0.999836	0.738003

From table 4.3 can be seen that the XGBoost model yielded an R^2 score close to 1 which could indicate that the model is overfitting, meaning it is yielding a regression which fits the training data while failing to generalize. However, the R^2 score of the test data is still high, indicating that the generalization of the algorithm is acceptable, although a higher value is desired.

When considering the model performance per element it was found that some predictions were negative and some unrealistically low, e.g. 3 orders of magnitude lower than the lowest true value. Negative values were deemed as misleading, as the values being predicted (FIAP%) are

correlated to concentration, which cannot be negative. Low values were also deemed misleading due to the considerable difference between them, and the lowest true values found in the database. All misleading predictions were correlated to the true values which were imputed, meaning the true values of 0. Which is reasonable when considering the model's performance (both R^2 scores), and the complexity of the system it is trying to predict. The explanation for the low values, could be that the model is yielding predictions as close to 0 as possible. Which is why a postprocessing step was deemed necessary to clean the test and training data of this kind of misleading values. The postprocessing considers the lowest value of each element's training data as a threshold of lowest possible value for that element and removes each prediction/true value pair where the prediction is below this threshold. This way the negative and low predictions are discarded. Worth mentioning however, is that the threshold value for each element might not be the lowest value for that specific element in the database due to the randomized sampling of training data.

While investigating model performance per element it was discovered that R^2 values differed for each element, after applying postprocessing it was also evident that R^2 values increased. A summary of R^2 values obtained for each element after postprocessing can be seen in table 4.4. For a visual representation of model performance, prediction/true value graphs of the training and test data of the elements with highest (Pr) and lowest (La) test R^2 value, excluding elements only documented by one study, are shown in Figure 4.19 and 4.22. From Figure 4.19 and 4.21 it is evident that the training phase of the model is yielding predictions with a high accuracy as both the slopes of the regression lines and the R^2 values are close to 1. Indicating that the predictions have an almost linear correlation to the true values and that the scattering of the points from the line is very low. Further considering Figure 4.20 and 4.22 it is evident that even after postprocessing, the prediction accuracy differs between elements. Figure 4.20 shows that the Pr predictions of test data have a relatively high accuracy, slope and R^2 close to 1, as compared to La, Figure 4.22. A suspicion that the reason behind the vast difference in performance of Pr and La depends on amount of data available in the database was investigated. Reasonably, a larger number of non-imputed values available for the predictions, should yield a more accurate training for the element. However, from the database can be seen that Pr and La have a total of 153 and 209 non-missing datapoints respectively. The difference in accuracy of predictions could be attributed to the random sampling of training data. The number of datapoints used for training is the same for all elements, but the datasets randomly chosen as training data could contain more imputed values than true values for varying elements. However, when investigating the number of true values used as training data it was found that the number of true values used for Pr and La were 118 and 164 respectively. As La has the higher number of true values, meaning non-zero values, in its training dataset, the previous reasoning does not hold. On other hand, the fact that La uses more true values than Pr in its training yet still yields lower accuracy for predictions does strengthen the argument for imputing zeros as missing values. Replacing missing values with zeros does not seem to affect the model's ability to predict non-zero values. In addition, imputing zeros facilitates the postprocessing step which is necessary to be able to discard of the misleading predictions.

Table 4.4 Summary of training and testing R^2 yielded by the XGBoost model for each element after postprocessing.

Element	Training R^2	Test R^2
Praseodymium	0.9998	0.9844
Barium	0.9998	0.9827
Cerium	0.9998	0.9346
Americium	0.9998	0.9331
Technetium	0.9999	0.9092
Caesium	0.9998	0.8534
Curium	0.9997	0.8451
Zirconium	0.9998	0.8427
Plutonium	0.9996	0.831
Molybdenum	0.9998	0.7768
Neptunium	0.9998	0.7741
Yttrium	0.9999	0.7598
Neodymium	0.9999	0.7418
Rubidium	0.9998	0.6696
Ruthenium	0.9998	0.6488
Europium	0.9999	0.6298
Rhodium	0.9999	0.6028
Iodine-129	0.9997	0.5999
Strontium	0.9999	0.4893
Lanthanum	0.9998	0.0747
Silver*	1	0.9858
Tellurium*	1	0.9401
Promethium*	1	1
Samarium*	1	1
Cadmium*	1	1
Model Total	0.999836	0.738003

*Elements only documented by one study.

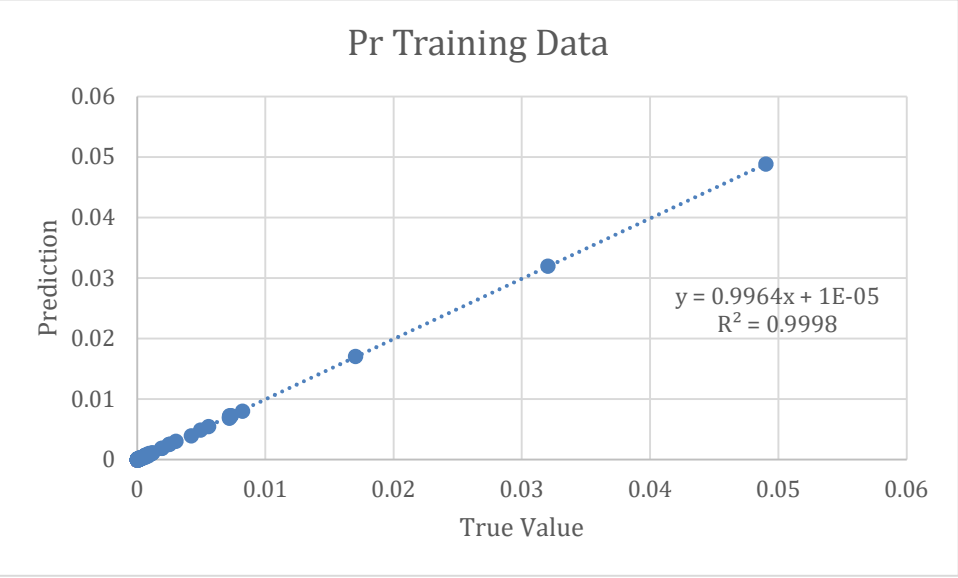

Figure 4.19 Predictions plotted against true values of Pr training data with regression line added.

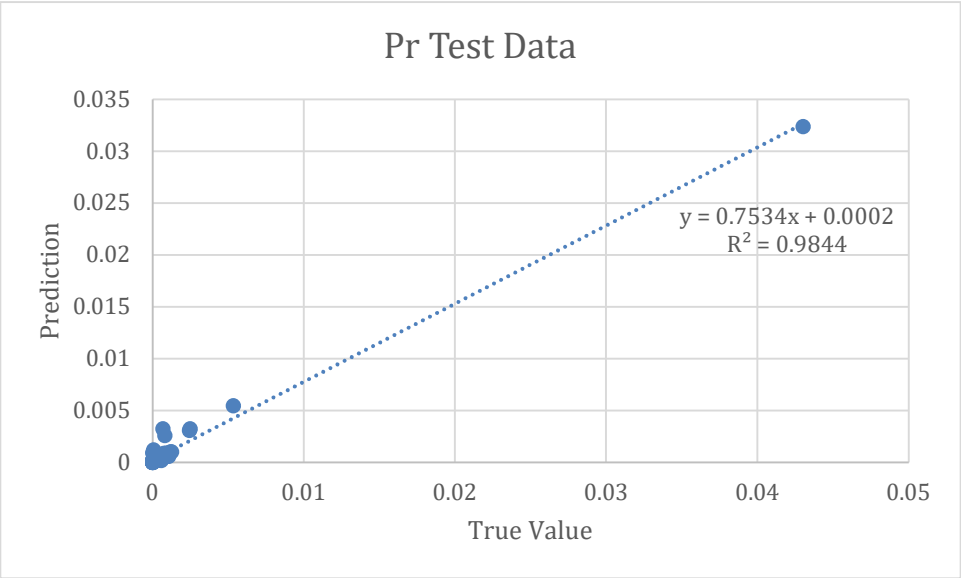

Figure 4.20 Predictions plotted against true values of Pr test data with regression line added.

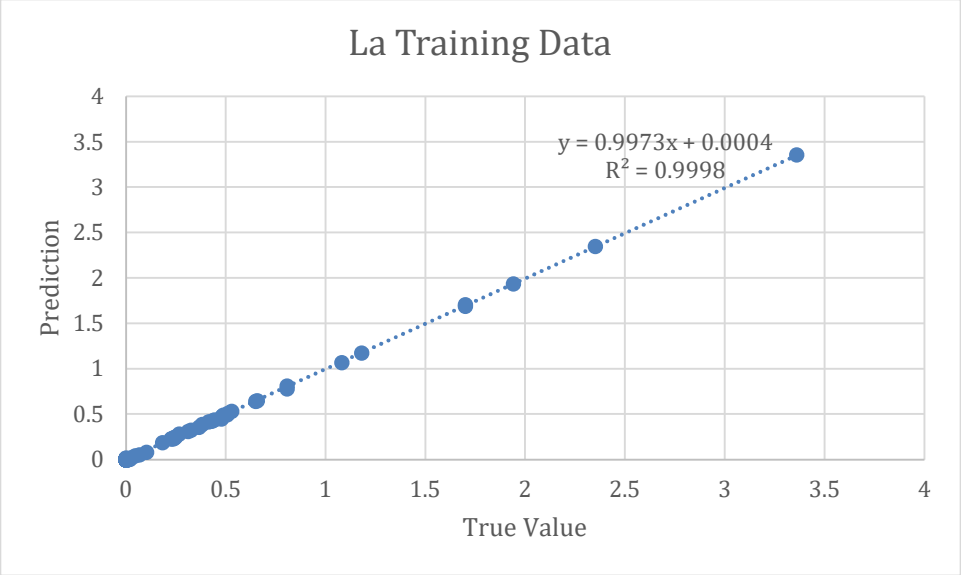

Figure 4.21 Predictions plotted against true values of La training data with regression line added.

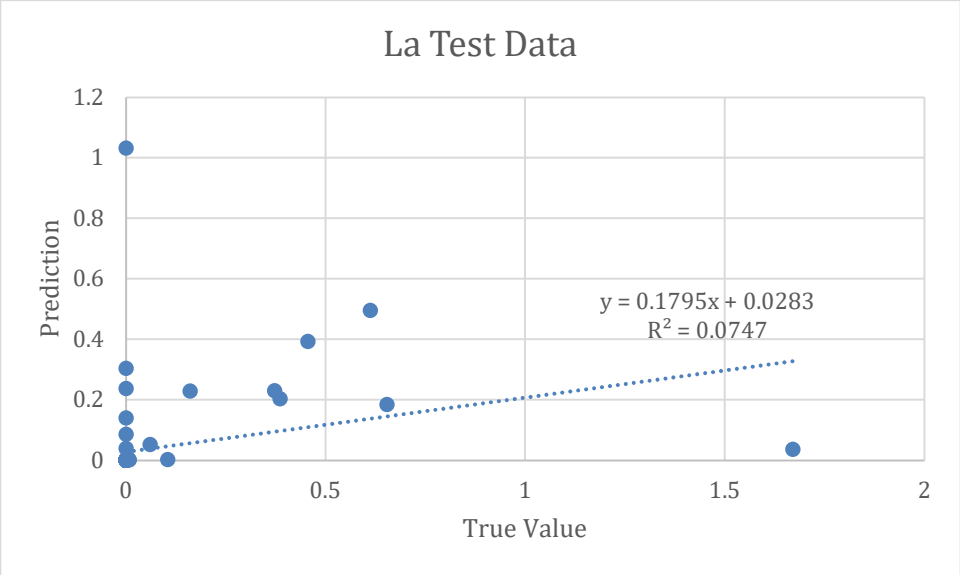

Figure 4.22 Predictions plotted against true values of La test data with regression line added.

As explained in section 3.2, all ANN models were run while imputing zeros and column mean values respectively. Imputing zeros however, yielded the weakest performance, mostly negative R^2 scores. Therefore, the model shown here uses column mean values instead of missing values. This made a postprocessing step difficult to obtain as the mean value of each element's release is in between the range of the highest and lowest release datapoints, hence no postprocessing was done for the ANN model.

The R^2 scores in table 4.3 indicate that the performance of the ANN model is inferior to that of the XGBoost model. Further investigating the R^2 values of training and test data per element of the ANN model, shown in table 4.5, it is evident that in some cases, e.g. Cs and Tc, the training R^2 is higher than the test R^2. This would suggest that the model is more capable of predicting data than learning which is a further indication that the ANN model is performing more poorly than the XGBoost model.

Figure 4.23-4.26 show the prediction/true value graphs of the elements with highest (Sr) and lowest (Eu) R^2. Comparing Figure 4.19 and 4.20 to Figure 4.23 and 4.24 it is evident that ANN yields less linearity between prediction and true value while also yielding a higher amount of scattering of the points. Further comparing Figure 4.21 and 4.22 to Figure 4.25 and 4.26, both slopes and R^2, it is evident that XGBoost's worst performance yields more true predictions that ANN's worst performance. Since the ANN models where zeros were imputed had weaker performance than the ANN models imputing column mean values, the difference in performance between XGBoost and ANN cannot be attributed to the missing value imputation. Further indicating that XGBoost is a better suited algorithm for this complex system.

Table 4.5 Summary of training and testing R^2 yielded by the ANN model for each element.

Element	Training R^2	Test R^2
Iodine-129	0.1575	0.0572
Rubidium	0.5829	0.4604
Caesium	0.6162	0.6488
Strontium	0.8106	0.7492
Barium	0.451	0.3665
Molybdenum	0.661	0.6847
Technetium	0.6196	0.6735
Neptunium	0.6399	0.6045
Plutonium	0.7559	0.5482
Curium	0.6756	0.2587
Lanthanum	0.6482	0.3964
Cerium	0.1603	0.2776
Praseodymium	0.1834	0.2809
Neodymium	0.5511	0.5712
Europium	0.0063	0.0365
Ruthenium	0.3964	0.3368
Yttrium	0.5972	0.5002
Zirconium	0.6223	0.2151
Rhodium	0.3295	0.3258
Americium	0.6174	0.4409
Silver*	0.1301	0.412
Cadmium*	0.2474	0.2637
Tellurium*	0.6789	0.4991
Promethium*	0.1795	0.1123
Samarium*	0.1989	0.1531
Model Total	0.4205	0.314832

*Elements only documented by one study.

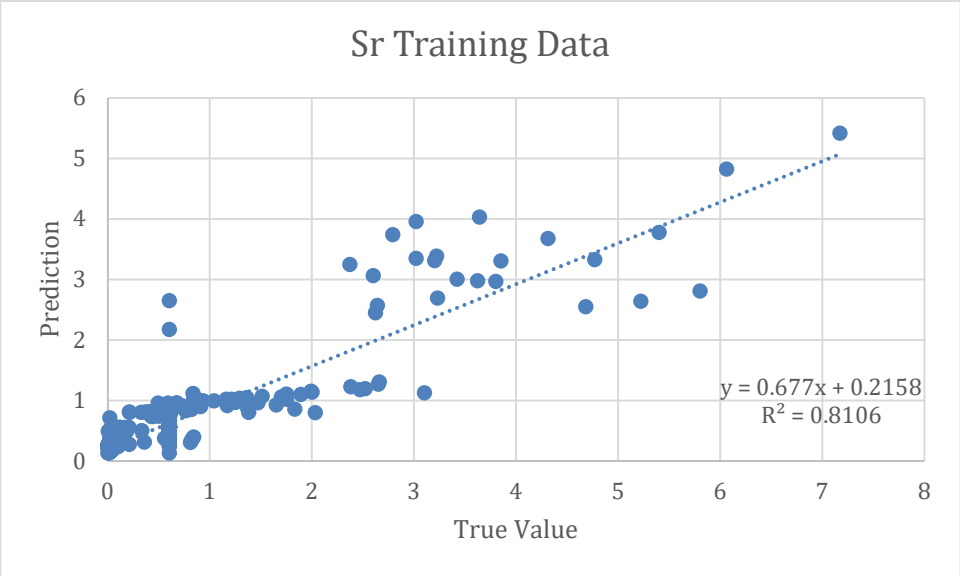

Figure 4.23 Prediction/ground truth relationship of Sr training data from best performing ANN model.

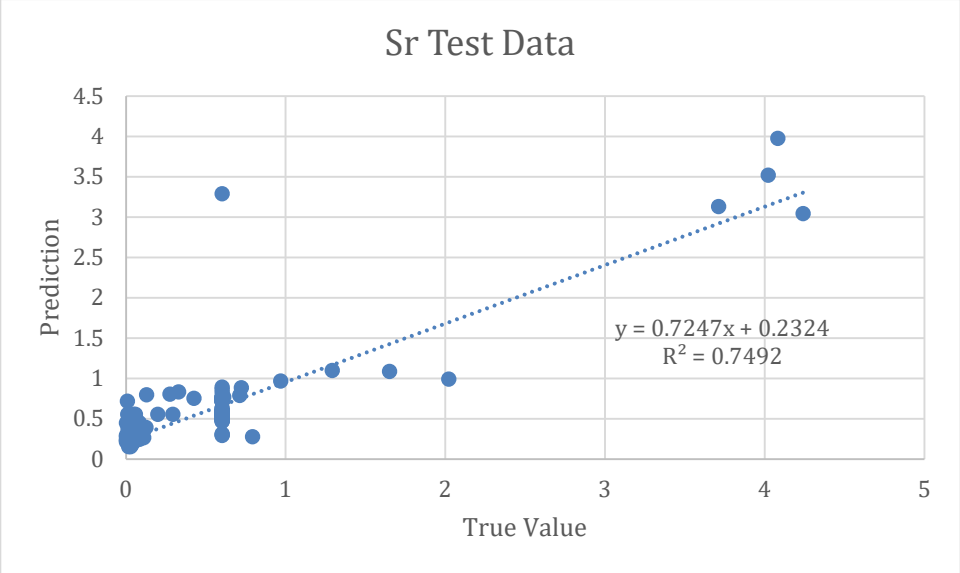

Figure 4.24 Prediction/ground truth relationship of Sr test data from best performing ANN model.

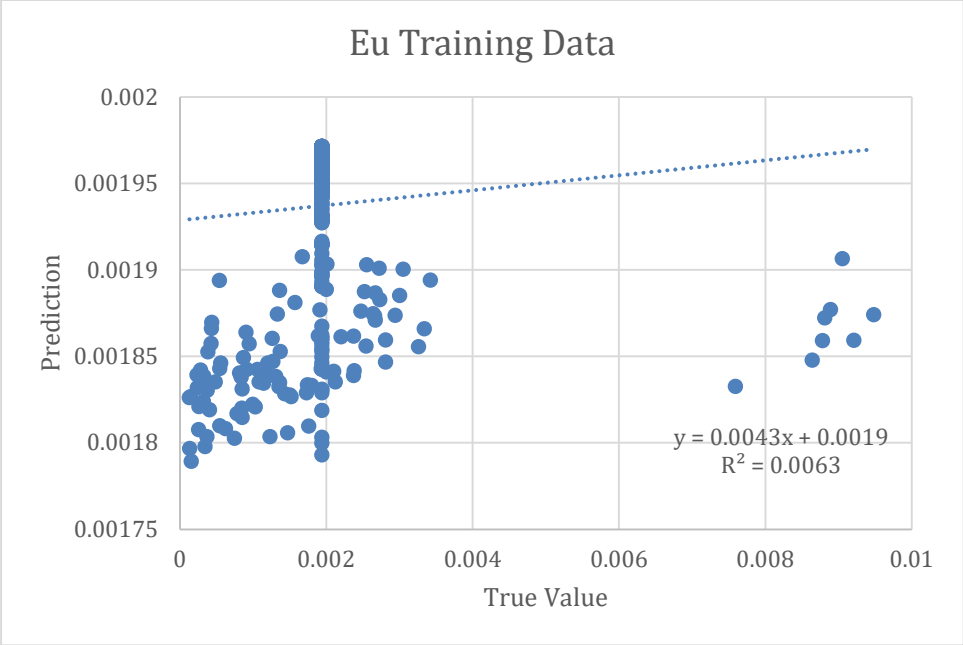

Figure 4.25 Prediction/ground truth relationship of Eu training data from best performing ANN model.

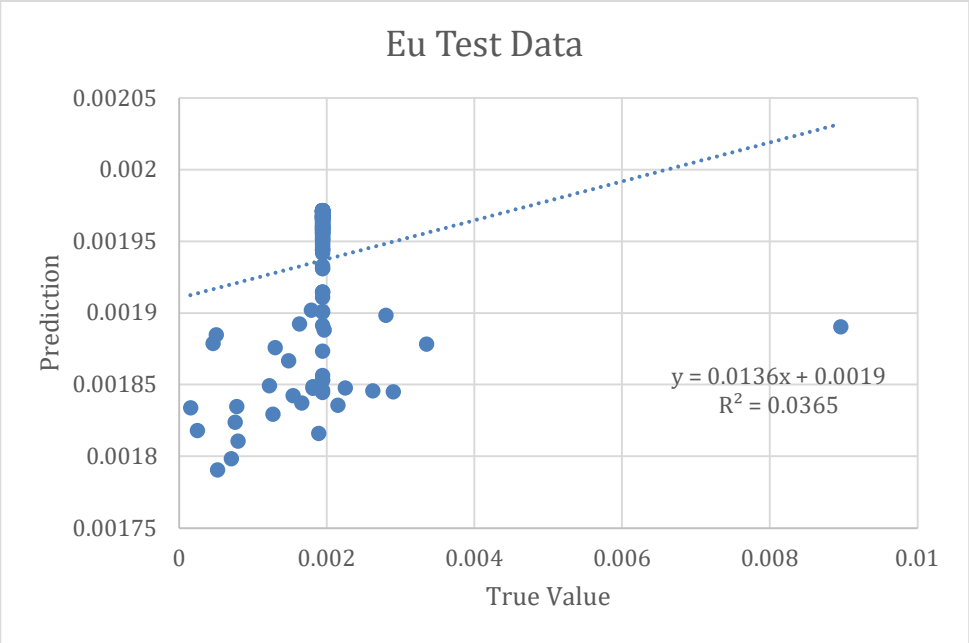

Figure 4.26 Prediction/ground truth relationship of Eu test data from best performing ANN model.

6 Conclusions and future work

In summary a database of radionuclide release during spent nuclear fuel dissolution has been expanded and further developed. The database was used to 1. Map out radionuclide release trends during spent fuel dissolution and group elements based on these trends and 2. Train and evaluate machine learning models as tools to be used to predict radionuclide release trends. The conclusions found from this work are summarised below.

Behavioural trends

- Overall, the groups of radionuclides showing similar behaviour during spent nuclear fuel dissolution found in this thesis coincide with existing literature. However, the releases of Se, C, Ag, Pd, Cd, Te, Pm and Sm have been measured in one study each. This entails less certainty on the behaviour of these elements and more data is desired in order to draw more certain conclusions.
- Due to the number of parameters considered and their varying effects on the release of radionuclides, as explained in section 4.1, it would be preferred that further experiments follow a template. In this template sample characteristics like sample size for each type of sample and solution type to be used as well as their composition are specified.
- Due to the large amount of missing values in the database, the template should also contain elements and isotopes to be measured at each experiment.

Machine learning for predictions

The machine learning model has been used in this study to get an understanding of the capacity of this approach to train a machine with experimental data to be able, in a second step, to predict independent experimental data which have not been used in the previous training process. Therefore, the machine learning model is not related to models based on physical-chemical processes which are designed to give an understanding on the behaviour of a system from a set of parameters and experimental data. However, what has been seen through this thesis work is that:

- Using machine learning models to predict radionuclide release is still a young concept, however this thesis has shown that the XGBoost algorithm in combination with the Optuna optimizer is performing better than Artificial Neural Network models.
- More data is required to gain models with more accurate predictions and reduce risk of overfitting.
- Since FIAP(U)% has been used as an input feature for models in this work it would be interesting during the continuation of this work to only use the radionuclides that show U dependent release (group 1a) and 1b)) as output features. This is because the other groups have not shown to be as dependent on the U release, yet it is used as one of the conditions that the algorithm determines predictions on.

References

[1] Office of Nuclear Energy. 2021. *3 Reasons Why Nuclear is Clean and Sustainable*. [online] Available at: https://www.energy.gov/ne/articles/3-reasons-why-nuclear-clean-and-sustainable [Accessed 8 April 2022].

[2] Miller, W., 2000. *Geological disposal of radioactive wastes and natural analogues*. Amsterdam: Pergamon.

[3] Liu, Y. Y. (2015). Wet storage of spent nuclear fuel. In *Safe and Secure Transport and Storage of Radioactive Materials* (pp. 299-310). Woodhead Publishing.

[4] European Commission, 2014. DELIVERABLE (D-N°:5.4) Final (3rd) Annual Workshop Proceedings. FIRST-Nuclides.

[5] Riba, O., Duro, L., & Bruno, J., 2011. *Evolución físico-química del combustible nuclear gastado durante la etapa de almacenamiento en seco,* Proyecto de combustible ENRESA-CG3. Grupo de Modelización. Parte II.

[6] Chandramouli, S., Dutt, S., & Das, A. (2018). *Machine Learning* (1st ed.).

[7] European Commission, 2021. DELIVERABLE D1.25 Final Conference Proceedings. DisCo.

[8] Liljenzin, J., Rydberg, J., & Choppin, G. (2016). *Radiochemistry and Nuclear Chemistry*: 2nd Edition of Nuclear Chemistry, Theory and Applications. Butterworth-Heinemann.

[9] Rondinella, V. and Wiss, T., 2010. *The high burn-up structure in nuclear fuel. Materials Today*, 13(12), pp.24-32.

[10] Martínez-Torrents, A., Serrano-Purroy, D., Sureda, R., Casas, I. and de Pablo, J., 2017. *Instant release fraction corrosion studies of commercial UO 2 BWR spent nuclear fuel*. Journal of Nuclear Materials, 488, pp.302-313.

[11] Kleykamp, H. (1988) *The chemical state of fission products in oxide fuels at different stages of the nuclear fuel cycle*. Nuclear Technology, 80, 412.

[12] Johnson, L.H. y McGinnes D.F, (2002) *Partitioning of radionuclides in Swiss power reactor fuels*, Nagra Technical Report NTB 02-07.

[13] Srivastava, N., Hinton, G., Krizhevsky, A., Sutskever, I., & Salakhutdinov, R., 2014. *Dropout: a simple way to prevent neural networks from overfitting.* The journal of machine learning research, 15(1), pp. 1929-1958.

[14] Biau, G. and Scornet, E., 2016. *A random forest guided tour*. TEST, 25(2), pp.197-227.

[15] Breiman, L., 2001. *Machine Learning*, 45(1), pp.5-32.

[16] Limited, Q., 2022. *Graph Grabber 2.0.2 | Downloads And Demos | Software | Quintessa Limited | Scientific and Mathematical Consultancy*. [online] Quintessa.org. Available at: https://www.quintessa.org/software/downloads-and-demos/graph-grabber-2.0.2 [Accessed 22 July 2022].

[17] TensorFlow. 2022. *Why TensorFlow*. [online] Available at: https://www.tensorflow.org/about [Accessed 29 May 2022].

[18] Chen, T. and Guestrin, C., 2016. *XGBoost: A Scalable Tree Boosting System*. Proceedings of the 22nd ACM SIGKDD International Conference on Knowledge Discovery and Data Mining,.

[19] Optuna. 2022. Optuna - A hyperparameter optimization framework. [online] Available at: https://optuna.org/ [Accessed 10 June 2022].

[20] Chicco, D., Warrens, M. and Jurman, G., 2021. *The coefficient of determination R-squared is more informative than SMAPE, MAE, MAPE, MSE and RMSE in regression analysis evaluation*. PeerJ Computer Science, 7, p.e623.

[21] Roth, O., Cui, D., Askeljung, C., Puranen, A., Evins, L., & Spahiu, K. (2019*). Leaching of spent nuclear fuels in aerated conditions: Influences of sample preparation on radionuclide release patterns*. Journal Of Nuclear Materials, 527, 151789.

[22] Gonzalez-Robles, E. (2011). *Study of Radionuclide Release in commercials UO2 Spent Nuclear Fuels Effect of Burn-up and High Burn-up Structure* (Ph.D). UNIVERSITAT POLITÈCNICA DE CATALUNYA.

Appendix

A.1 Scatterplots Group 1a

Appendix A.1 shows all the plots of the elements in group 1a (Y, Np and Sr), both plots used and not used in section 4. The plots are shown by element.

Yttrium

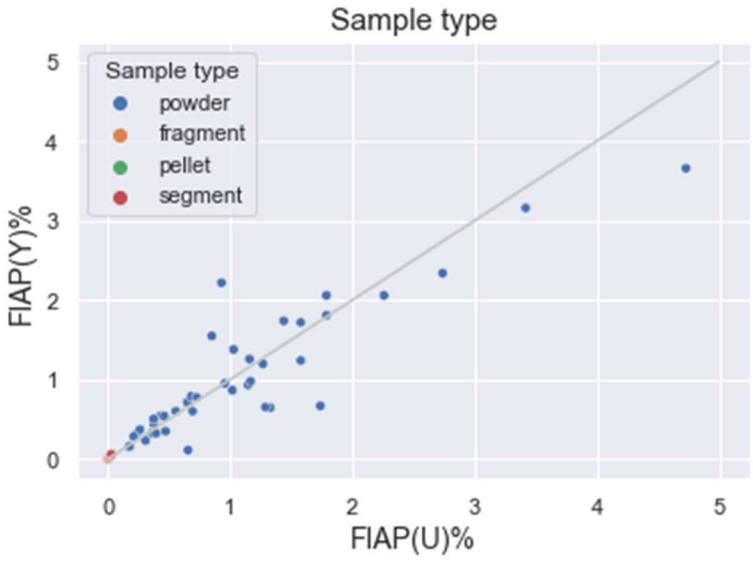

Fig A1.1 Scatterplot of Y release in relation to U release, where points have been categorized by colour depending on sample type and the grey line is a straight y = x line.

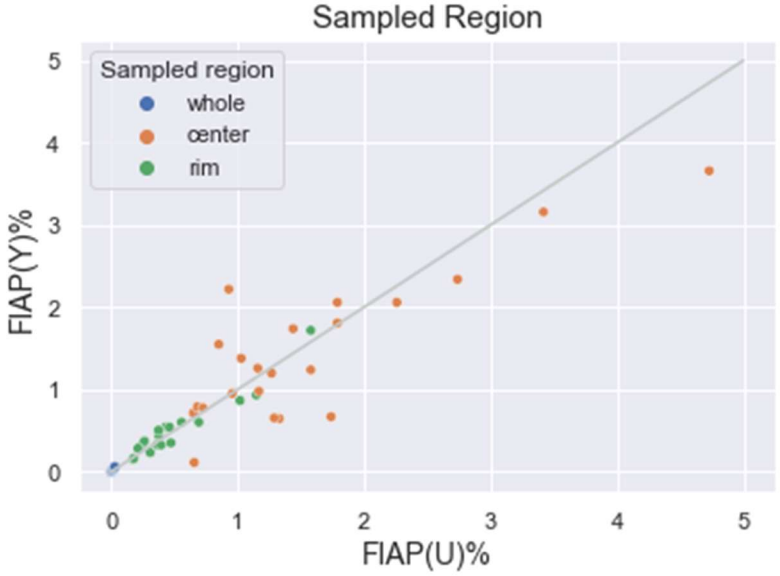

Fig A1.2 Scatterplot of Y release in relation to U release, where points have been categorized by colour depending on sampled region and the grey line is a straight y = x line.

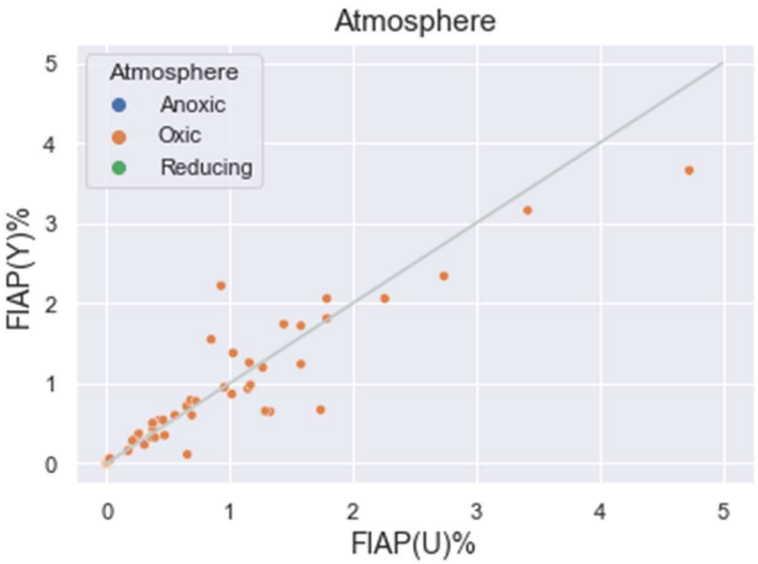

Fig A1.3 Scatterplot of Y release in relation to U release, where points have been categorized by colour depending on atmosphere and the grey line is a straight y = x line.

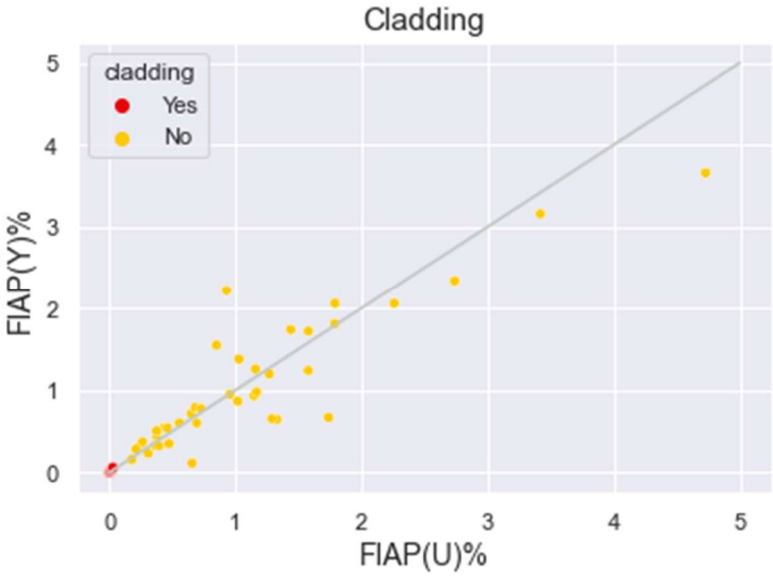

Fig A1.4 Scatterplot of Y release in relation to U release, where points have been categorized by colour depending on presence of cladding and the grey line is a straight y = x line.

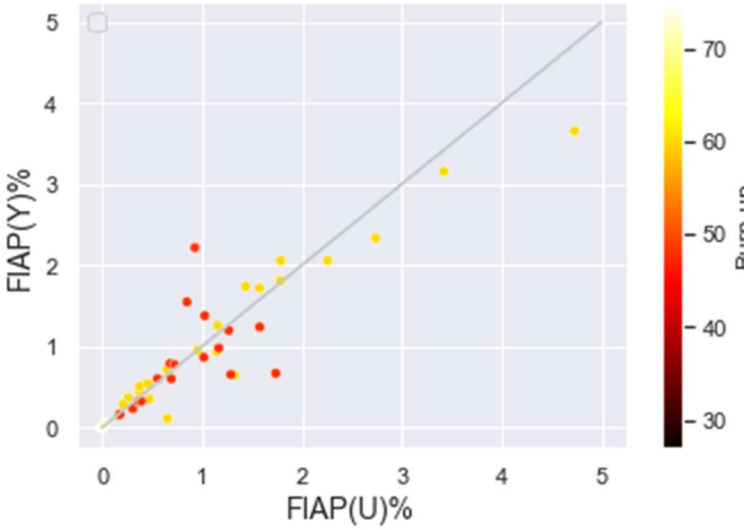

Fig A1.5 Scatterplot of Y release in relation to U release, where points have been categorized by colour depending on BU and the grey line is a straight y = x line.

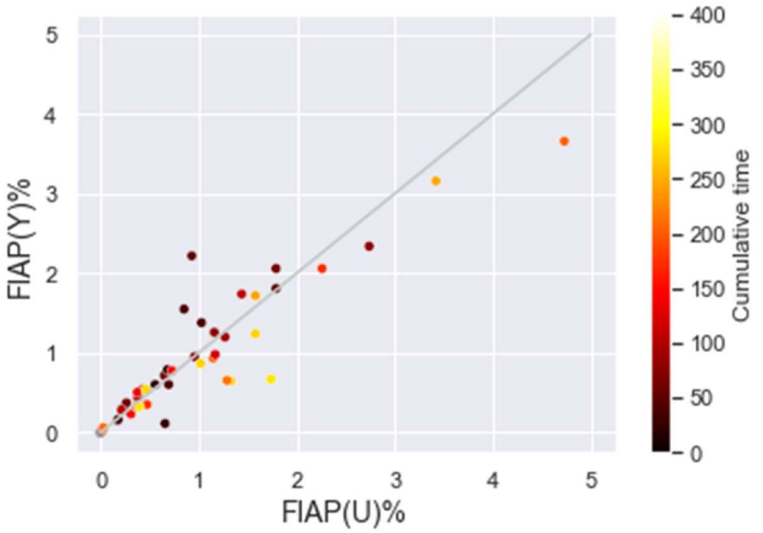

Fig A1.6 Scatterplot of Y release in relation to U release, where points have been categorized by colour depending on cumulative time and the grey line is a straight y = x line.

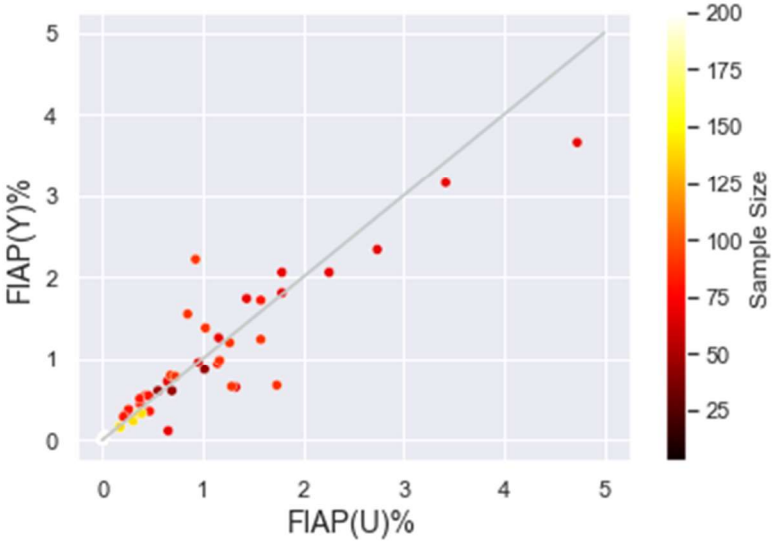

Fig A1.7 Scatterplot of Y release in relation to U release, where points have been categorized by colour depending on sample size and the grey line is a straight y = x line.

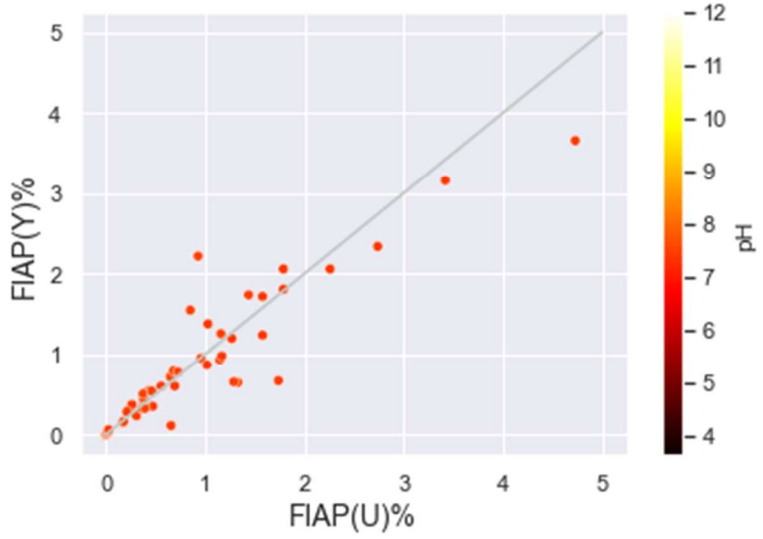

Fig A1.8 Scatterplot of Y release in relation to U release, where points have been categorized by colour depending on pH and the grey line is a straight y = x line.

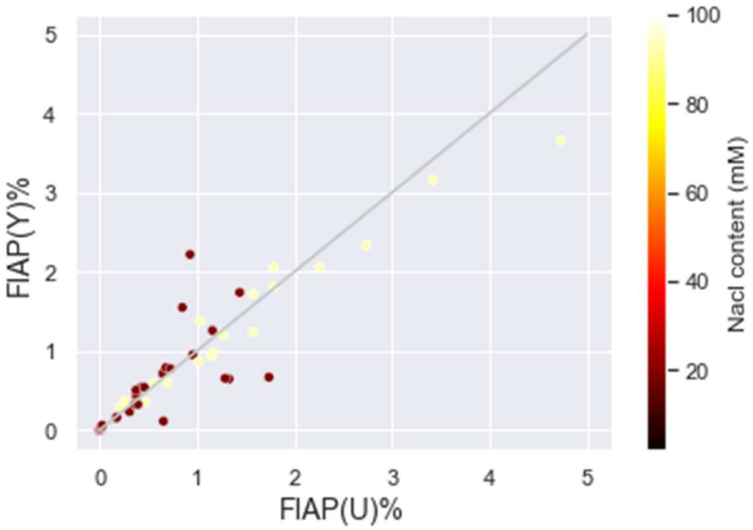

Fig A1.9 Scatterplot of Y release in relation to U release, where points have been categorized by colour depending on NaCl content and the grey line is a straight y = x line.

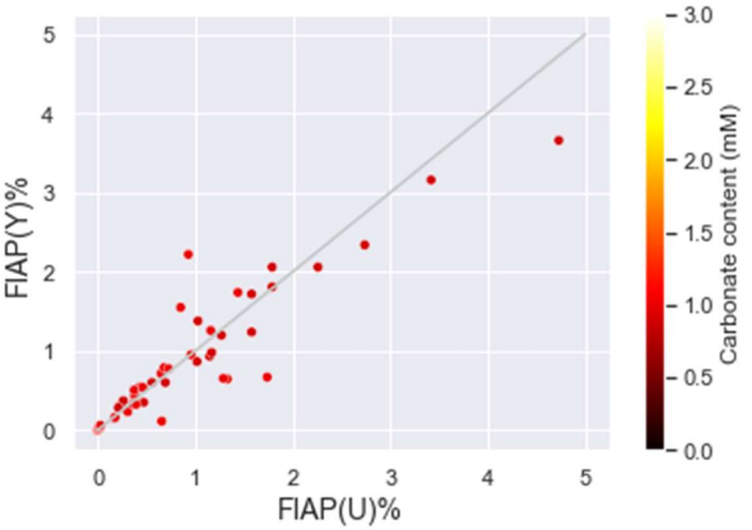

Fig A1.10 Scatterplot of Y release in relation to U release, where points have been categorized by colour depending on carbonate content and the grey line is a straight y = x line.

Neptunium

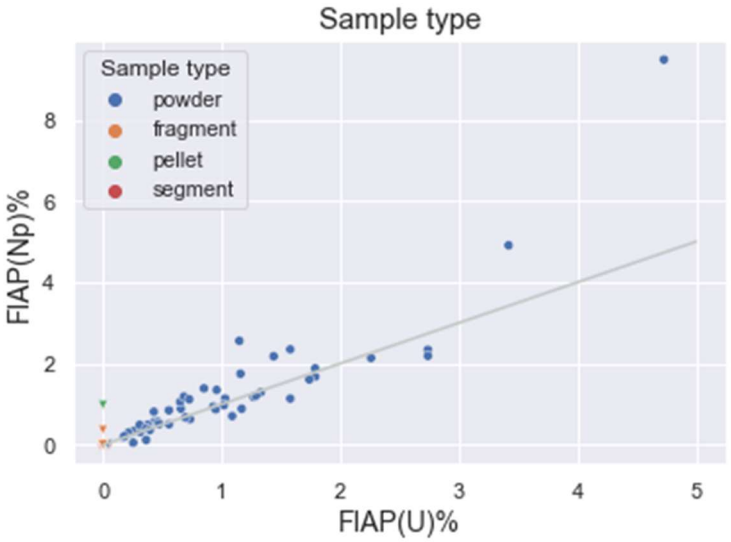

Fig A1.11 Scatterplot of Np release in relation to U release, where points have been categorized by colour depending on sample type and the grey line is a straight y = x line. Circles represent unspecified Np and triangles Np-237.

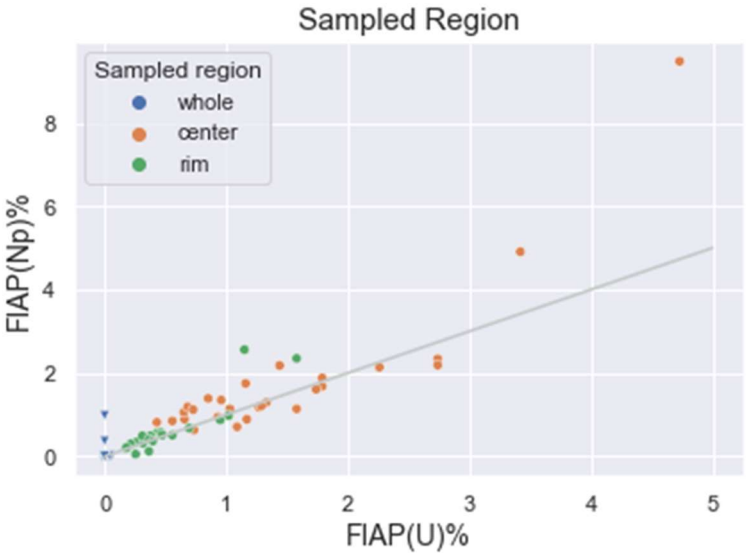

Fig A1.12 Scatterplot of Np release in relation to U release, where points have been categorized by colour depending on sampled region and the grey line is a straight y = x line. Circles represent unspecified Np and triangles Np-237.

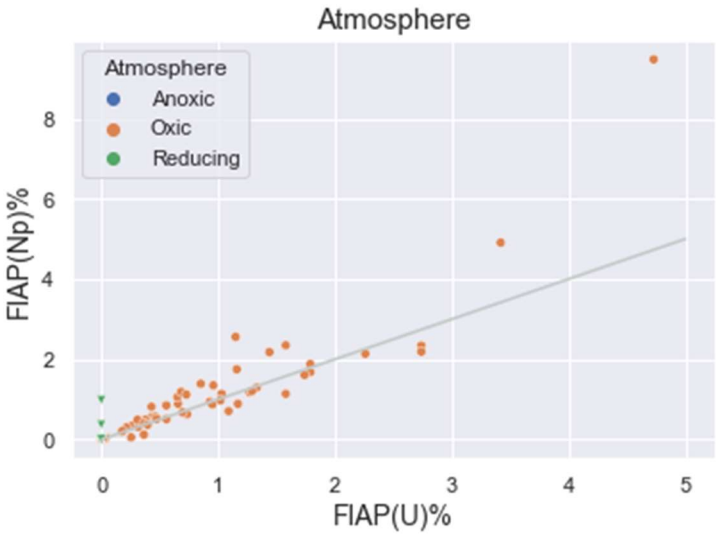

Fig A1.13 Scatterplot of Np release in relation to U release, where points have been categorized by colour depending on atmosphere and the grey line is a straight y = x line. Circles represent unspecified Np and triangles Np-237.

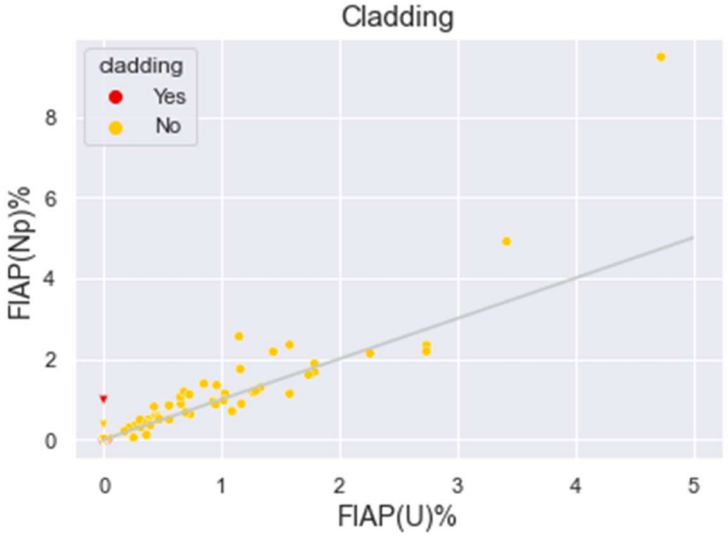

Fig A1.14 Scatterplot of Np release in relation to U release, where points have been categorized by colour depending on presence of cladding and the grey line is a straight y = x line. Circles represent unspecified Np and triangles Np-237.

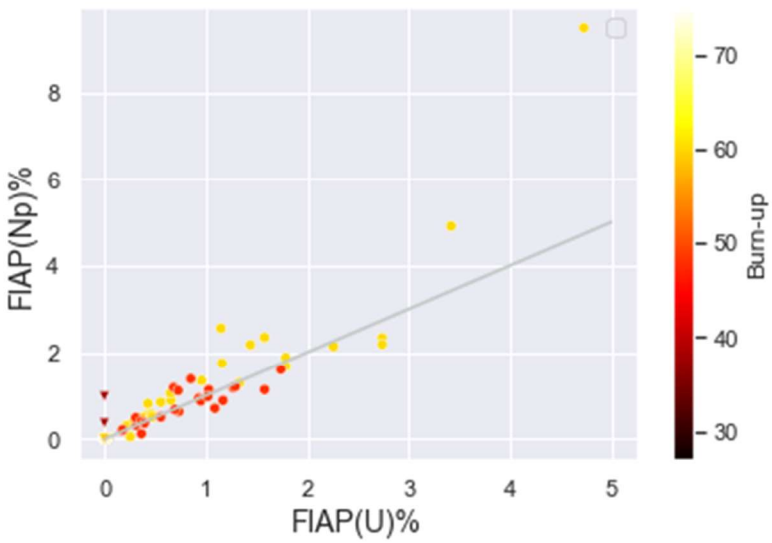

Fig A1.15 Scatterplot of Np release in relation to U release, where points have been categorized by colour depending on BU and the grey line is a straight y = x line. Circles represent unspecified Np and triangles Np-237.

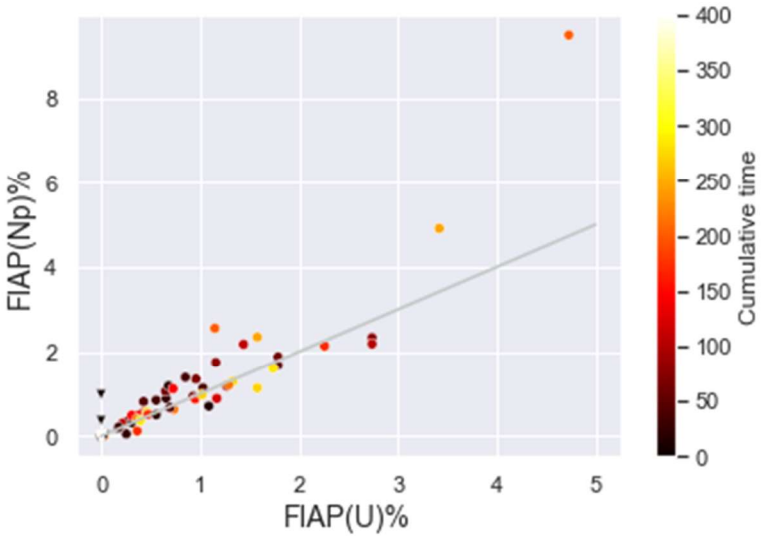

Fig A1.16 Scatterplot of Np release in relation to U release, where points have been categorized by colour depending on cumulative time and the grey line is a straight y = x line. Circles represent unspecified Np and triangles Np-237.

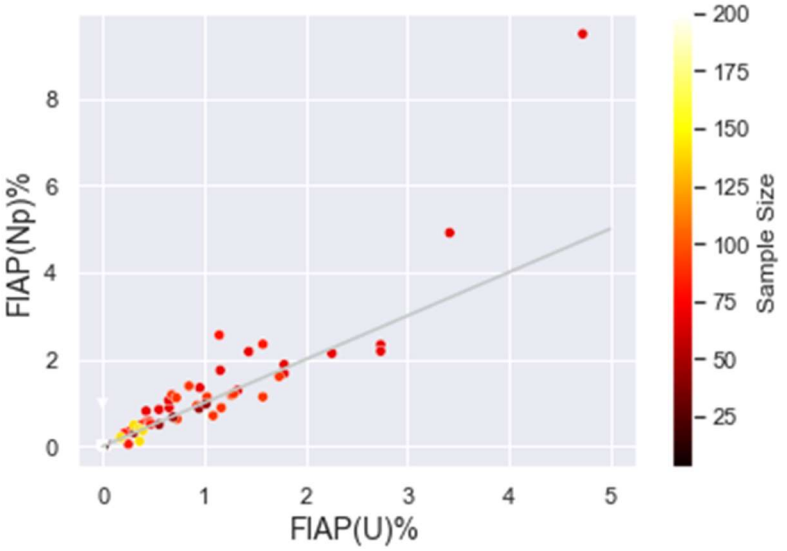

Fig A1.17 Scatterplot of Np release in relation to U release, where points have been categorized by colour depending on sample size and the grey line is a straight y = x line. Circles represent unspecified Np and triangles Np-237.

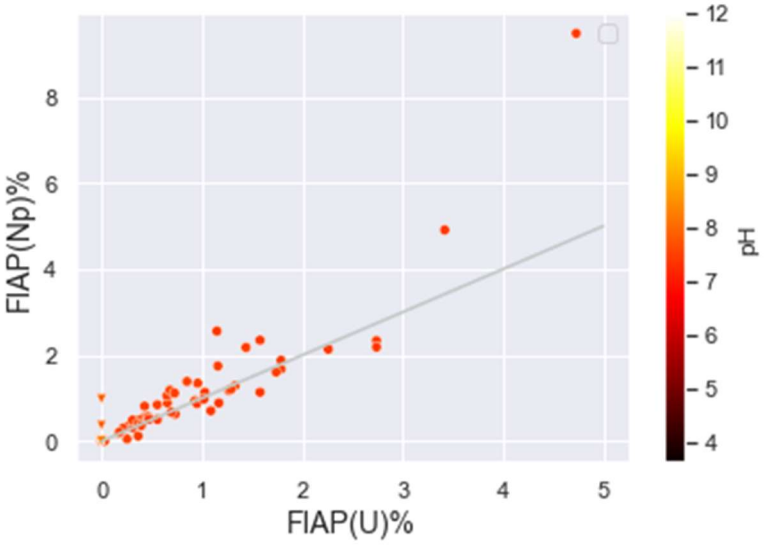

Fig A1.18 Scatterplot of Np release in relation to U release, where points have been categorized by colour depending on pH and the grey line is a straight y = x line. Circles represent unspecified Np and triangles Np-237.

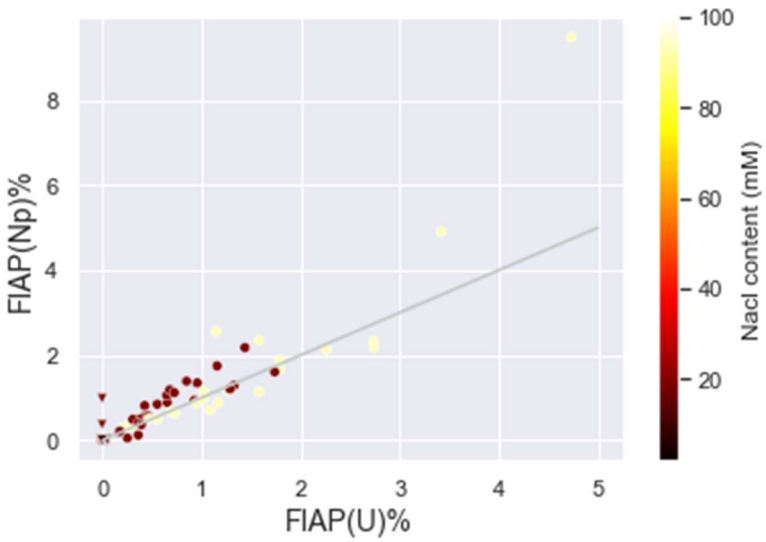

Fig A1.19 Scatterplot of Np release in relation to U release, where points have been categorized by colour depending on NaCl content and the grey line is a straight y = x line. Circles represent unspecified Np and triangles Np-237.

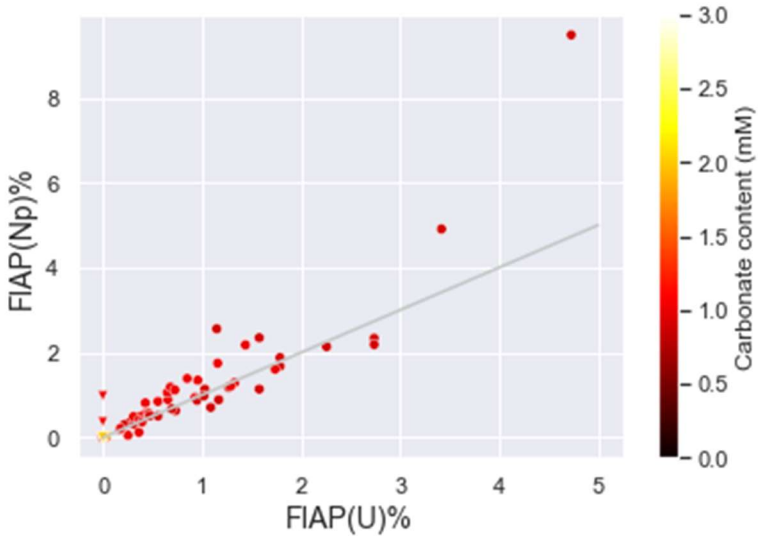

Fig A1.20 Scatterplot of Np release in relation to U release, where points have been categorized by colour depending on carbonate content and the grey line is a straight y = x line. Circles represent unspecified Np and triangles Np-237.

Strontium

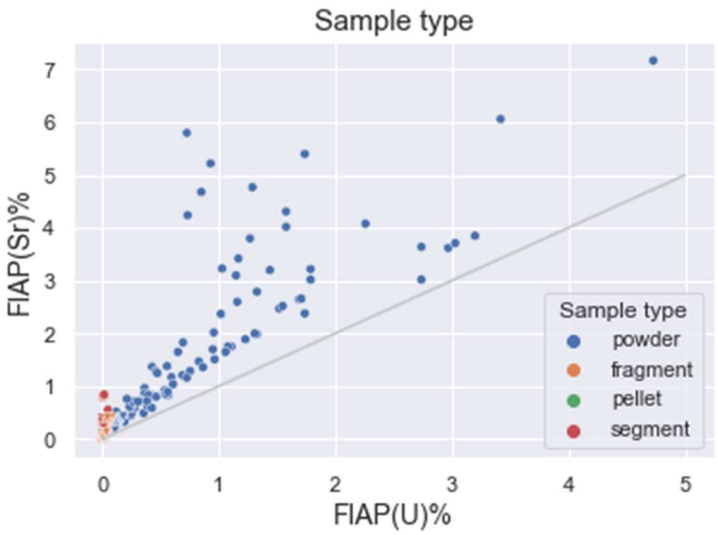

Fig A1.21 Scatterplot of Sr release in relation to U release, where points have been categorized by colour depending on sample type and the grey line is a straight y = x line. Circles represent unspecified Sr and triangles Sr-90.

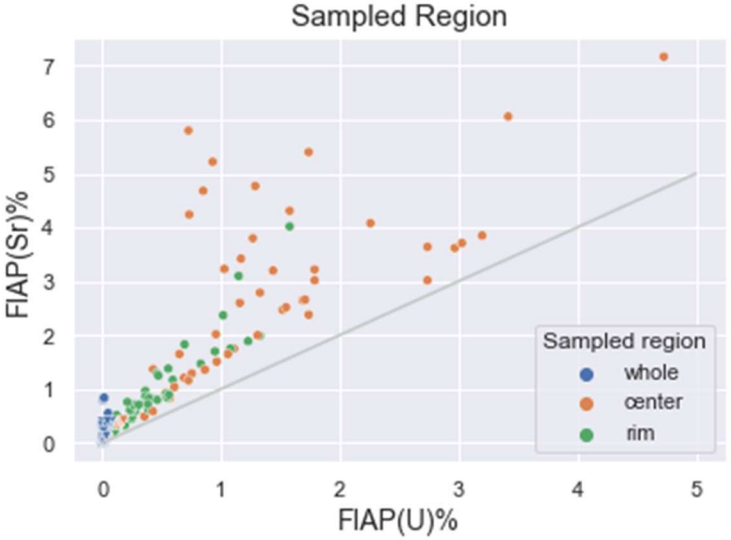

Fig A1.22 Scatterplot of Sr release in relation to U release, where points have been categorized by colour depending on sampled region and the grey line is a straight y = x line. Circles represent unspecified Sr and triangles Sr-90.

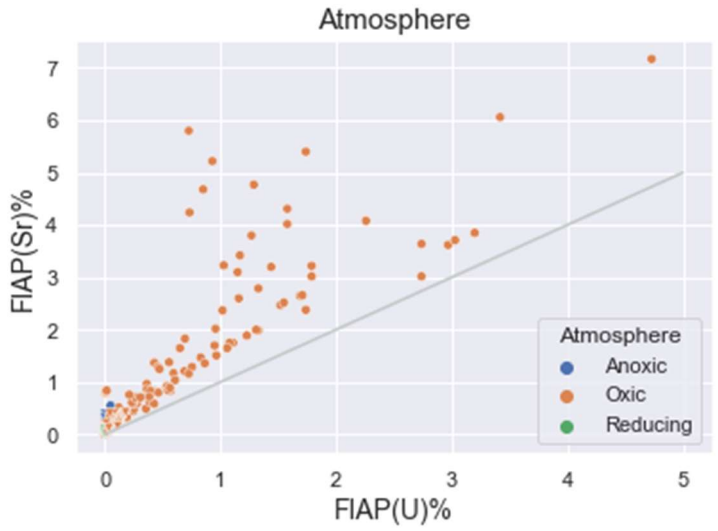

Fig A1.23 Scatterplot of Sr release in relation to U release, where points have been categorized by colour depending on atmosphere and the grey line is a straight y = x line. Circles represent unspecified Sr and triangles Sr-90.

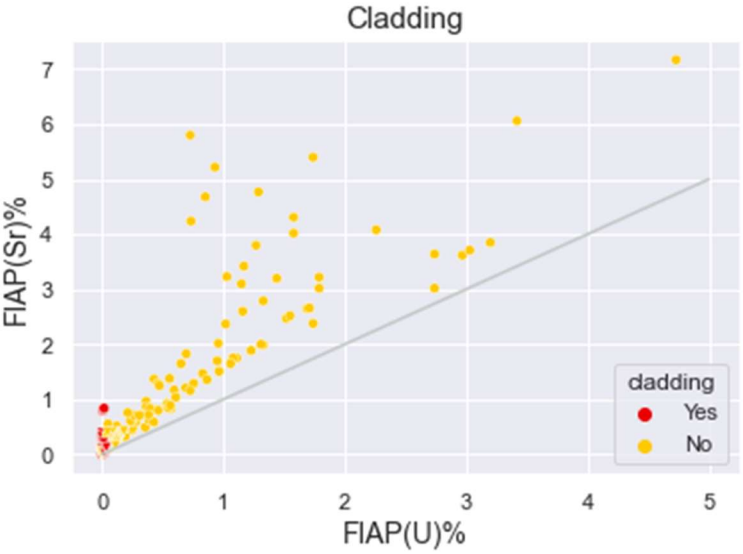

Fig A1.24 Scatterplot of Sr release in relation to U release, where points have been categorized by colour depending on presence of cladding and the grey line is a straight y = x line. Circles represent unspecified Sr and triangles Sr-90.

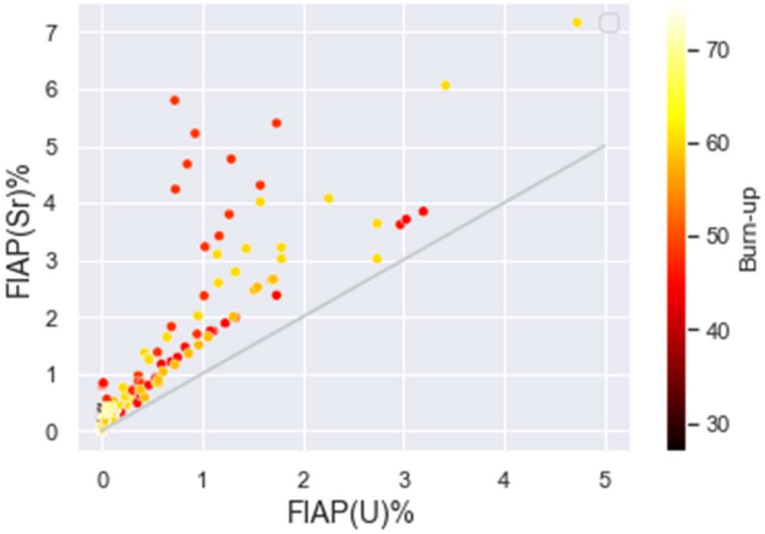

Fig A1.25 Scatterplot of Sr release in relation to U release, where points have been categorized by colour depending on BU and the grey line is a straight y = x line. Circles represent unspecified Sr and triangles Sr-90.

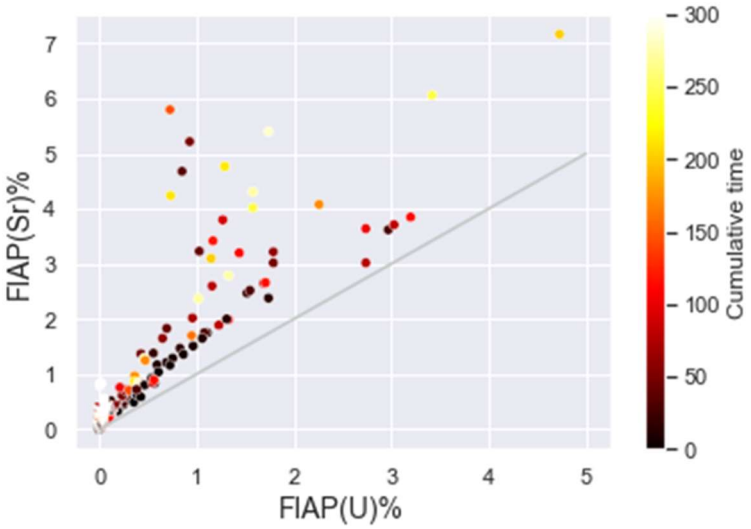

Fig A1.26 Scatterplot of Sr release in relation to U release, where points have been categorized by colour depending on cumulative time and the grey line is a straight y = x line. Circles represent unspecified Sr and triangles Sr-90.

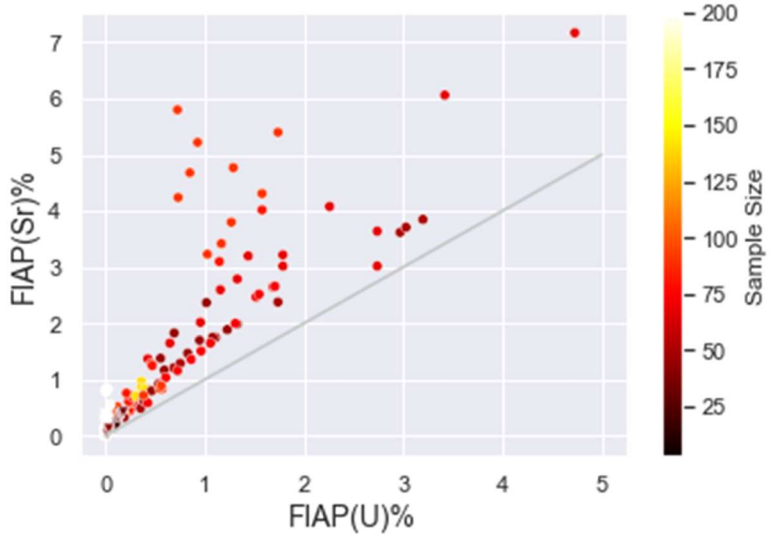

Fig A1.27 Scatterplot of Sr release in relation to U release, where points have been categorized by colour depending on sample size and the grey line is a straight y = x line. Circles represent unspecified Sr and triangles Sr-90.

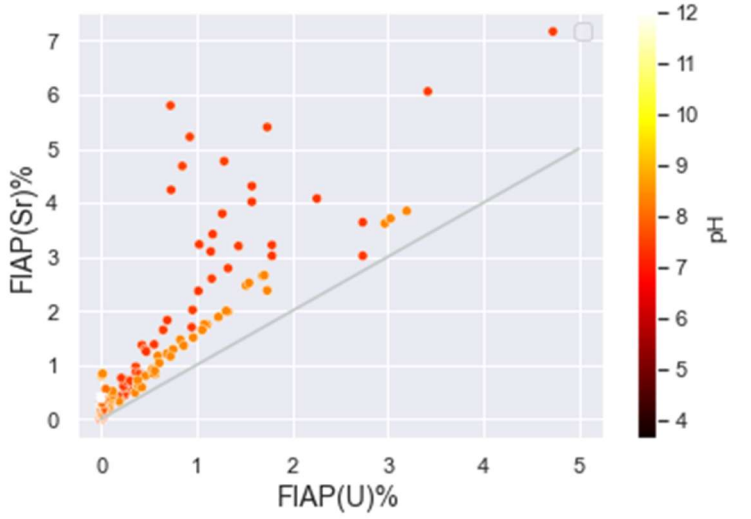

Fig A1.28 Scatterplot of Sr release in relation to U release, where points have been categorized by colour depending on pH and the grey line is a straight y = x line. Circles represent unspecified Sr and triangles Sr-90.

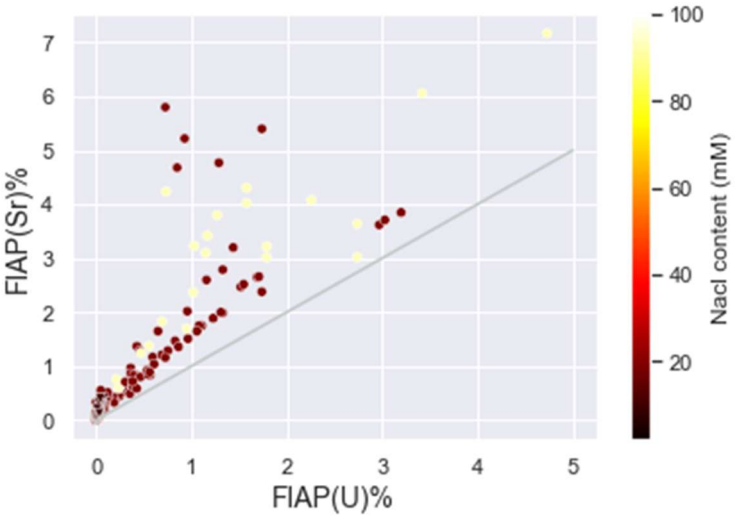

Fig A1.29 Scatterplot of Sr release in relation to U release, where points have been categorized by colour depending on NaCl content and the grey line is a straight y = x line. Circles represent unspecified Sr and triangles Sr-90.

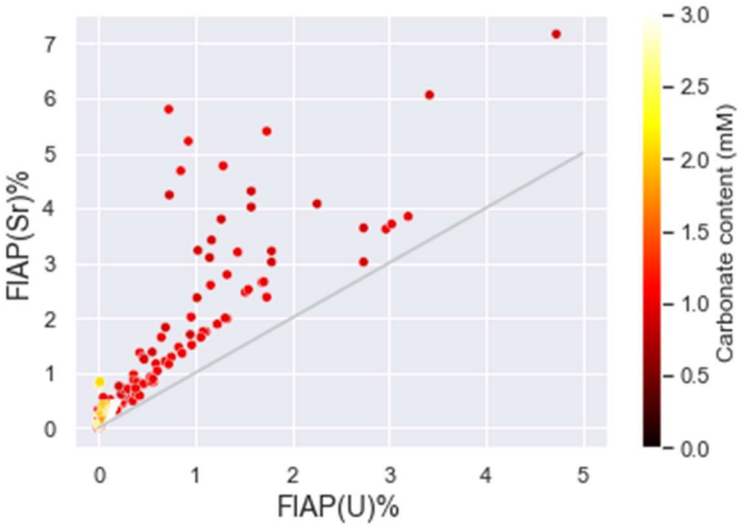

Fig A1.30 Scatterplot of Sr release in relation to U release, where points have been categorized by colour depending on carbonate content and the grey line is a straight y = x line. Circles represent unspecified Sr and triangles Sr-90.

A.2 Scatterplots Group 1b

Appendix A.2 shows all the plots of the elements in group 1b (Pu, Am, Cm, Nd, La, Zr), both plots used and not used in section 4. The plots are shown by element.

Plutonium

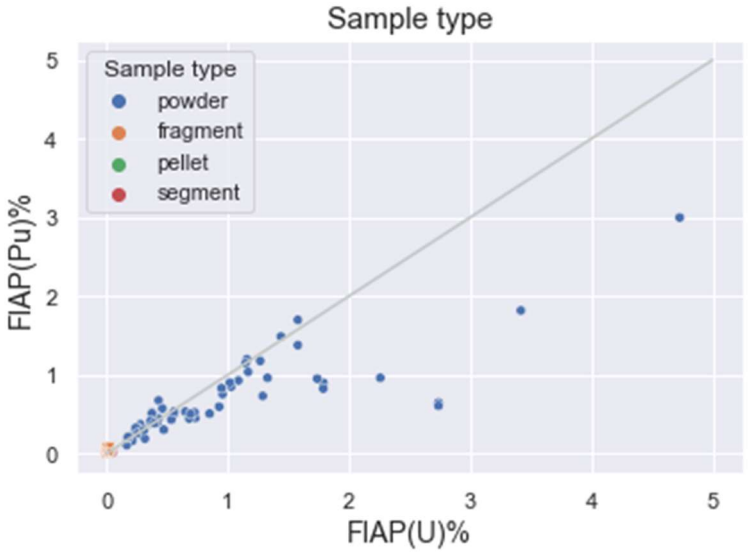

Fig A2.1 Scatterplot of Pu release in relation to U release, where points have been categorized by colour depending on sample type and the grey line is a straight y = x line. Circles represent unspecified Pu and triangles Pu-239.

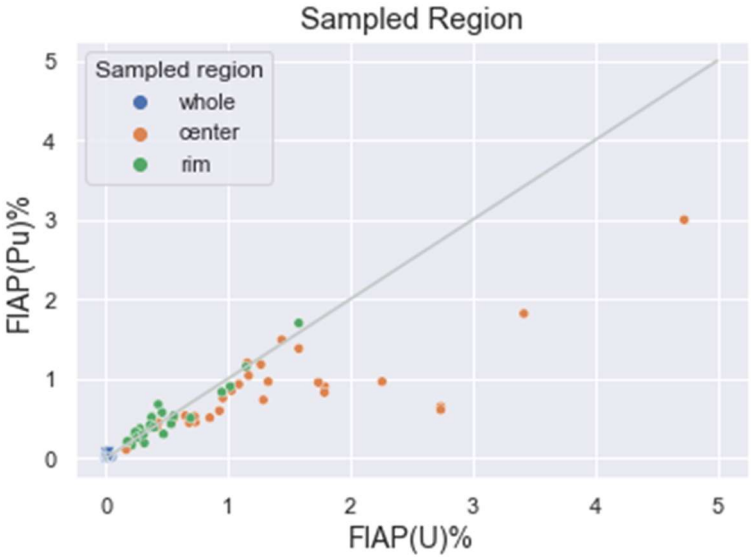

Fig A2.2 Scatterplot of Pu release in relation to U release, where points have been categorized by colour depending on sample region and the grey line is a straight y = x line. Circles represent unspecified Pu and triangles Pu-239.

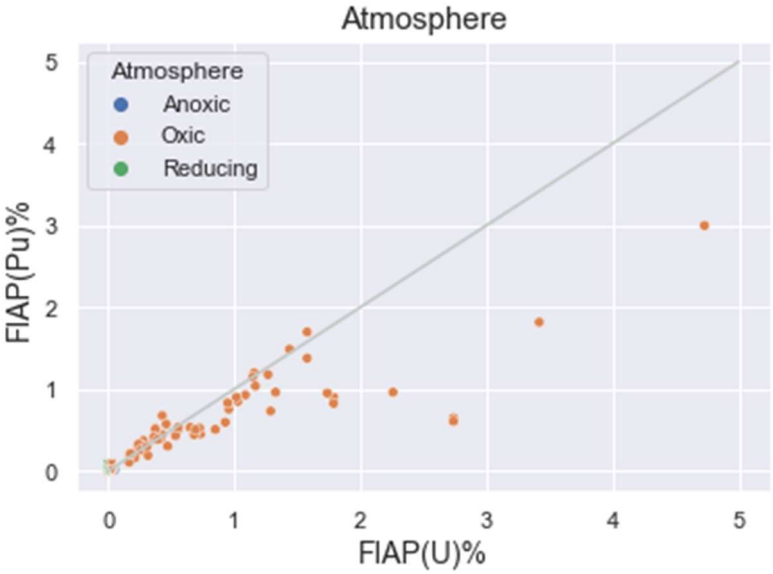

Fig A2.3 Scatterplot of Pu release in relation to U release, where points have been categorized by colour depending on atmosphere and the grey line is a straight y = x line. Circles represent unspecified Pu and triangles Pu-239.

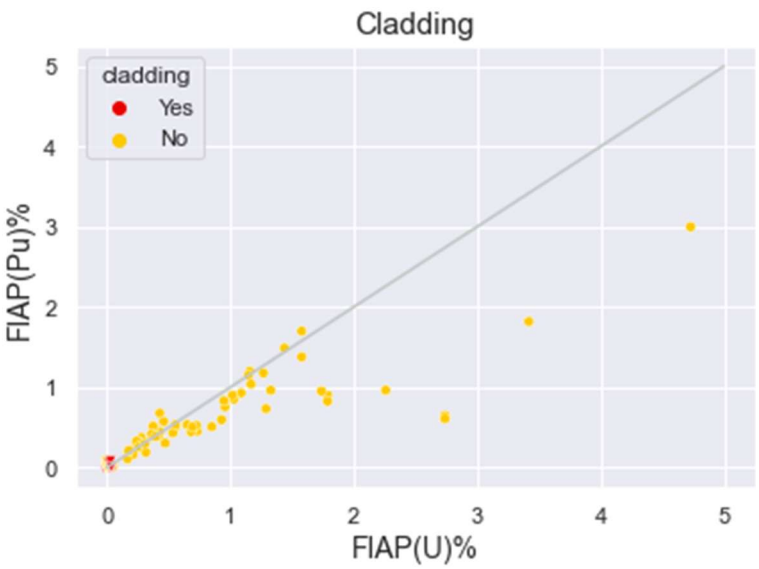

Fig A2.4 Scatterplot of Pu release in relation to U release, where points have been categorized by colour depending on presence of cladding and the grey line is a straight y = x line. Circles represent unspecified Pu and triangles Pu-239.

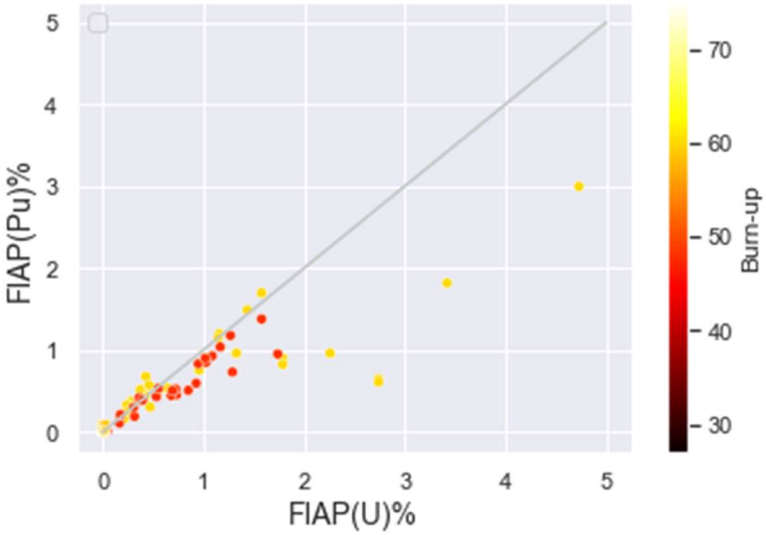

Fig A2.5 Scatterplot of Pu release in relation to U release, where points have been categorized by colour depending on BU and the grey line is a straight y = x line. Circles represent unspecified Pu and triangles Pu-239.

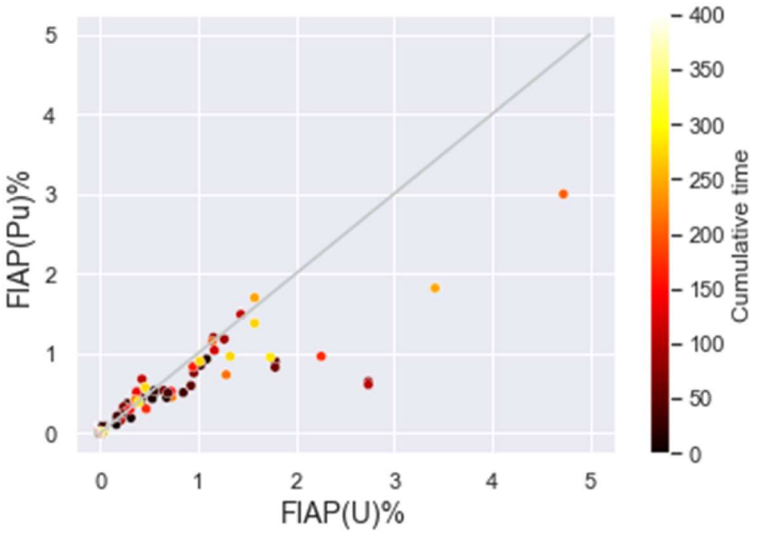

Fig A2.6 Scatterplot of Pu release in relation to U release, where points have been categorized by colour depending on cumulative time and the grey line is a straight y = x line. Circles represent unspecified Pu and triangles Pu-239.

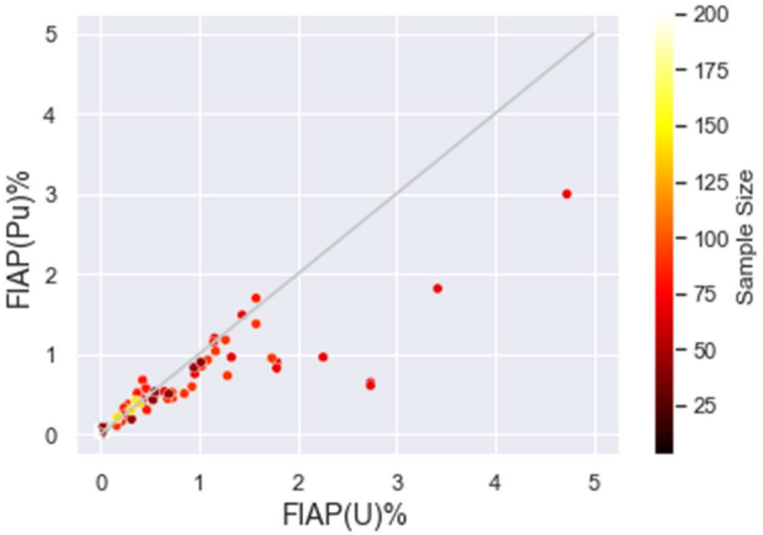

Fig A2.7 Scatterplot of Pu release in relation to U release, where points have been categorized by colour depending on sample size and the grey line is a straight y = x line. Circles represent unspecified Pu and triangles Pu-239.

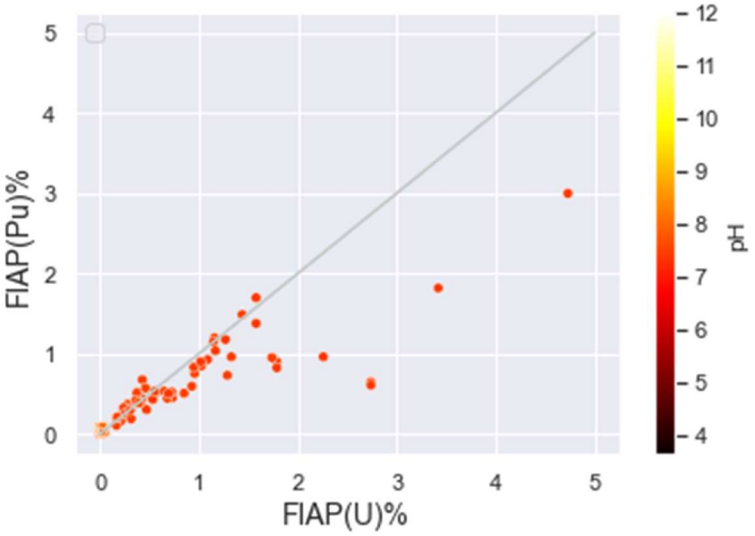

Fig A2.8 Scatterplot of Pu release in relation to U release, where points have been categorized by colour depending on pH and the grey line is a straight y = x line. Circles represent unspecified Pu and triangles Pu-239.

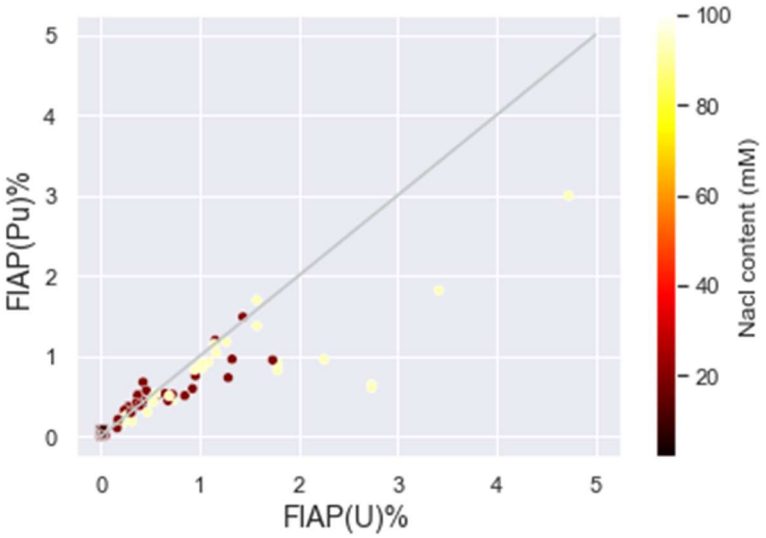

Fig A2.9 Scatterplot of Pu release in relation to U release, where points have been categorized by colour depending on NaCl content and the grey line is a straight y = x line. Circles represent unspecified Pu and triangles Pu-239.

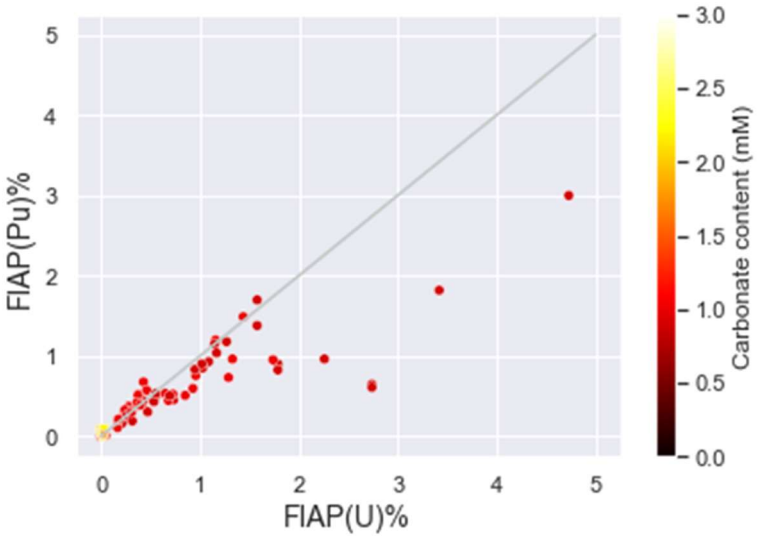

Fig A2.10 Scatterplot of Pu release in relation to U release, where points have been categorized by colour depending on carbonate content and the grey line is a straight y = x line. Circles represent unspecified Pu and triangles Pu-239.

Curium

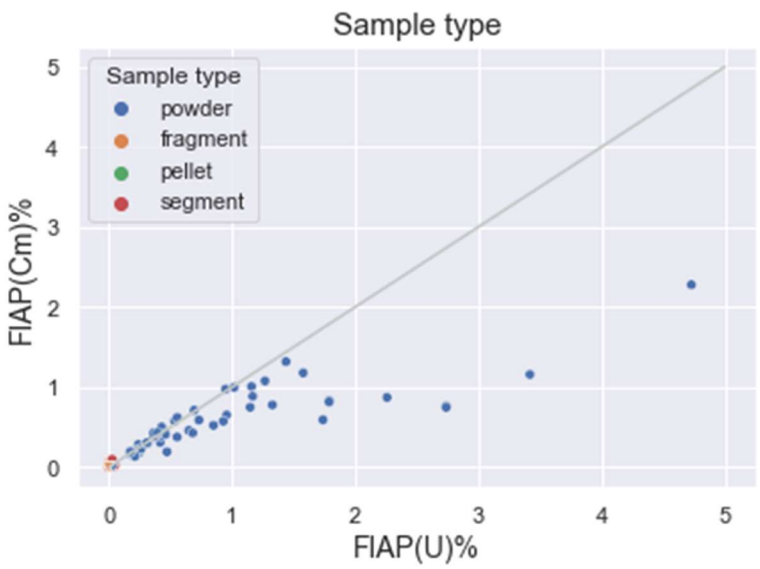

Fig A2.11 Scatterplot of Cm release in relation to U release, where points have been categorized by colour depending on sample type and the grey line is a straight y = x line. Circles represent unspecified Cm and triangles Cm-244.

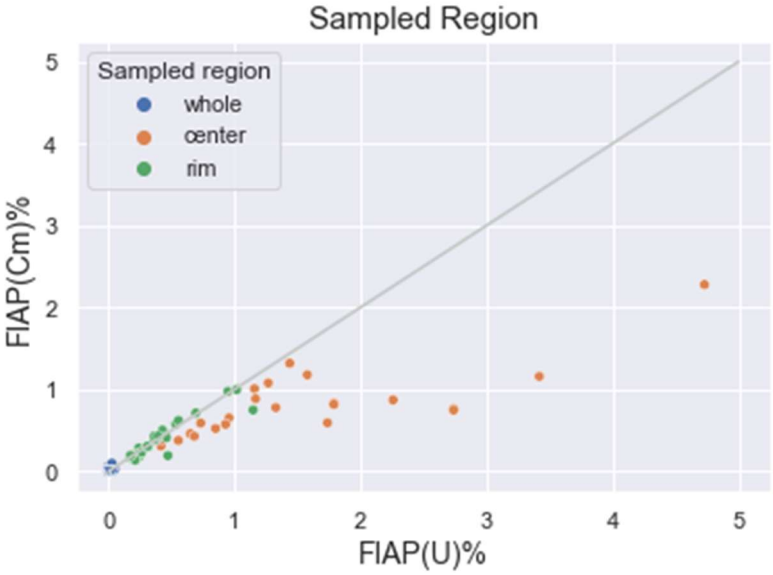

Fig A2.12 Scatterplot of Cm release in relation to U release, where points have been categorized by colour depending on sampled region and the grey line is a straight y = x line. Circles represent unspecified Cm and triangles Cm-244.

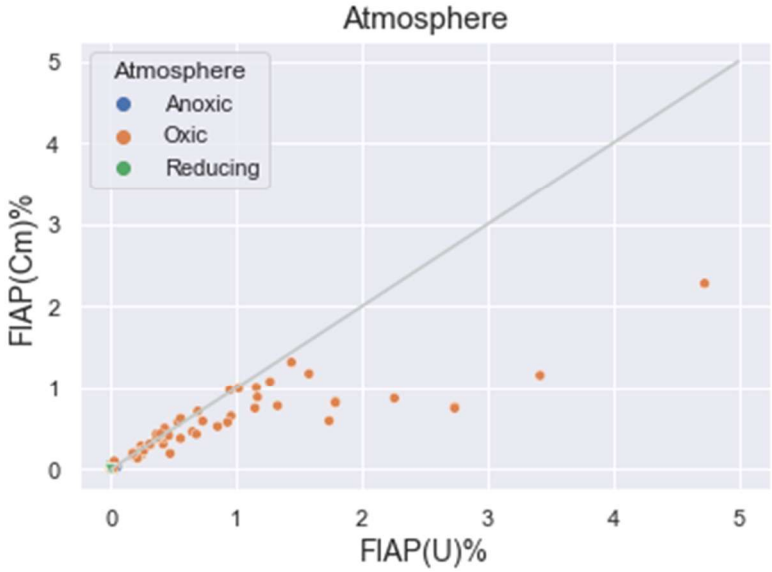

Fig A2.13 Scatterplot of Cm release in relation to U release, where points have been categorized by colour depending on atmosphere and the grey line is a straight y = x line. Circles represent unspecified Cm and triangles Cm-244.

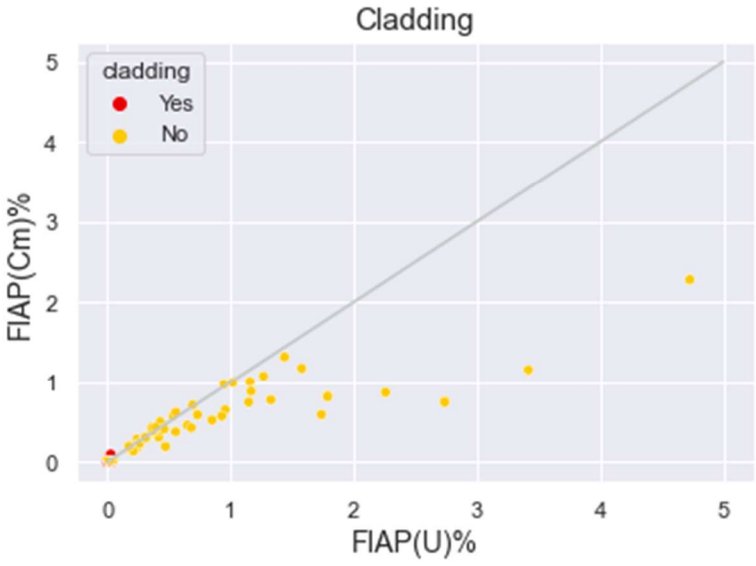

Fig A2.14 Scatterplot of Cm release in relation to U release, where points have been categorized by colour depending on presence of cladding and the grey line is a straight y = x line. Circles represent unspecified Cm and triangles Cm-244.

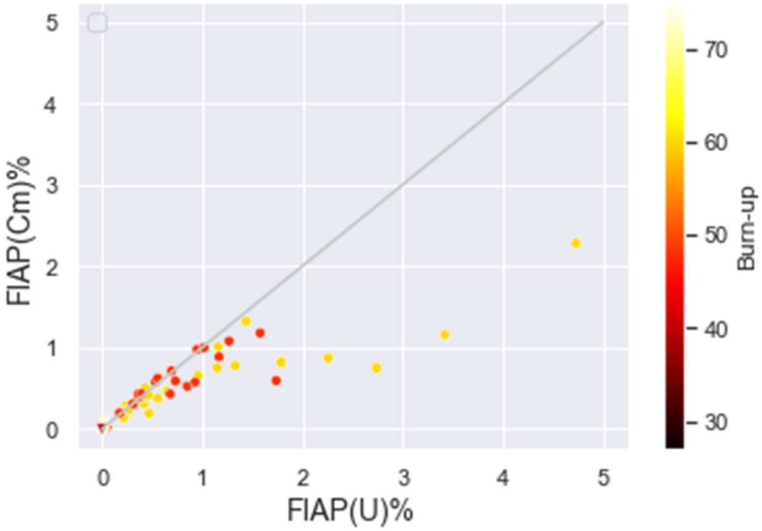

Fig A2.15 Scatterplot of Cm release in relation to U release, where points have been categorized by colour depending on BU and the grey line is a straight y = x line. Circles represent unspecified Cm and triangles Cm-244.

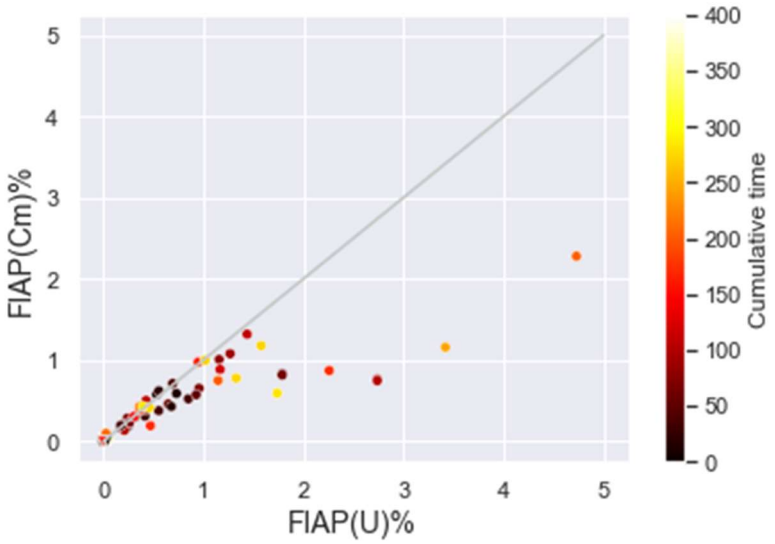

Fig A2.16 Scatterplot of Cm release in relation to U release, where points have been categorized by colour depending on cumulative time and the grey line is a straight y = x line. Circles represent unspecified Cm and triangles Cm-244.

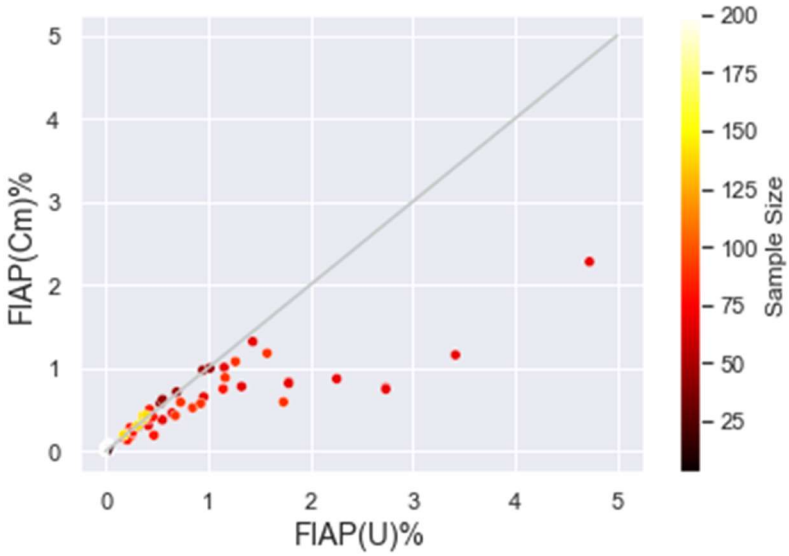

Fig A2.17 Scatterplot of Cm release in relation to U release, where points have been categorized by colour depending on sample size and the grey line is a straight y = x line. Circles represent unspecified Cm and triangles Cm-244.

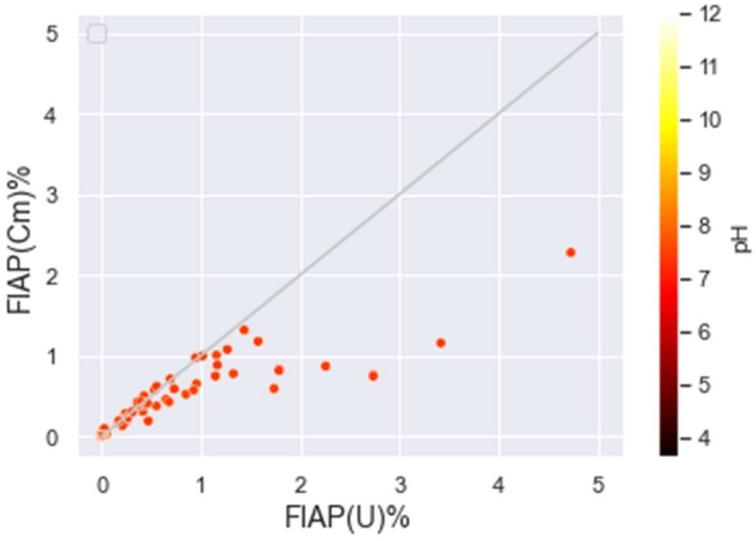

Fig A2.18 Scatterplot of Cm release in relation to U release, where points have been categorized by colour depending on pH and the grey line is a straight y = x line. Circles represent unspecified Cm and triangles Cm-244.

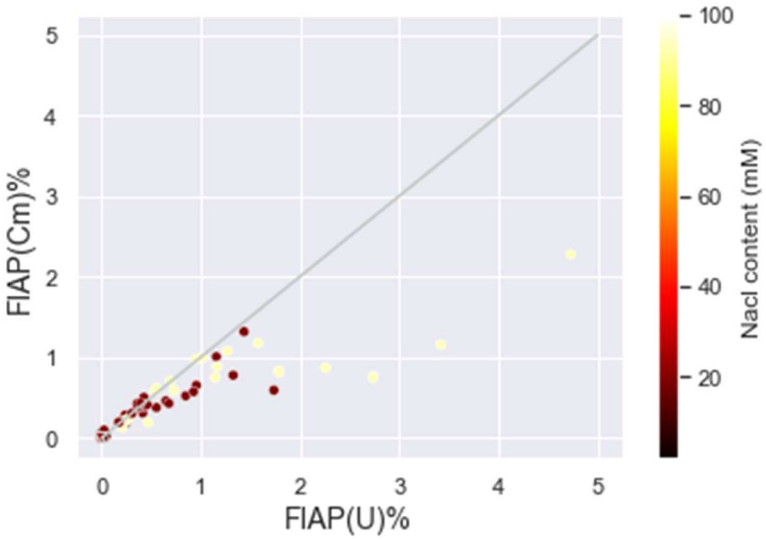

Fig A2.19 Scatterplot of Cm release in relation to U release, where points have been categorized by colour depending on NaCl content and the grey line is a straight y = x line. Circles represent unspecified Cm and triangles Cm-244.

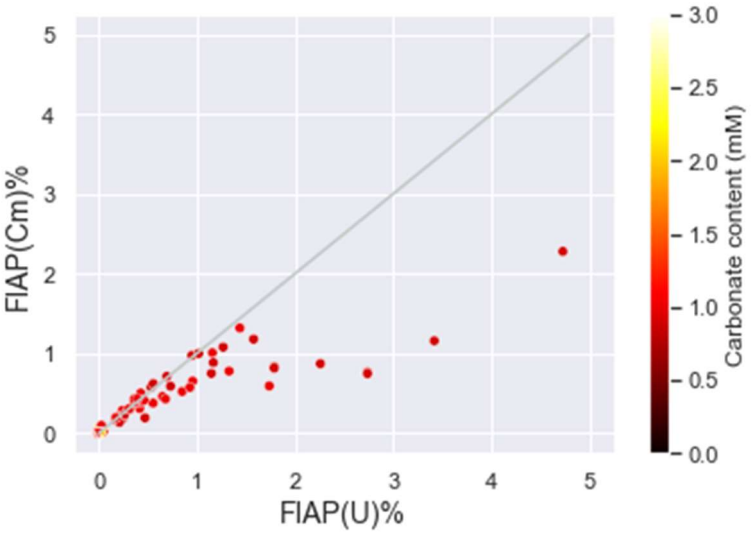

Fig A2.20 Scatterplot of Cm release in relation to U release, where points have been categorized by colour depending on carbonate content and the grey line is a straight y = x line. Circles represent unspecified Cm and triangles Cm-244.

Americium

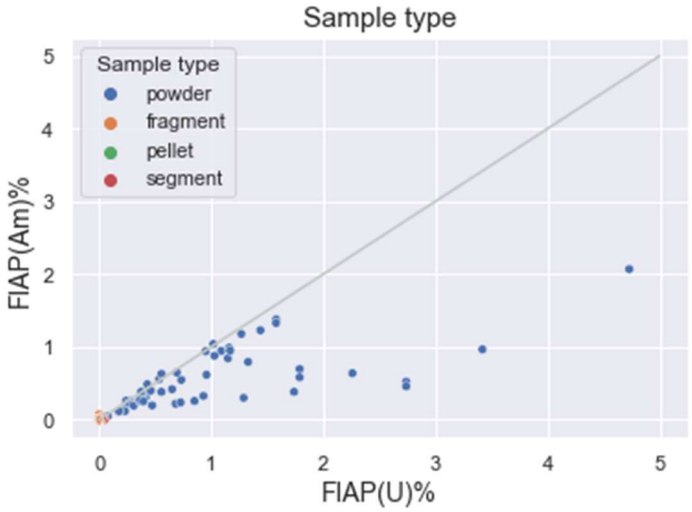

Fig A2.21 Scatterplot of Am release in relation to U release, where points have been categorized by colour depending on sample type and the grey line is a straight y = x line. Circles represent unspecified Am, triangles Am-241 and diamonds Am-243.

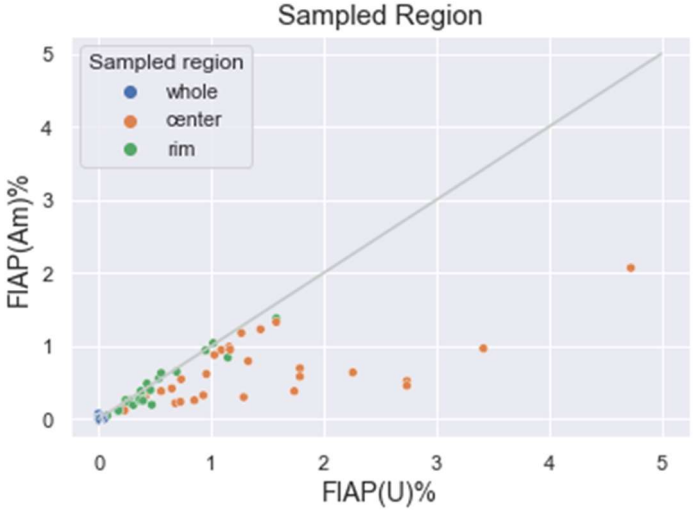

Fig A2.22 Scatterplot of Am release in relation to U release, where points have been categorized by colour depending on sample region and the grey line is a straight y = x line. Circles represent unspecified Am, triangles Am-241 and Am-243.

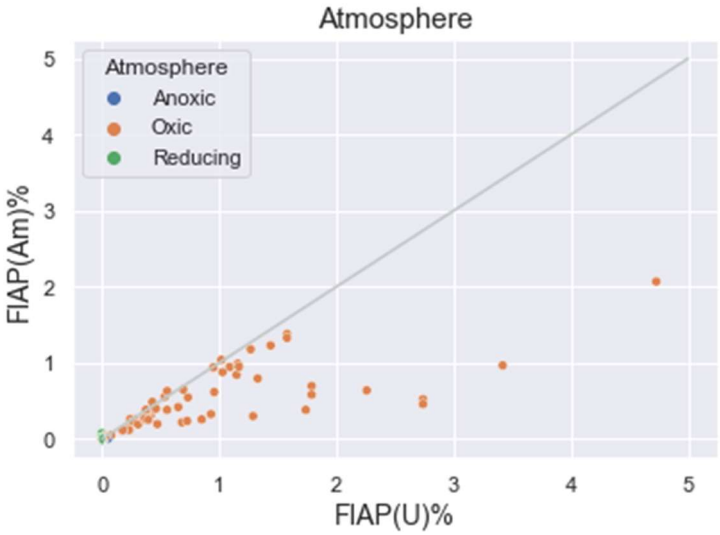

Fig A2.23 Scatterplot of Am release in relation to U release, where points have been categorized by colour depending on atmosphere and the grey line is a straight y = x line. Circles represent unspecified Am, triangles Am-241 and diamonds Am -243.

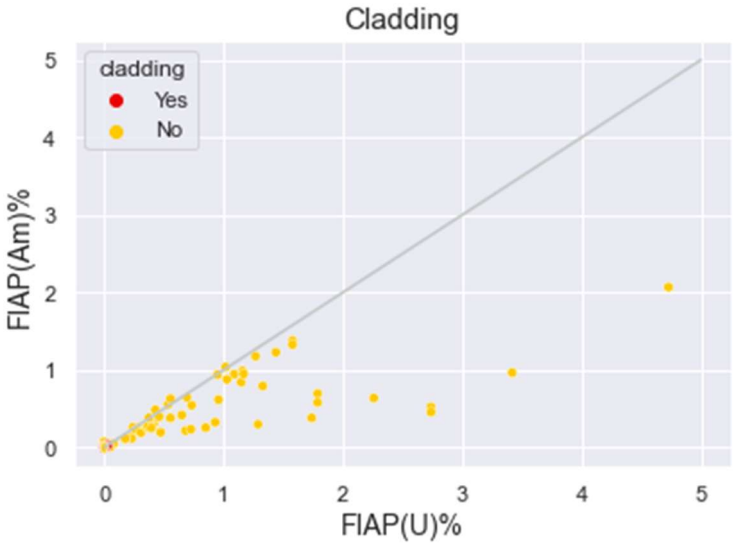

Fig A2.24 Scatterplot of Am release in relation to U release, where points have been categorized by colour depending on presence of cladding and the grey line is a straight y = x line. Circles represent unspecified Am, triangles Am-241 and diamonds Am -243.

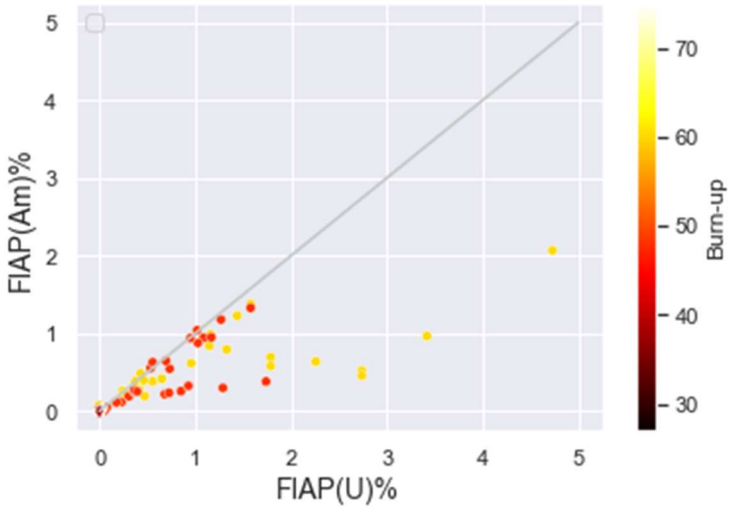

Fig A2.25 Scatterplot of Am release in relation to U release, where points have been categorized by colour depending on BU and the grey line is a straight y = x line. Circles represent unspecified Am, triangles Am-241 and diamonds Am -243.

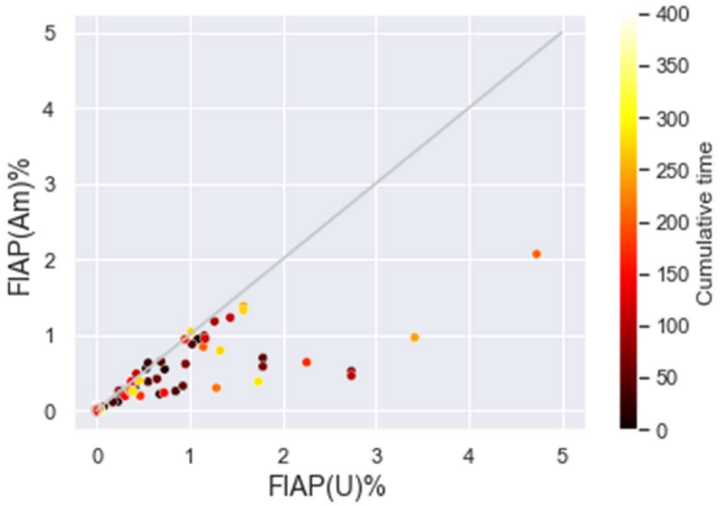

Fig A2.26 Scatterplot of Am release in relation to U release, where points have been categorized by colour depending on cumulative time and the grey line is a straight y = x line. Circles represent unspecified Am, triangles Am-241 and diamonds Am -243.

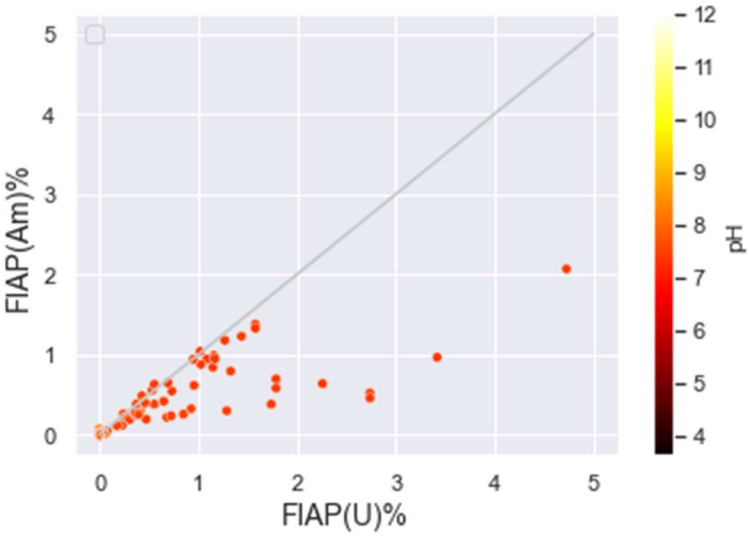

Fig A2.27 Scatterplot of Am release in relation to U release, where points have been categorized by colour depending on pH and the grey line is a straight y = x line. Circles represent unspecified Am, triangles Am-241 and diamonds Am -243.

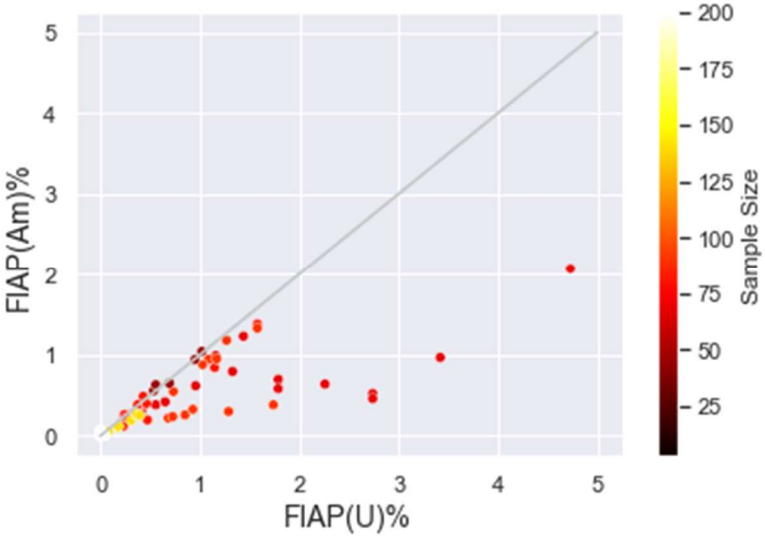

Fig A2.28 Scatterplot of Am release in relation to U release, where points have been categorized by colour depending on sample size and the grey line is a straight y = x line. Circles represent unspecified Am, triangles Am-241 and diamonds Am -243.

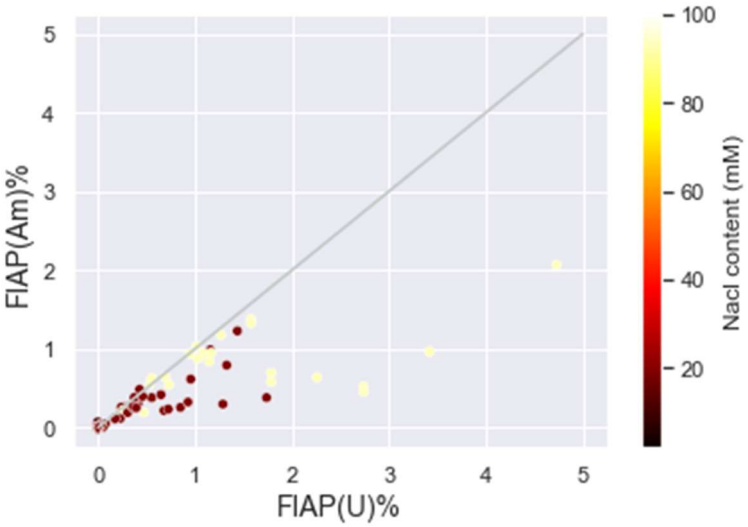

Fig A2.29 Scatterplot of Am release in relation to U release, where points have been categorized by colour depending on NaCl content and the grey line is a straight y = x line. Circles represent unspecified Am, triangles Am-241 and diamonds Am - 243.

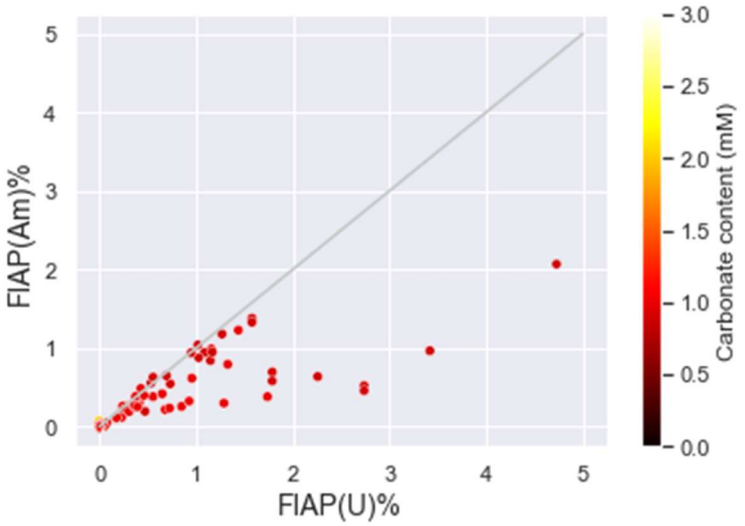

Fig A2.30 Scatterplot of Am release in relation to U release, where points have been categorized by colour depending on carbonate content and the grey line is a straight y = x line. Circles represent unspecified Am, triangles Am-241 and diamonds Am - 243.

Neodymium

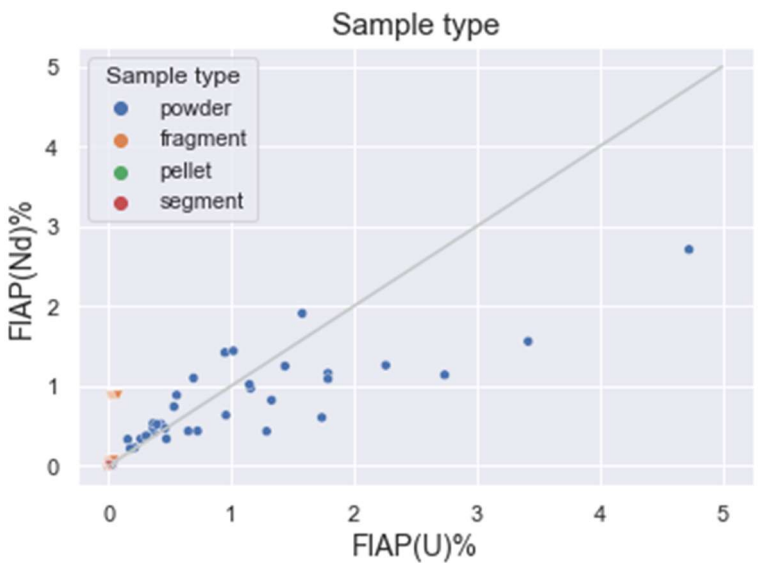

Fig A2.31 Scatterplot of Nd release in relation to U release, where points have been categorized by colour depending on sample type and the grey line is a straight y = x line. Circles represent unspecified Nd and triangles Nd-144.

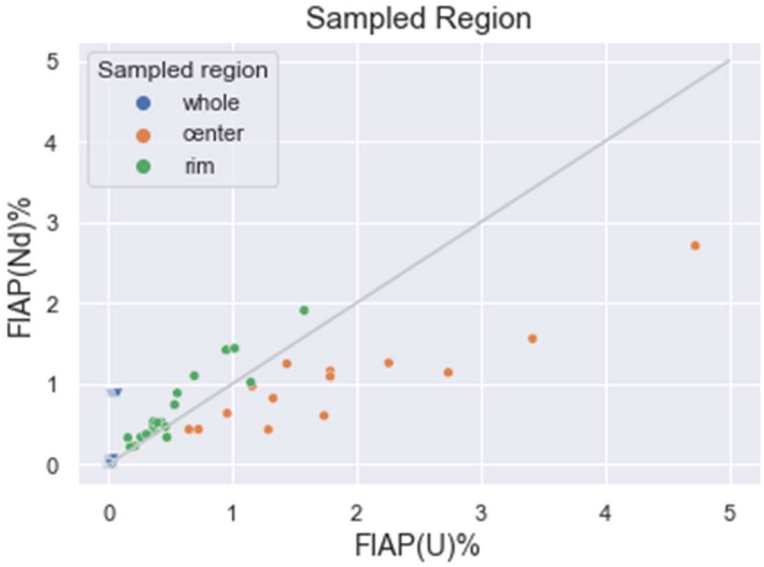

Fig A2.32 Scatterplot of Nd release in relation to U release, where points have been categorized by colour depending on sampled region and the grey line is a straight y = x line. Circles represent unspecified Nd and triangles Nd-144.

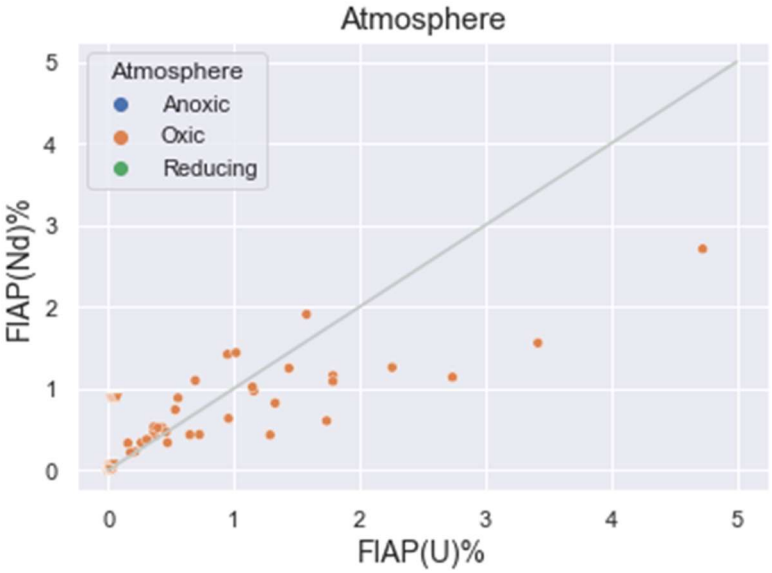

Fig A2.33 Scatterplot of Nd release in relation to U release, where points have been categorized by colour depending on atmosphere and the grey line is a straight y = x line. Circles represent unspecified Nd and triangles Nd-144.

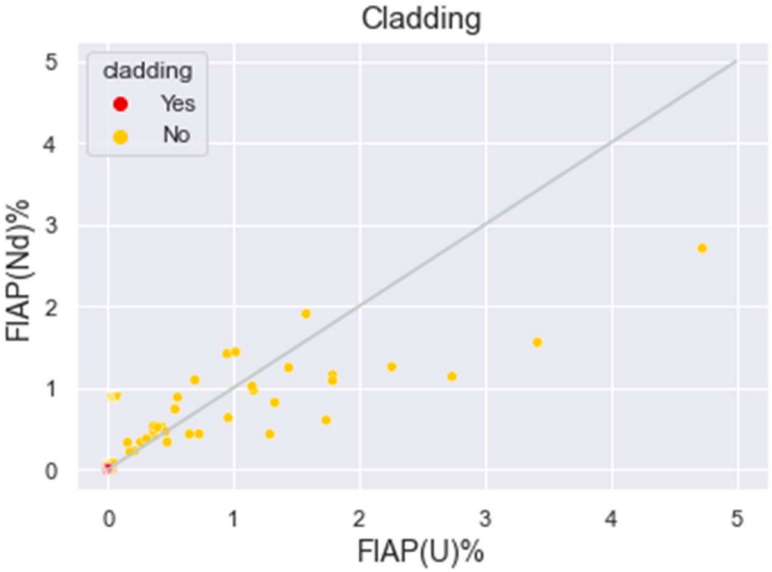

Fig A2.34 Scatterplot of Nd release in relation to U release, where points have been categorized by colour depending on presence of cladding and the grey line is a straight y = x line. Circles represent unspecified Nd and triangles Nd-144.

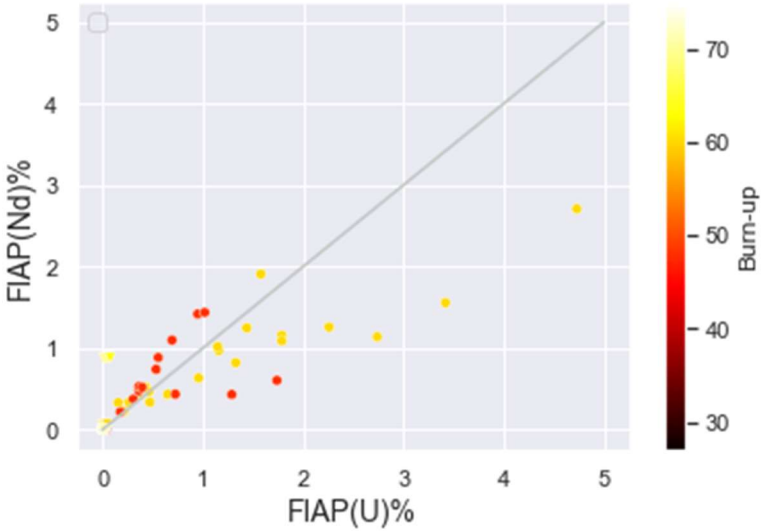

Fig A2.35 Scatterplot of Nd release in relation to U release, where points have been categorized by colour depending on BU and the grey line is a straight y = x line. Circles represent unspecified Nd and triangles Nd-144.

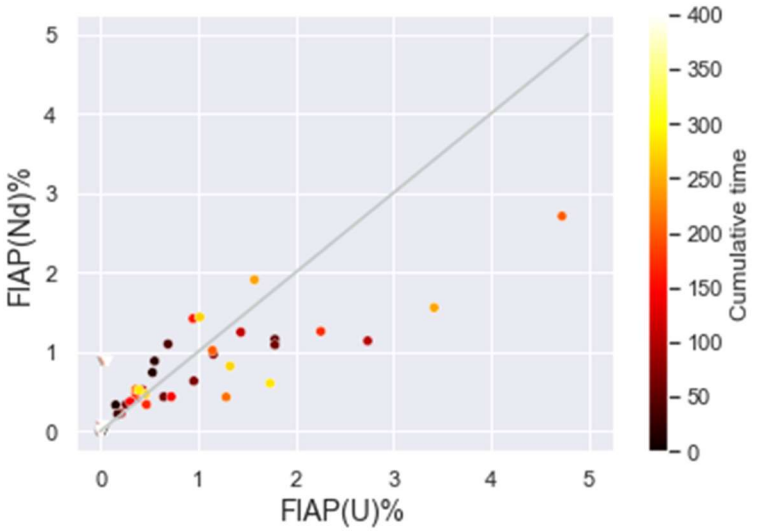

Fig A2.36 Scatterplot of Nd release in relation to U release, where points have been categorized by colour depending on cumulative time and the grey line is a straight y = x line. Circles represent unspecified Nd and triangles Nd-144.

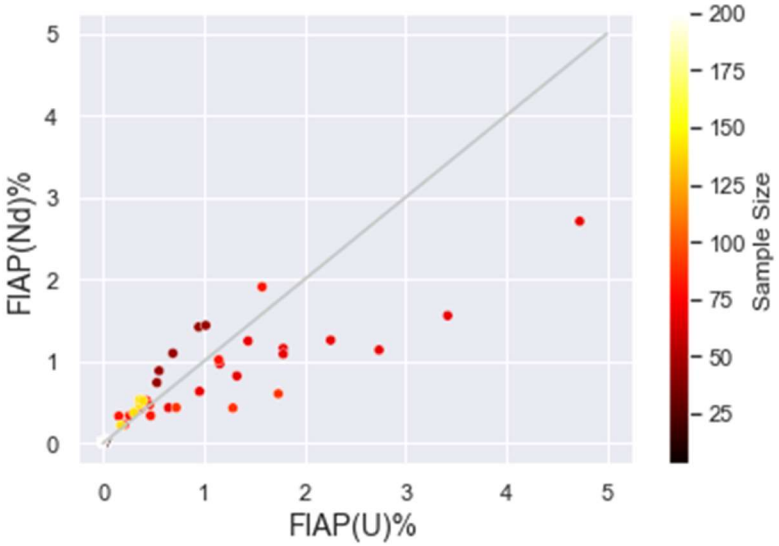

Fig A2.37 Scatterplot of Nd release in relation to U release, where points have been categorized by colour depending on sample size and the grey line is a straight y = x line. Circles represent unspecified Nd and triangles Nd-144.

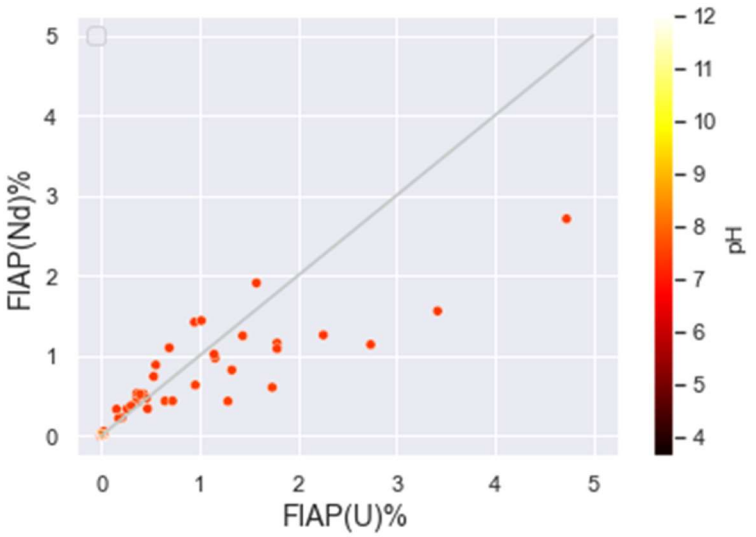

Fig A2.38 Scatterplot of Nd release in relation to U release, where points have been categorized by colour depending on pH and the grey line is a straight y = x line. Circles represent unspecified Nd and triangles Nd-144.

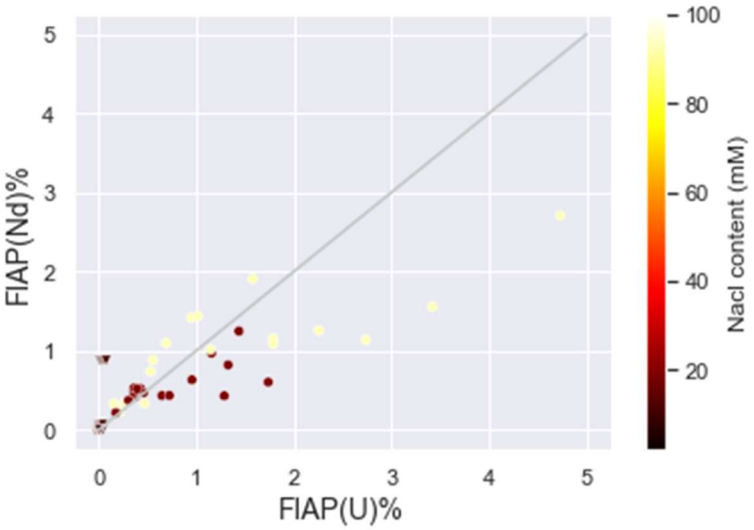

Fig A2.39 Scatterplot of Nd release in relation to U release, where points have been categorized by colour depending on NaCl content and the grey line is a straight y = x line. Circles represent unspecified Nd and triangles Nd-144.

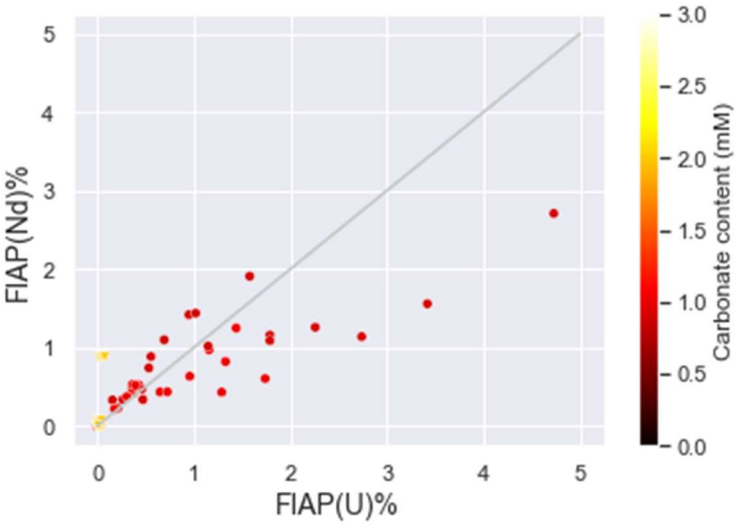

Fig A2.40 Scatterplot of Nd release in relation to U release, where points have been categorized by colour depending on carbonate content and the grey line is a straight y = x line. Circles represent unspecified Nd and triangles Nd-144.

Lanthanum

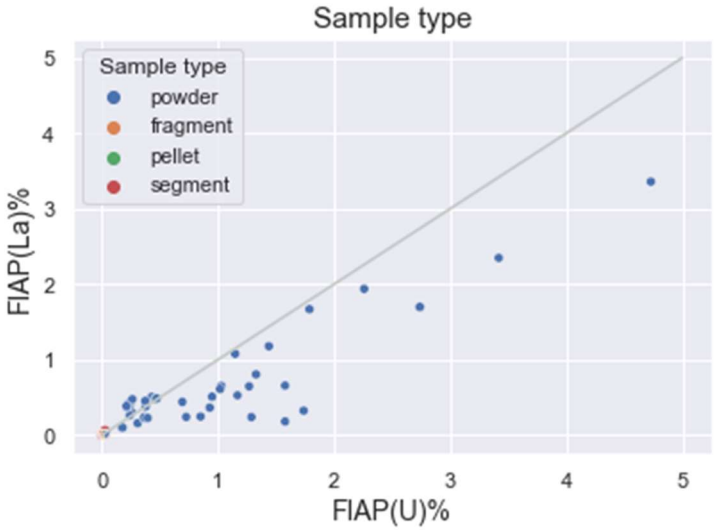

Fig A2.41 Scatterplot of La release in relation to U release, where points have been categorized by colour depending on sample type and the grey line is a straight y = x line. Circles represent unspecified La and triangles La-139.

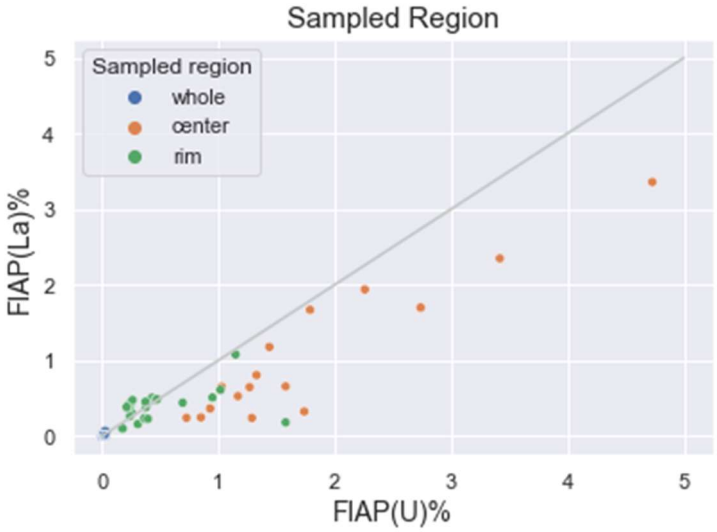

Fig A2.42 Scatterplot of La release in relation to U release, where points have been categorized by colour depending on sample region and the grey line is a straight y = x line. Circles represent unspecified La and triangles La-139.

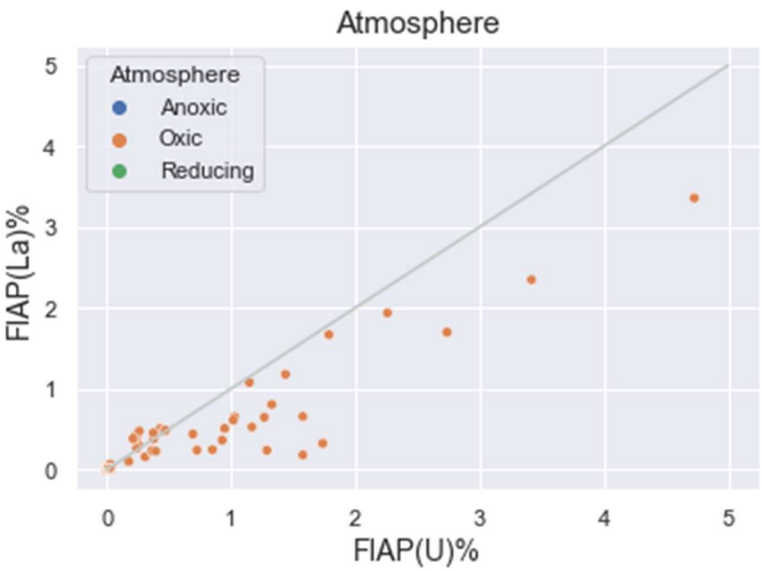

Fig A2.43 Scatterplot of La release in relation to U release, where points have been categorized by colour depending on atmosphere and the grey line is a straight y = x line. Circles represent unspecified La and triangles La-139.

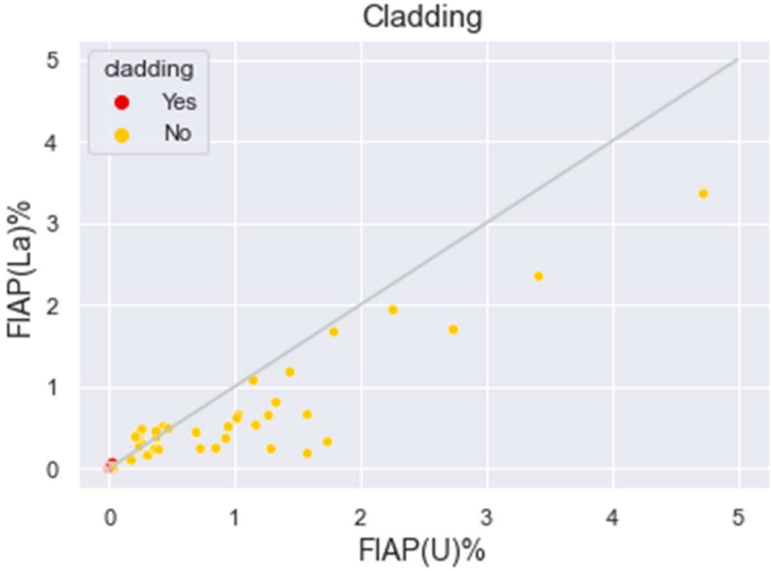

Fig A2.44 Scatterplot of La release in relation to U release, where points have been categorized by colour depending on presence of cladding and the grey line is a straight y = x line. Circles represent unspecified La and triangles La-139.

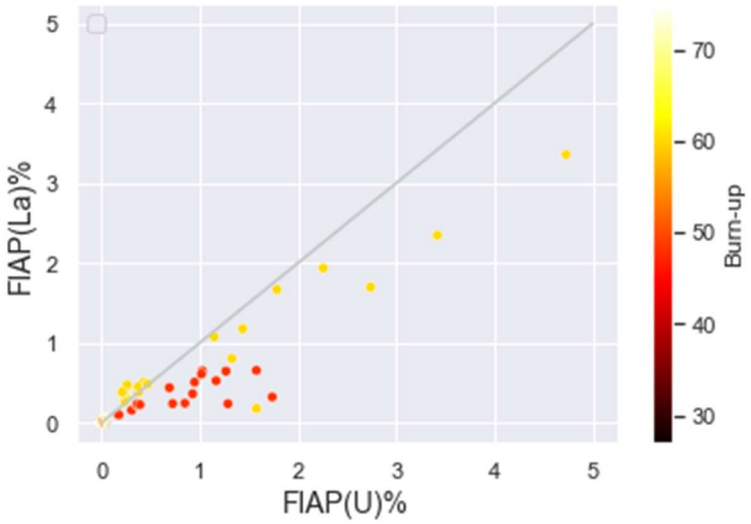

Fig A2.45 Scatterplot of La release in relation to U release, where points have been categorized by colour depending on BU and the grey line is a straight y = x line. Circles represent unspecified La and triangles La-139.

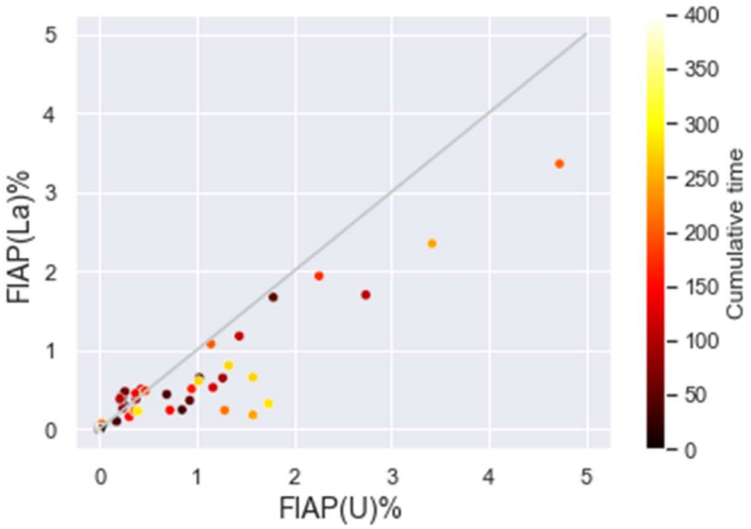

Fig A2.46 Scatterplot of La release in relation to U release, where points have been categorized by colour depending on cumulative time and the grey line is a straight y = x line. Circles represent unspecified La and triangles La-139.

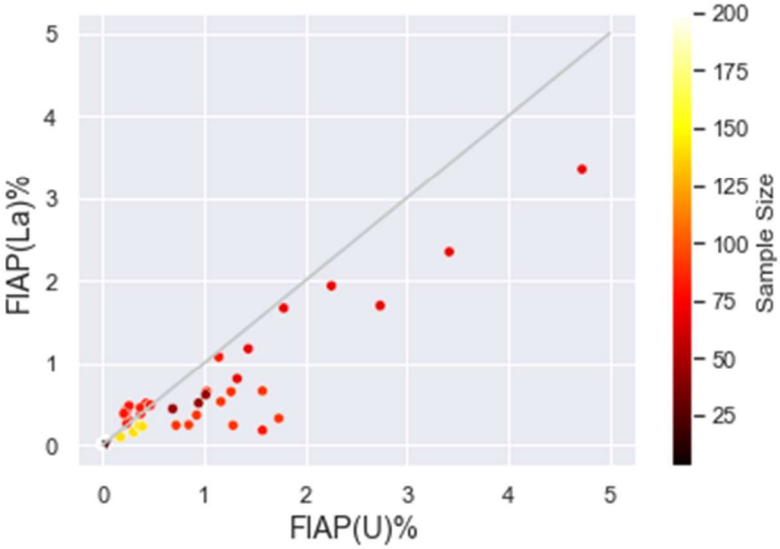

Fig A2.47 Scatterplot of La release in relation to U release, where points have been categorized by colour depending on sample size and the grey line is a straight y = x line. Circles represent unspecified La and triangles La-139.

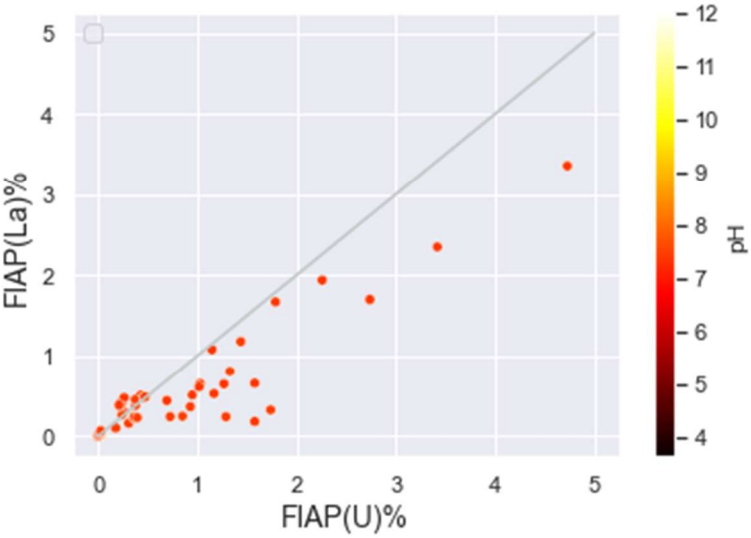

Fig A2.48 Scatterplot of La release in relation to U release, where points have been categorized by colour depending on pH and the grey line is a straight y = x line. Circles represent unspecified La and triangles La-139.

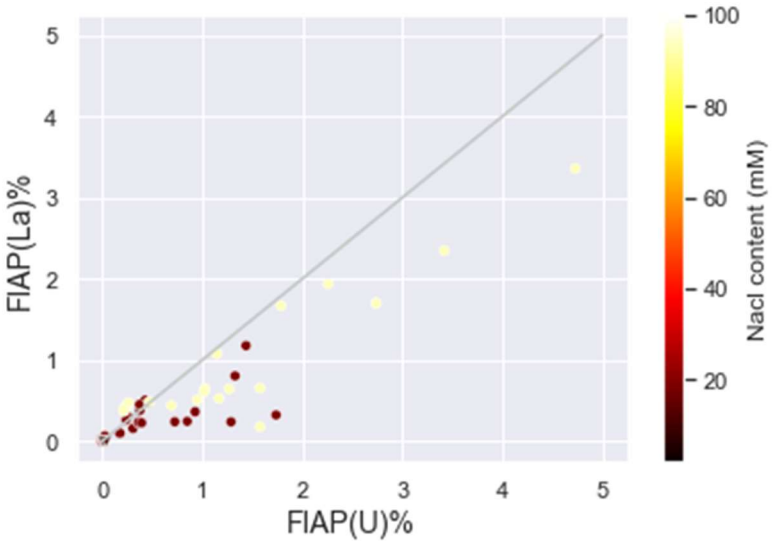

Fig A2.49 Scatterplot of La release in relation to U release, where points have been categorized by colour depending on NaCl content and the grey line is a straight y = x line. Circles represent unspecified La and triangles La-139.

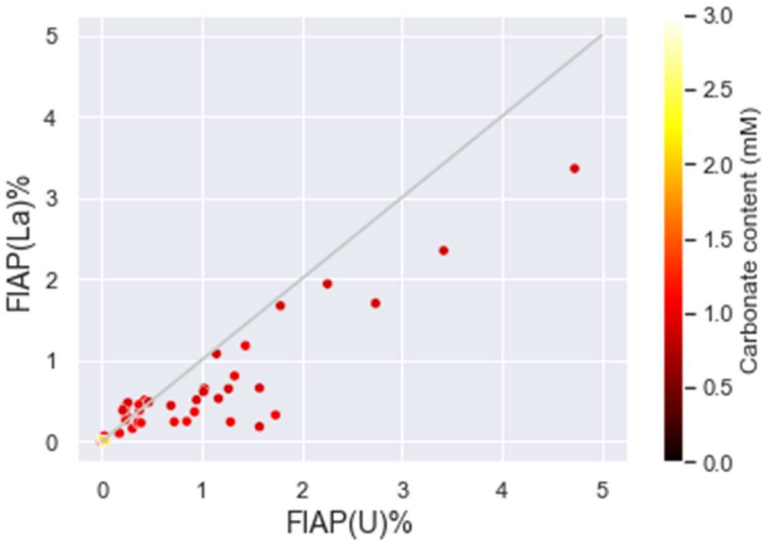

Fig A2.50 Scatterplot of La release in relation to U release, where points have been categorized by colour depending on carbonate content and the grey line is a straight y = x line. Circles represent unspecified La and triangles La-139.

Zirconium

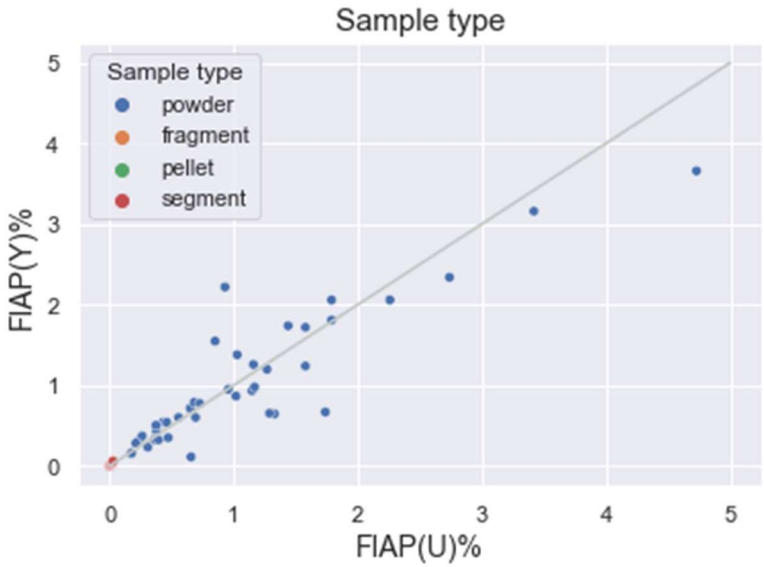

Fig A2.51 Scatterplot of Zr release in relation to U release, where points have been categorized by colour depending on sample type and the grey line is a straight y = x line.

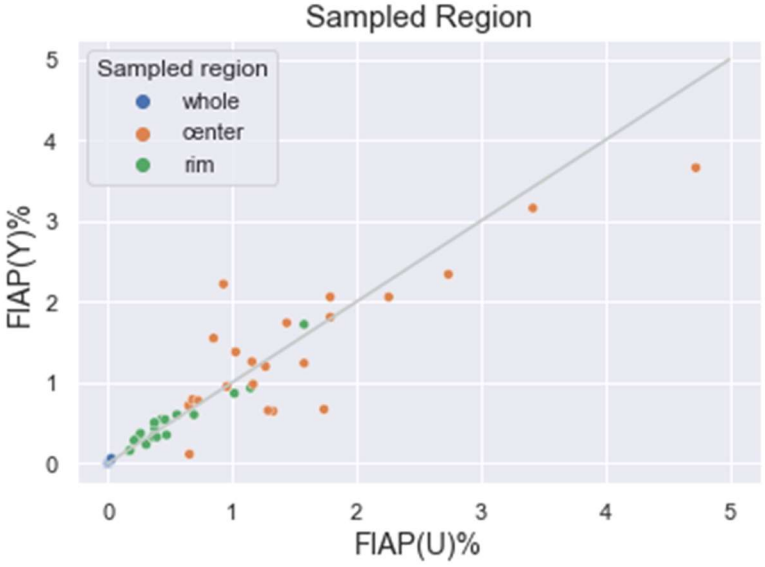

Fig A2.52 Scatterplot of Zr release in relation to U release, where points have been categorized by colour depending on sample region and the grey line is a straight y = x line.

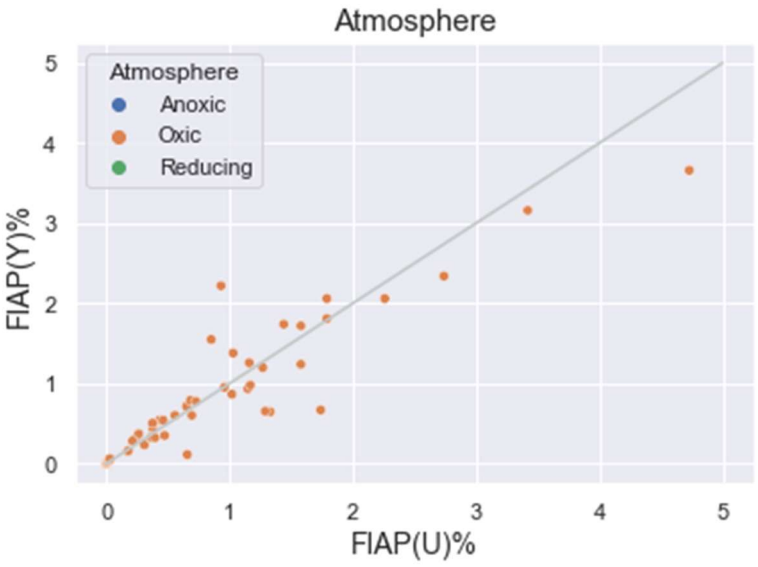

Fig A2.53 Scatterplot of Zr release in relation to U release, where points have been categorized by colour depending on atmosphere and the grey line is a straight y = x line.

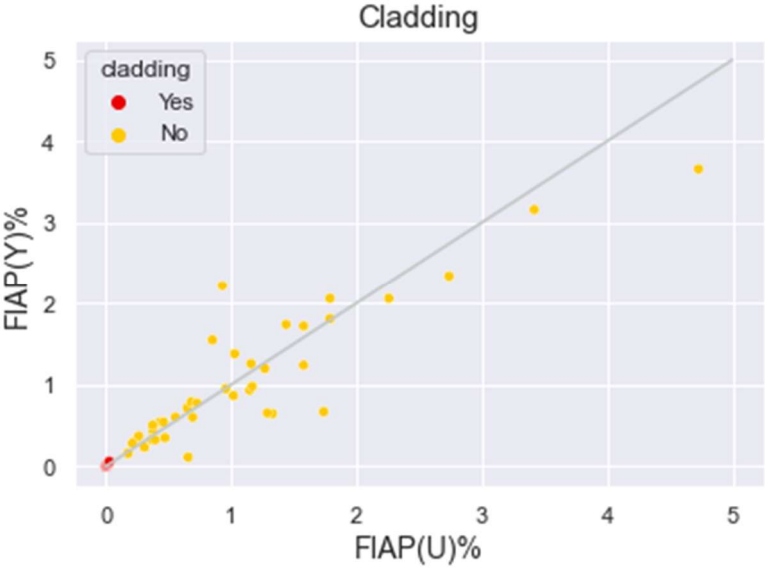

Fig A2.54 Scatterplot of Zr release in relation to U release, where points have been categorized by colour depending on presence of cladding and the grey line is a straight y = x line.

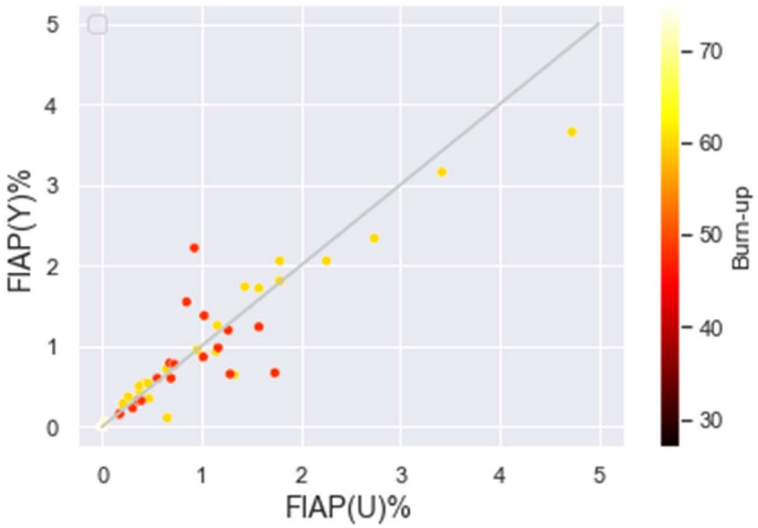

Fig A2.55 Scatterplot of Zr release in relation to U release, where points have been categorized by colour depending on BU and the grey line is a straight y = x line.

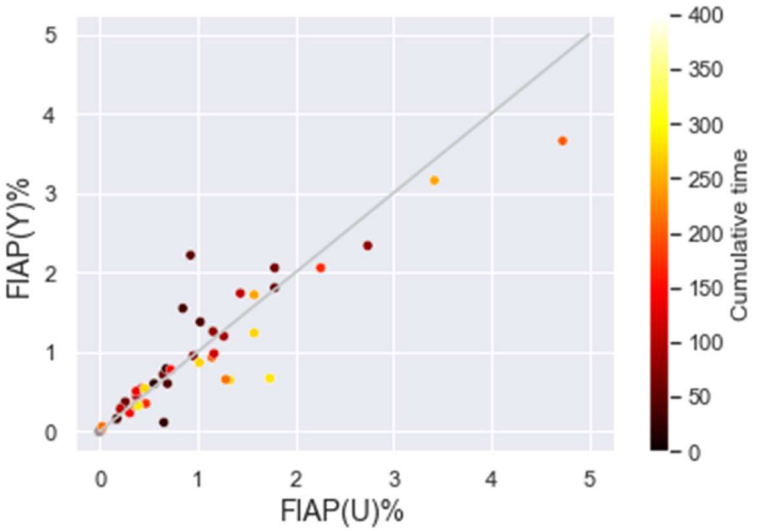

Fig A2.56 Scatterplot of Zr release in relation to U release, where points have been categorized by colour depending on cumulative time and the grey line is a straight y = x line.

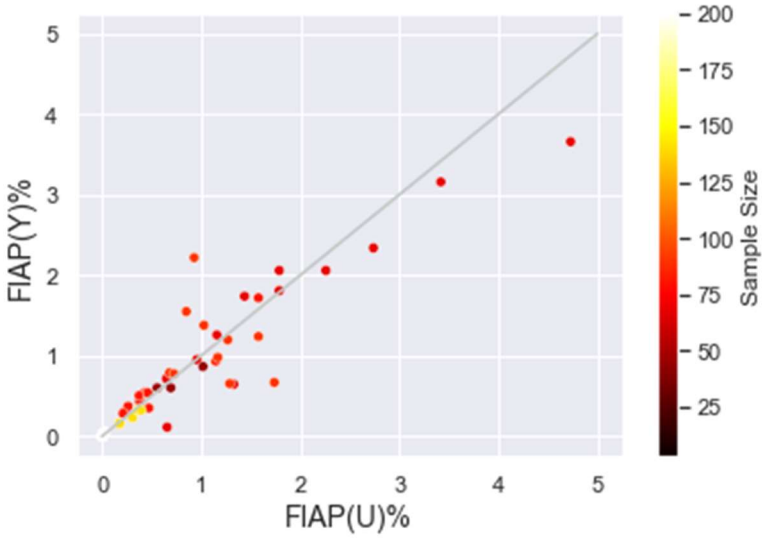

Fig A2.57 Scatterplot of Zr release in relation to U release, where points have been categorized by colour depending on sample size and the grey line is a straight y = x line.

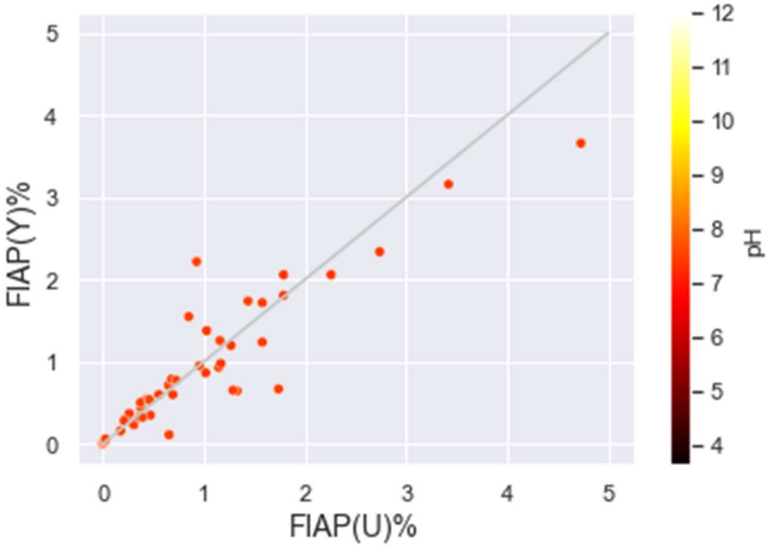

Fig A2.58 Scatterplot of Zr release in relation to U release, where points have been categorized by colour depending on pH and the grey line is a straight y = x line.

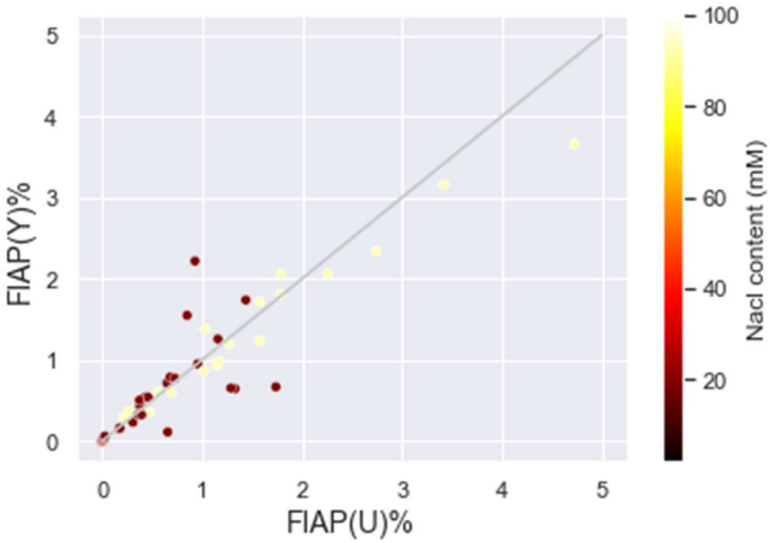

Fig A2.59 Scatterplot of Zr release in relation to U release, where points have been categorized by colour depending on NaCl content and the grey line is a straight y = x line.

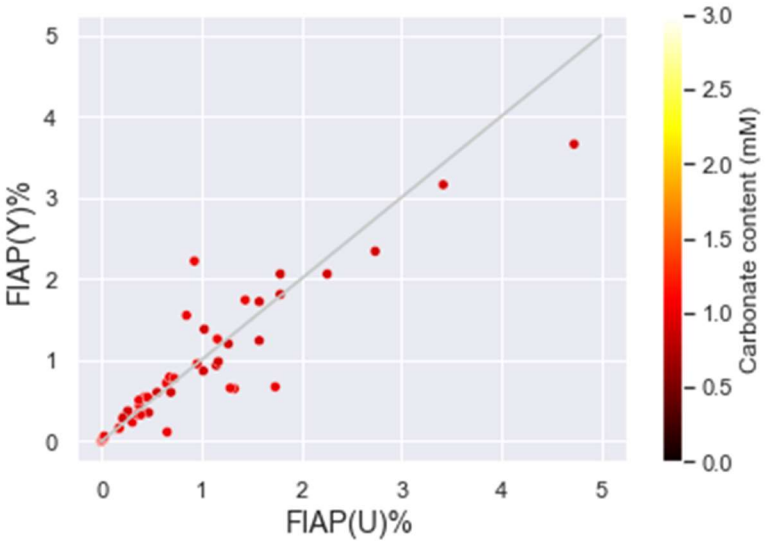

Fig A2.51 Scatterplot of Zr release in relation to U release, where points have been categorized by colour depending on carbonate content and the grey line is a straight y = x line.

A.3 Scatterplots Group 1c

Appendix A.3 shows all the plots of the elements in group 1c (Eu, Ce, Pr, Pm), both plots used and not used in section 4. The plots are shown by element.

Europium

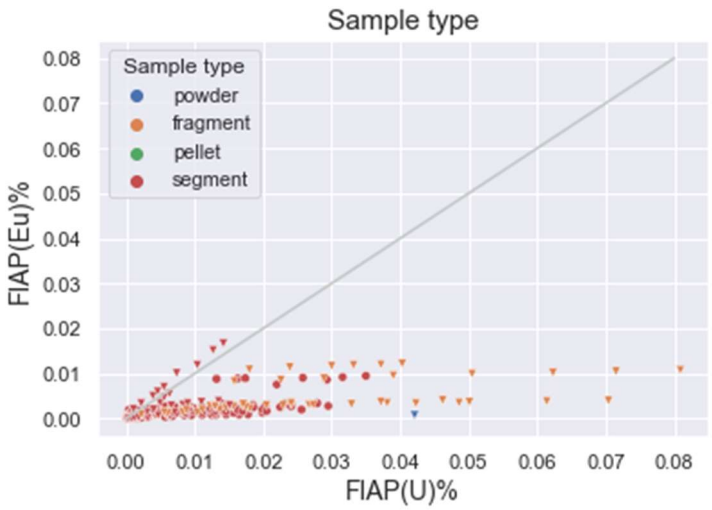

Fig A3.1 Scatterplot of Eu release in relation to U release, where points have been categorized by colour depending on sample type and the grey line is a straight y = x line. Circles represent unspecified Eu, triangles Eu-153 and diamonds Eu-154.

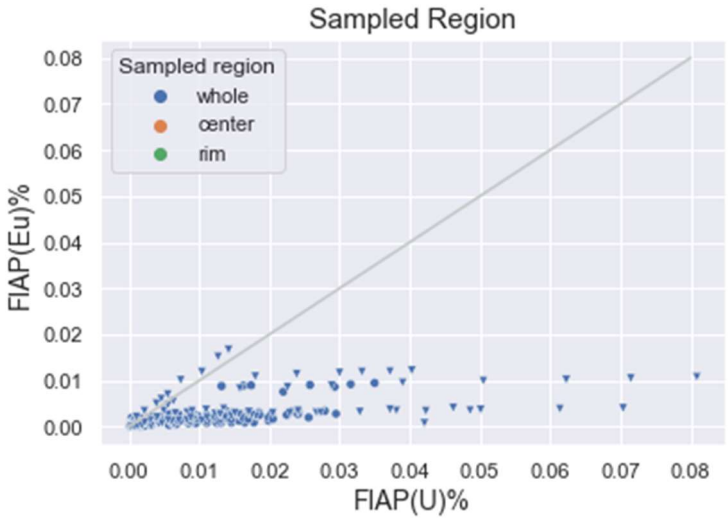

Fig A3.2 Scatterplot of Eu release in relation to U release, where points have been categorized by colour depending on sampled region and the grey line is a straight y = x line. Circles represent unspecified Eu, triangles Eu-153 and diamonds Eu-154.

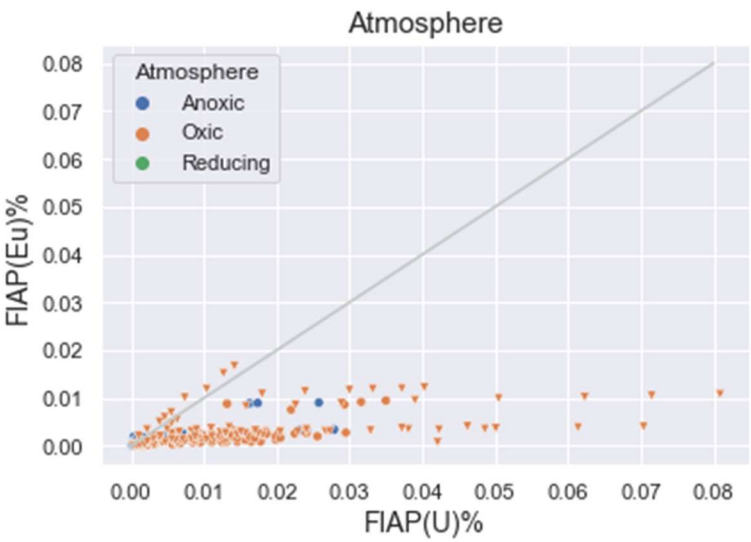

Fig A3.3 Scatterplot of Eu release in relation to U release, where points have been categorized by colour depending on atmosphere and the grey line is a straight y = x line. Circles represent unspecified Eu, triangles Eu-153 and diamonds Eu-154.

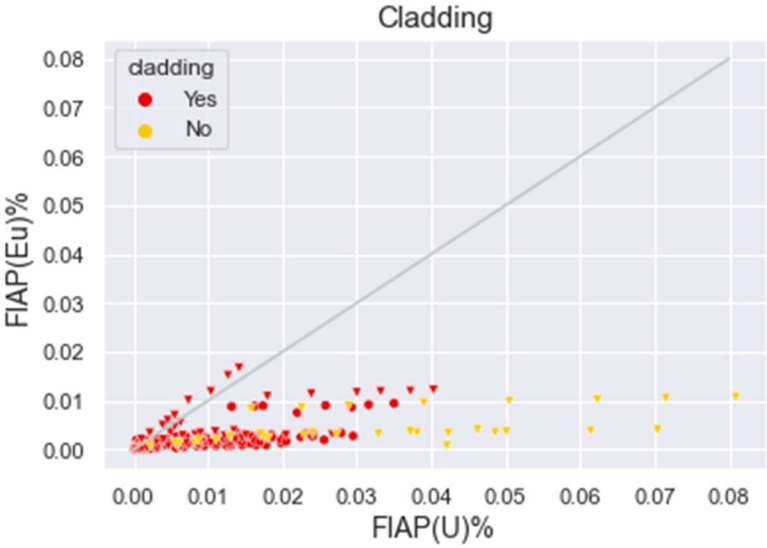

Fig A3.4 Scatterplot of Eu release in relation to U release, where points have been categorized by colour depending on presence of cladding and the grey line is a straight y = x line. Circles represent unspecified Eu, triangles Eu-153 and diamonds Eu-154.

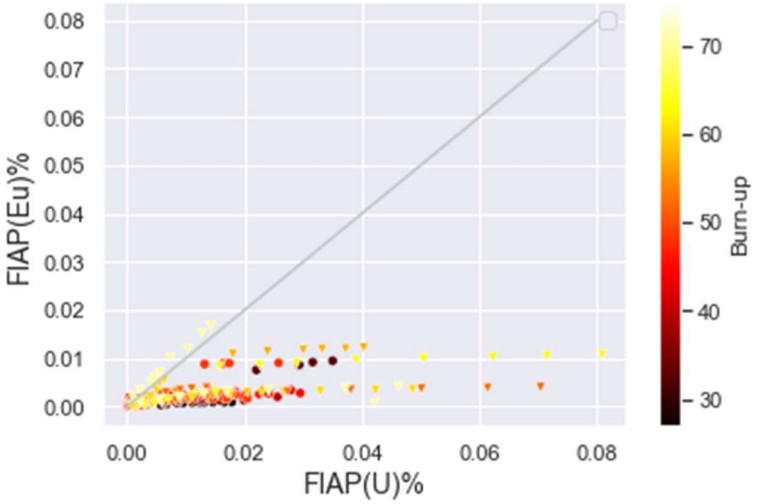

Fig A3.5 Scatterplot of Eu release in relation to U release, where points have been categorized by colour depending on BU and the grey line is a straight y = x line. Circles represent unspecified Eu, triangles Eu-153 and diamonds Eu-154.

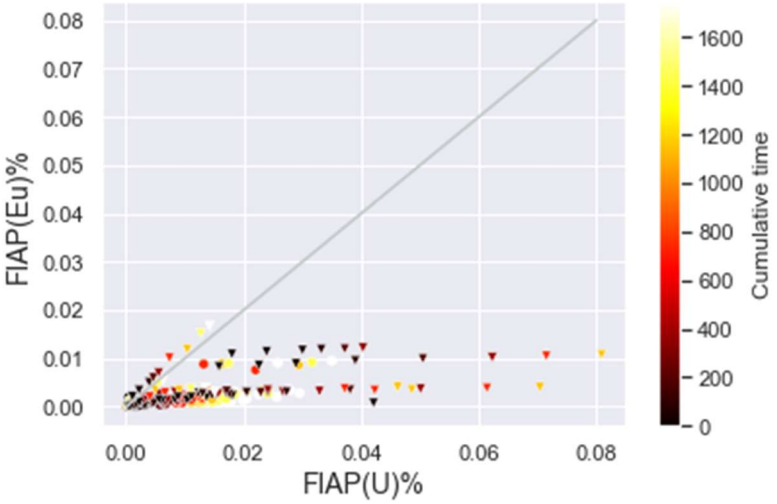

Fig A3.6 Scatterplot of Eu release in relation to U release, where points have been categorized by colour depending on cumulative time and the grey line is a straight y = x line. Circles represent unspecified Eu, triangles Eu-153 and diamonds Eu-154.

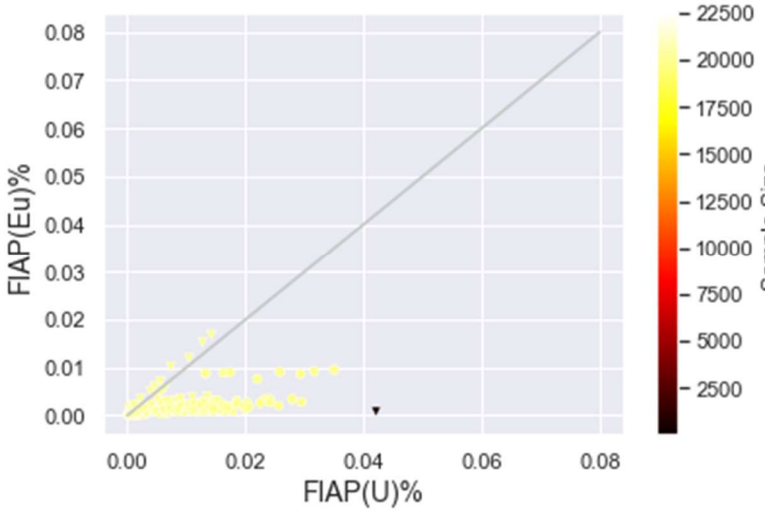

Fig A3.7 Scatterplot of Eu release in relation to U release, where points have been categorized by colour depending on sample size and the grey line is a straight y = x line. Circles represent unspecified Eu, triangles Eu-153 and diamonds Eu-154.

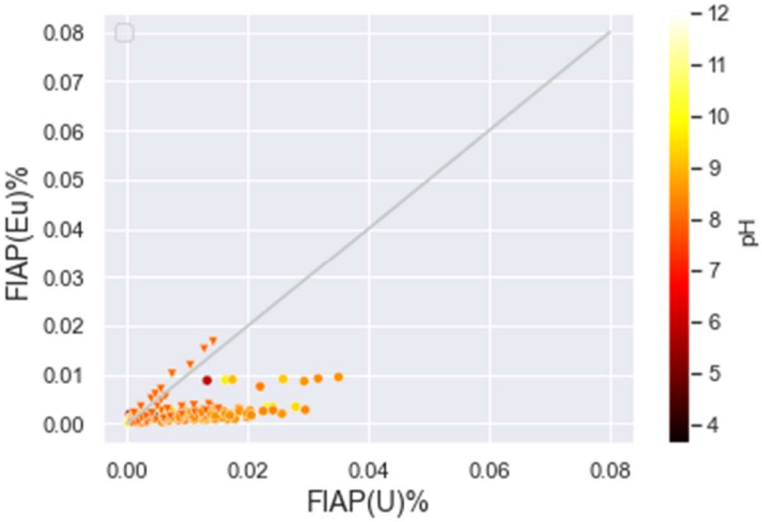

Fig A3.8 Scatterplot of Eu release in relation to U release, where points have been categorized by colour depending on pH and the grey line is a straight y = x line. Circles represent unspecified Eu, triangles Eu-153 and diamonds Eu-154.

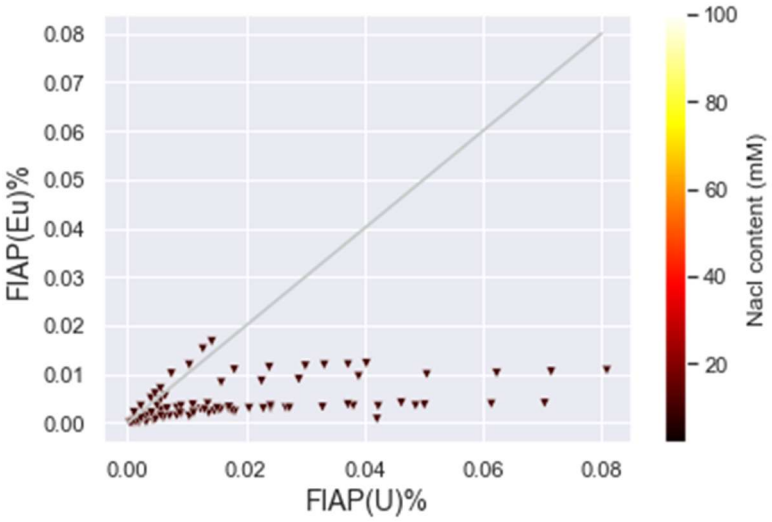

Fig A3.9 Scatterplot of Eu release in relation to U release, where points have been categorized by colour depending on NaCl content and the grey line is a straight y = x line. Circles represent unspecified Eu, triangles Eu-153 and diamonds Eu-154.

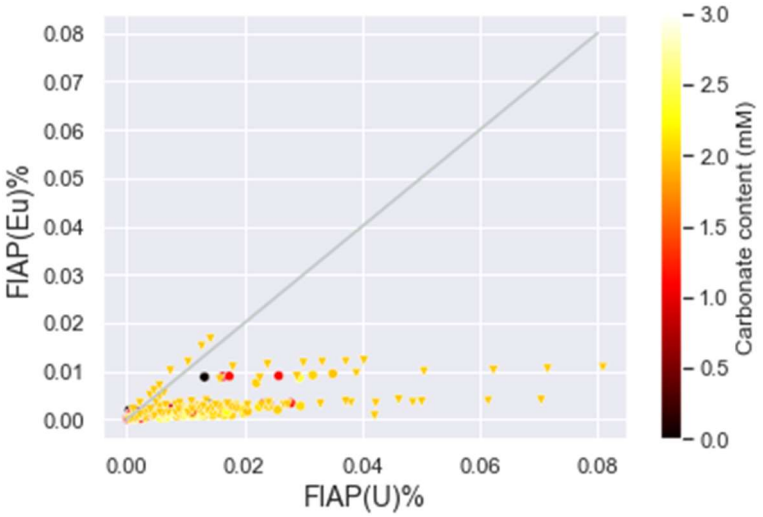

Fig A3.10 Scatterplot of Eu release in relation to U release, where points have been categorized by colour depending on carbonate content and the grey line is a straight y = x line. Circles represent unspecified Eu, triangles Eu-153 and diamonds Eu-154.

Cerium

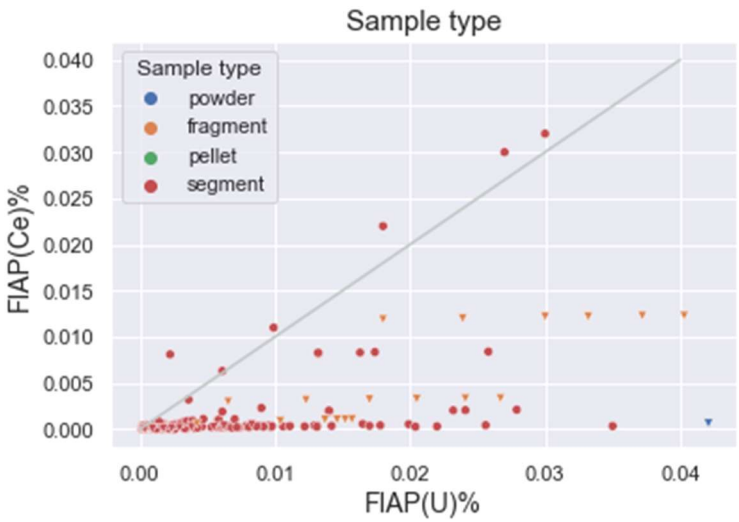

Fig A3.11 Scatterplot of Ce release in relation to U release, where points have been categorized by colour depending on sample type and the grey line is a straight y = x line. Circles represent unspecified Ce, triangles Ce-140 and diamonds Ce-144.

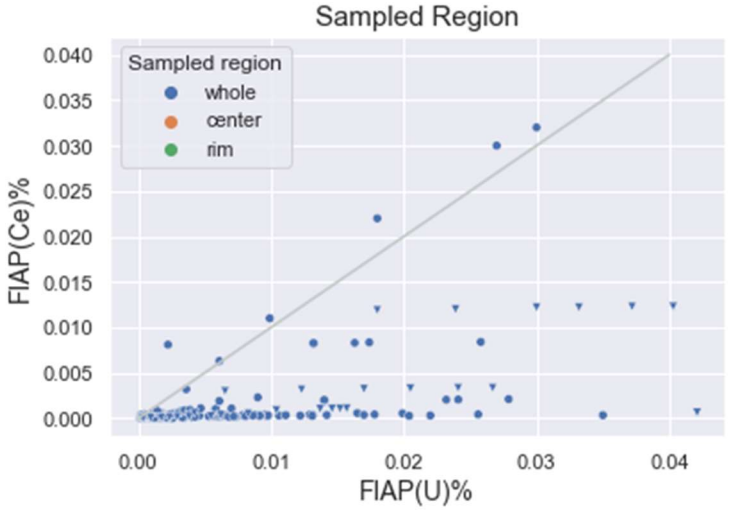

Fig A3.12 Scatterplot of Ce release in relation to U release, where points have been categorized by colour depending on sampled region and the grey line is a straight y = x line. Circles represent unspecified Ce, triangles Ce-140 and diamonds Ce-144.

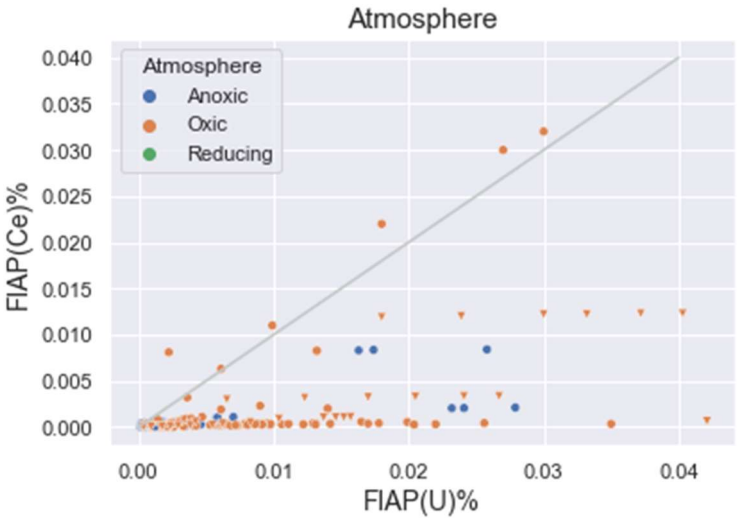

Fig A3.13 Scatterplot of Ce release in relation to U release, where points have been categorized by colour depending on atmosphere and the grey line is a straight y = x line. Circles represent unspecified Ce, triangles Ce-140 and diamonds Ce-144.

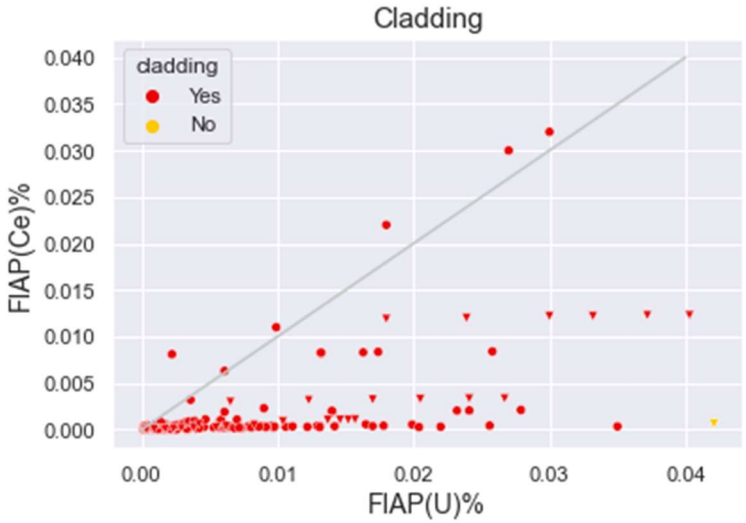

Fig A3.14 Scatterplot of Ce release in relation to U release, where points have been categorized by colour depending on presence of cladding and the grey line is a straight y = x line. Circles represent unspecified Ce, triangles Ce-140 and diamonds Ce-144.

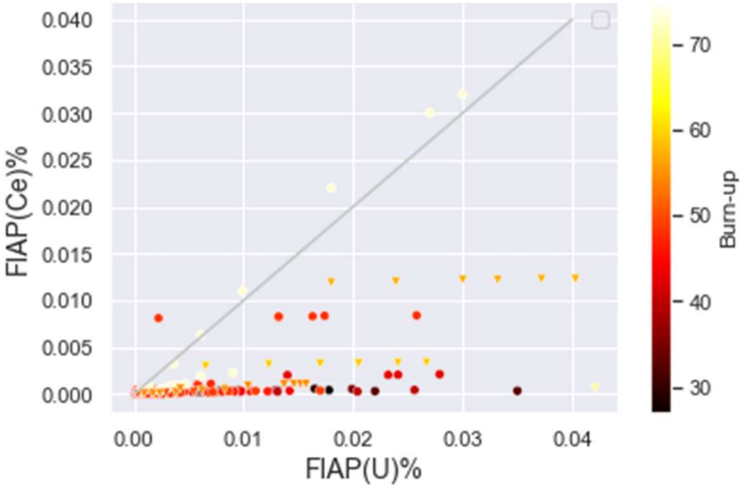

Fig A3.15 Scatterplot of Ce release in relation to U release, where points have been categorized by colour depending on BU type and the grey line is a straight y = x line. Circles represent unspecified Ce, triangles Ce-140 and diamonds Ce-144.

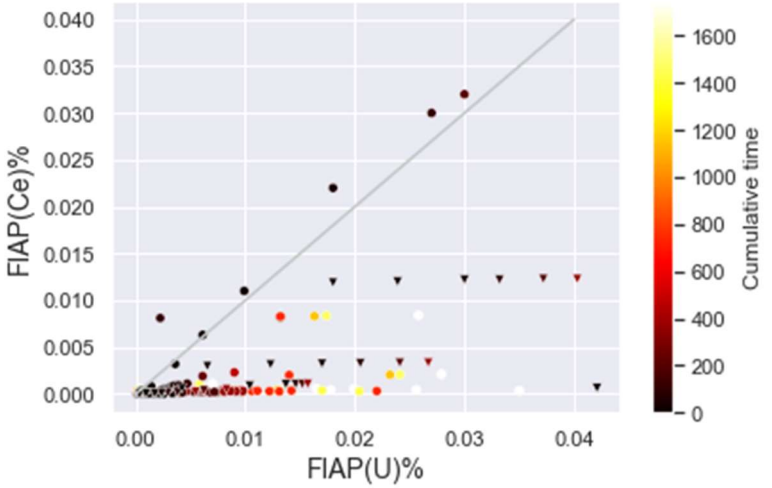

Fig A3.16 Scatterplot of Ce release in relation to U release, where points have been categorized by colour depending on cumulative time and the grey line is a straight y = x line. Circles represent unspecified Ce, triangles Ce-140 and diamonds Ce-144.

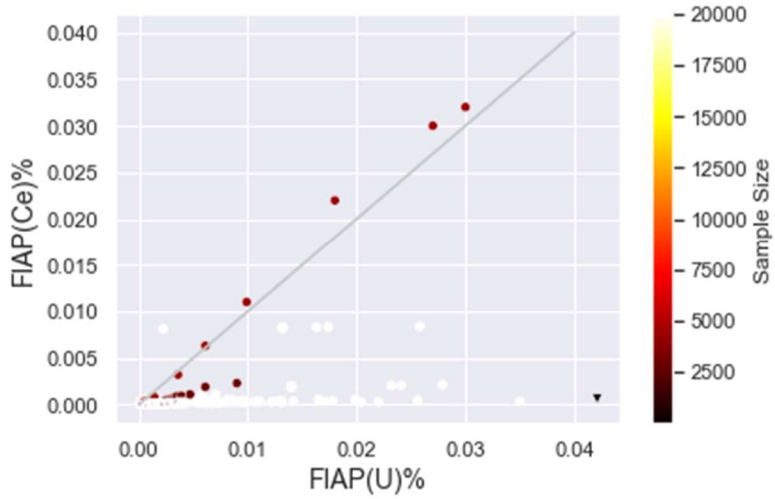

Fig A3.17 Scatterplot of Ce release in relation to U release, where points have been categorized by colour depending on sample size and the grey line is a straight y = x line. Circles represent unspecified Ce, triangles Ce-140 and diamonds Ce-144.

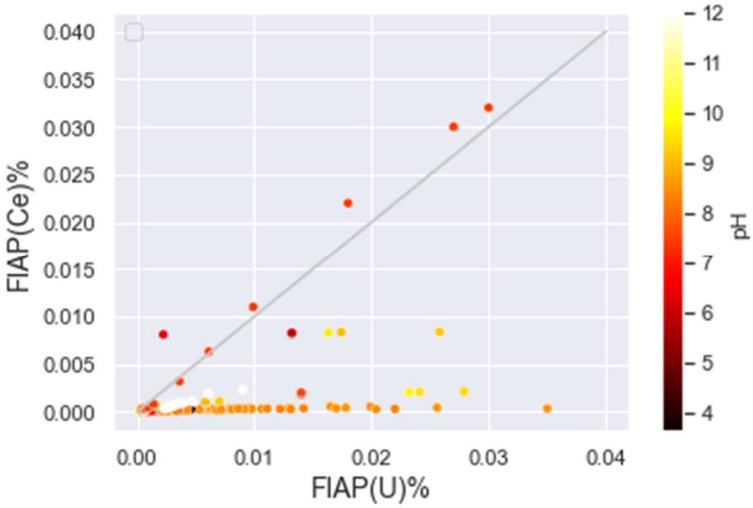

Fig A3.18 Scatterplot of Ce release in relation to U release, where points have been categorized by colour depending on pH and the grey line is a straight y = x line. Circles represent unspecified Ce, triangles Ce-140 and diamonds Ce-144.

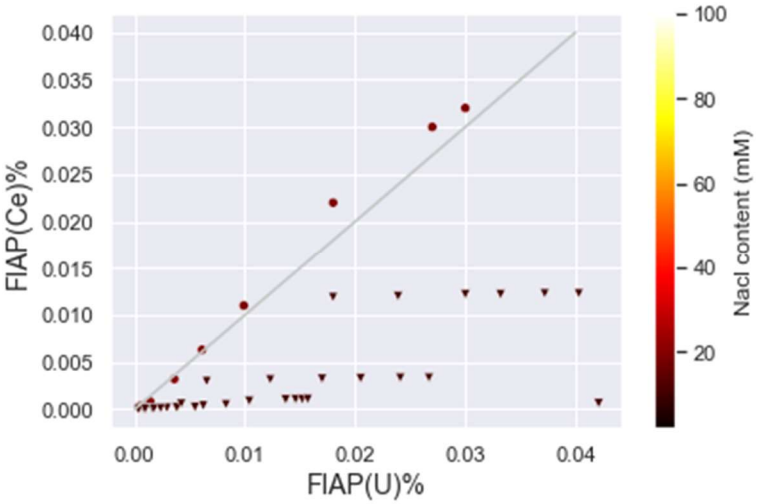

Fig A3.19 Scatterplot of Ce release in relation to U release, where points have been categorized by colour depending on NaCl content and the grey line is a straight y = x line. Circles represent unspecified Ce, triangles Ce-140 and diamonds Ce-144.

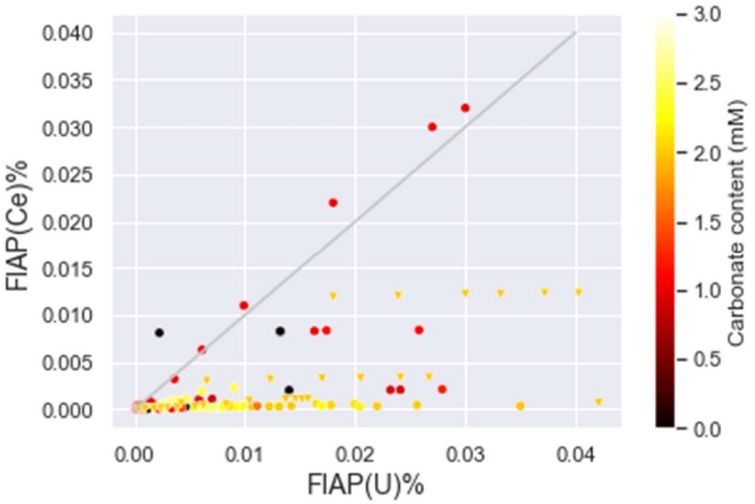

Fig A3.20 Scatterplot of Ce release in relation to U release, where points have been categorized by colour depending on carbonate content and the grey line is a straight y = x line. Circles represent unspecified Ce, triangles Ce-140 and diamonds Ce-144.

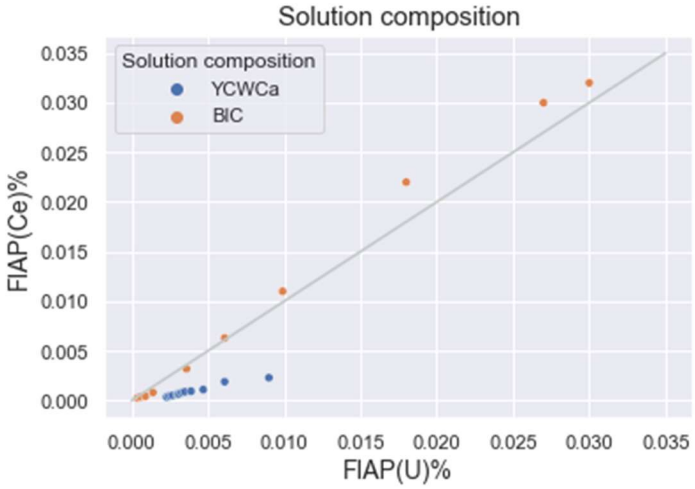

Fig A3.21 Scatterplot of Ce release in relation to U release, where points have been categorized by colour depending on solution composition of Clarens et al. [9] samples and the grey line is a straight y = x line.

Praseodymium

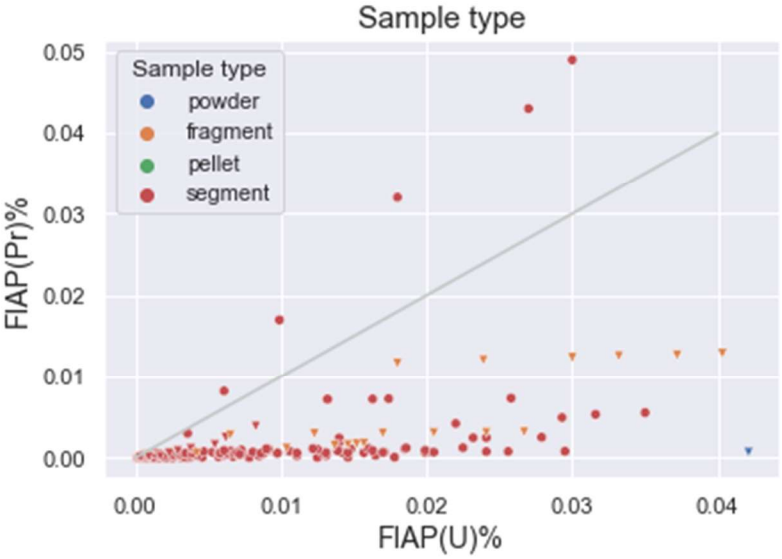

Fig A3.22 Scatterplot of Pr release in relation to U release, where points have been categorized by colour depending on sample type and the grey line is a straight y = x line. Circles represent unspecified Pr and triangles Pr-141.

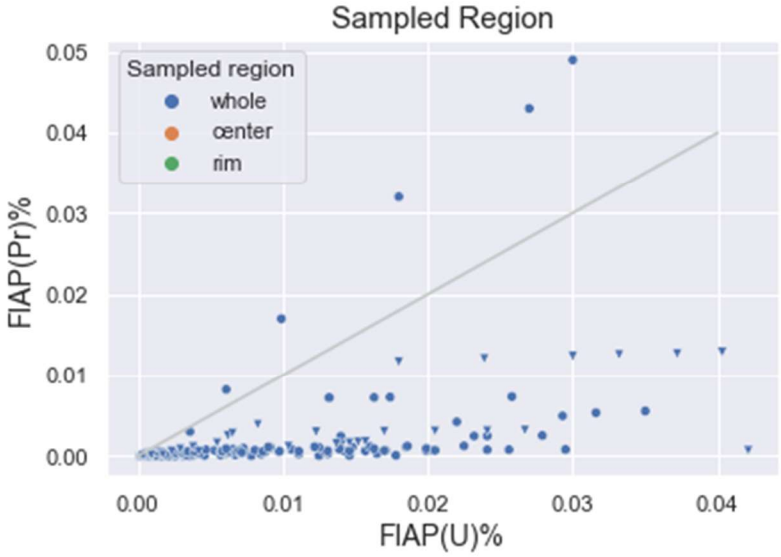

Fig A3.23 Scatterplot of Pr release in relation to U release, where points have been categorized by colour depending on sample region and the grey line is a straight y = x line. Circles represent unspecified Pr and triangles Pr-141.

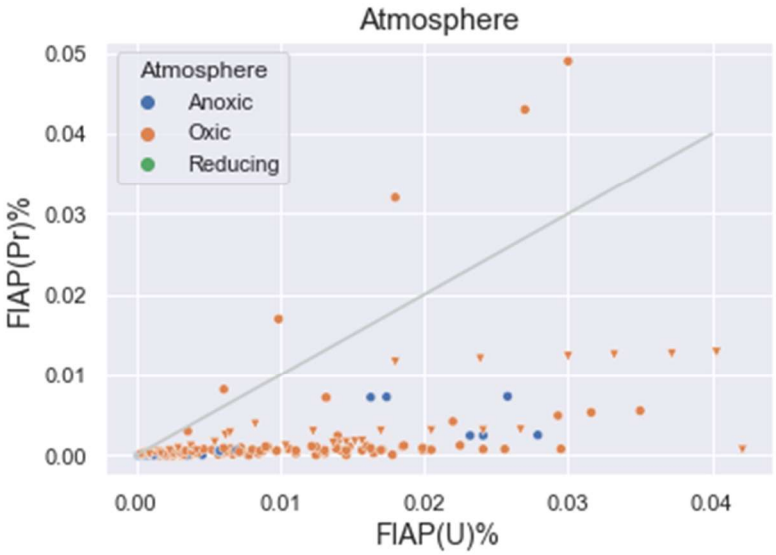

Fig A3.24 Scatterplot of Pr release in relation to U release, where points have been categorized by colour depending on atmosphere and the grey line is a straight y = x line. Circles represent unspecified Pr and triangles Pr-141.

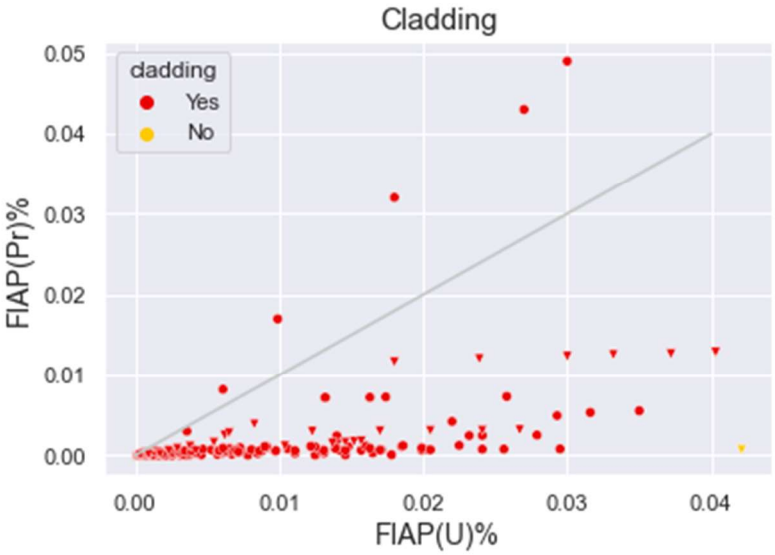

Fig A3.25 Scatterplot of Pr release in relation to U release, where points have been categorized by colour depending on presence of cladding and the grey line is a straight y = x line. Circles represent unspecified Pr and triangles Pr-141.

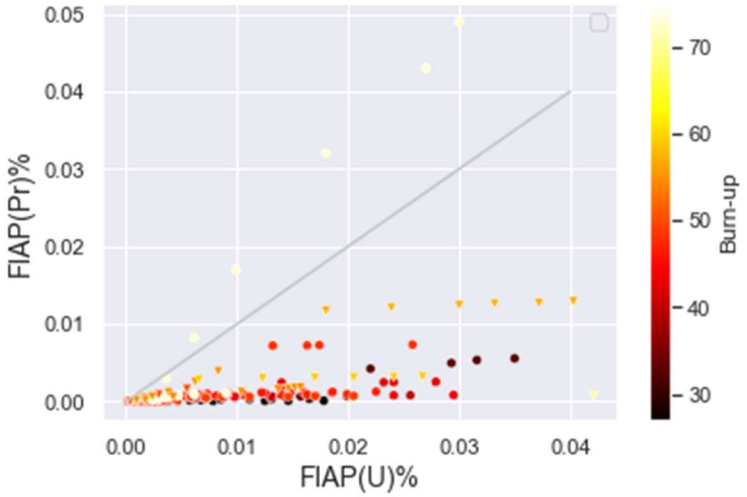

Fig A3.26 Scatterplot of Pr release in relation to U release, where points have been categorized by colour depending on BU and the grey line is a straight y = x line. Circles represent unspecified Pr and triangles Pr-141.

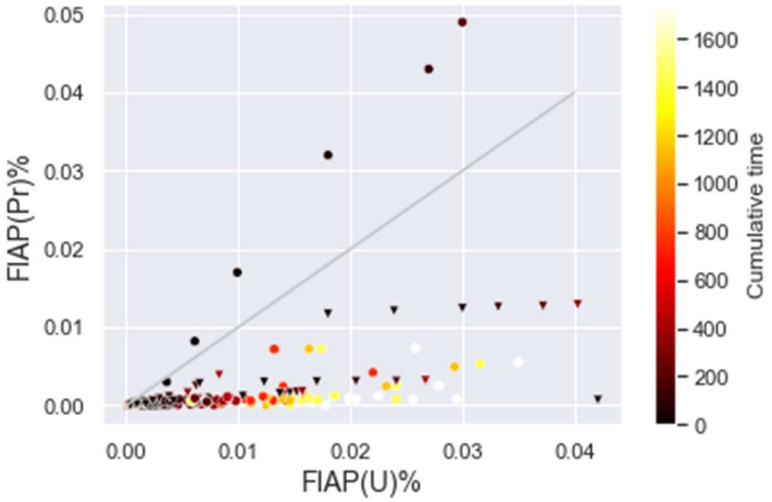

Fig A3.27 Scatterplot of Pr release in relation to U release, where points have been categorized by colour depending on cumulative time and the grey line is a straight y = x line. Circles represent unspecified Pr and triangles Pr-141.

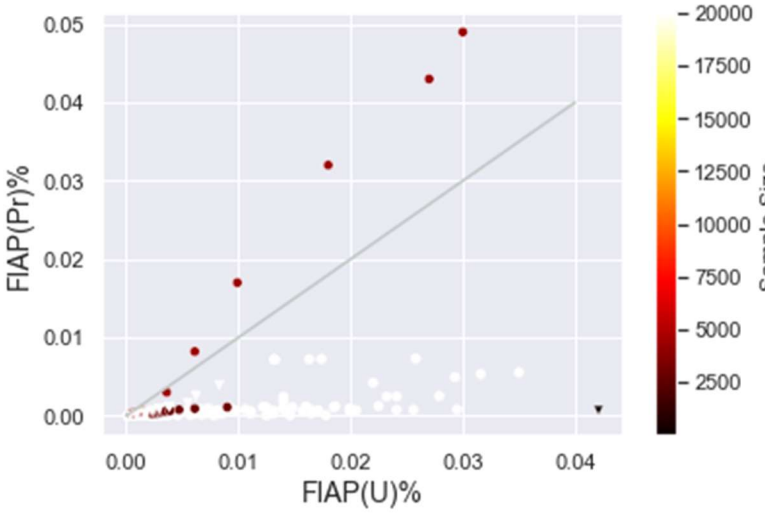

Fig A3.28 Scatterplot of Pr release in relation to U release, where points have been categorized by colour depending on sample size and the grey line is a straight y = x line. Circles represent unspecified Pr and triangles Pr-141.

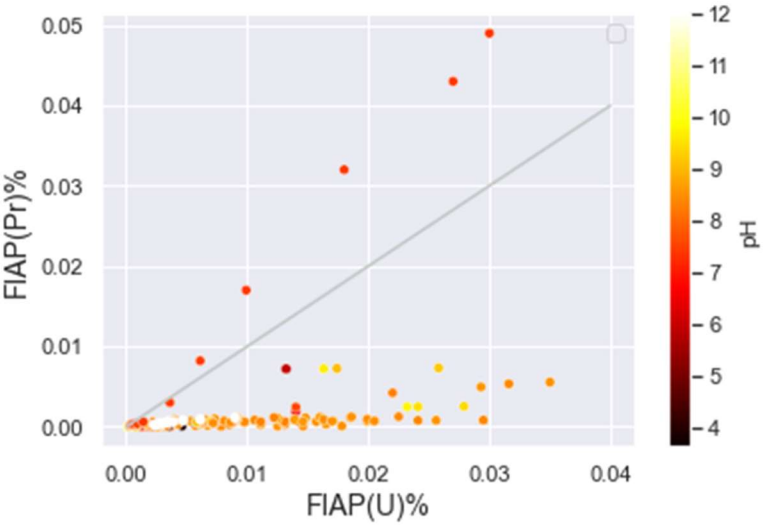

Fig A3.29 Scatterplot of Pr release in relation to U release, where points have been categorized by colour depending on pH and the grey line is a straight y = x line. Circles represent unspecified Pr and triangles Pr-141.

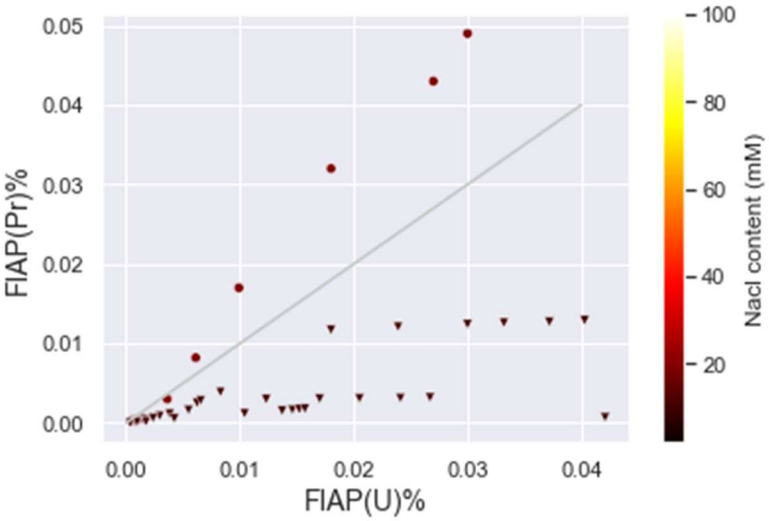

Fig A3.30 Scatterplot of Pr release in relation to U release, where points have been categorized by colour depending on NaCl content and the grey line is a straight y = x line. Circles represent unspecified Pr and triangles Pr-141.

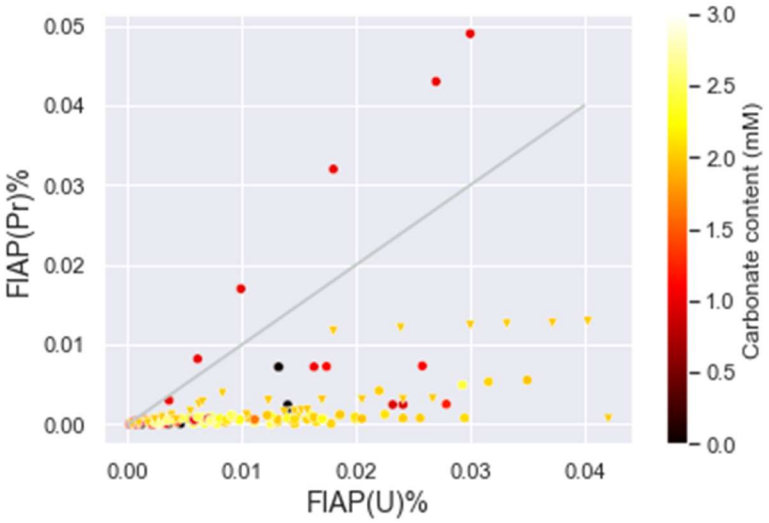

Fig A3.31 Scatterplot of Pr release in relation to U release, where points have been categorized by colour depending on carbonate content and the grey line is a straight y = x line. Circles represent unspecified Pr and triangles Pr-141.

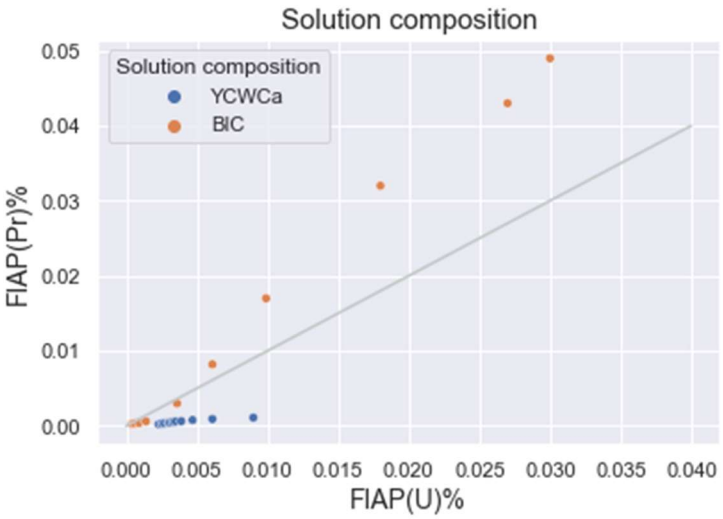

Fig A3.32 Scatterplot of Pr release in relation to U release, where points have been categorized by colour depending on solution composition of the Clarens et al. samples and the grey line is a straight y = x line.

Promethium

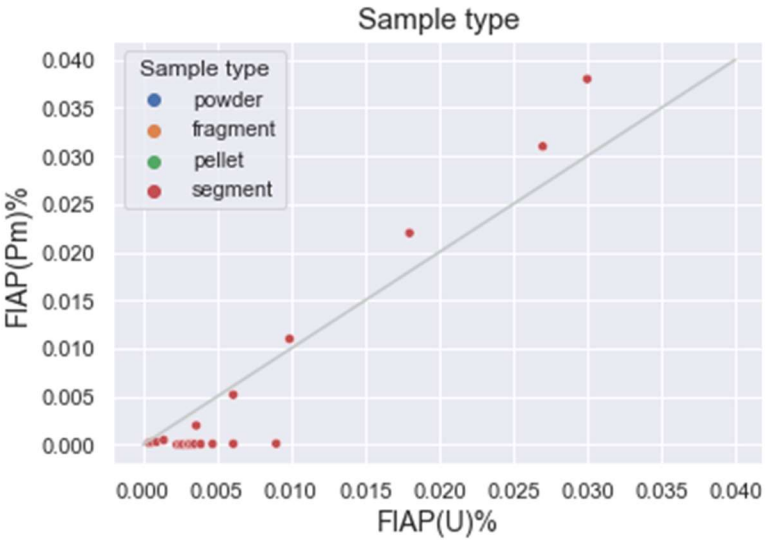

Fig A3.33 Scatterplot of Pm release in relation to U release, where points have been categorized by colour depending on sample type and the grey line is a straight y = x line.

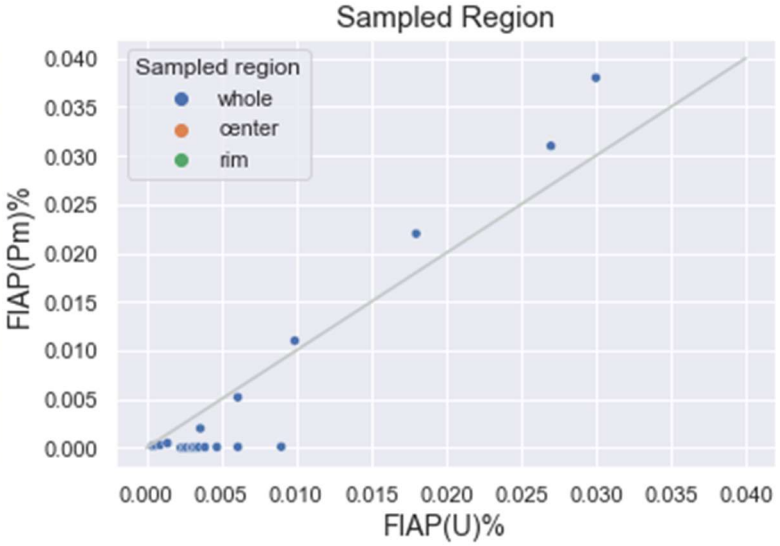

Fig A3.34 Scatterplot of Pm release in relation to U release, where points have been categorized by colour depending on sample region and the grey line is a straight y = x line.

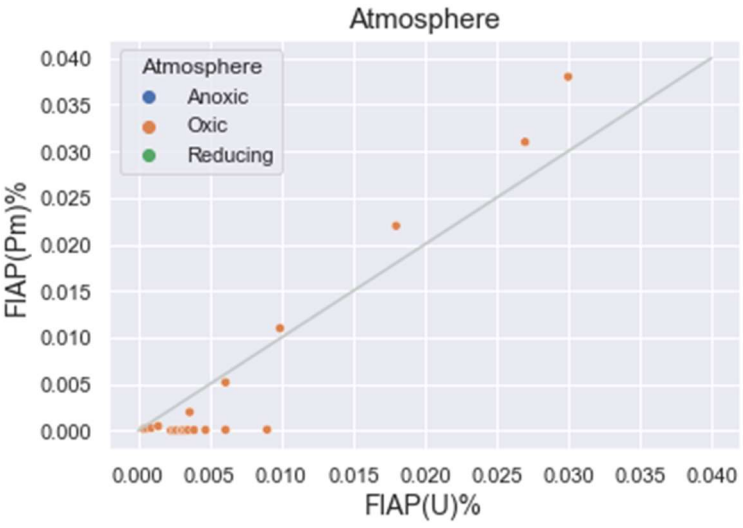

Fig A3.35 Scatterplot of Pm release in relation to U release, where points have been categorized by colour depending on atmosphere and the grey line is a straight y = x line.

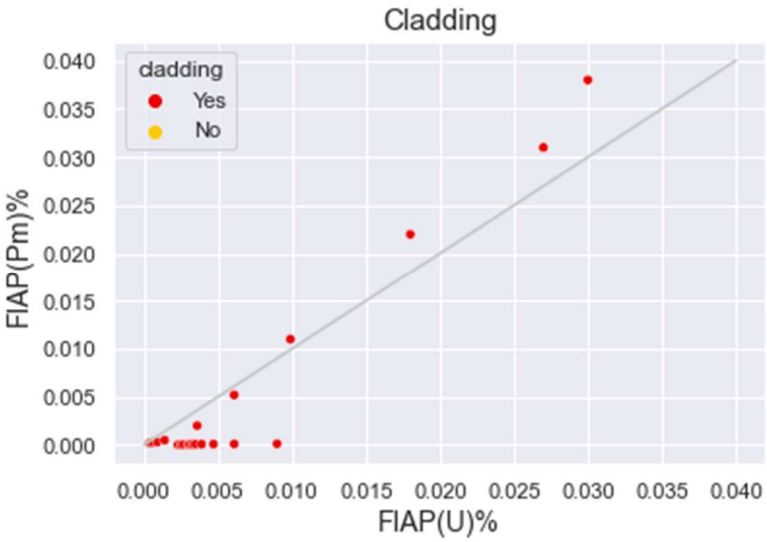

Fig A3.36 Scatterplot of Pm release in relation to U release, where points have been categorized by colour depending on presence of cladding and the grey line is a straight y = x line.

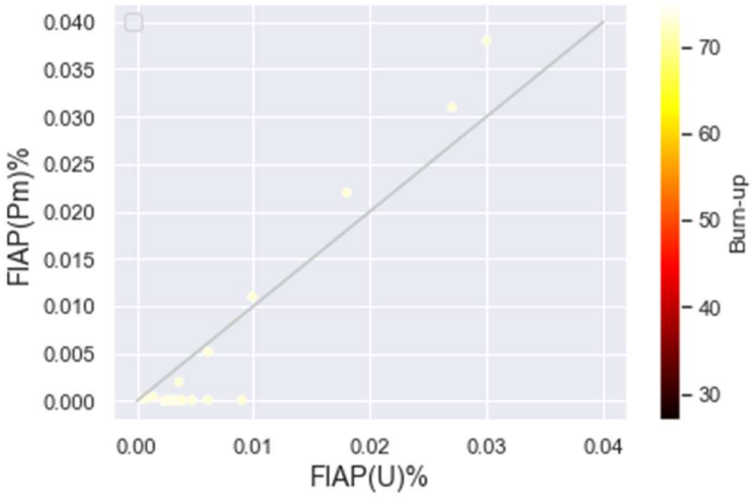

Fig A3.37 Scatterplot of Pm release in relation to U release, where points have been categorized by colour depending on BU and the grey line is a straight y = x line.

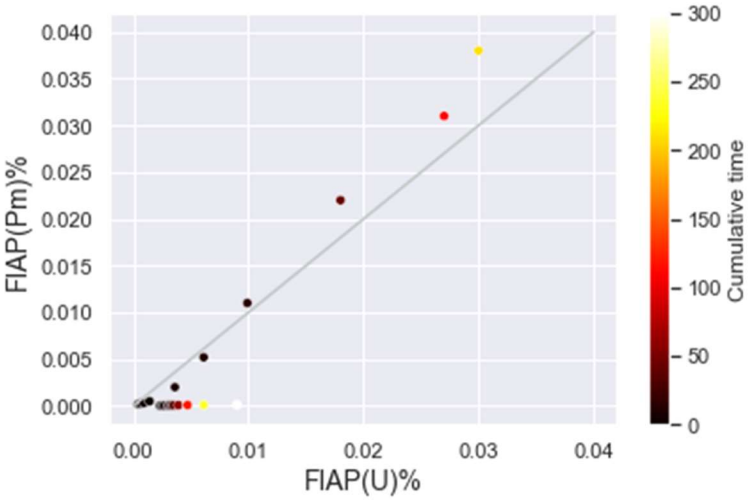

Fig A3.38 Scatterplot of Pm release in relation to U release, where points have been categorized by colour depending on cumulative time and the grey line is a straight y = x line.

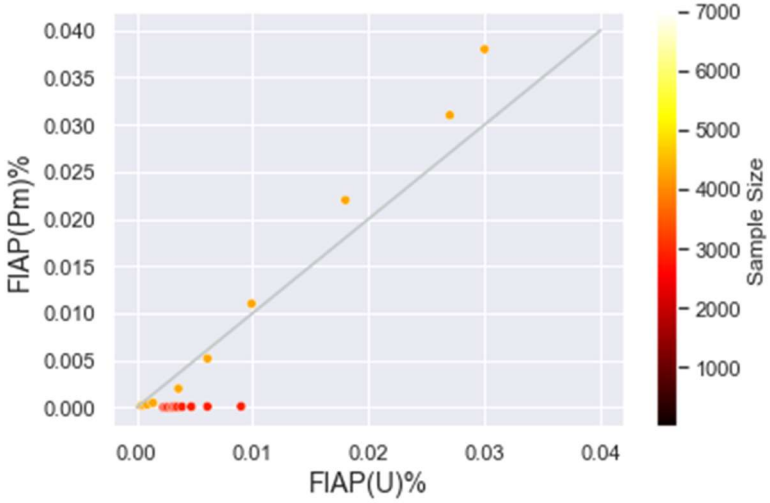

Fig A3.39 Scatterplot of Pm release in relation to U release, where points have been categorized by colour depending on sample size and the grey line is a straight y = x line.

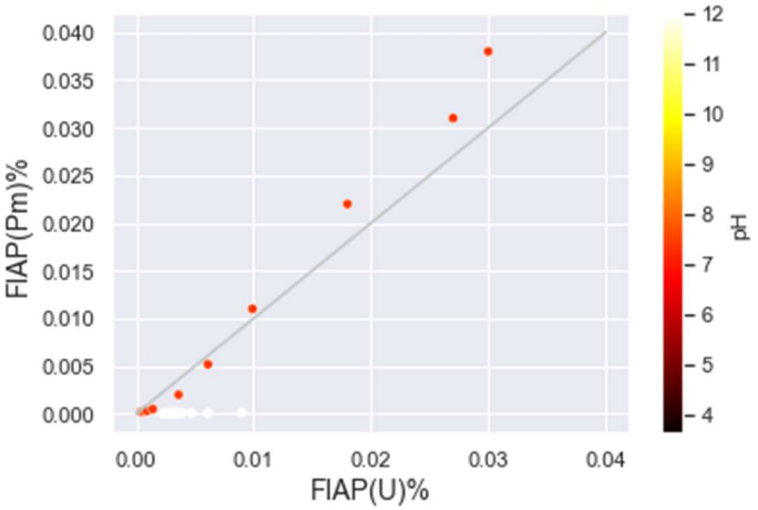

Fig A3.40 Scatterplot of Pm release in relation to U release, where points have been categorized by colour depending on pH and the grey line is a straight y = x line.

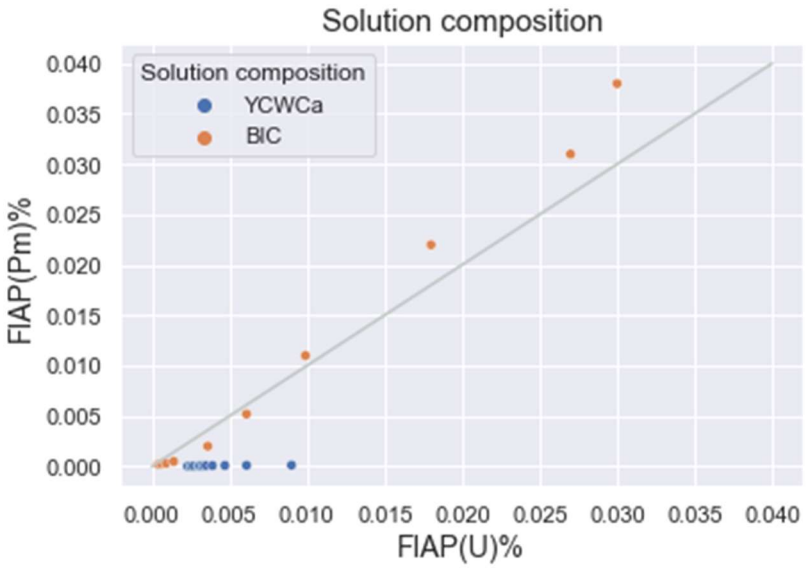

Fig A3.41 Scatterplot of Pm release in relation to U release, where points have been categorized by colour depending on solution composition and the grey line is a straight y = x line.

A.4 Scatterplots Group 2a

Appendix A.4 shows all the plots of the elements in group 2a (Pd, Ag, Sm), both plots used and not used in section 4. The plots are shown by element.

Palladium

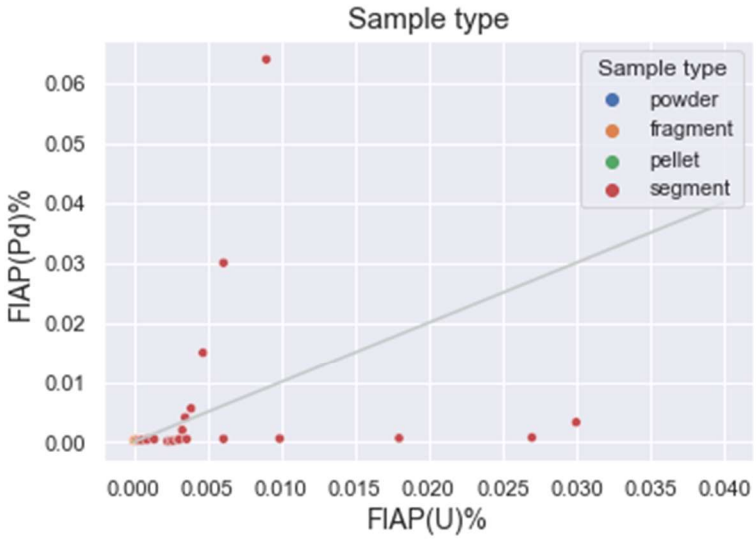

Fig A4.1 Scatterplot of Pd release in relation to U release, where points have been categorized by colour depending on sample type and the grey line is a straight y = x line.

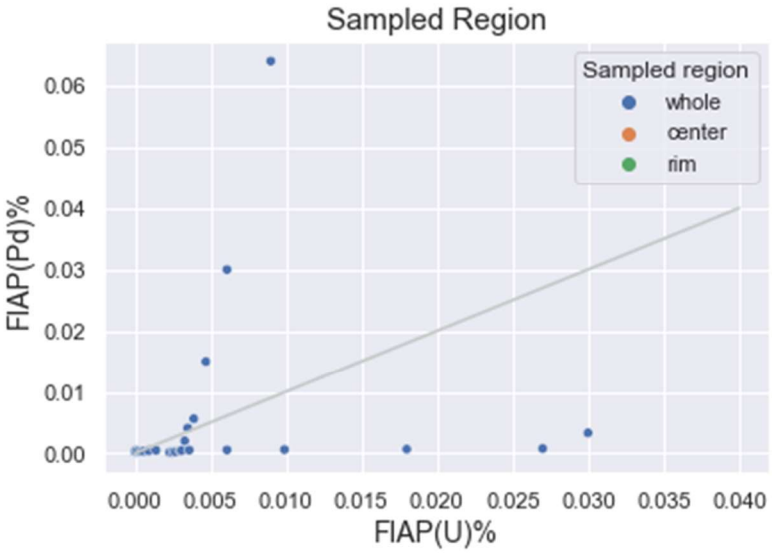

Fig A4.2 Scatterplot of Pd release in relation to U release, where points have been categorized by colour depending on sampled region and the grey line is a straight y = x line.

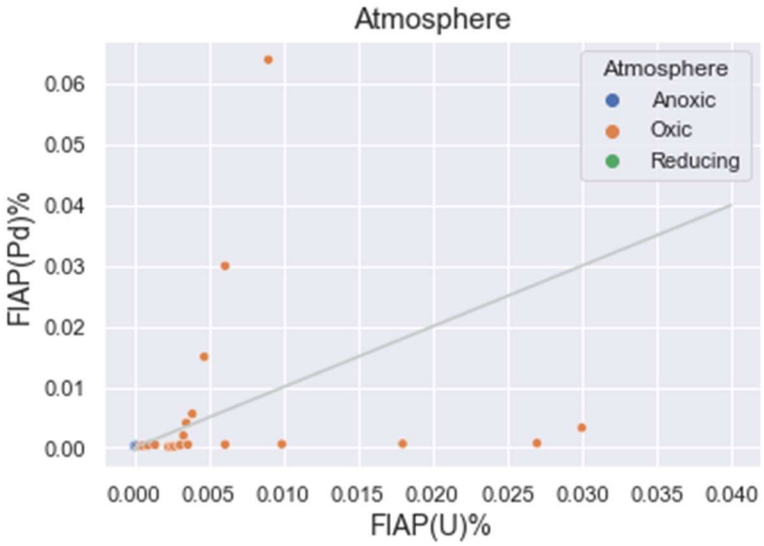

Fig A4.3 Scatterplot of Pd release in relation to U release, where points have been categorized by colour depending on atmosphere and the grey line is a straight y = x line.

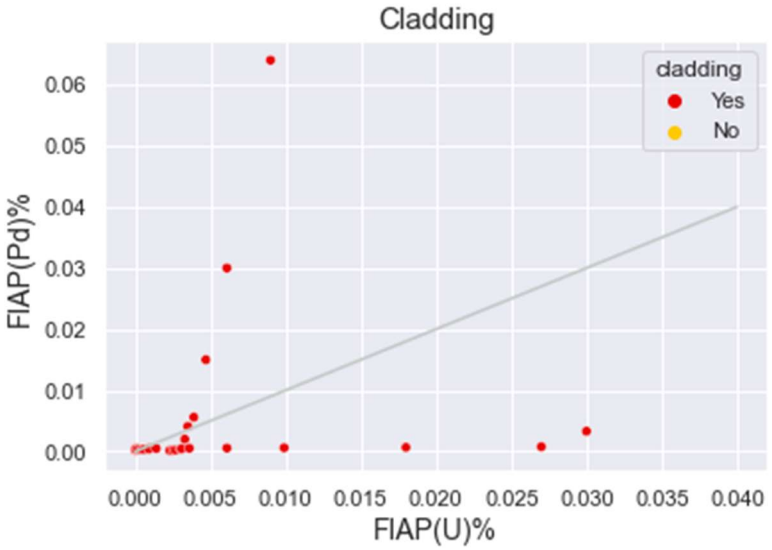

Fig A4.4 Scatterplot of Pd release in relation to U release, where points have been categorized by colour depending on presence of cladding and the grey line is a straight y = x line.

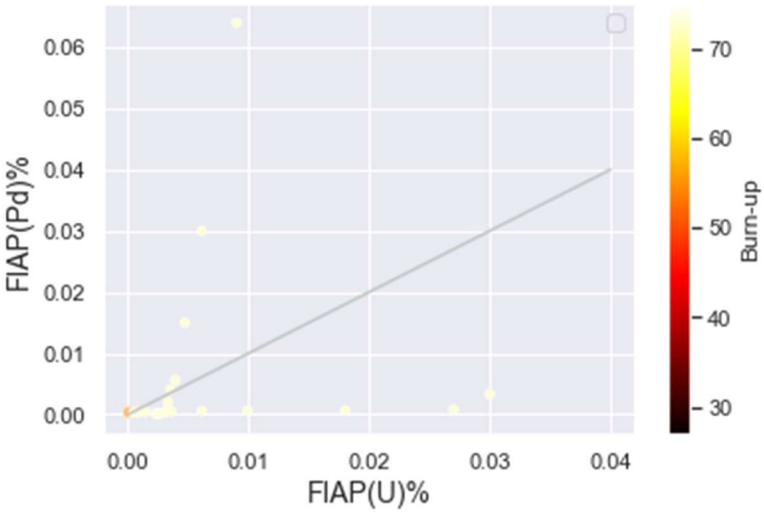

Fig A4.5 Scatterplot of Pd release in relation to U release, where points have been categorized by colour depending on BU and the grey line is a straight y = x line.

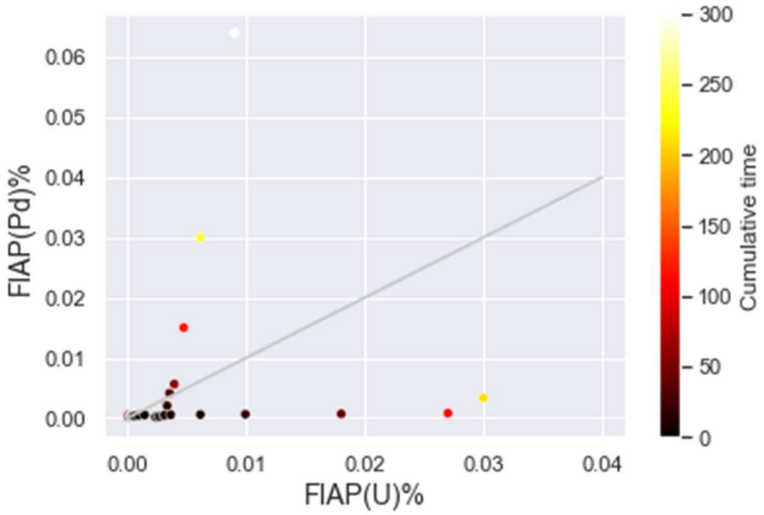

Fig A4.6 Scatterplot of Pd release in relation to U release, where points have been categorized by colour depending on cumulative time and the grey line is a straight y = x line.

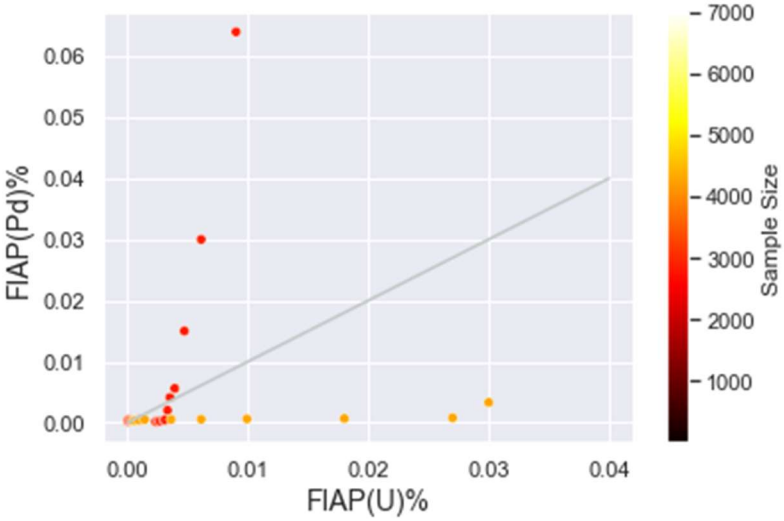

Fig A4.7 Scatterplot of Pd release in relation to U release, where points have been categorized by colour depending on sample size and the grey line is a straight y = x line.

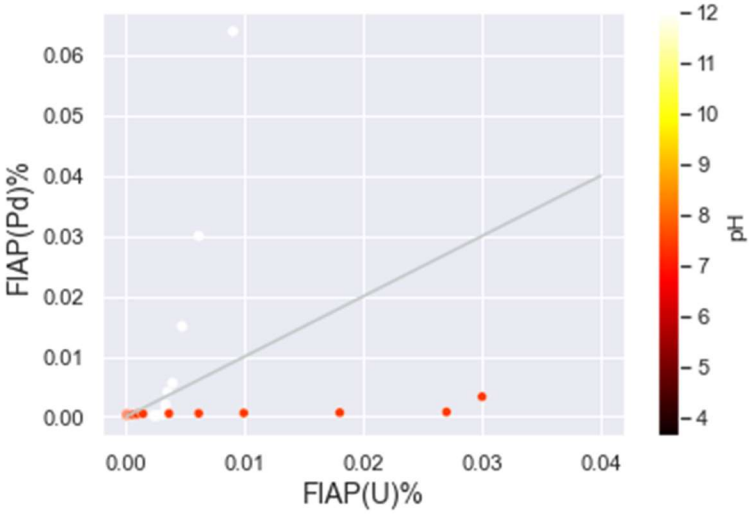

Fig A4.8 Scatterplot of Pd release in relation to U release, where points have been categorized by colour depending on pH and the grey line is a straight y = x line.

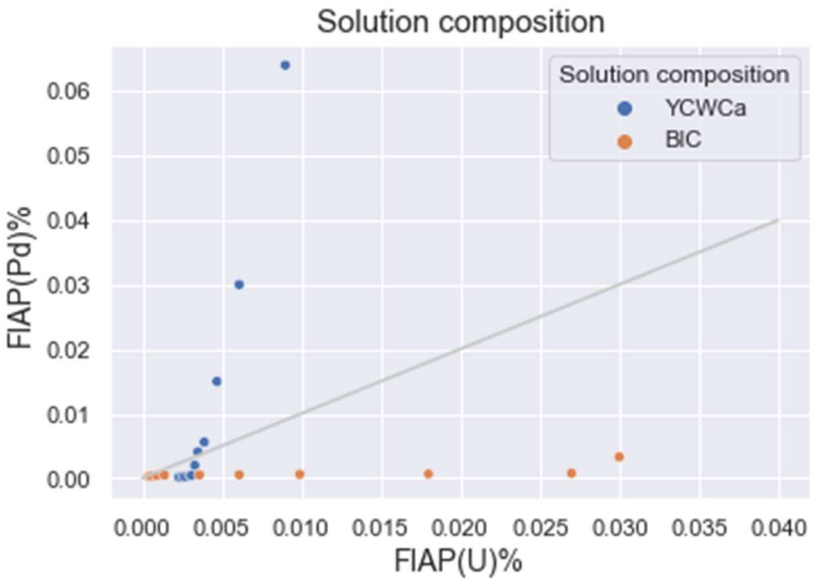

Fig A4.9 Scatterplot of Pd release in relation to U release, where points have been categorized by colour depending on solution composition and the grey line is a straight y = x line.

Silver

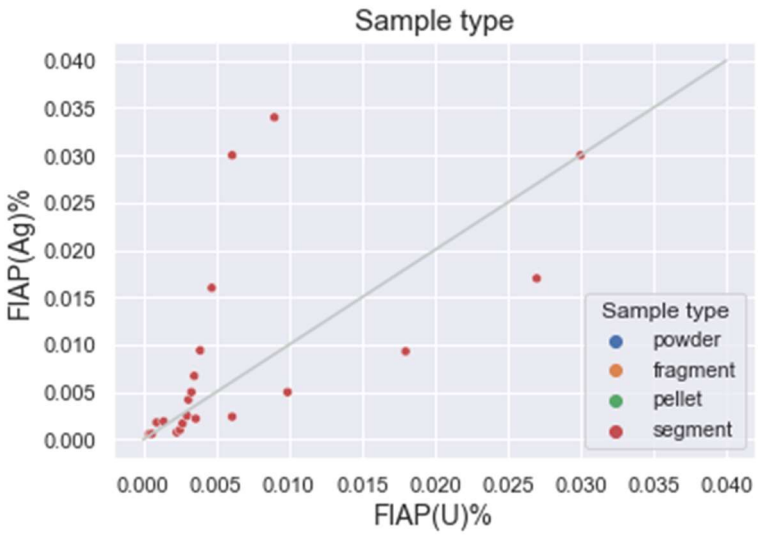

Fig A4.10 Scatterplot of Ag release in relation to U release, where points have been categorized by colour depending on sample type and the grey line is a straight y = x line.

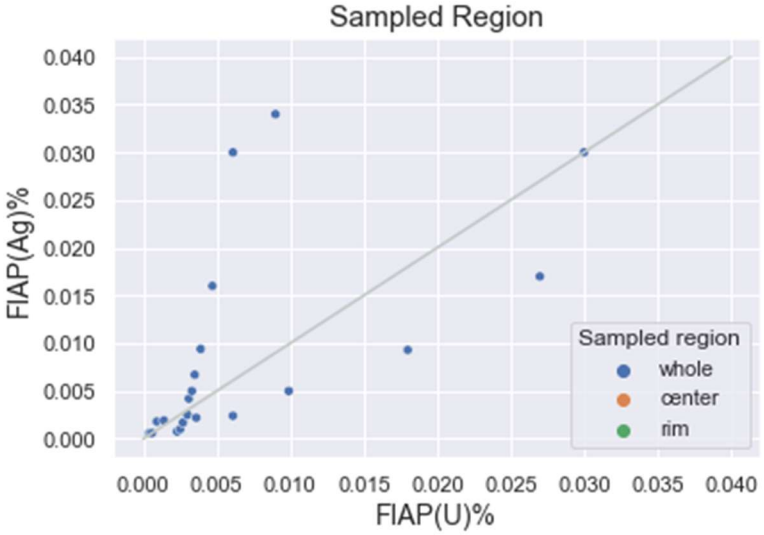

Fig A4.11 Scatterplot of Ag release in relation to U release, where points have been categorized by colour depending on sampled region and the grey line is a straight y = x line.

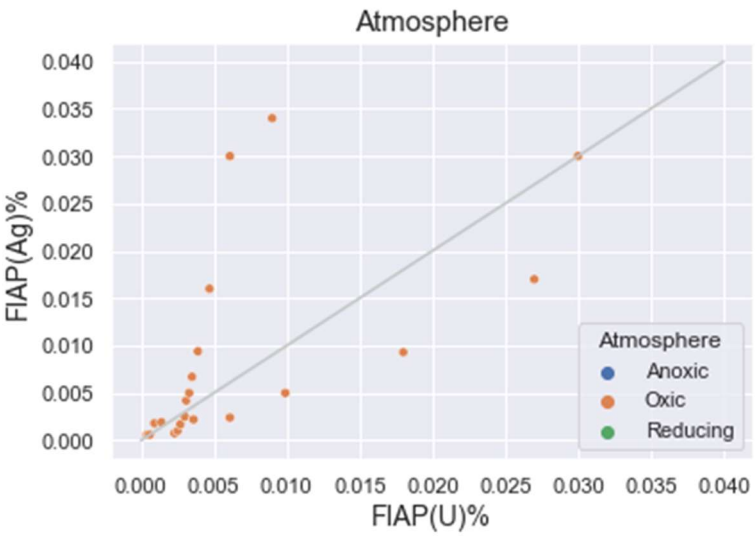

Fig A4.12 Scatterplot of Ag release in relation to U release, where points have been categorized by colour depending on atmosphere and the grey line is a straight y = x line.

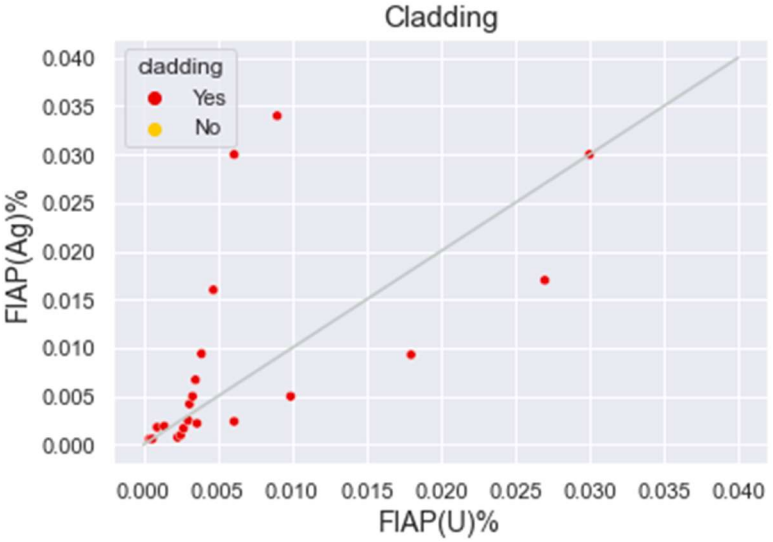

Fig A4.13 Scatterplot of Ag release in relation to U release, where points have been categorized by colour depending on presence of cladding and the grey line is a straight y = x line.

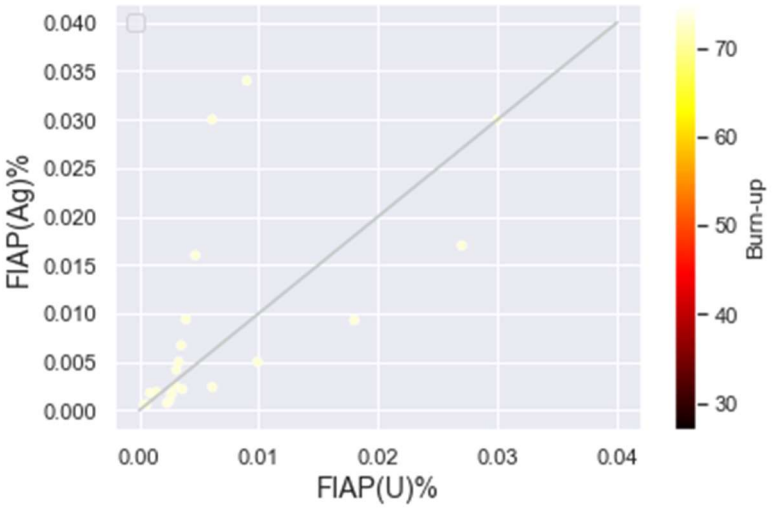

Fig A4.14 Scatterplot of Ag release in relation to U release, where points have been categorized by colour depending on BU and the grey line is a straight y = x line.

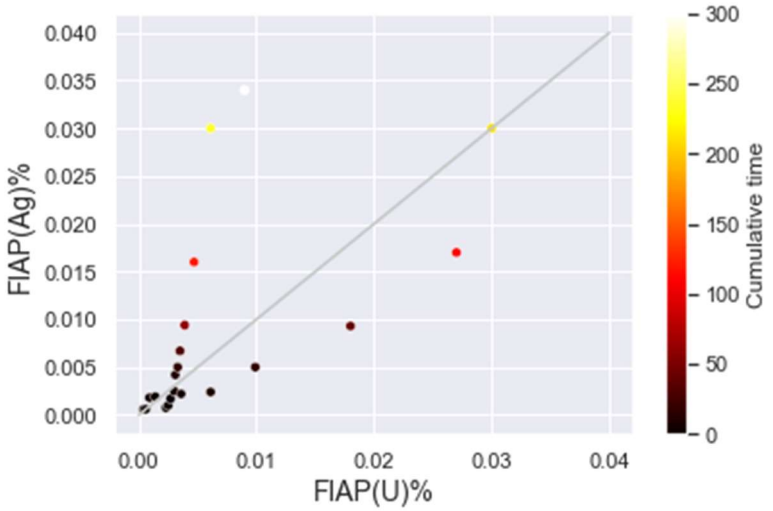

Fig A4.15 Scatterplot of Ag release in relation to U release, where points have been categorized by colour depending on cumulative time and the grey line is a straight y = x line.

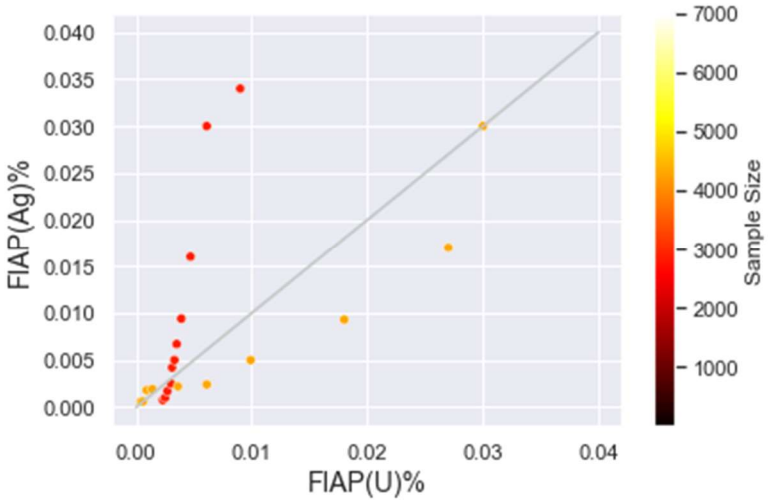

Fig A4.16 Scatterplot of Ag release in relation to U release, where points have been categorized by colour depending on sample size and the grey line is a straight y = x line.

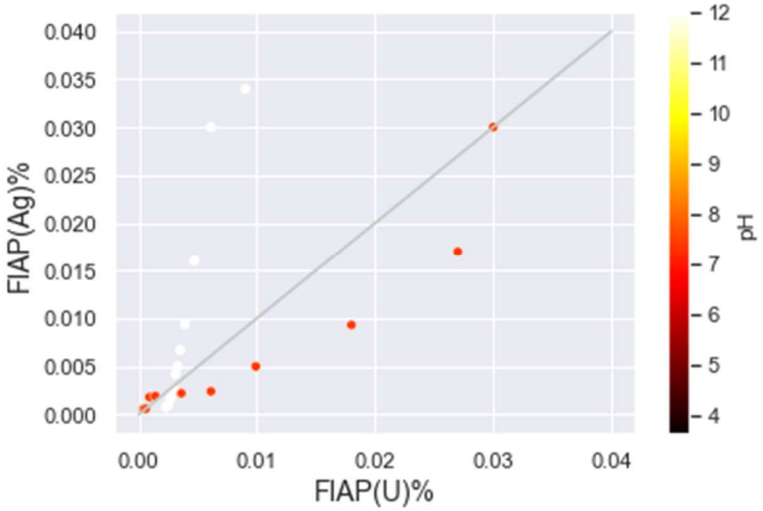

Fig A4.17 Scatterplot of Ag release in relation to U release, where points have been categorized by colour depending on pH and the grey line is a straight y = x line.

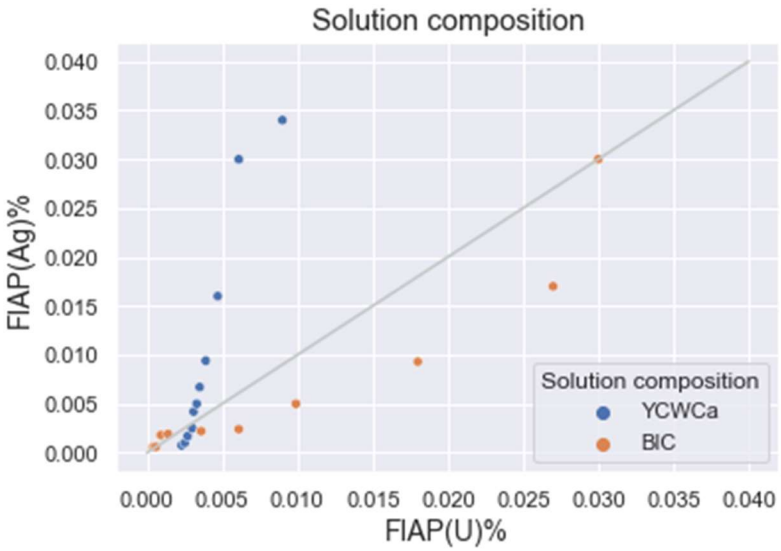

Fig A4.18 Scatterplot of Ag release in relation to U release, where points have been categorized by colour depending on solution composition and the grey line is a straight y = x line.

Samarium

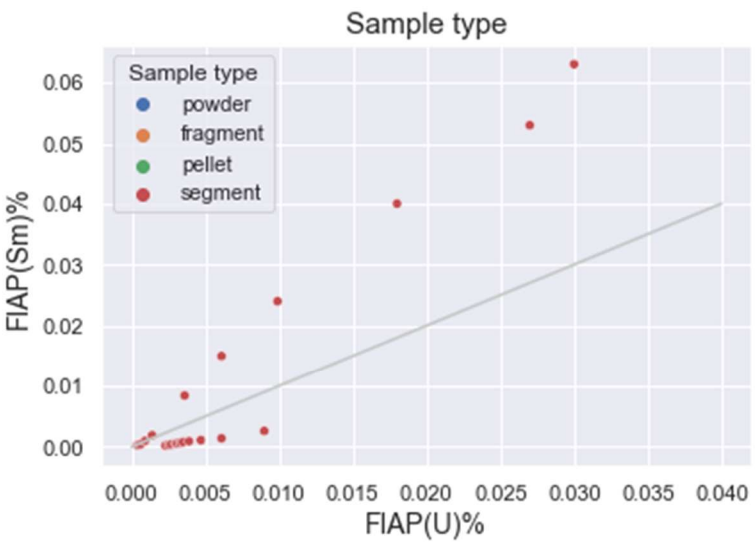

Fig A4.19 Scatterplot of Sm release in relation to U release, where points have been categorized by colour depending on sample type and the grey line is a straight y = x line.

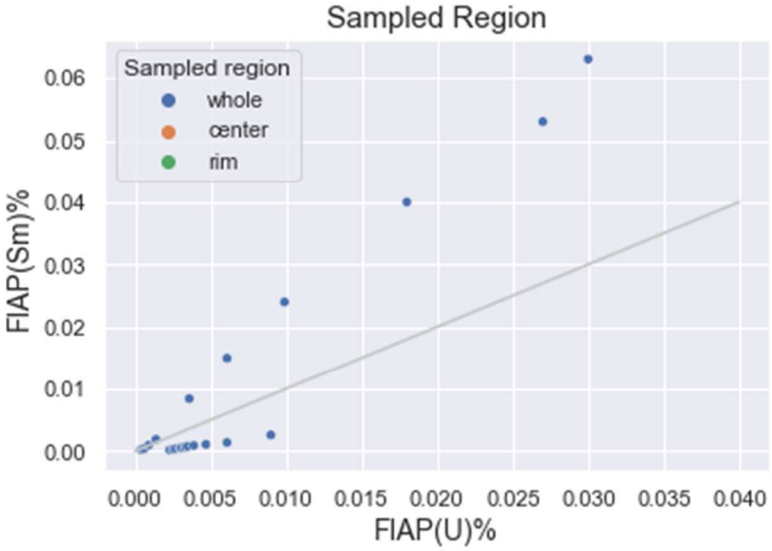

Fig A4.20 Scatterplot of Sm release in relation to U release, where points have been categorized by colour depending on sampled region and the grey line is a straight y = x line.

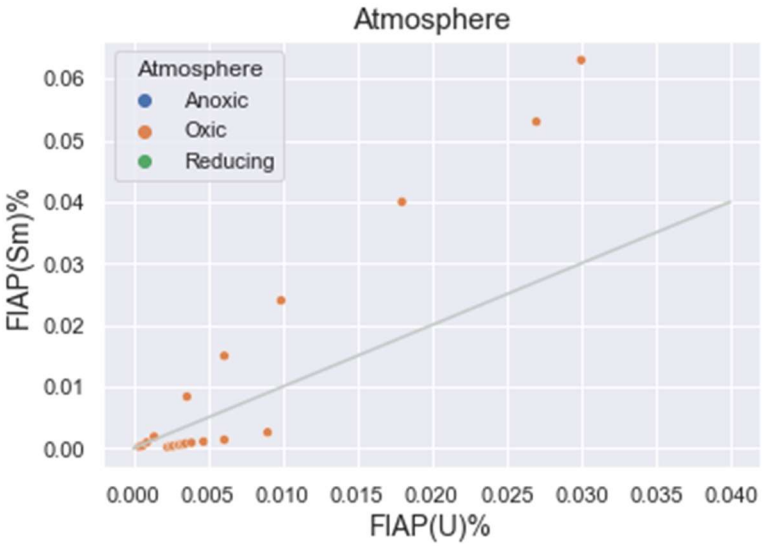

Fig A4.21 Scatterplot of Sm release in relation to U release, where points have been categorized by colour depending on atmosphere and the grey line is a straight y = x line.

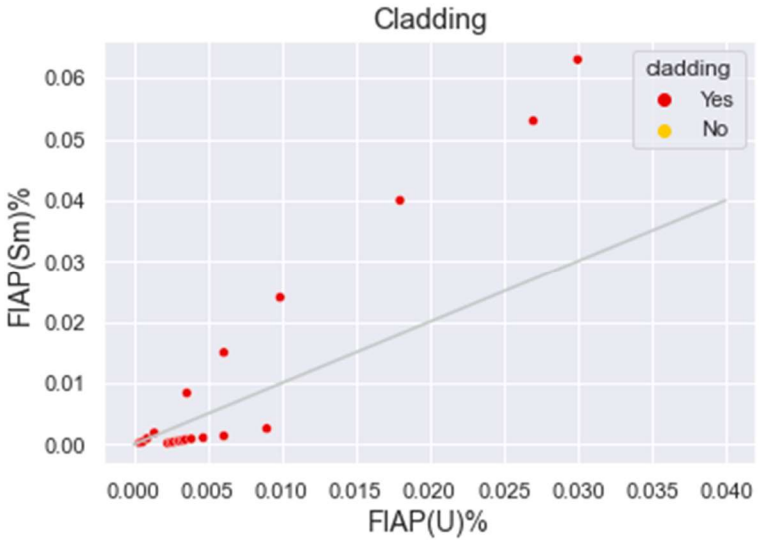

Fig A4.22 Scatterplot of Sm release in relation to U release, where points have been categorized by colour depending on presence of cladding and the grey line is a straight y = x line.

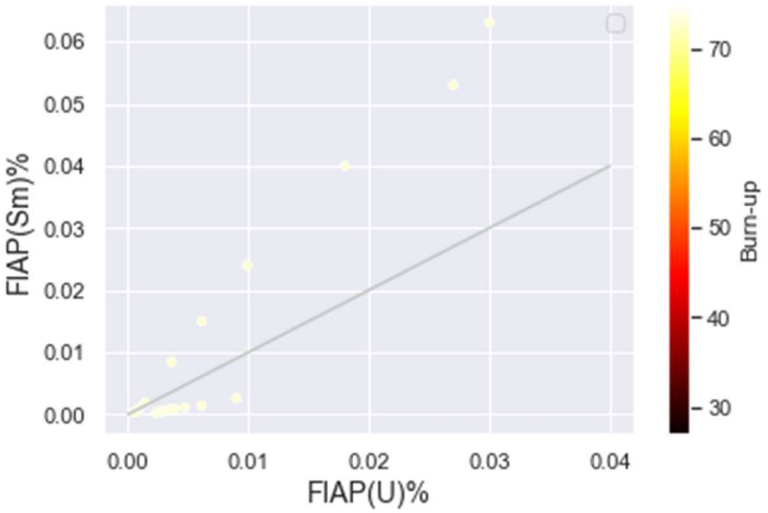

Fig A4.23 Scatterplot of Sm release in relation to U release, where points have been categorized by colour depending on BU and the grey line is a straight y = x line.

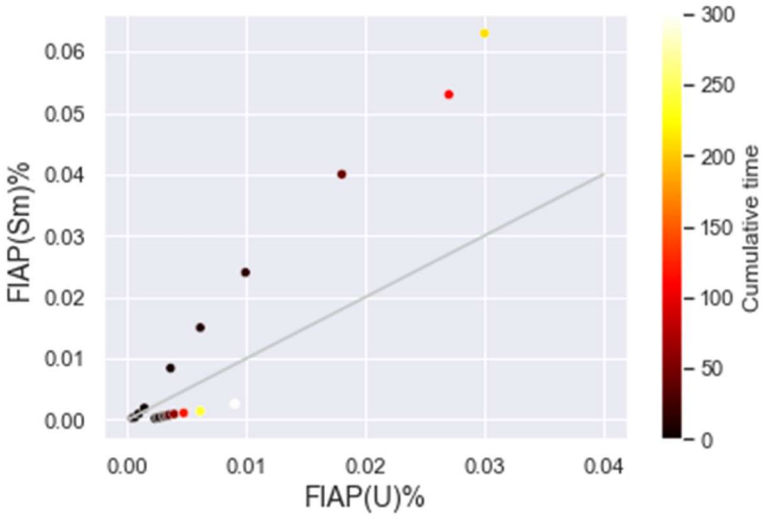

Fig A4.24 Scatterplot of Sm release in relation to U release, where points have been categorized by colour depending on cumulative time and the grey line is a straight y = x line.

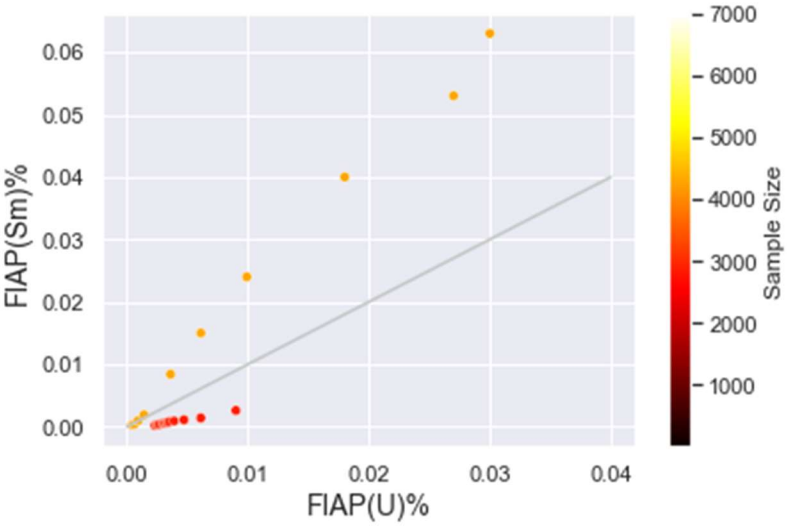

Fig A4.25 Scatterplot of Sm release in relation to U release, where points have been categorized by colour depending on sample size and the grey line is a straight y = x line.

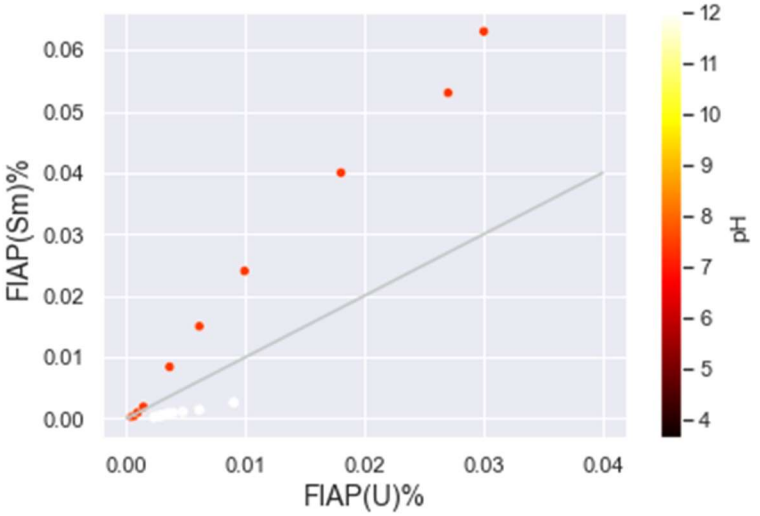

Fig A4.26 Scatterplot of Sm release in relation to U release, where points have been categorized by colour depending on pH and the grey line is a straight y = x line.

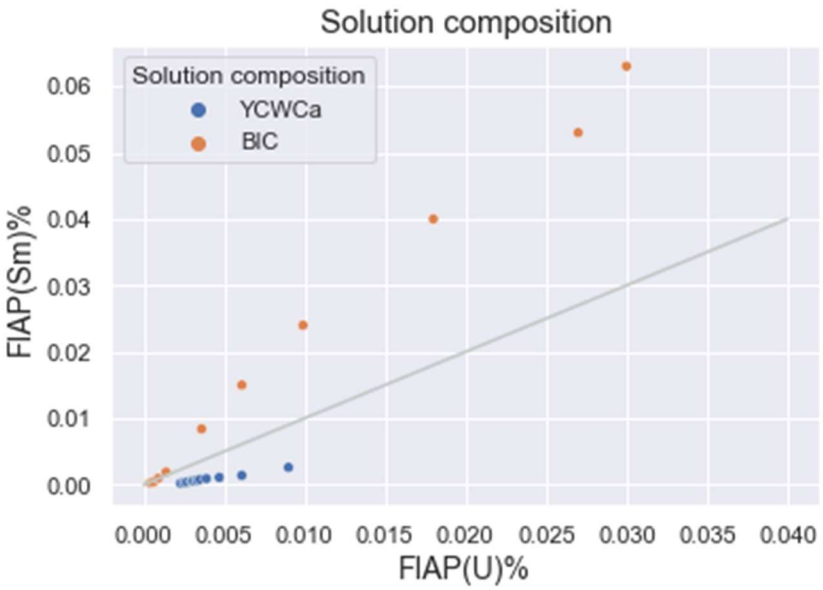

Fig A4.28 Scatterplot of Sm release in relation to U release, where points have been categorized by colour depending on solution composition and the grey line is a straight y = x line.

A.5 Scatterplots Group 2b

Appendix A.5 shows all the plots of the elements in group 2b (Ru, Rh), both plots used and not used in section 4. The plots are shown by element.

Ruthenium

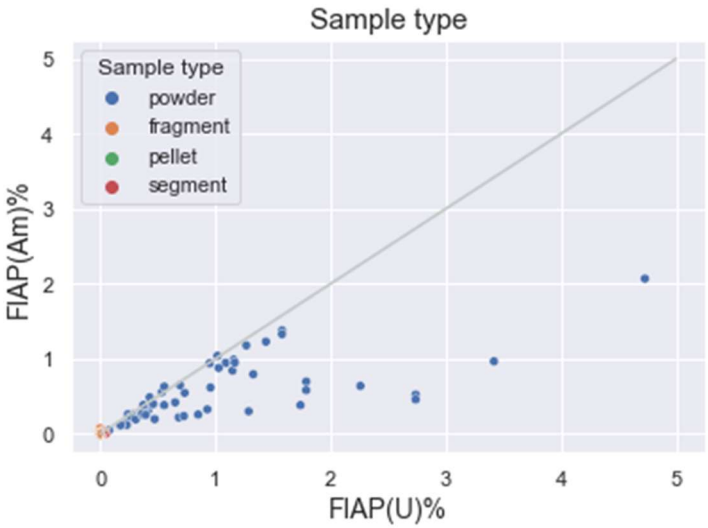

Fig A5.1 Scatterplot of Ru release in relation to U release, where points have been categorized by colour depending on sample type and the grey line is a straight y = x line.

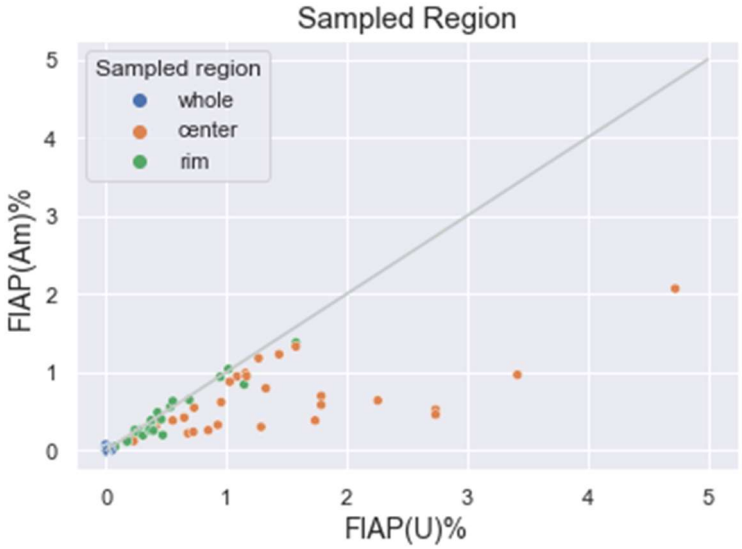

Fig A5.2 Scatterplot of Ru release in relation to U release, where points have been categorized by colour depending on sampled region and the grey line is a straight y = x line.

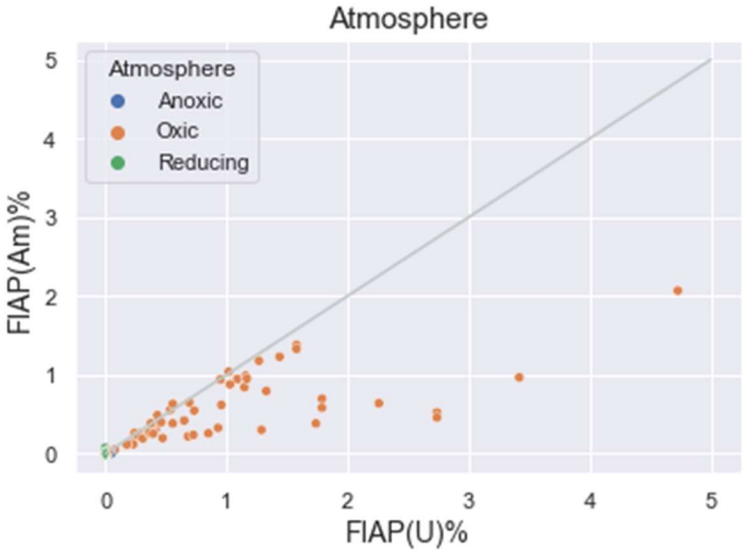

Fig A5.3 Scatterplot of Ru release in relation to U release, where points have been categorized by colour depending on atmosphere and the grey line is a straight y = x line.

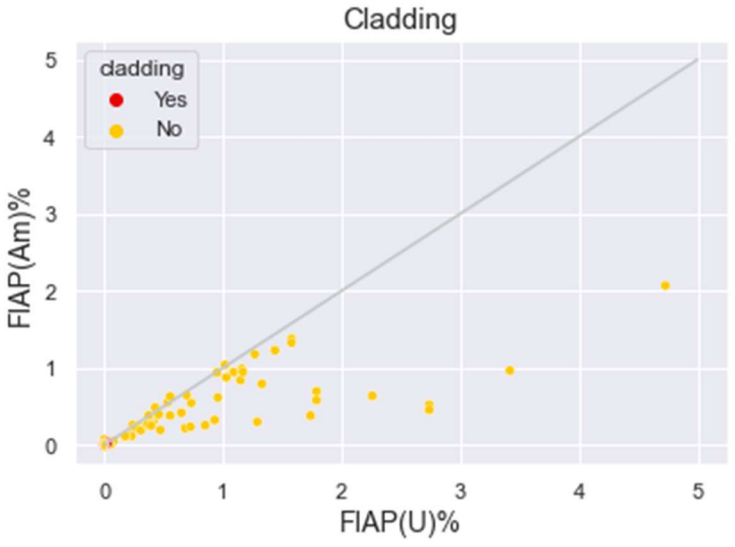

Fig A5.4 Scatterplot of Ru release in relation to U release, where points have been categorized by colour depending on presence of cladding and the grey line is a straight y = x line.

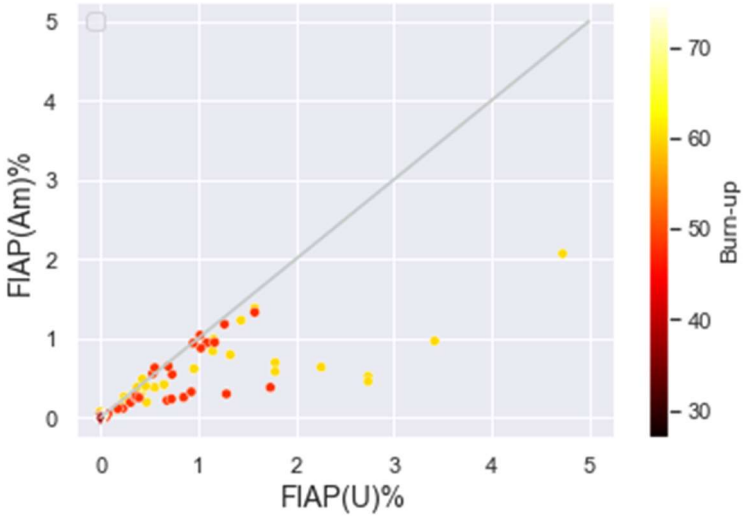

Fig A5.5 Scatterplot of Ru release in relation to U release, where points have been categorized by colour depending on BU and the grey line is a straight y = x line.

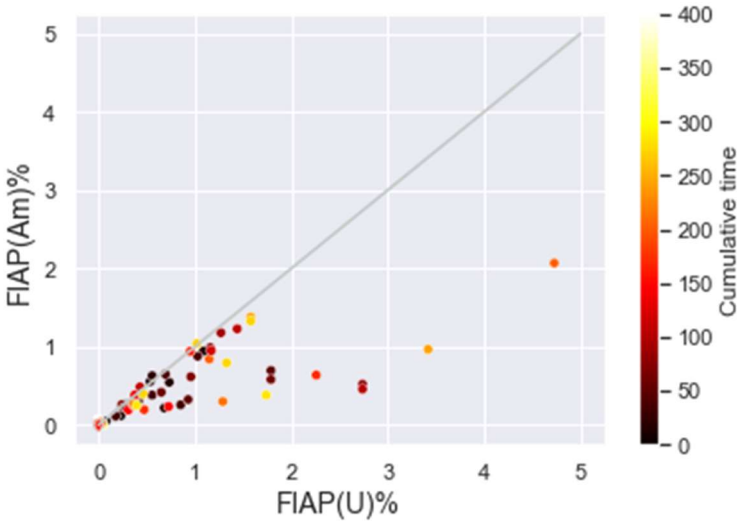

Fig A5.6 Scatterplot of Ru release in relation to U release, where points have been categorized by colour depending on cumulative time and the grey line is a straight y = x line.

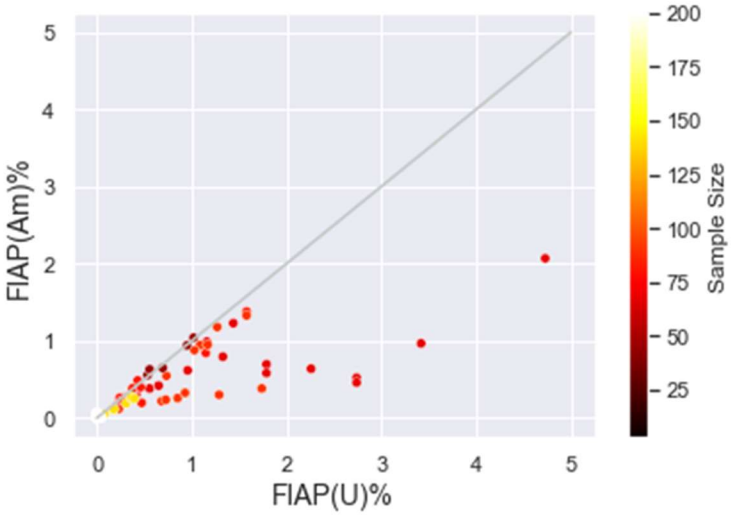

Fig A5.7 Scatterplot of Ru release in relation to U release, where points have been categorized by colour depending on sample size and the grey line is a straight y = x line.

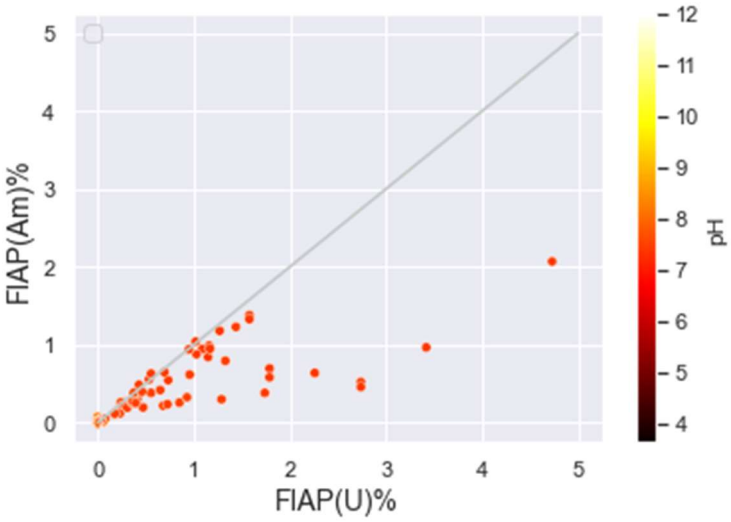

Fig A5.8 Scatterplot of Ru release in relation to U release, where points have been categorized by colour depending on pH and the grey line is a straight y = x line.

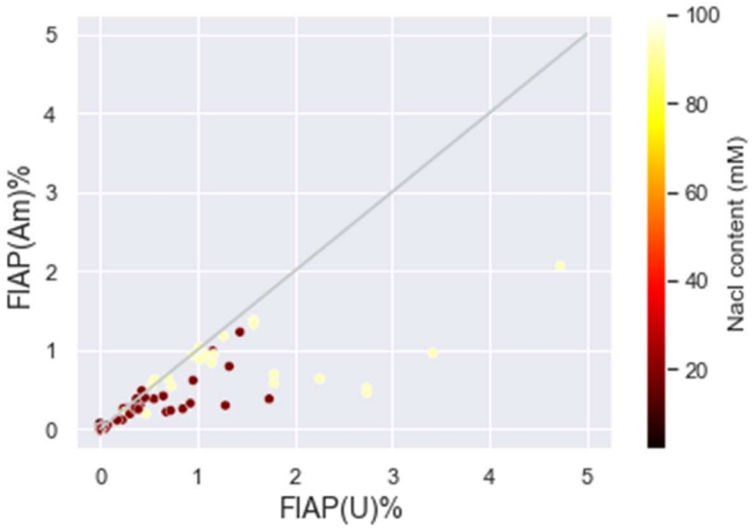

Fig A5.9 Scatterplot of Ru release in relation to U release, where points have been categorized by colour depending on NaCl content and the grey line is a straight y = x line.

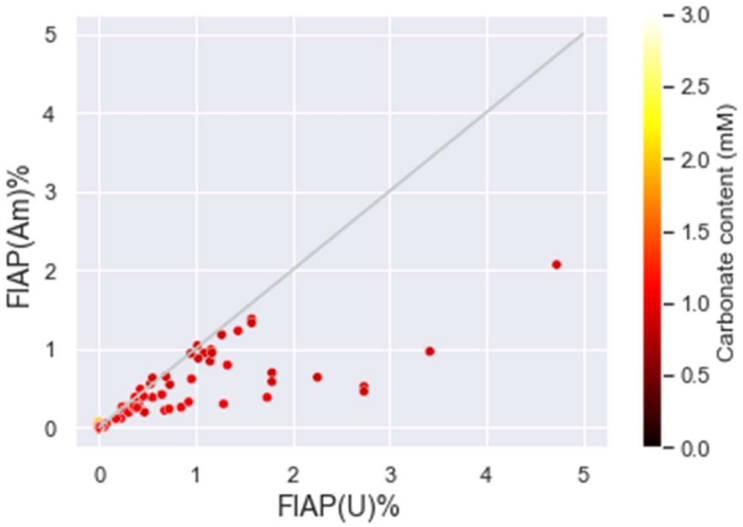

Fig A5.10 Scatterplot of Ru release in relation to U release, where points have been categorized by colour depending on carbonate content and the grey line is a straight y = x line.

Rhodium

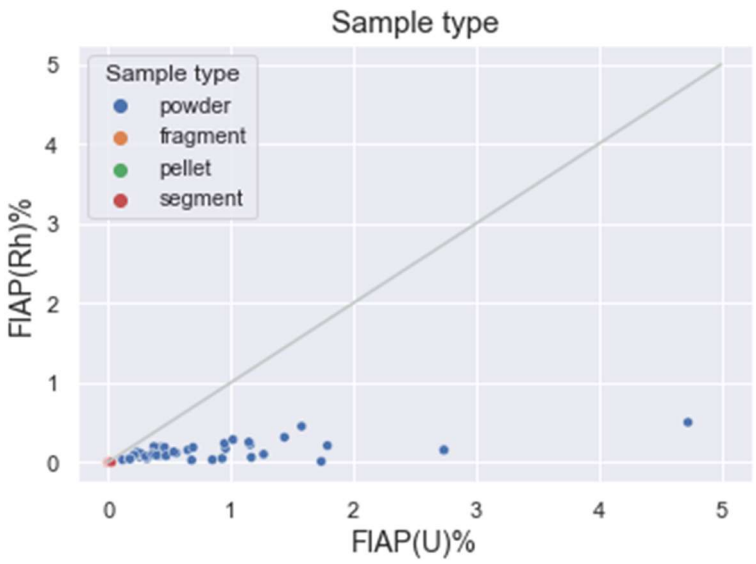

Fig A5.11 Scatterplot of Rh release in relation to U release, where points have been categorized by colour depending on sample type and the grey line is a straight y = x line.

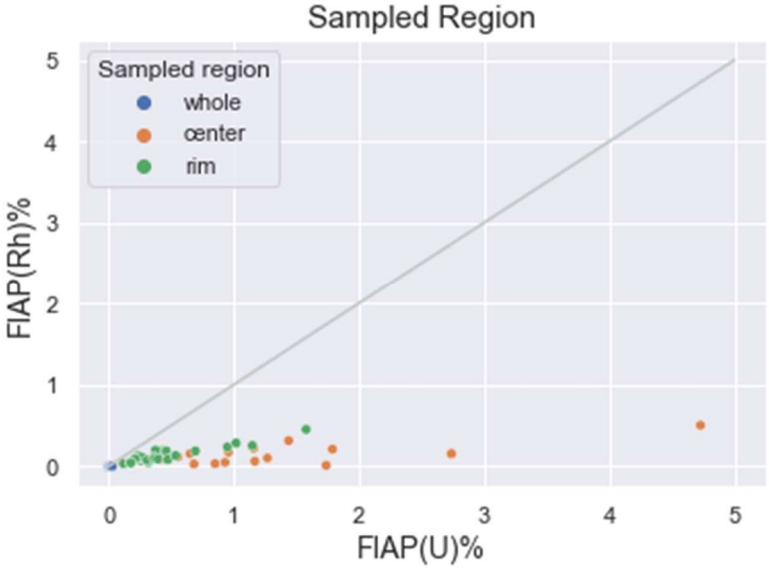

Fig A5.12 Scatterplot of Rh release in relation to U release, where points have been categorized by colour depending on sampled region and the grey line is a straight y = x line.

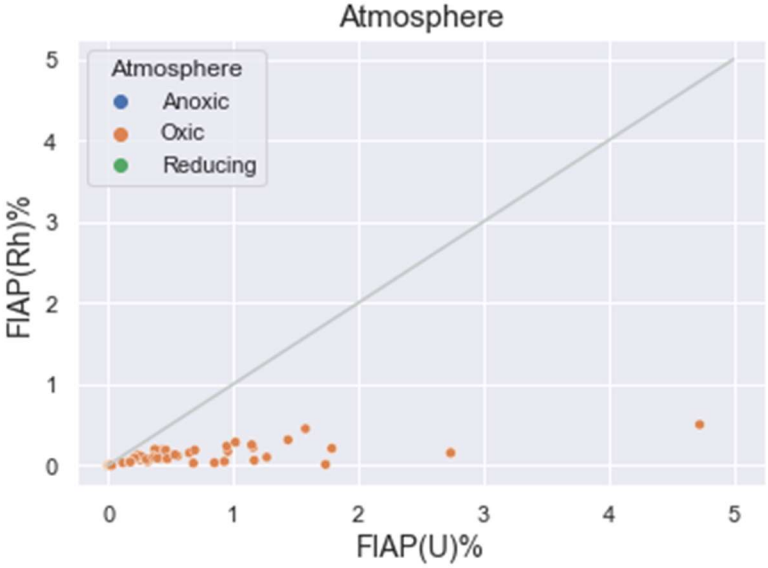

Fig A5.13 Scatterplot of Rh release in relation to U release, where points have been categorized by colour depending on atmosphere and the grey line is a straight y = x line.

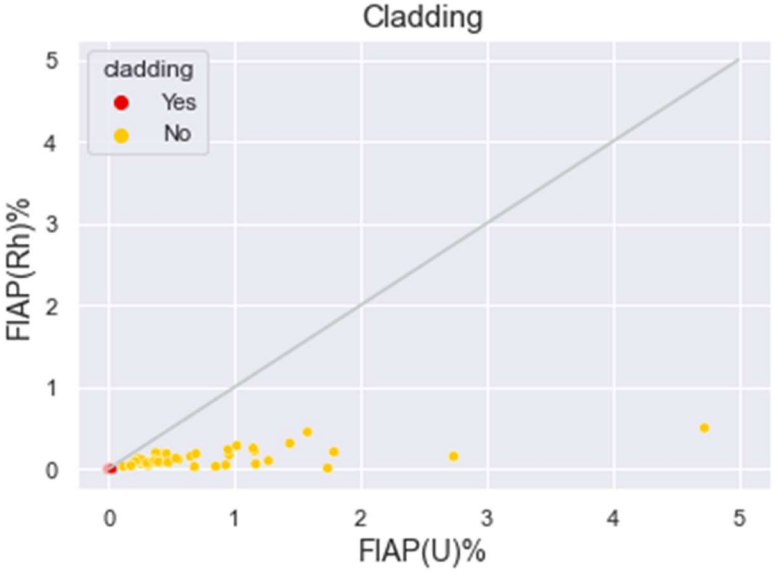

Fig A5.14 Scatterplot of Rh release in relation to U release, where points have been categorized by colour depending on presence of cladding and the grey line is a straight y = x line.

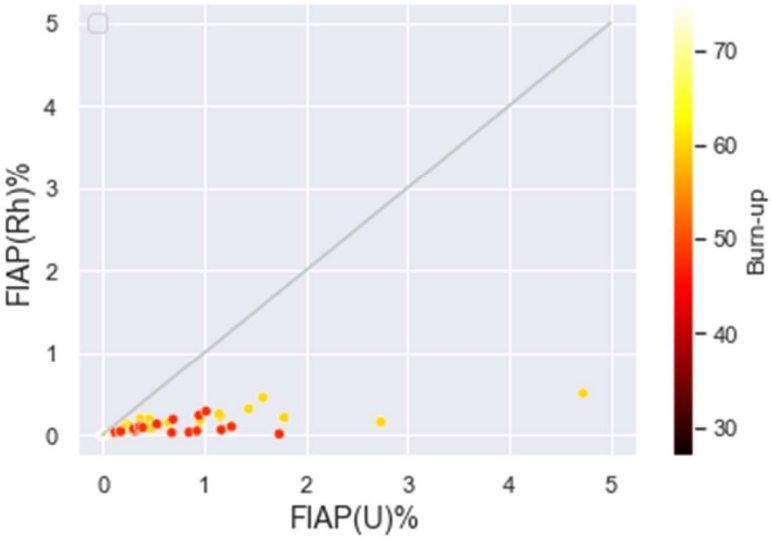

Fig A5.15 Scatterplot of Rh release in relation to U release, where points have been categorized by colour depending on BU and the grey line is a straight y = x line.

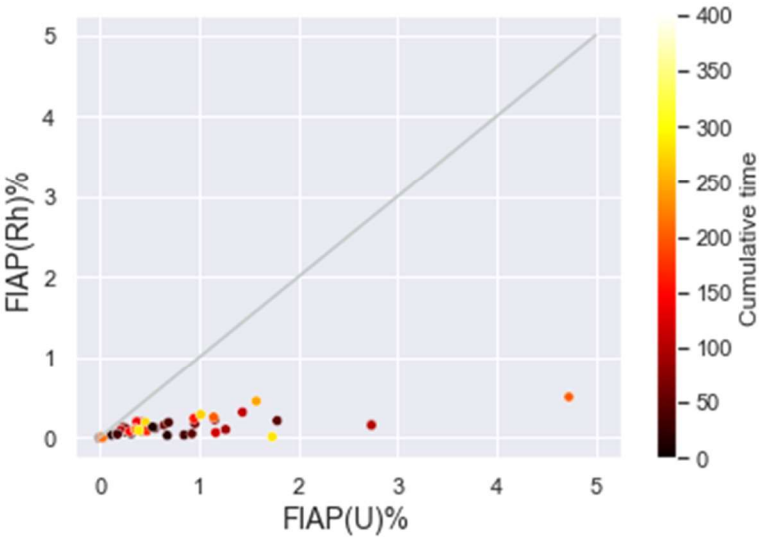

Fig A5.16 Scatterplot of Rh release in relation to U release, where points have been categorized by colour depending on cumulative time and the grey line is a straight y = x line.

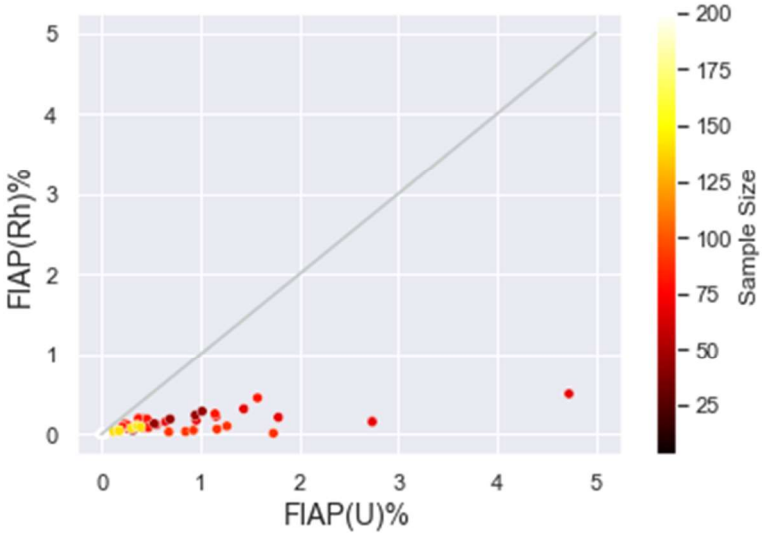

Fig A5.17 Scatterplot of Rh release in relation to U release, where points have been categorized by colour depending on sample size and the grey line is a straight y = x line.

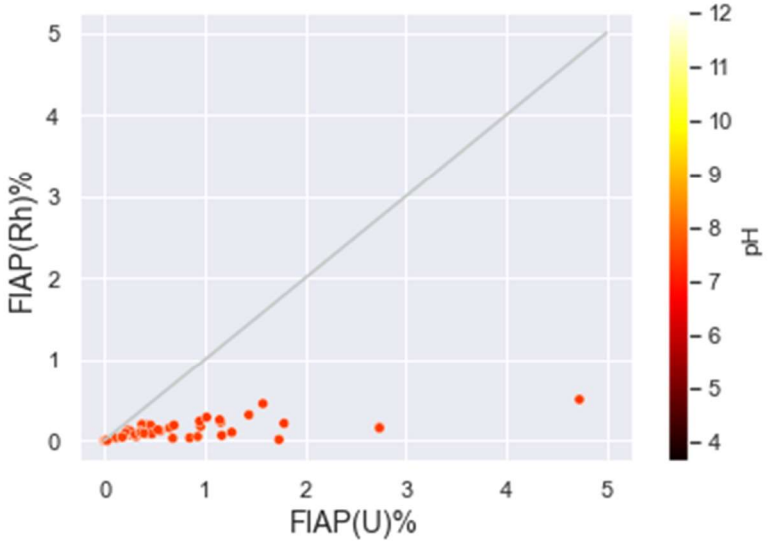

Fig A5.18 Scatterplot of Rh release in relation to U release, where points have been categorized by colour depending on pH and the grey line is a straight y = x line.

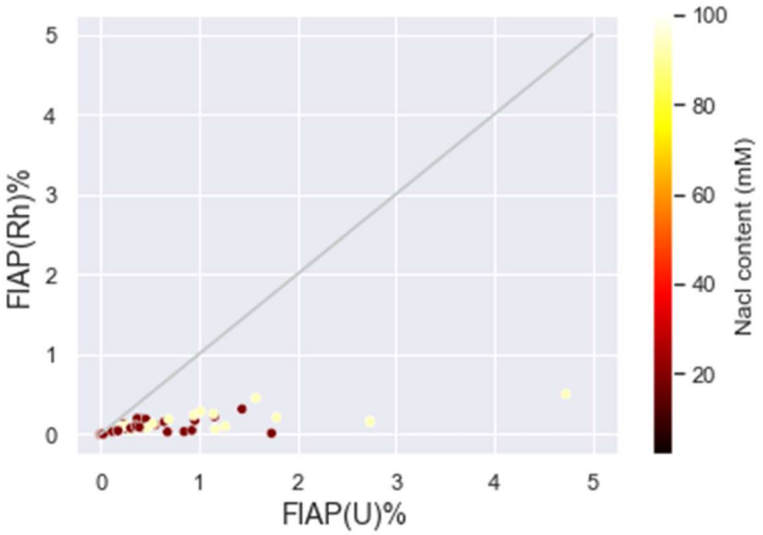

Fig A5.19 Scatterplot of Rh release in relation to U release, where points have been categorized by colour depending on NaCl content and the grey line is a straight y = x line.

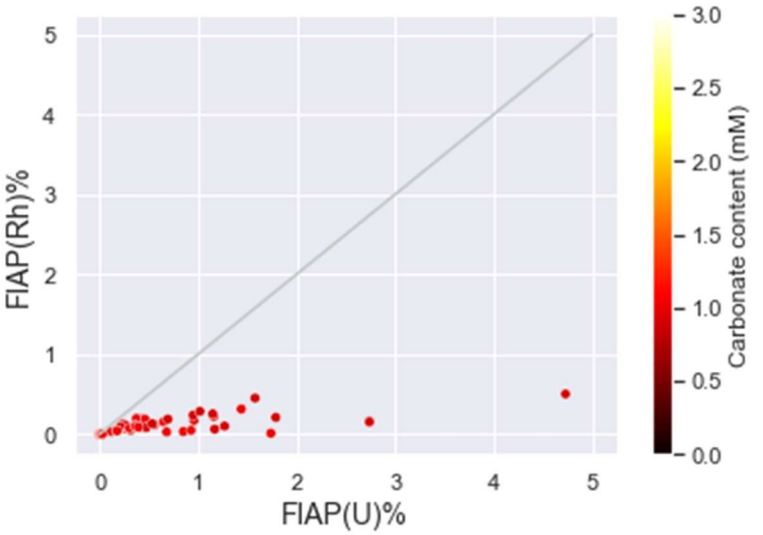

Fig A5.20 Scatterplot of Rh release in relation to U release, where points have been categorized by colour depending on carbonate content and the grey line is a straight y = x line.

A.6 Scatterplots Group 3a

Appendix A.6 shows all the plots of the elements in group 3a (I, Ba, Cd, Te), both plots used and not used in section 4. The plots are shown by element.

Iodine

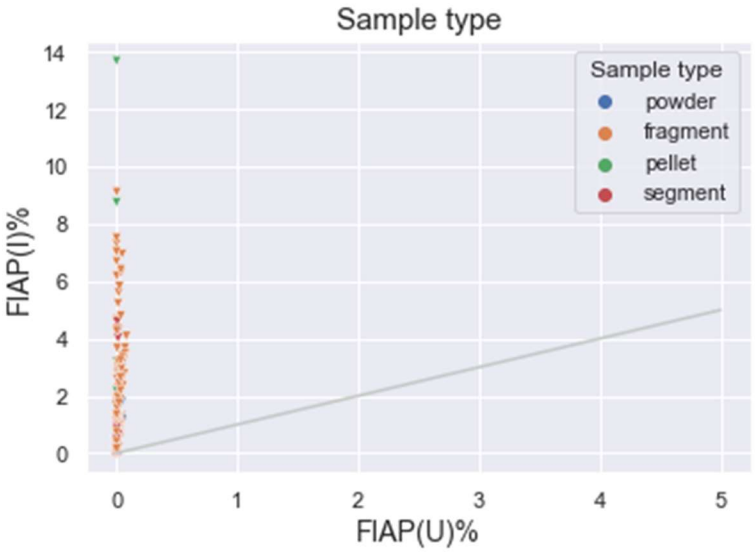

Fig A6.1 Scatterplot of I release in relation to U release, where points have been categorized by colour depending on sample type and the grey line is a straight y = x line. Circles represent I-129 and triangles I-127.

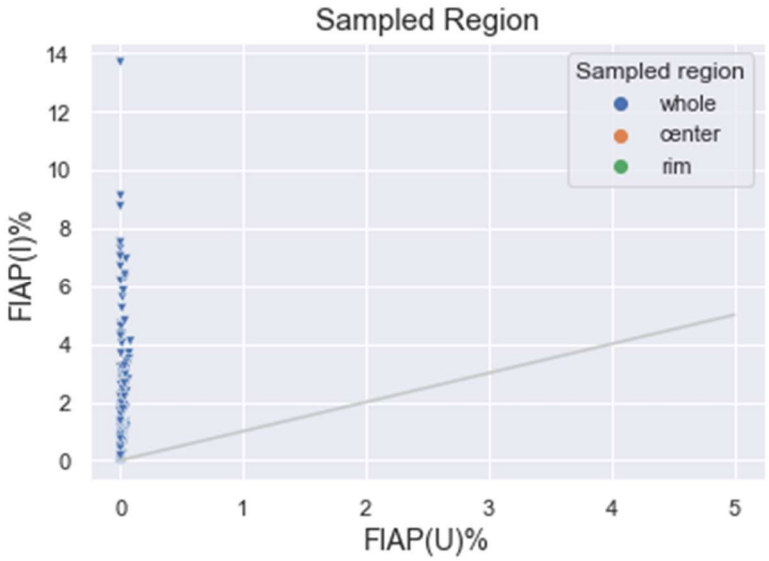

Fig A6.2 Scatterplot of I release in relation to U release, where points have been categorized by colour depending on sampled region and the grey line is a straight y = x line. Circles represent I-129 and triangles I-127.

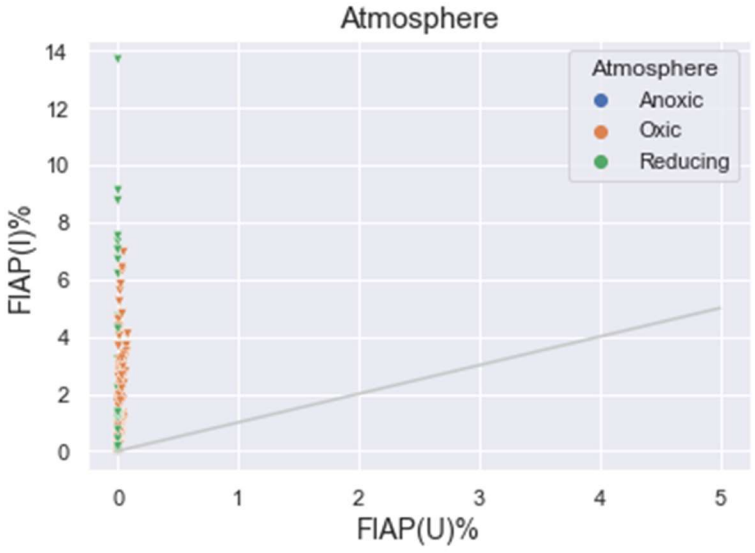

Fig A6.3 Scatterplot of I release in relation to U release, where points have been categorized by colour depending on atmosphere and the grey line is a straight y = x line. Circles represent I-129 and triangles I-127.

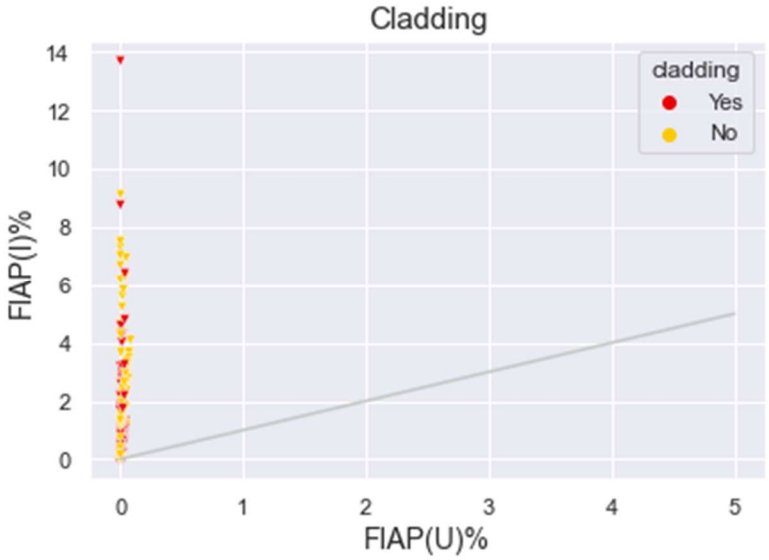

Fig A6.4 Scatterplot of I release in relation to U release, where points have been categorized by colour depending on presence of cladding and the grey line is a straight y = x line. Circles represent I-129 and triangles I-127.

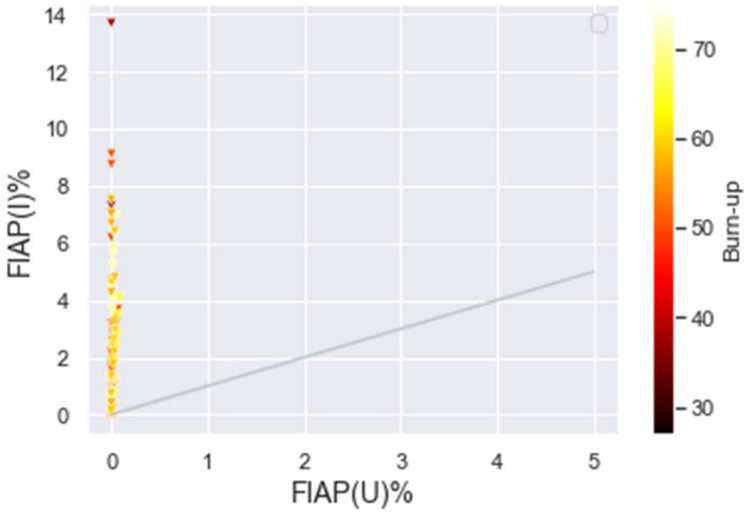

Fig A6.5 Scatterplot of I release in relation to U release, where points have been categorized by colour depending on BU and the grey line is a straight y = x line. Circles represent I-129 and triangles I-127.

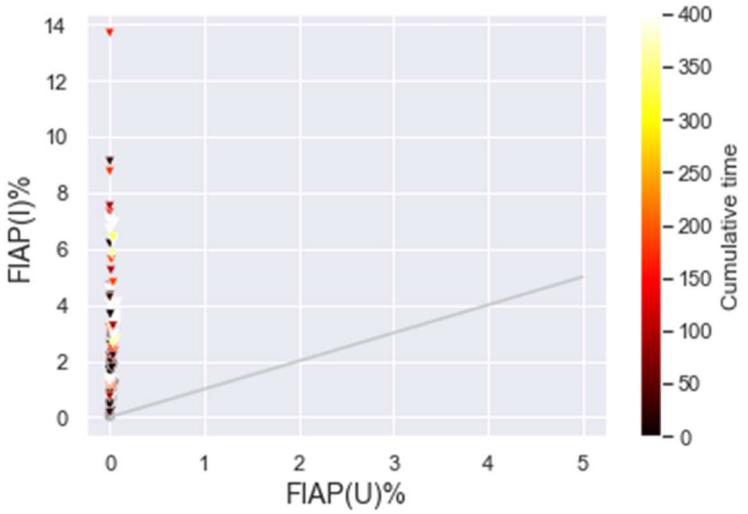

Fig A6.6 Scatterplot of I release in relation to U release, where points have been categorized by colour depending on cumulative time and the grey line is a straight y = x line. Circles represent I-129 and triangles I-127.

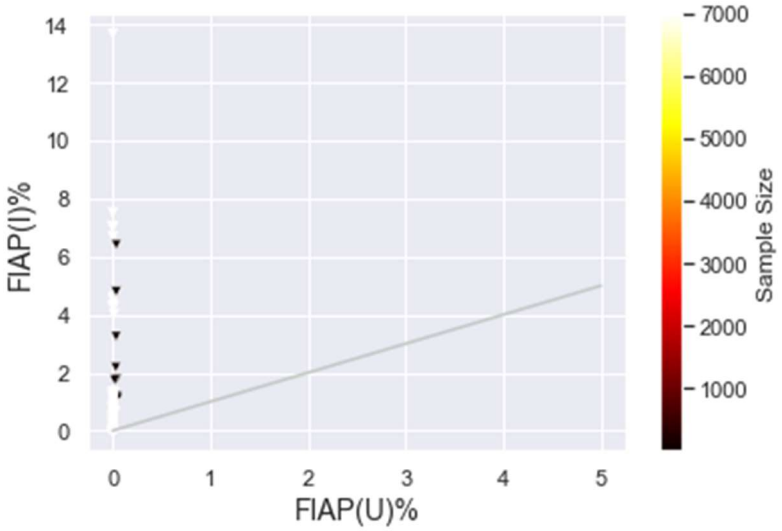

Fig A6.7 Scatterplot of I release in relation to U release, where points have been categorized by colour depending on sample size and the grey line is a straight y = x line. Circles represent I-129 and triangles I-127.

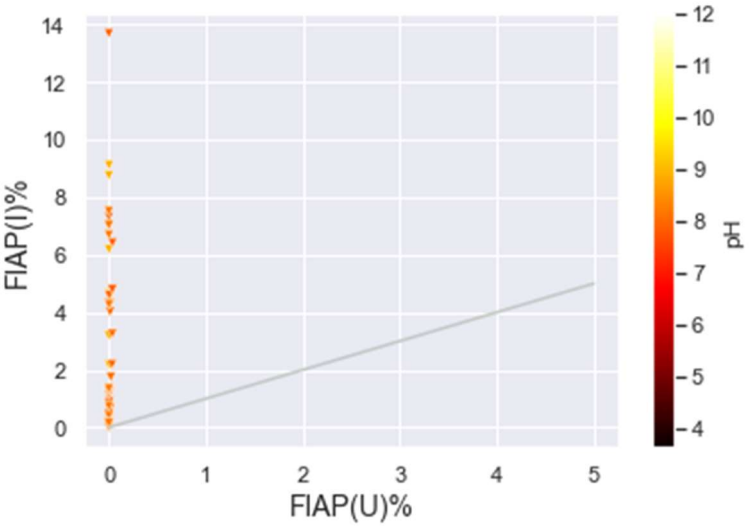

Fig A6.8 Scatterplot of I release in relation to U release, where points have been categorized by colour depending on pH and the grey line is a straight y = x line. Circles represent I-129 and triangles I-127.

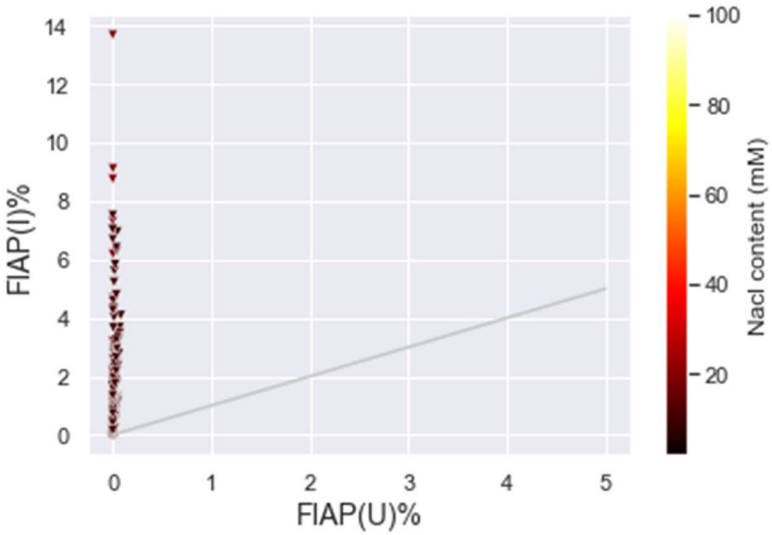

Fig A6.9 Scatterplot of I release in relation to U release, where points have been categorized by colour depending on NaCl content and the grey line is a straight y = x line. Circles represent I-129 and triangles I-127.

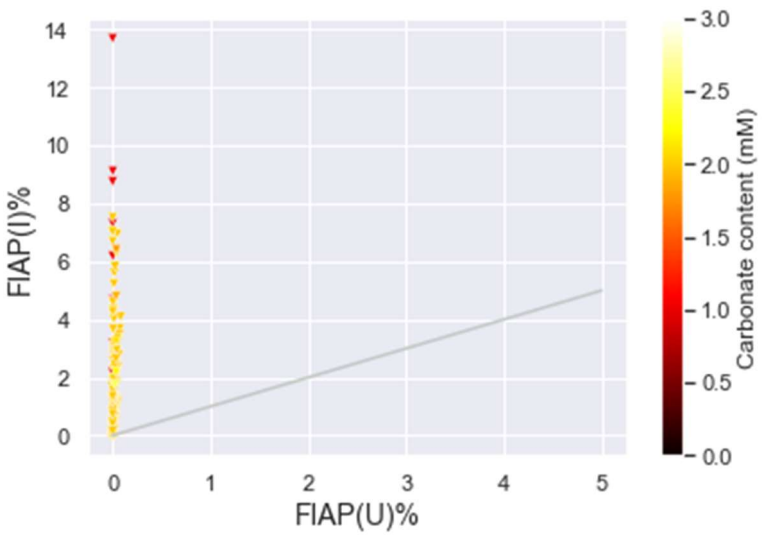

Fig A6.10 Scatterplot of I release in relation to U release, where points have been categorized by colour depending on carbonate content and the grey line is a straight y = x line. Circles represent I-129 and triangles I-127.

Barium

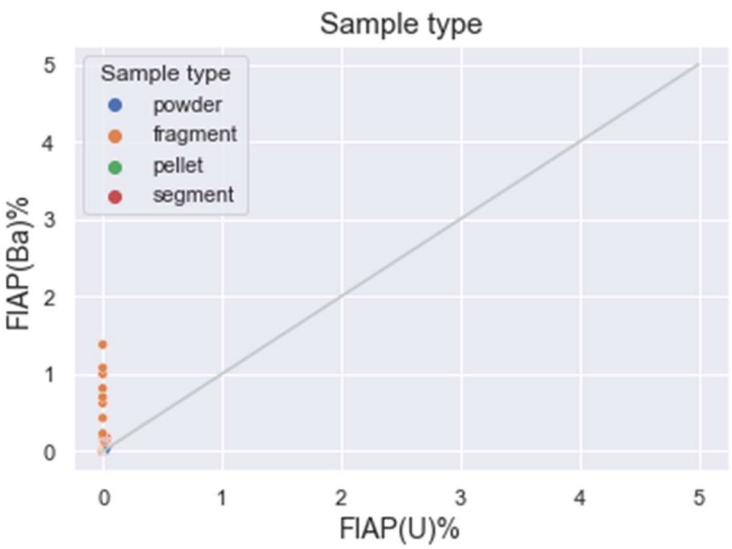

Fig A6.11 Scatterplot of Ba release in relation to U release, where points have been categorized by colour depending on sample type and the grey line is a straight y = x line. Circles represent Ba and triangles Ba-138.

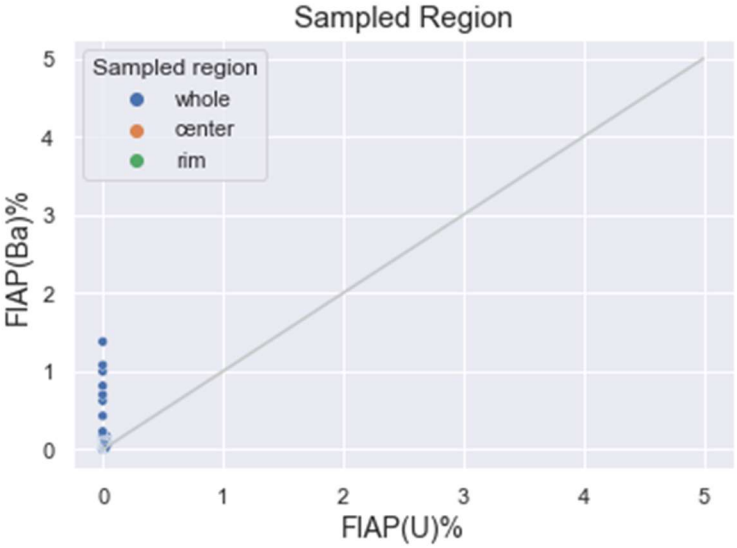

Fig A6.12 Scatterplot of I release in relation to U release, where points have been categorized by colour depending on sampled region and the grey line is a straight y = x line. Circles represent Ba and triangles Ba-138.

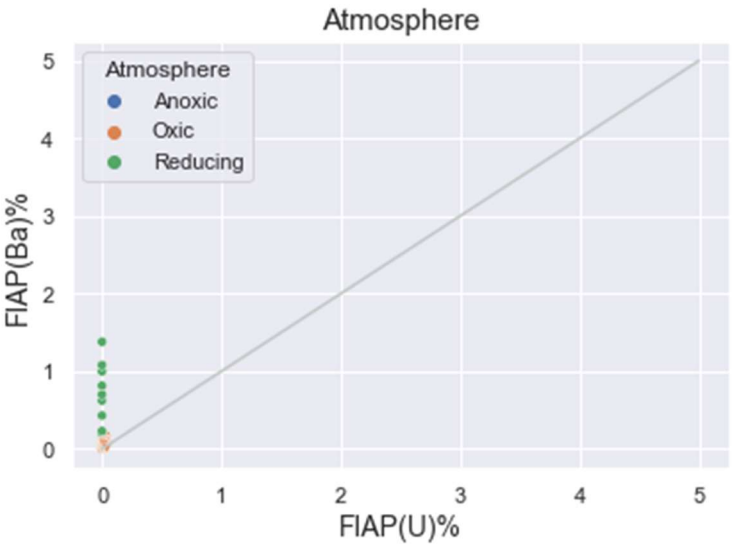

Fig A6.13 Scatterplot of Ba release in relation to U release, where points have been categorized by colour depending on atmosphere and the grey line is a straight y = x line. Circles represent Ba and triangles Ba-138.

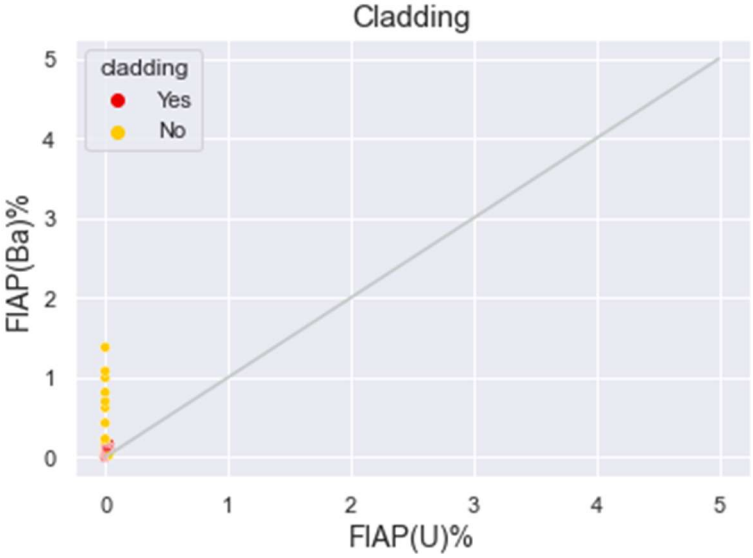

Fig A6.14 Scatterplot of Ba release in relation to U release, where points have been categorized by colour depending on presence of cladding and the grey line is a straight y = x line. Circles represent Ba and triangles Ba-138.

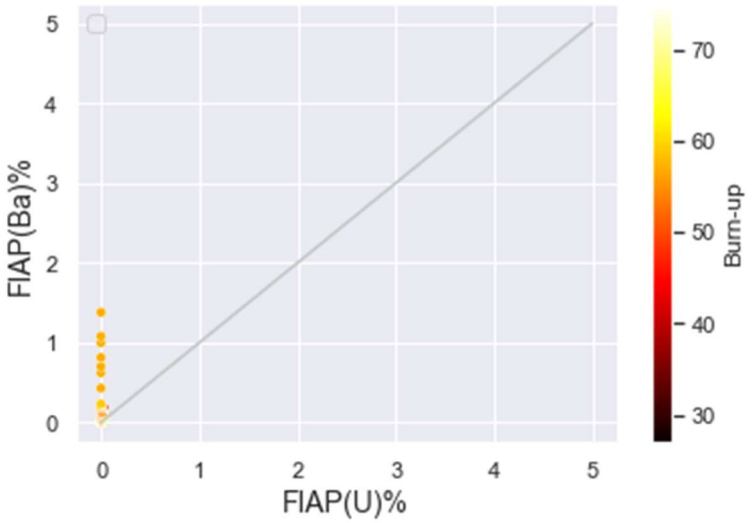

Fig A6.15 Scatterplot of Ba release in relation to U release, where points have been categorized by colour depending on BU and the grey line is a straight y = x line. Circles represent Ba and triangles Ba-138.

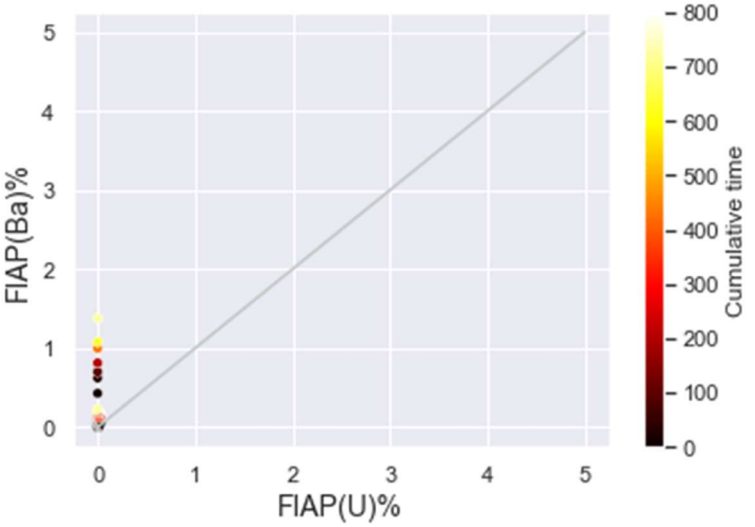

Fig A6.16 Scatterplot of Ba release in relation to U release, where points have been categorized by colour depending on cumulative time and the grey line is a straight y = x line. Circles represent Ba and triangles Ba-138.

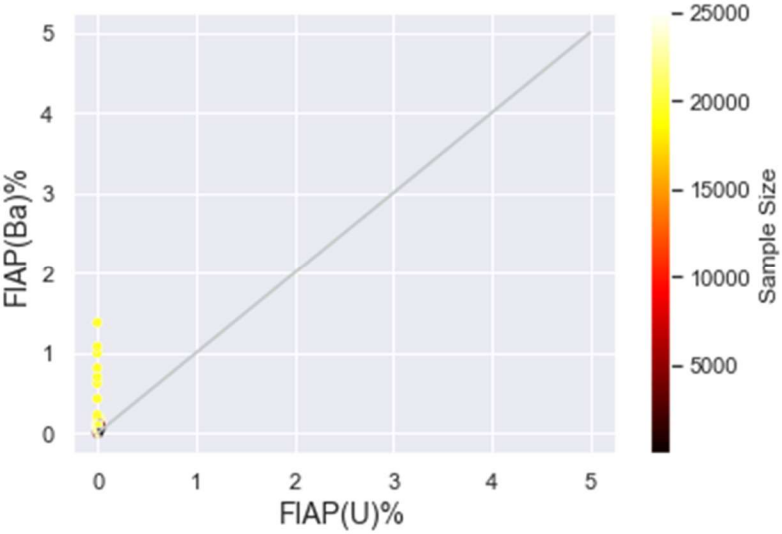

Fig A6.17 Scatterplot of Ba release in relation to U release, where points have been categorized by colour depending on sample size and the grey line is a straight y = x line. Circles represent Ba and triangles Ba-138.

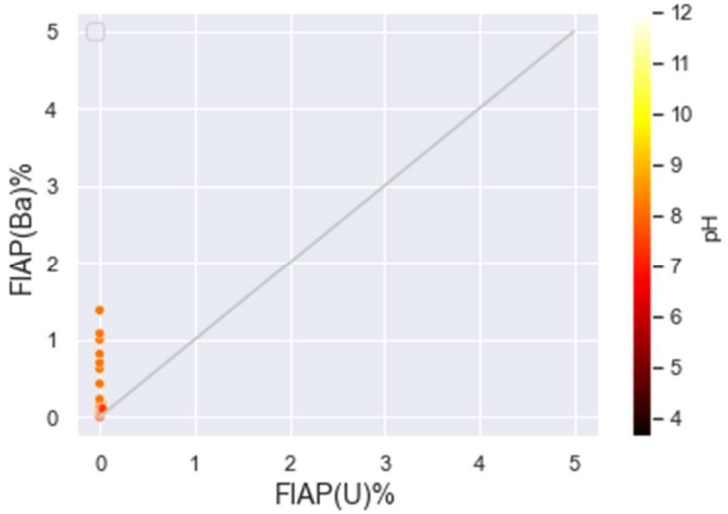

Fig A6.18 Scatterplot of Ba release in relation to U release, where points have been categorized by colour depending on pH and the grey line is a straight y = x line. Circles represent Ba and triangles Ba-138.

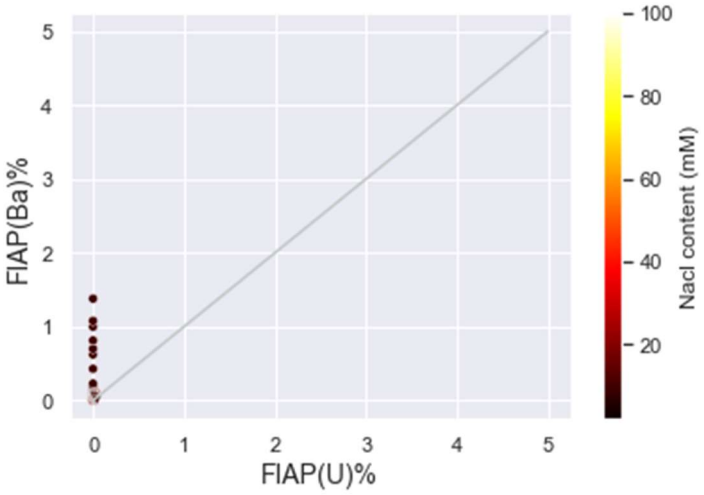

Fig A6.19 Scatterplot of Ba release in relation to U release, where points have been categorized by colour depending on NaCl content and the grey line is a straight y = x line. Circles represent Ba and triangles Ba-138.

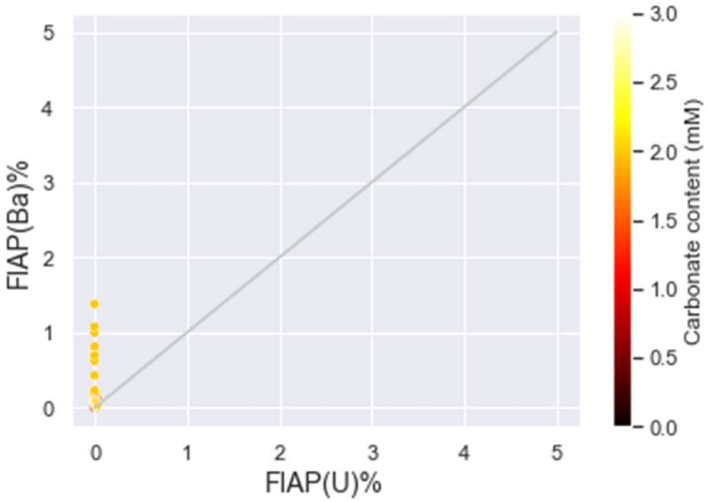

Fig A6.20 Scatterplot of Ba release in relation to U release, where points have been categorized by colour depending on carbonate content and the grey line is a straight y = x line. Circles represent Ba and triangles Ba-138.

Cadmium

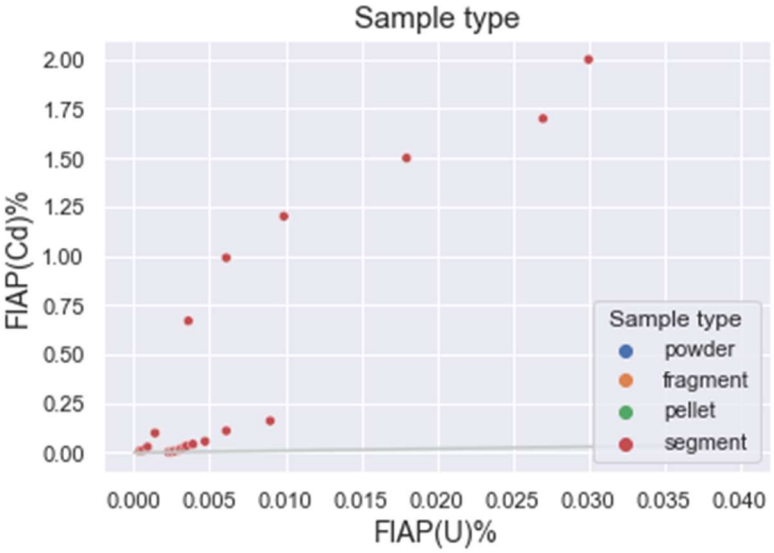

Fig A6.21 Scatterplot of Cd release in relation to U release, where points have been categorized by colour depending on sample type and the grey line is a straight y = x line.

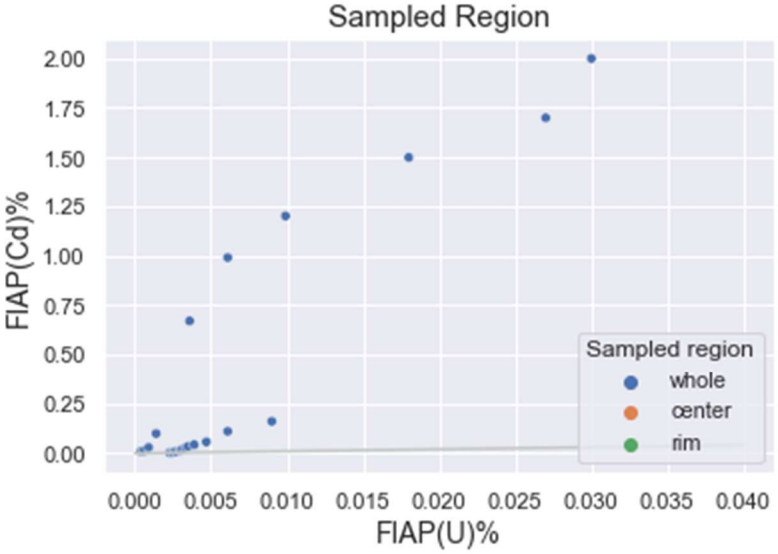

Fig A6.22 Scatterplot of Cd release in relation to U release, where points have been categorized by colour depending on sampled region and the grey line is a straight y = x line.

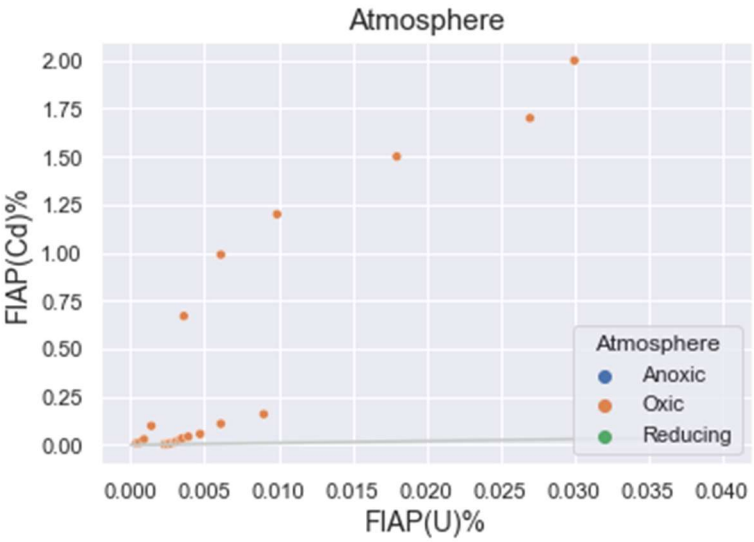

Fig A6.23 Scatterplot of Cd release in relation to U release, where points have been categorized by colour depending on atmosphere and the grey line is a straight y = x line.

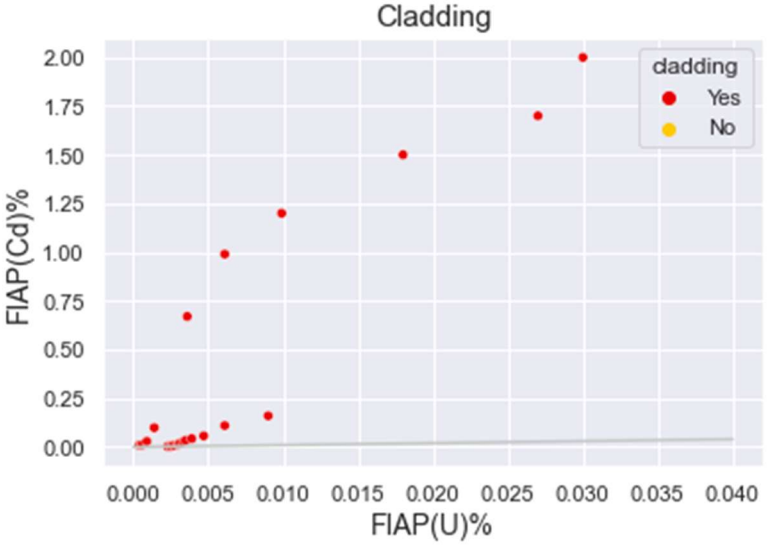

Fig A6.24 Scatterplot of Cd release in relation to U release, where points have been categorized by colour depending on sample type and the grey line is a straight y = x line.

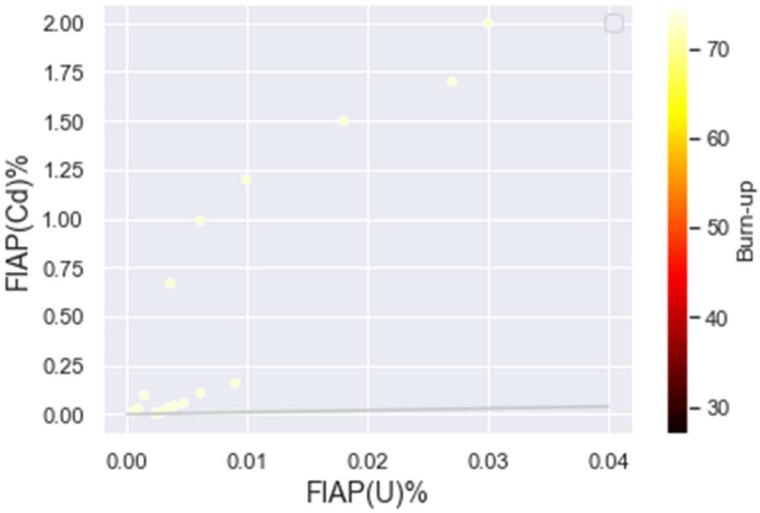

Fig A6.25 Scatterplot of Cd release in relation to U release, where points have been categorized by colour depending on BU and the grey line is a straight y = x line.

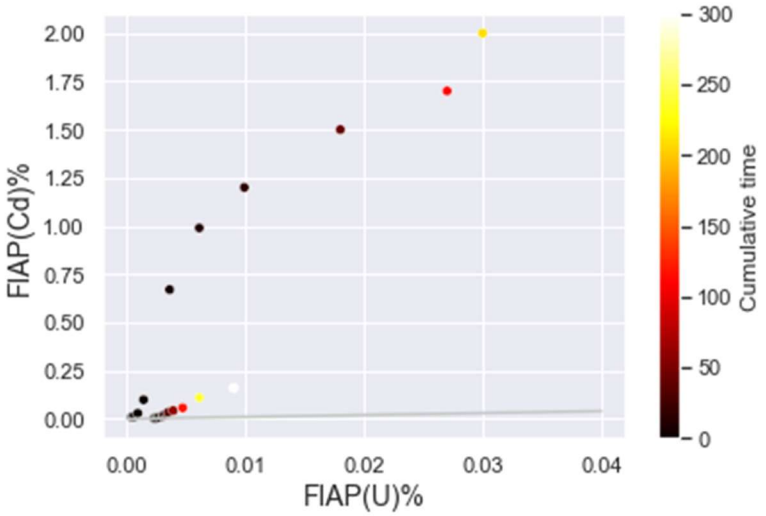

Fig A6.26 Scatterplot of Cd release in relation to U release, where points have been categorized by colour depending on cumulative time and the grey line is a straight y = x line.

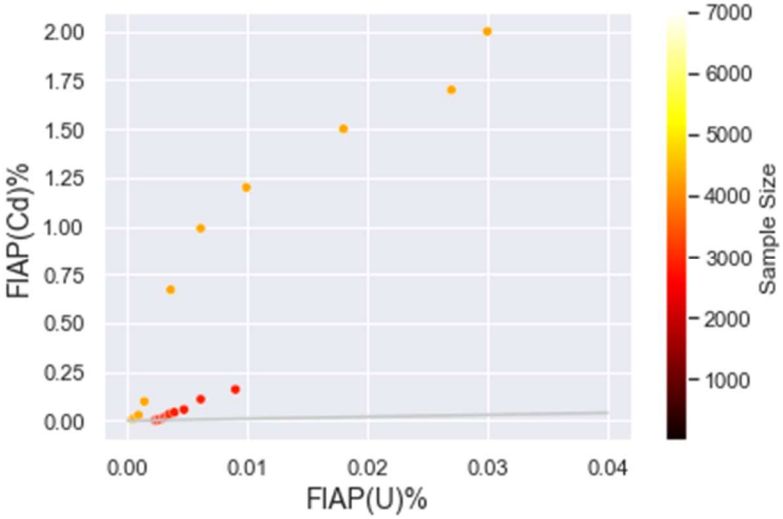

Fig A6.27 Scatterplot of Cd release in relation to U release, where points have been categorized by colour depending on sample size and the grey line is a straight y = x line.

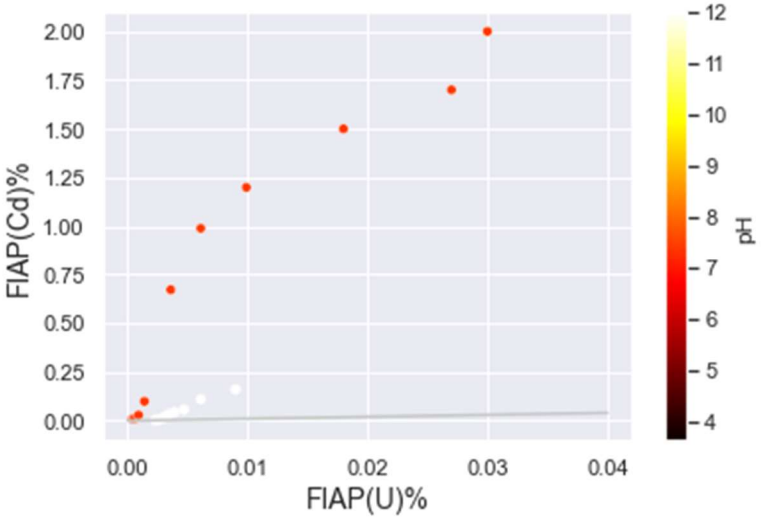

Fig A6.28 Scatterplot of Cd release in relation to U release, where points have been categorized by colour depending on pH and the grey line is a straight y = x line.

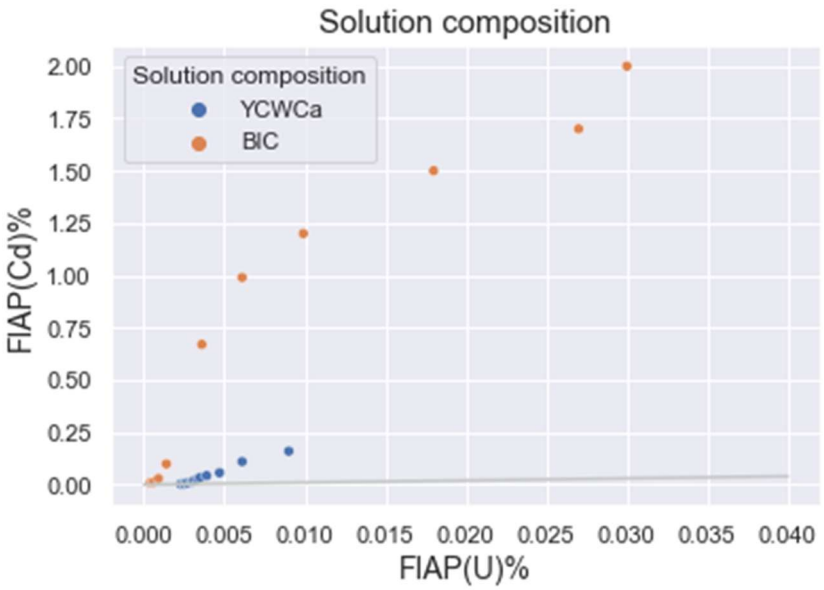

Fig A6.29 Scatterplot of Cd release in relation to U release, where points have been categorized by colour depending on solution composition and the grey line is a straight y = x line.

Tellurium

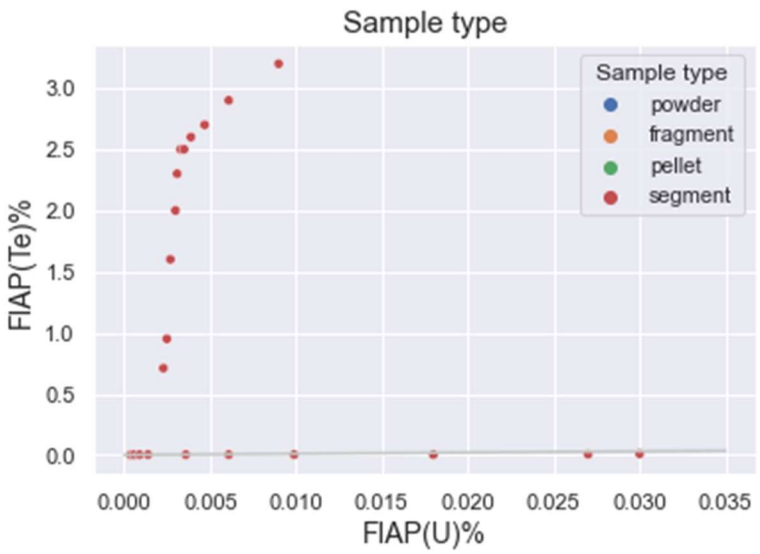

Fig A6.30 Scatterplot of Te release in relation to U release, where points have been categorized by colour depending on sample type and the grey line is a straight y = x line.

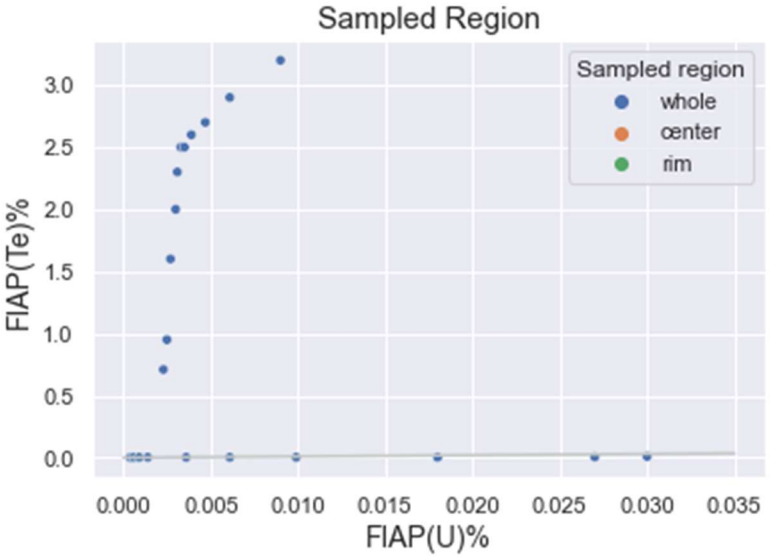

Fig A6.31 Scatterplot of Te release in relation to U release, where points have been categorized by colour depending on sampled region and the grey line is a straight y = x line.

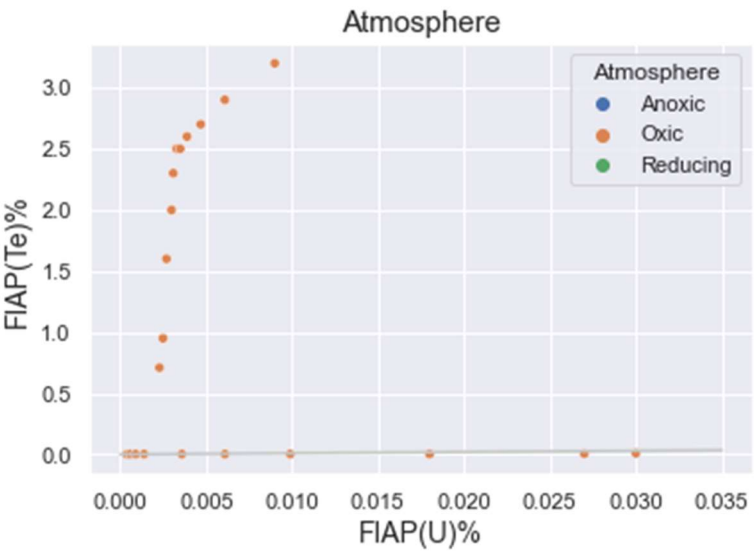

Fig A6.32 Scatterplot of Te release in relation to U release, where points have been categorized by colour depending on atmosphere and the grey line is a straight y = x line.

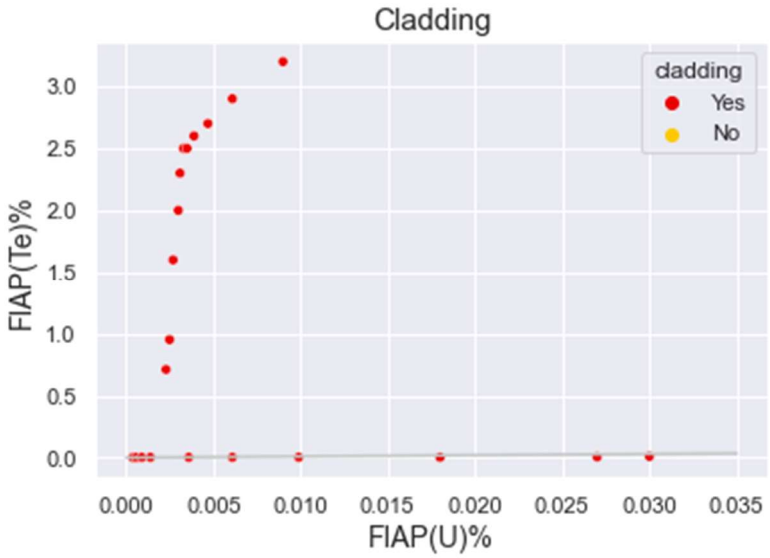

Fig A6.33 Scatterplot of Te release in relation to U release, where points have been categorized by colour depending on presence of cladding and the grey line is a straight y = x line.

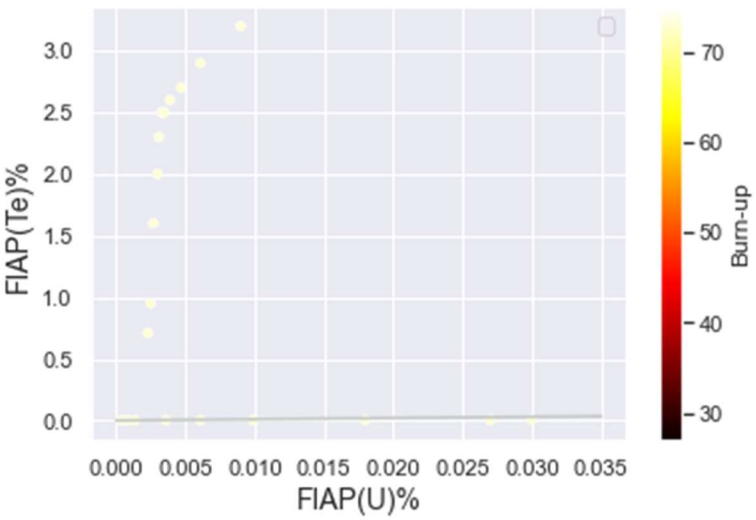

Fig A6.34 Scatterplot of Te release in relation to U release, where points have been categorized by colour depending on BU and the grey line is a straight y = x line.

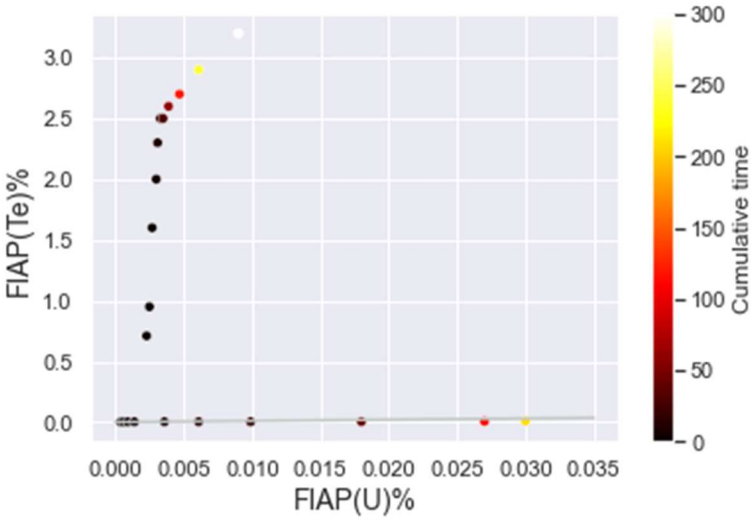

Fig A6.35 Scatterplot of Te release in relation to U release, where points have been categorized by colour depending on cumulative time and the grey line is a straight y = x line.

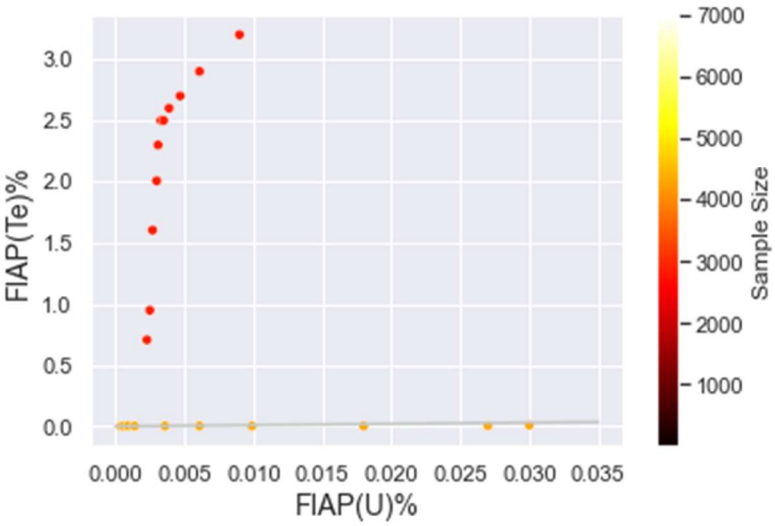

Fig A6.36 Scatterplot of Te release in relation to U release, where points have been categorized by colour depending on sample size and the grey line is a straight y = x line.

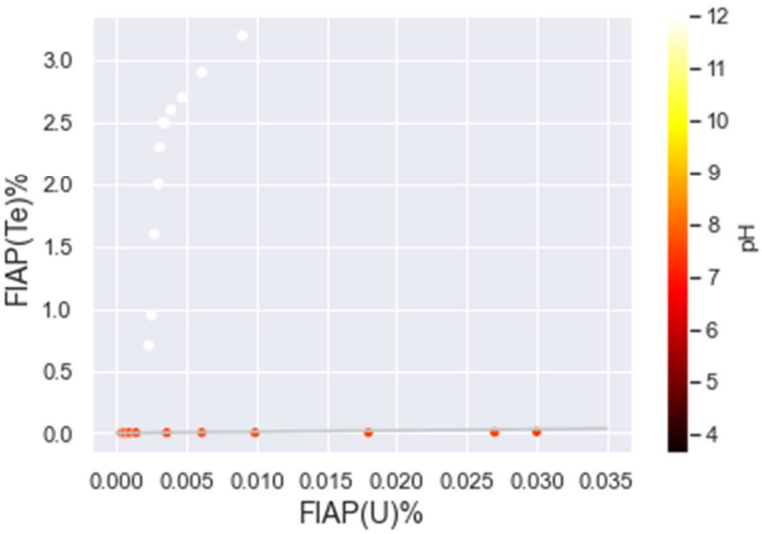

Fig A6.37 Scatterplot of Te release in relation to U release, where points have been categorized by colour depending on pH and the grey line is a straight y = x line.

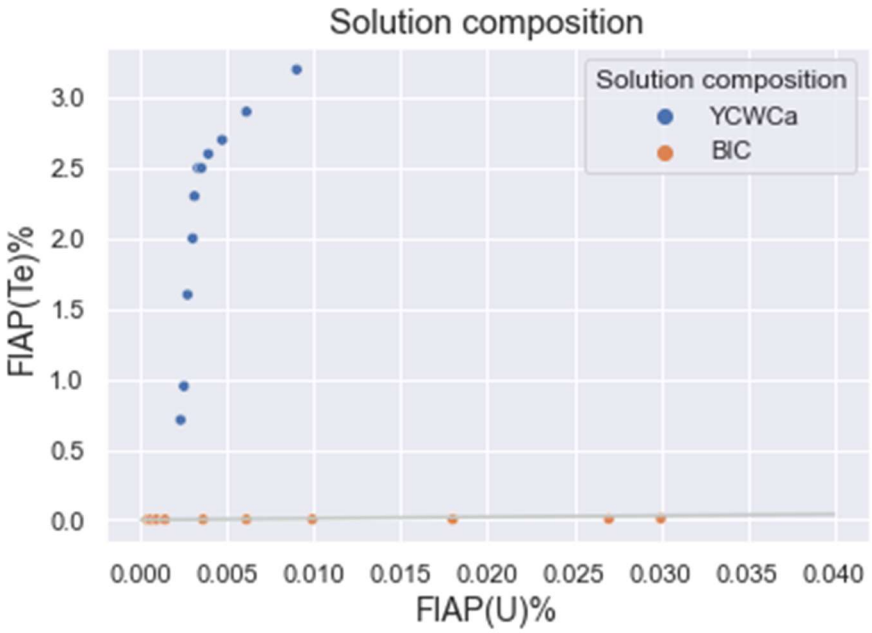

Fig A6.38 Scatterplot of Te release in relation to U release, where points have been categorized by colour depending on solution composition and the grey line is a straight y = x line.

A.7 Scatterplots Group 3b

Appendix A.7 shows all the plots of the elements in group 3b (Cs, Mo, Rb, Tc), both plots used and not used in section 4. The plots are shown by element.

Caesium

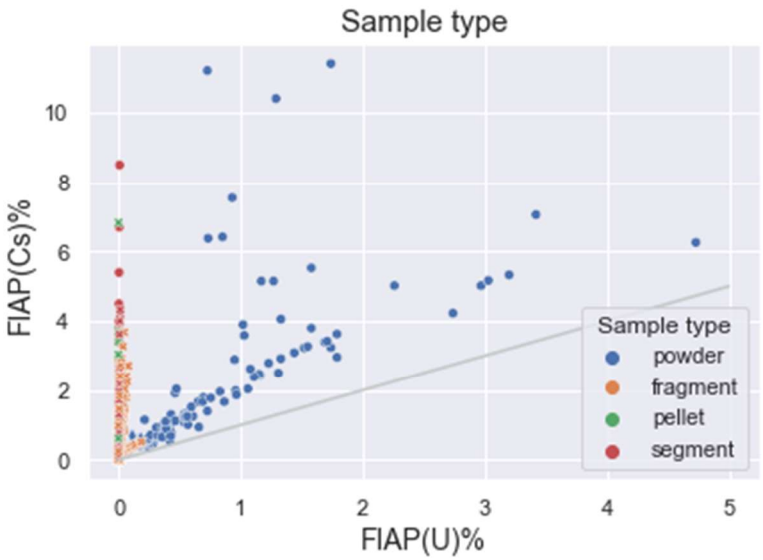

Fig A7.1 Scatterplot of Cs release in relation to U release, where points have been categorized by colour depending on sample type and the grey line is a straight y = x line. Circles represent unspecified Cs, triangles Cs-133, diamonds Cs-134, squares Cs-135 and crosses Cs-137.

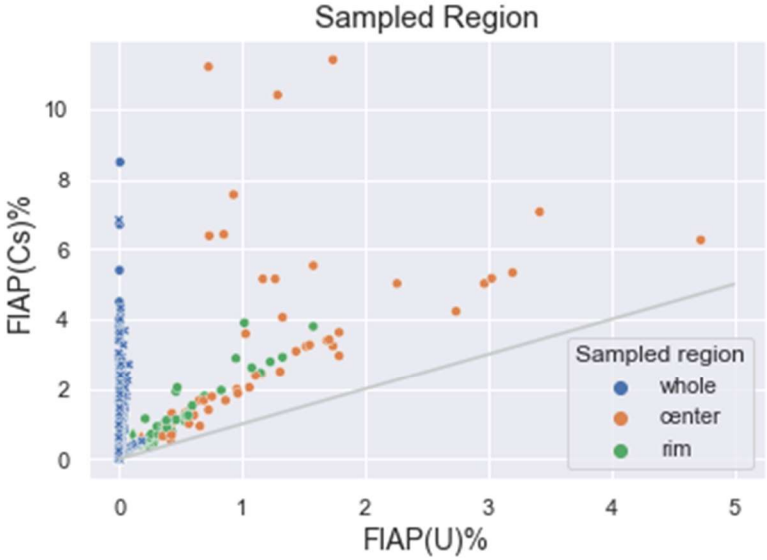

Fig A7.2 Scatterplot of Cs release in relation to U release, where points have been categorized by colour depending on sampled region and the grey line is a straight y = x line. Circles represent unspecified Cs, triangles Cs-133, diamonds Cs-134, squares Cs-135 and crosses Cs-137.

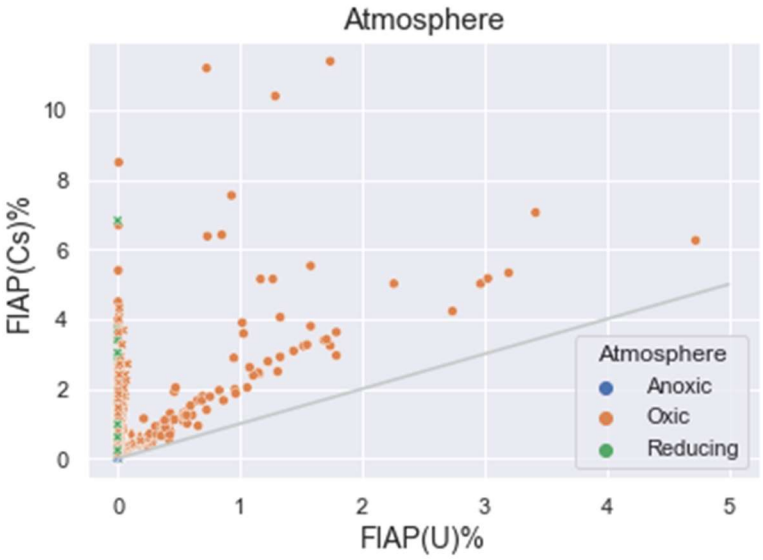

Fig A7.3 Scatterplot of Cs release in relation to U release, where points have been categorized by colour depending on atmosphere and the grey line is a straight y = x line. Circles represent unspecified Cs, triangles Cs-133, diamonds Cs-134, squares Cs-135 and crosses Cs-137.

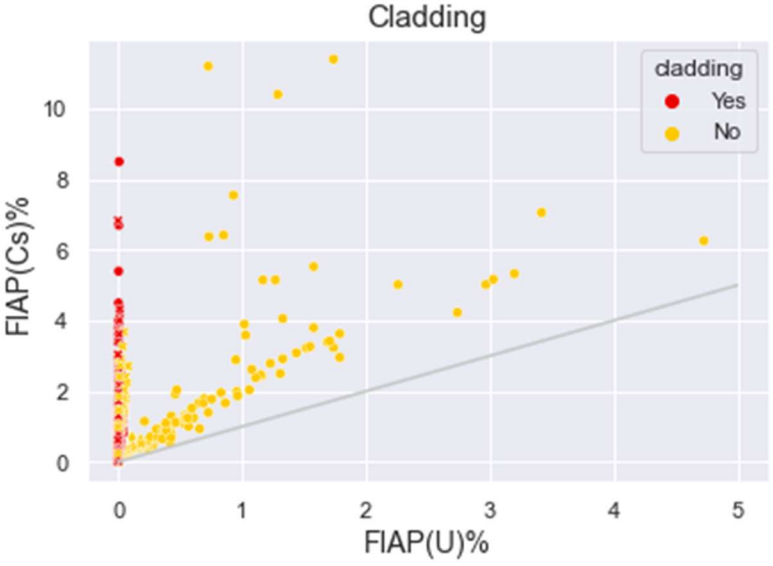

Fig A7.4 Scatterplot of Cs release in relation to U release, where points have been categorized by colour depending on presence of cladding and the grey line is a straight y = x line. Circles represent unspecified Cs, triangles Cs-133, diamonds Cs-134, squares Cs-135 and crosses Cs-137.

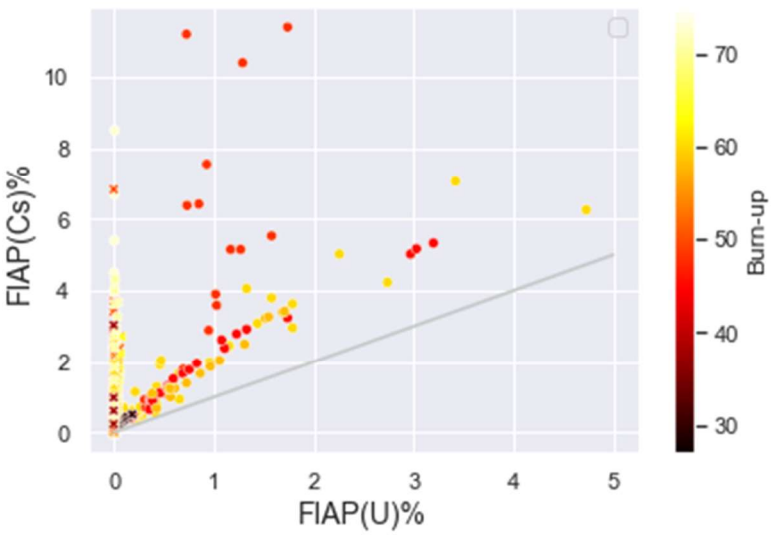

Fig A7.5 Scatterplot of Cs release in relation to U release, where points have been categorized by colour depending on BU content and the grey line is a straight y = x line. Circles represent unspecified Cs, triangles Cs-133, diamonds Cs-134, squares Cs-135 and crosses Cs-137.

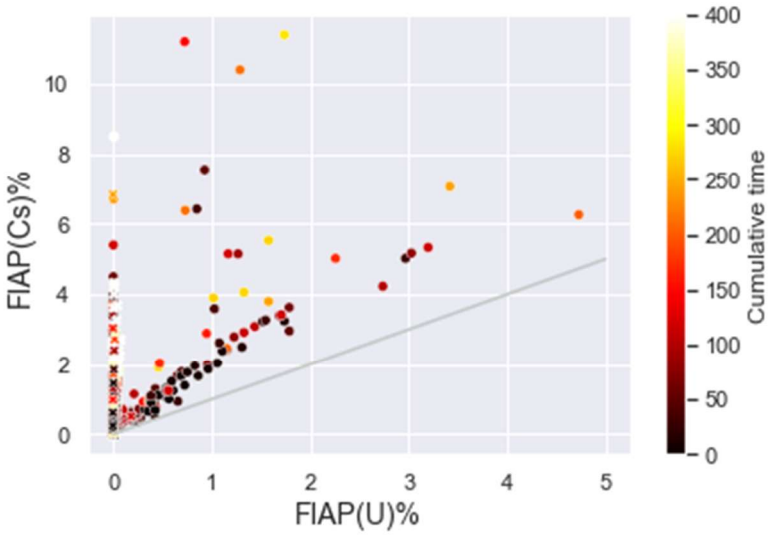

Fig A7.6 Scatterplot of Cs release in relation to U release, where points have been categorized by colour depending on cumulative time and the grey line is a straight y = x line. Circles represent unspecified Cs, triangles Cs-133, diamonds Cs-134, squares Cs-135 and crosses Cs-137.

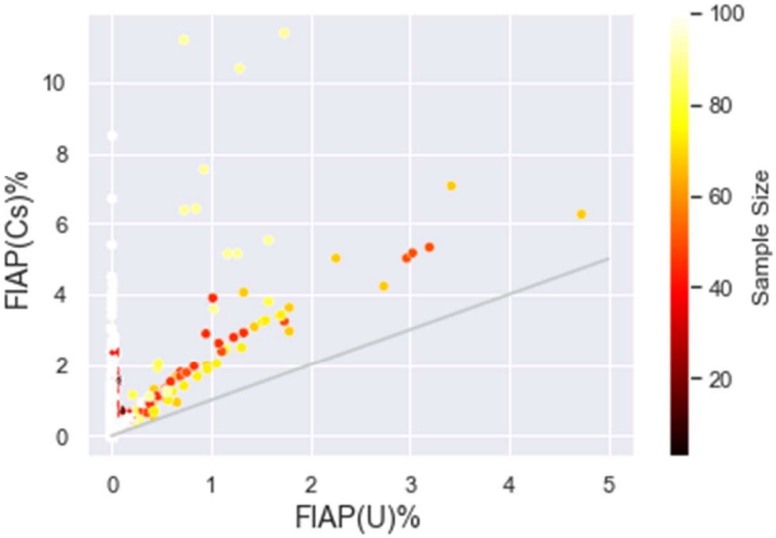

Fig A7.7 Scatterplot of Cs release in relation to U release, where points have been categorized by colour depending on sample size and the grey line is a straight y = x line. Circles represent unspecified Cs, triangles Cs-133, diamonds Cs-134, squares Cs-135 and crosses Cs-137.

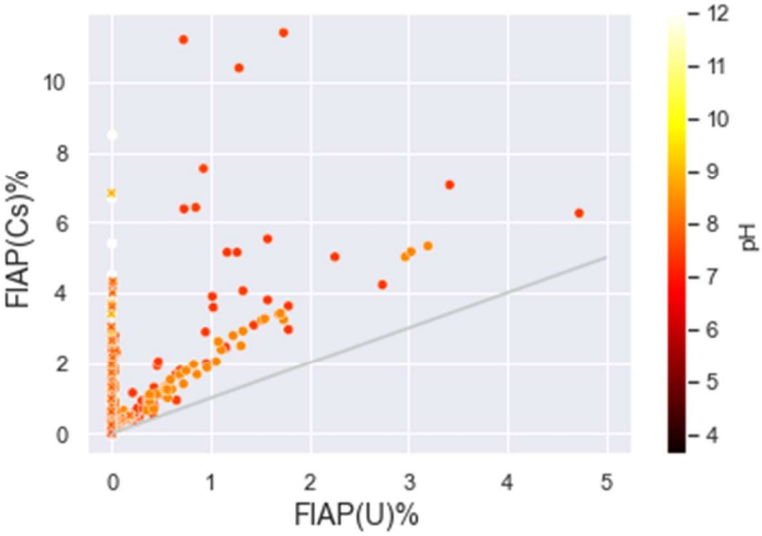

Fig A7.8 Scatterplot of Cs release in relation to U release, where points have been categorized by colour depending on pH and the grey line is a straight y = x line. Circles represent unspecified Cs, triangles Cs-133, diamonds Cs-134, squares Cs-135 and crosses Cs-137.

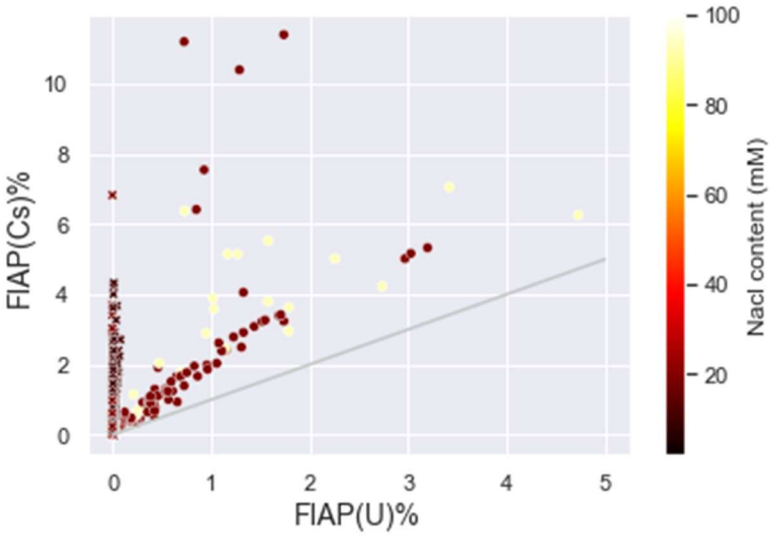

Fig A7.9 Scatterplot of Cs release in relation to U release, where points have been categorized by colour depending on NaCl content and the grey line is a straight y = x line. Circles represent unspecified Cs, triangles Cs-133, diamonds Cs-134, squares Cs-135 and crosses Cs-137.

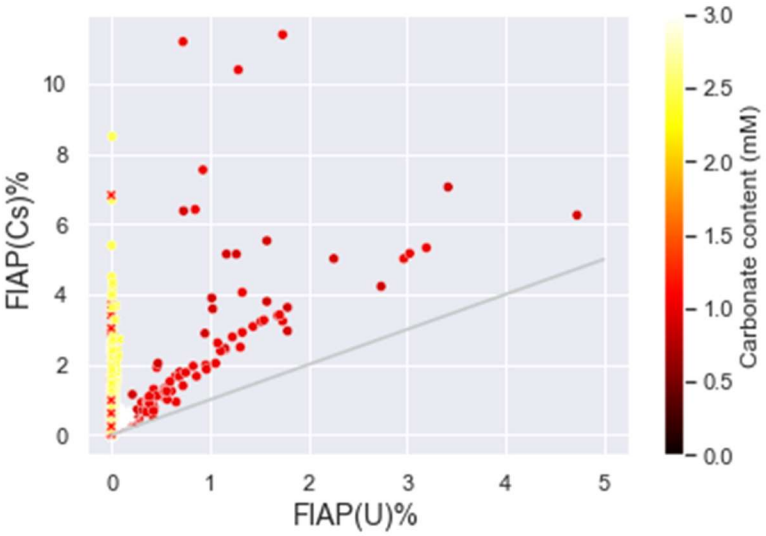

Fig A7.10 Scatterplot of Cs release in relation to U release, where points have been categorized by colour depending on carbonate content and the grey line is a straight y = x line. Circles represent unspecified Cs, triangles Cs-133, diamonds Cs-134, squares Cs-135 and crosses Cs-137.

Molybdenum

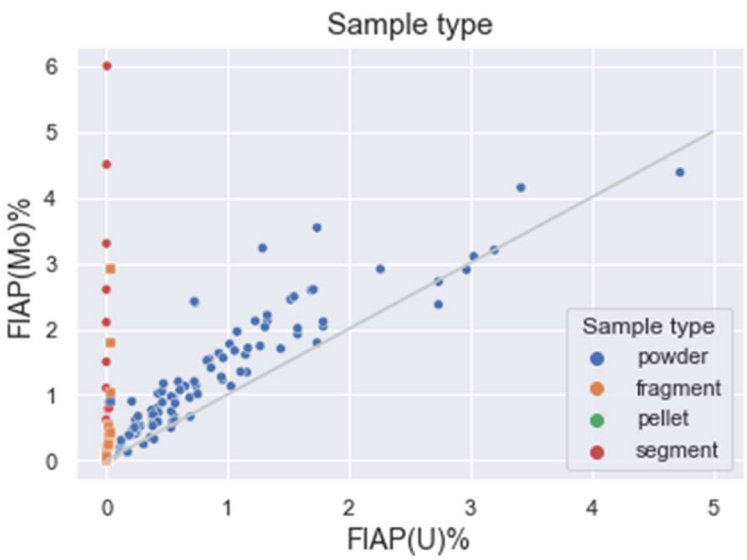

Fig A7.11 Scatterplot of Mo release in relation to U release, where points have been categorized by colour depending on sample type and the grey line is a straight y = x line. Circles represent unspecified Mo, triangles Mo-97, diamonds Mo-98 and squares Mo-100.

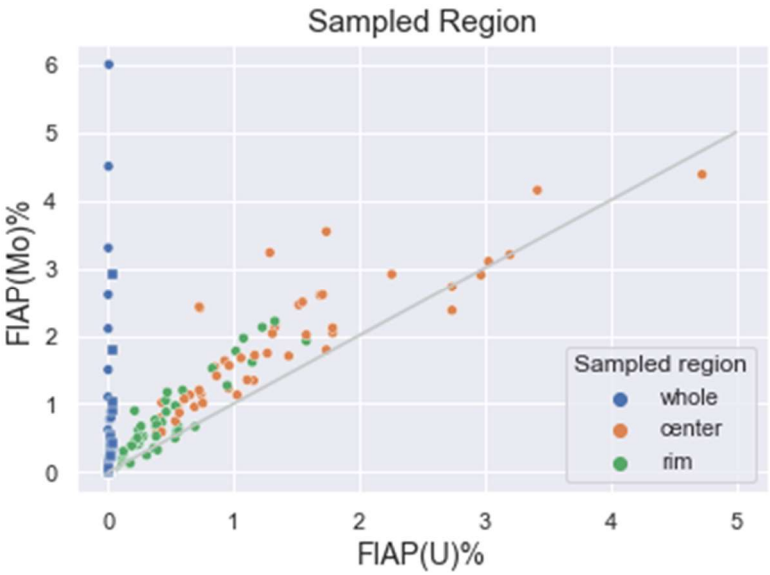

Fig A7.12 Scatterplot of Mo release in relation to U release, where points have been categorized by colour depending on sampled region and the grey line is a straight y = x line. . Circles represent unspecified Mo, triangles Mo-97, diamonds Mo-98 and squares Mo-100.

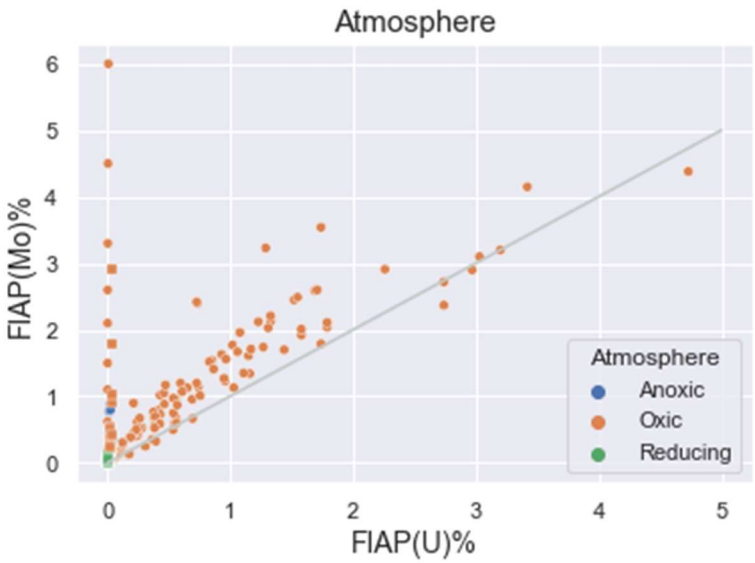

Fig A7.13 Scatterplot of Mo release in relation to U release, where points have been categorized by colour depending on atmosphere and the grey line is a straight y = x line. Circles represent unspecified Mo, triangles Mo-97, diamonds Mo-98 and squares Mo-100.

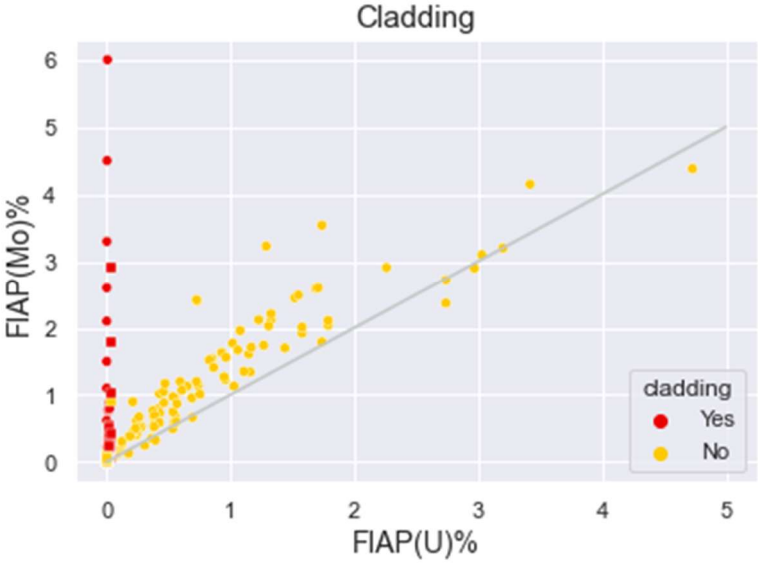

Fig A7.14 Scatterplot of Mo release in relation to U release, where points have been categorized by colour depending on presence of cladding and the grey line is a straight y = x line. Circles represent unspecified Mo, triangles Mo-97, diamonds Mo-98 and squares Mo-100.

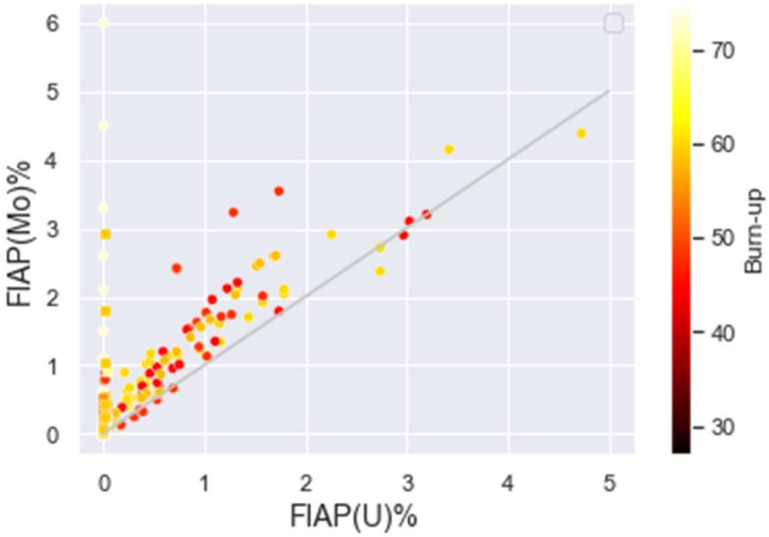

Fig A7.15 Scatterplot of Mo release in relation to U release, where points have been categorized by colour depending on BU and the grey line is a straight y = x line. Circles represent unspecified Mo, triangles Mo-97, diamonds Mo-98 and squares Mo-100.

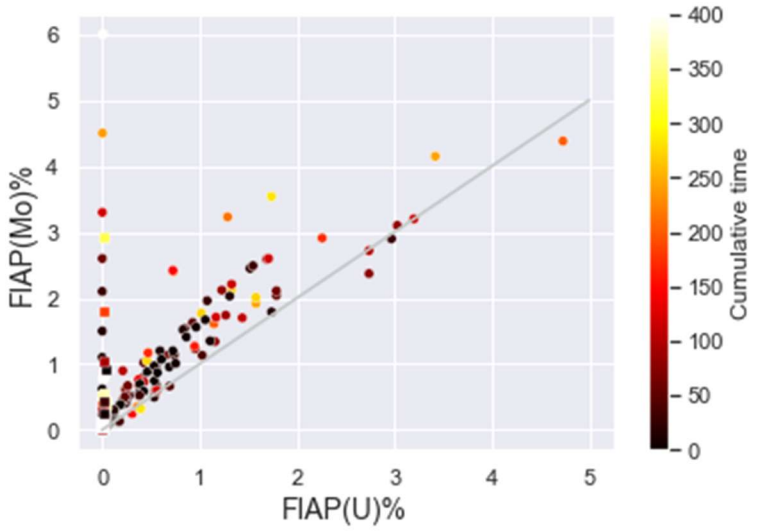

Fig A7.16 Scatterplot of Mo release in relation to U release, where points have been categorized by colour depending on cumulative time and the grey line is a straight y = x line. Circles represent unspecified Mo, triangles Mo-97, diamonds Mo-98 and squares Mo-100.

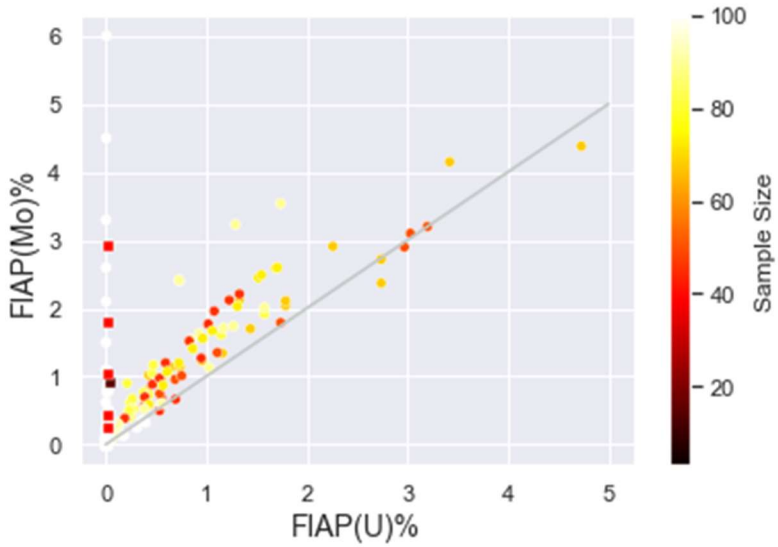

Fig A7.17 Scatterplot of Mo release in relation to U release, where points have been categorized by colour depending on sample size and the grey line is a straight y = x line. Circles represent unspecified Mo, triangles Mo-97, diamonds Mo-98 and squares Mo-100.

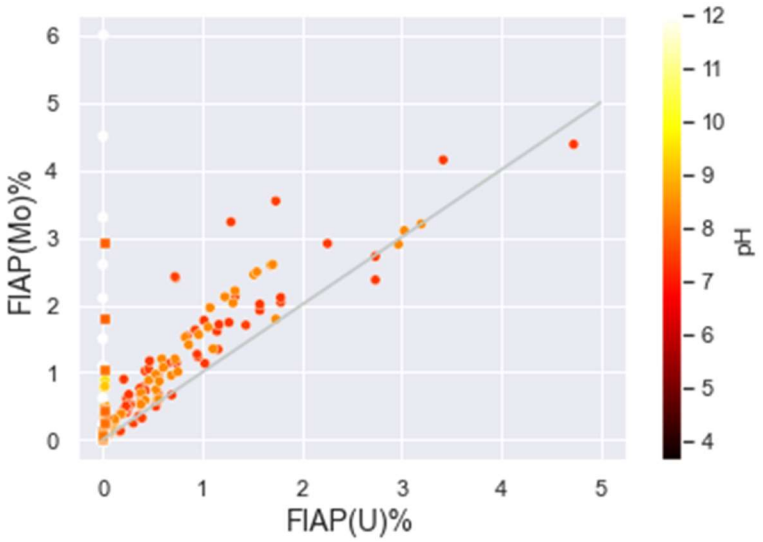

Fig A7.18 Scatterplot of Mo release in relation to U release, where points have been categorized by colour depending on pH and the grey line is a straight y = x line. Circles represent unspecified Mo, triangles Mo-97, diamonds Mo-98 and squares Mo-100.

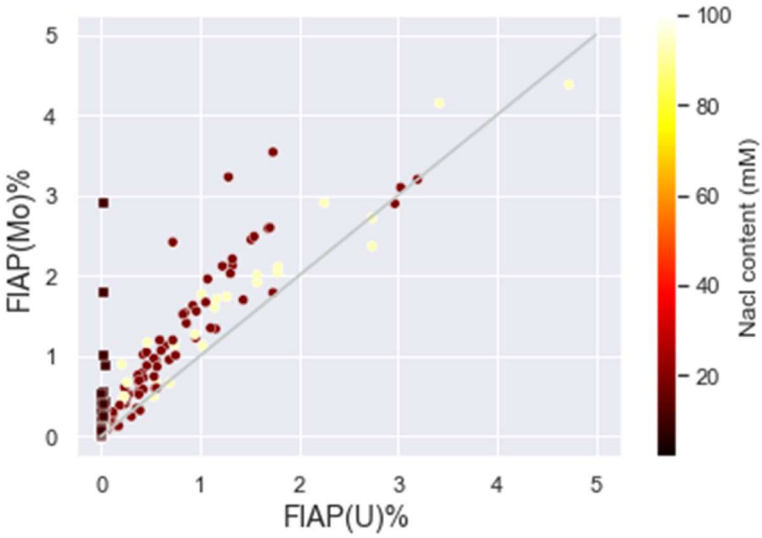

Fig A7.19 Scatterplot of Mo release in relation to U release, where points have been categorized by colour depending on NaCl content and the grey line is a straight y = x line. Circles represent unspecified Mo, triangles Mo-97, diamonds Mo-98 and squares Mo-100.

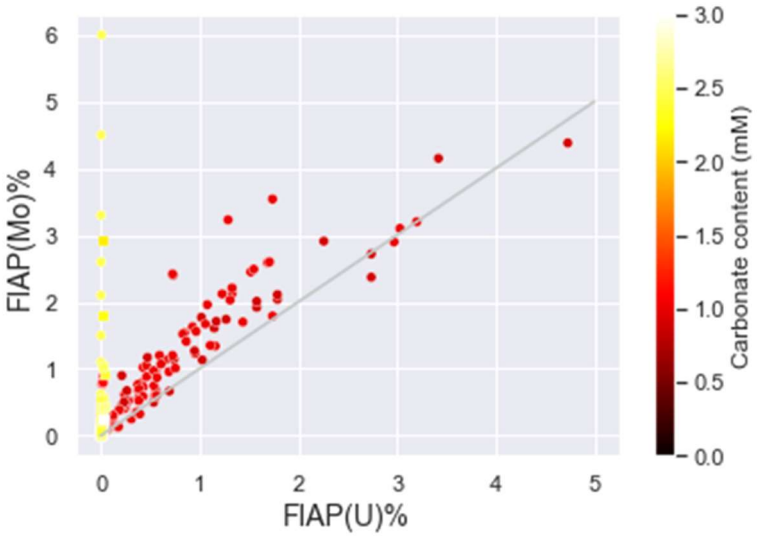

Fig A7.20 Scatterplot of Mo release in relation to U release, where points have been categorized by colour depending on carbonate content and the grey line is a straight y = x line. Circles represent unspecified Mo, triangles Mo-97, diamonds Mo-98 and squares Mo-100.

Rubidium

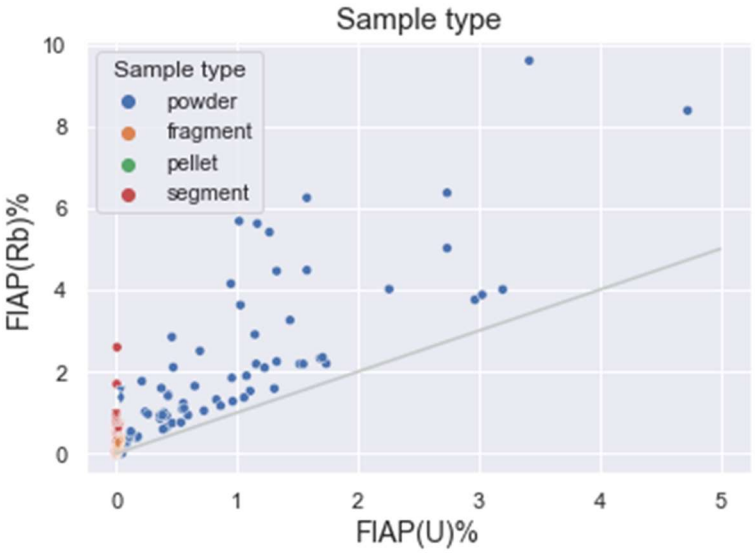

Fig A7.21 Scatterplot of Rb release in relation to U release, where points have been categorized by colour depending on sample type and the grey line is a straight y = x line. Circles represent unspecified Rb, triangles Rb-85 and diamonds Rb-87.

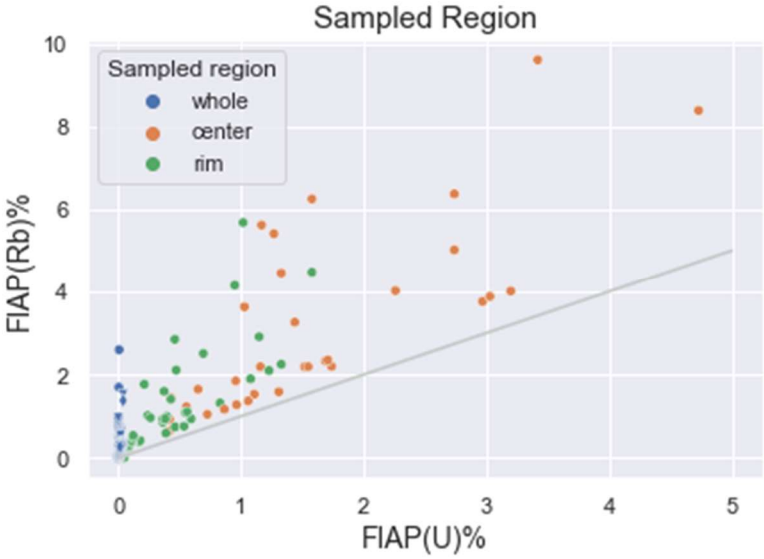

Fig A7.22 Scatterplot of Rb release in relation to U release, where points have been categorized by colour depending on sampled region and the grey line is a straight y = x line. Circles represent unspecified Rb, triangles Rb-85 and diamonds Rb-87.

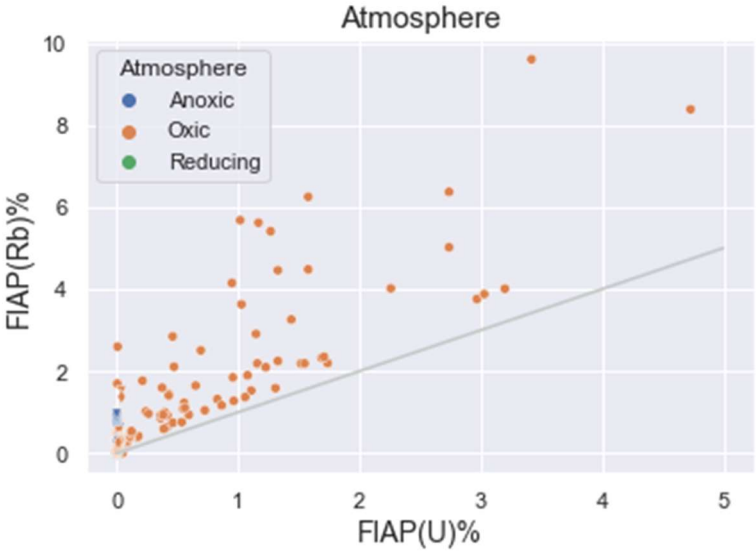

Fig A7.23 Scatterplot of Rb release in relation to U release, where points have been categorized by colour depending on atmosphere and the grey line is a straight y = x line. Circles represent unspecified Rb, triangles Rb-85 and diamonds Rb-87.

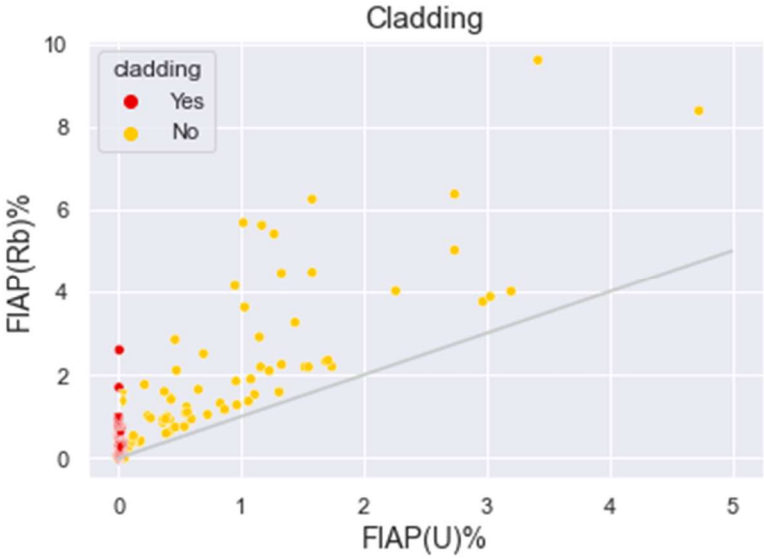

Fig A7.24 Scatterplot of Rb release in relation to U release, where points have been categorized by colour depending on presence of cladding and the grey line is a straight y = x line. Circles represent unspecified Rb, triangles Rb-85 and diamonds Rb-87.

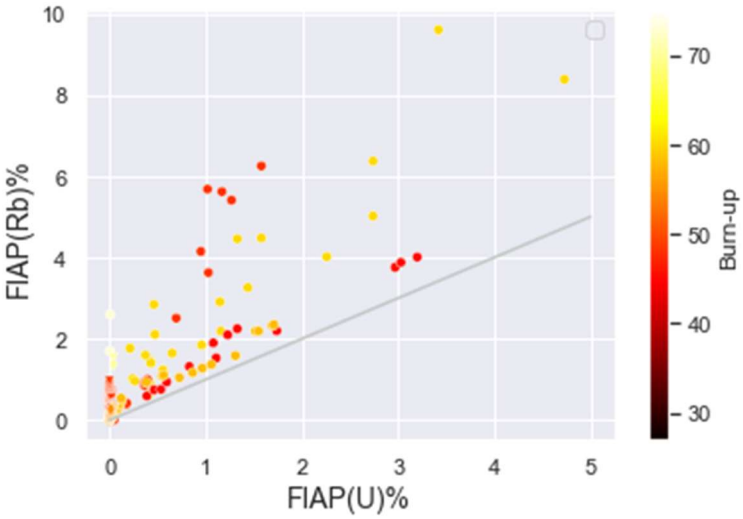

Fig A7.25 Scatterplot of Rb release in relation to U release, where points have been categorized by colour depending on BU and the grey line is a straight y = x line. Circles represent unspecified Rb, triangles Rb-85 and diamonds Rb-87.

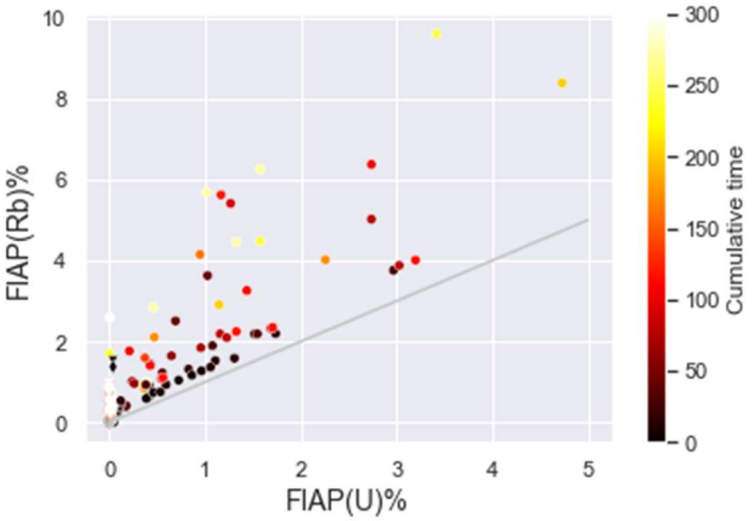

Fig A7.26 Scatterplot of Rb release in relation to U release, where points have been categorized by colour depending on cumulative time and the grey line is a straight y = x line. Circles represent unspecified Rb, triangles Rb-85 and diamonds Rb-87.

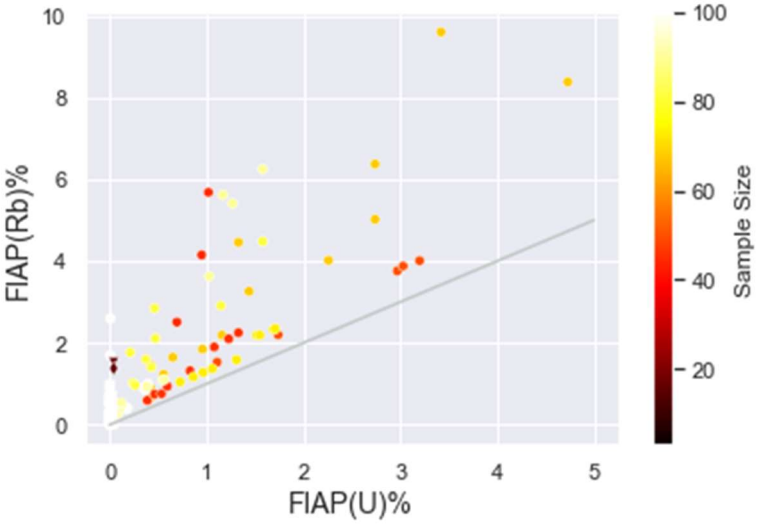

Fig A7.27 Scatterplot of Rb release in relation to U release, where points have been categorized by colour depending on sample size and the grey line is a straight y = x line. Circles represent unspecified Rb, triangles Rb-85 and diamonds Rb-87.

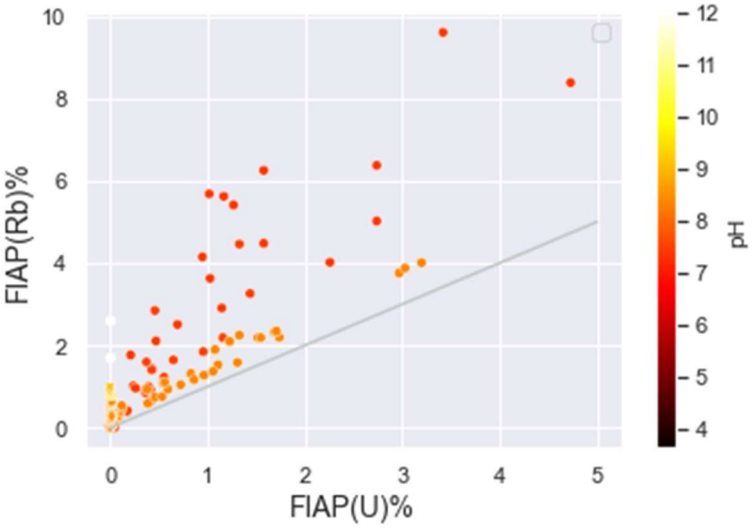

Fig A7.28 Scatterplot of Rb release in relation to U release, where points have been categorized by colour depending on pH and the grey line is a straight y = x line. Circles represent unspecified Rb, triangles Rb-85 and diamonds Rb-87.

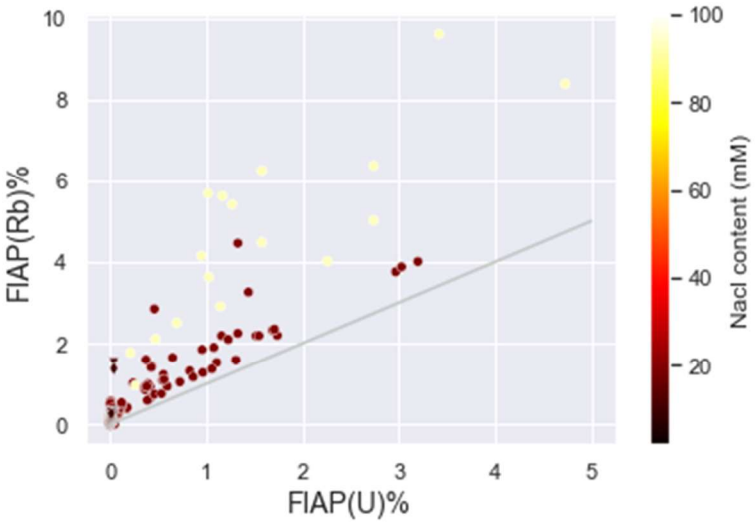

Fig A7.29 Scatterplot of Rb release in relation to U release, where points have been categorized by colour depending on NaCl content and the grey line is a straight y = x line. Circles represent unspecified Rb, triangles Rb-85 and diamonds Rb-87.

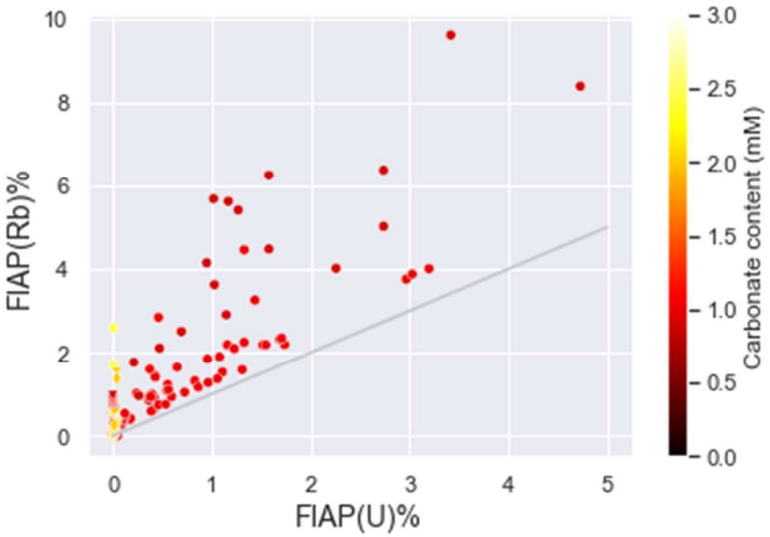

Fig A7.30 Scatterplot of Rb release in relation to U release, where points have been categorized by colour depending on carbonate content and the grey line is a straight y = x line. Circles represent unspecified Rb, triangles Rb-85 and diamonds Rb-87.

Technetium

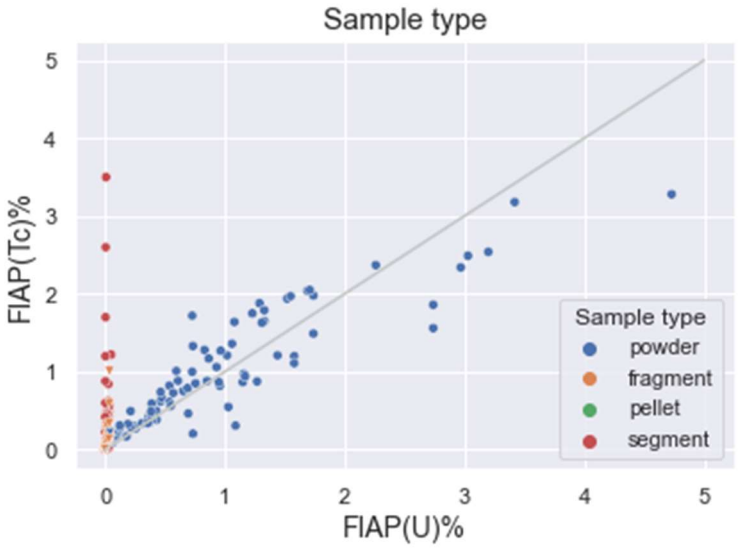

Fig A7.31 Scatterplot of Tc release in relation to U release, where points have been categorized by colour depending on sample type and the grey line is a straight y = x line.

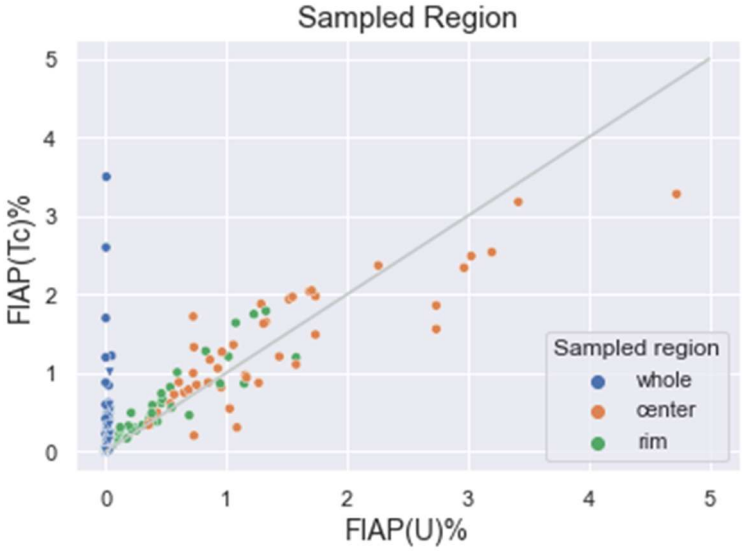

Fig A7.32 Scatterplot of Tc release in relation to U release, where points have been categorized by colour depending on sampled region and the grey line is a straight y = x line.

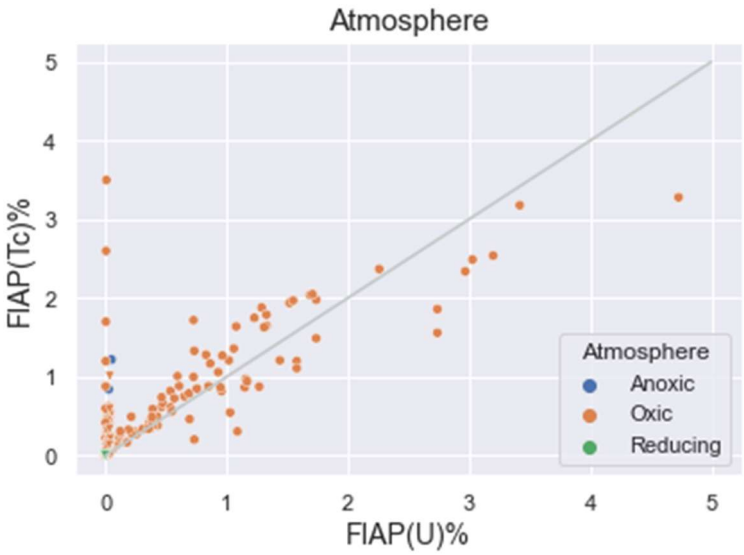

Fig A7.33 Scatterplot of Tc release in relation to U release, where points have been categorized by colour depending on atmosphere and the grey line is a straight y = x line.

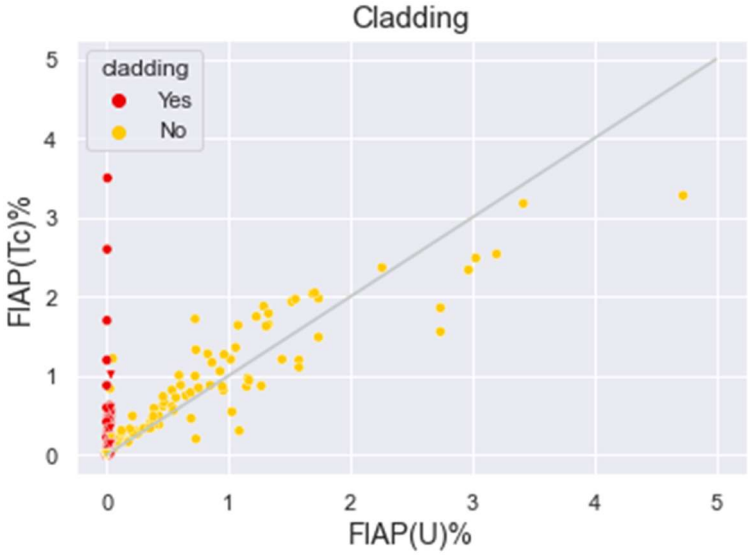

Fig A7.34 Scatterplot of Tc release in relation to U release, where points have been categorized by colour depending on presence of cladding and the grey line is a straight y = x line.

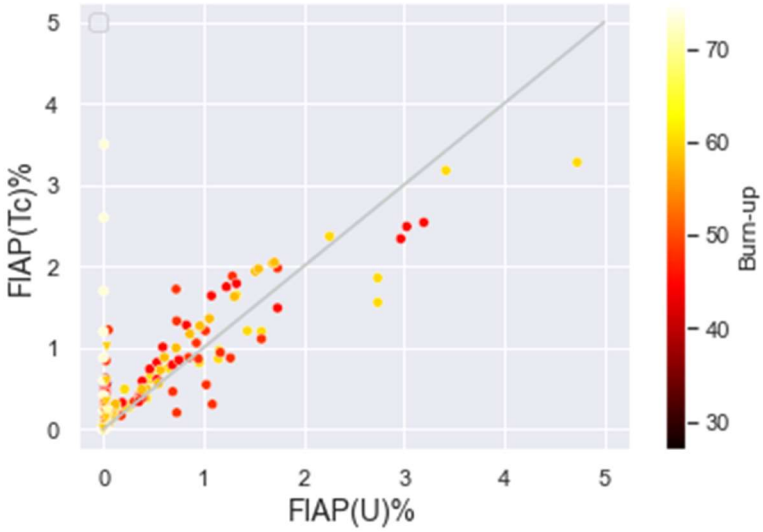

Fig A7.35 Scatterplot of Tc release in relation to U release, where points have been categorized by colour depending on BU and the grey line is a straight y = x line.

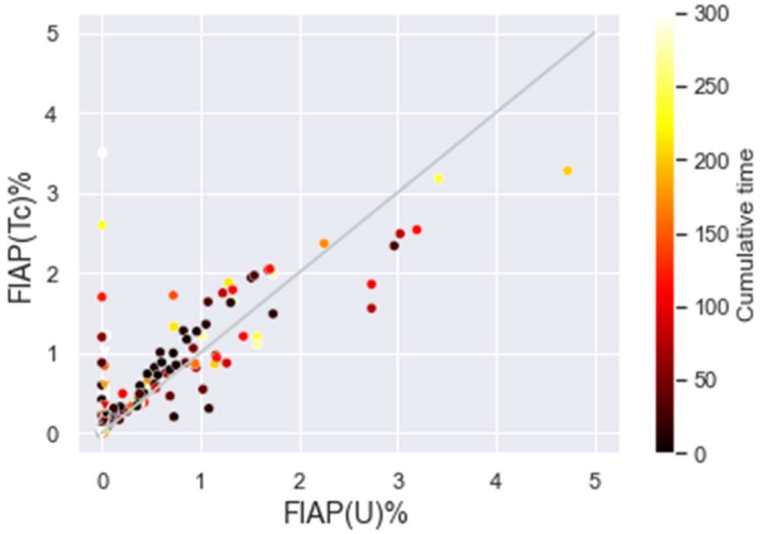

Fig A7.36 Scatterplot of Tc release in relation to U release, where points have been categorized by colour depending on cumulative time and the grey line is a straight y = x line.

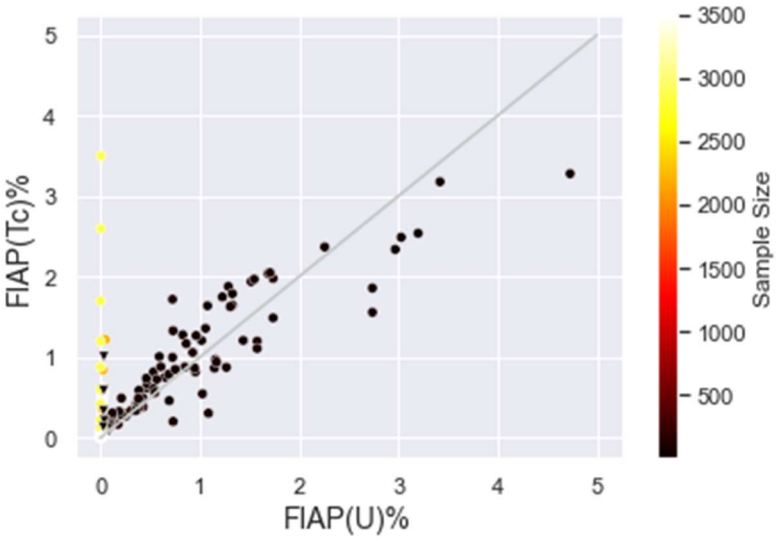

Fig A7.37 Scatterplot of Tc release in relation to U release, where points have been categorized by colour depending on sample size of higher range and the grey line is a straight y = x line.

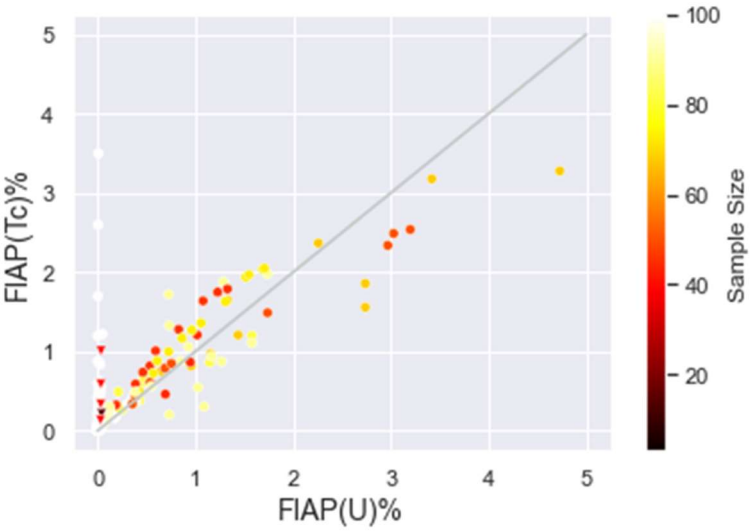

Fig A7.38 Scatterplot of Tc release in relation to U release, where points have been categorized by colour depending on sample size of lower range and the grey line is a straight y = x line.

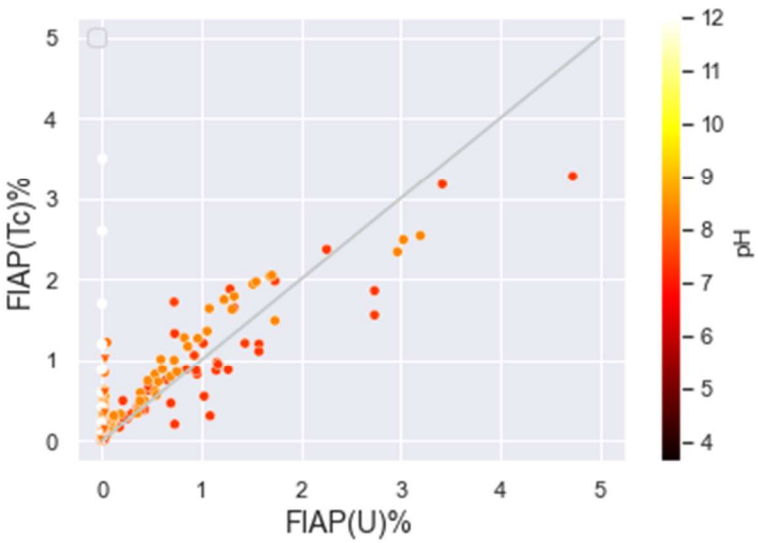

Fig A7.39 Scatterplot of Tc release in relation to U release, where points have been categorized by colour depending on pH and the grey line is a straight y = x line.

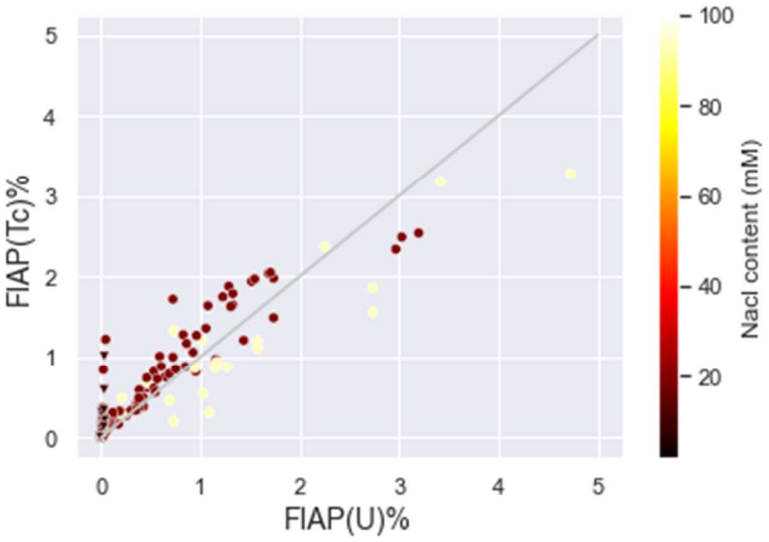

Fig A7.40 Scatterplot of Tc release in relation to U release, where points have been categorized by colour depending on NaCl content and the grey line is a straight y = x line.

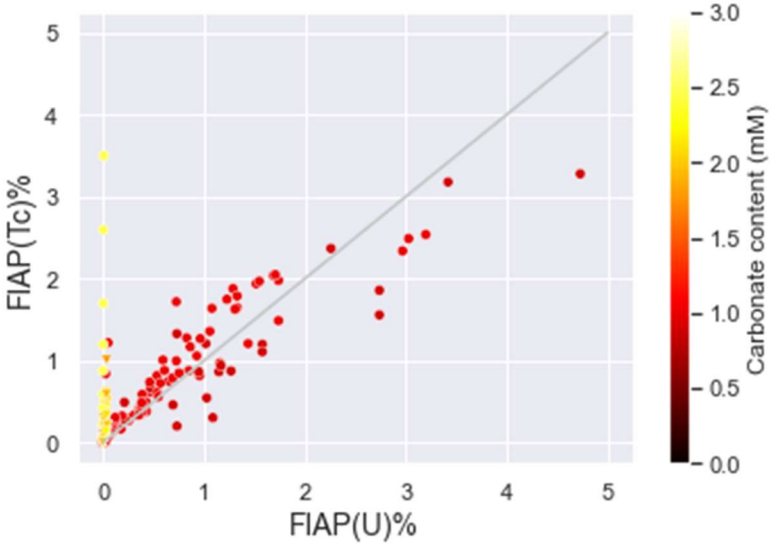

Fig A7.41 Scatterplot of Tc release in relation to U release, where points have been categorized by colour depending on carbonate content and the grey line is a straight y = x line.

A.8 Scatterplots Group 4

Appendix A.6 shows all the plots of the elements in group 3a (I, Ba, Cd, Te), both plots used and not used in section 4. The plots are shown by element.

Selenium

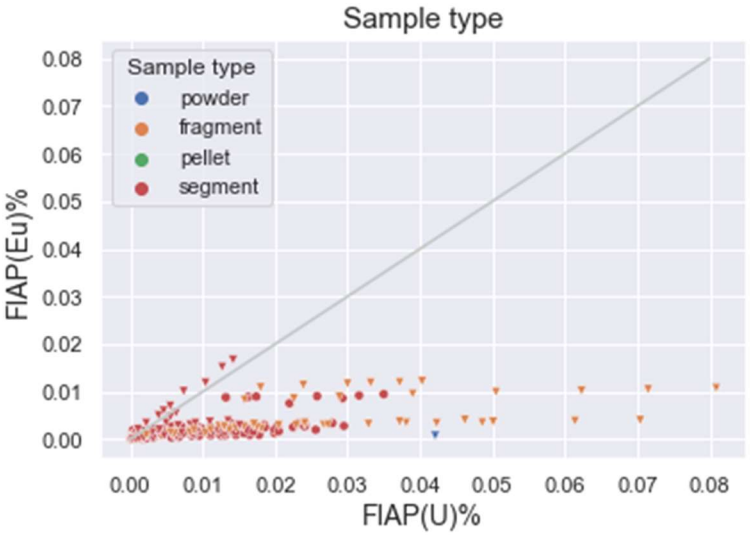

Fig A8.1 Scatterplot of Se release in relation to U release, where points have been categorized by colour depending on sample type and the grey line is a straight y = x line. Circles represent Se-79, triangles Se-80 and diamonds Se-82.

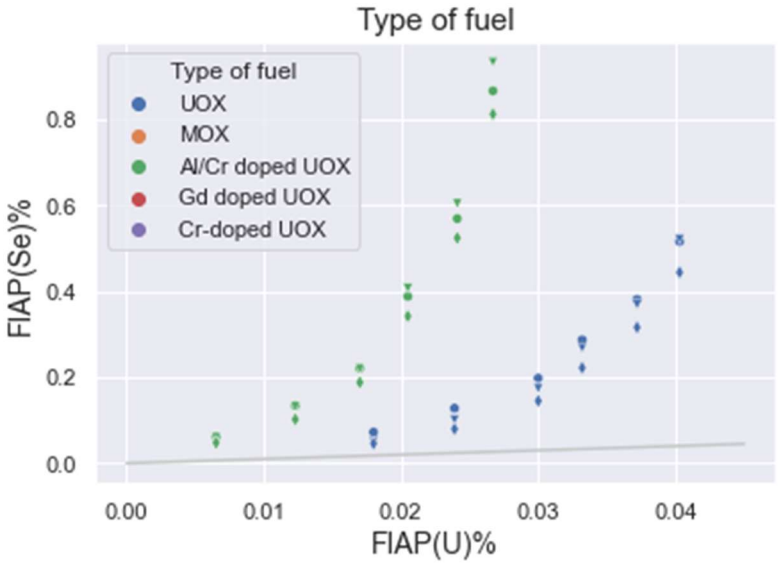

Fig A8.2 Scatterplot of Se release in relation to U release, where points have been categorized by colour depending on type of fuel and the grey line is a straight y = x line. Circles represent Se-79, triangles Se-80 and diamonds Se-82.

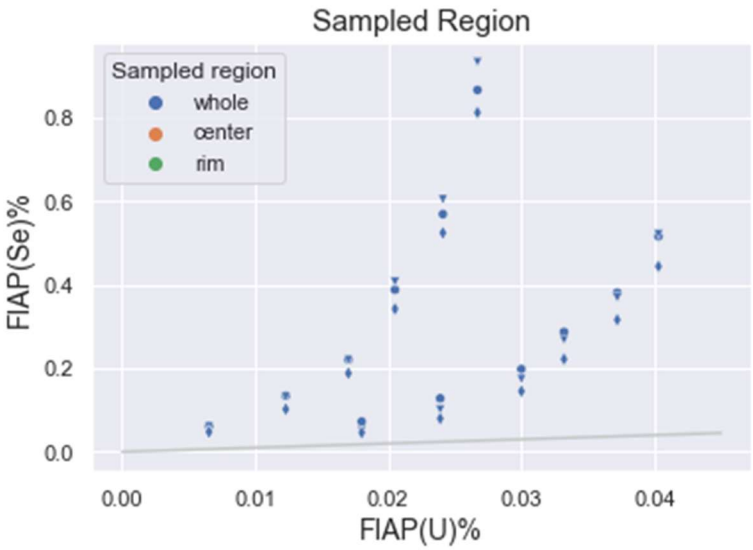

Fig A8.3 Scatterplot of Se release in relation to U release, where points have been categorized by colour depending on sampled region and the grey line is a straight y = x line. Circles represent Se-79, triangles Se-80 and diamonds Se-82.

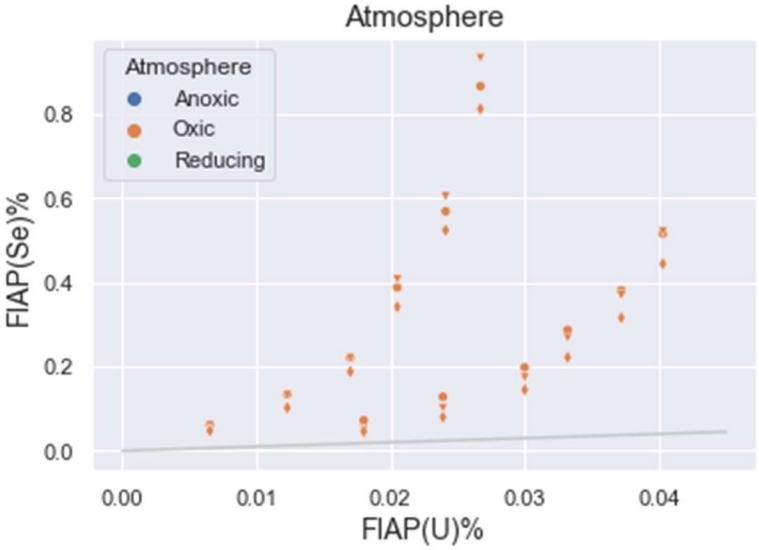

Fig A8.4 Scatterplot of Se release in relation to U release, where points have been categorized by colour depending on atmosphere and the grey line is a straight y = x line. Circles represent Se-79, triangles Se-80 and diamonds Se-82.

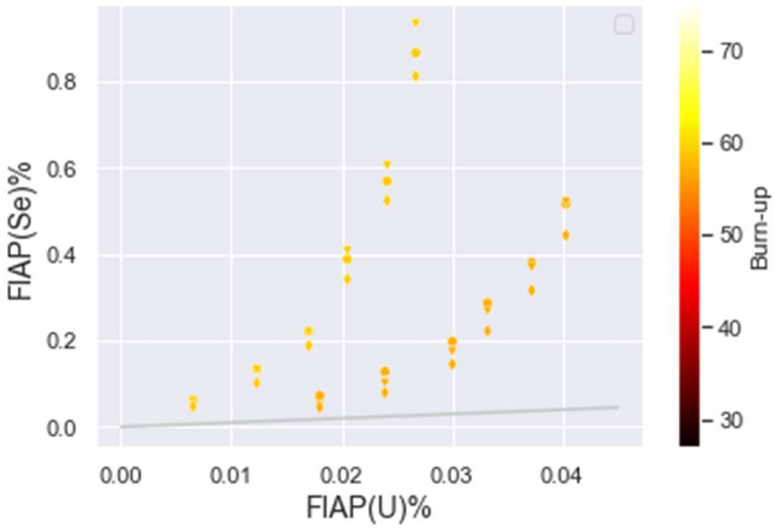

Fig A8.5 Scatterplot of Se release in relation to U release, where points have been categorized by colour depending on BU and the grey line is a straight y = x line. Circles represent Se-79, triangles Se-80 and diamonds Se-82.

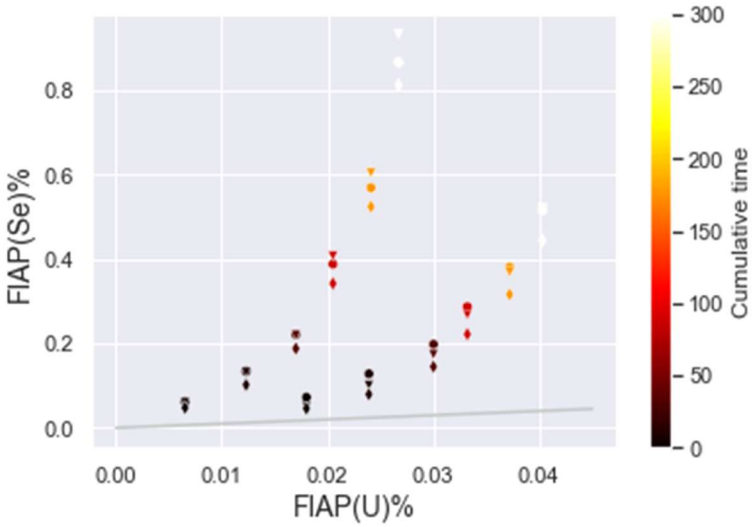

Fig A8.6 Scatterplot of Se release in relation to U release, where points have been categorized by colour depending on cumulative time and the grey line is a straight y = x line. Circles represent Se-79, triangles Se-80 and diamonds Se-82.

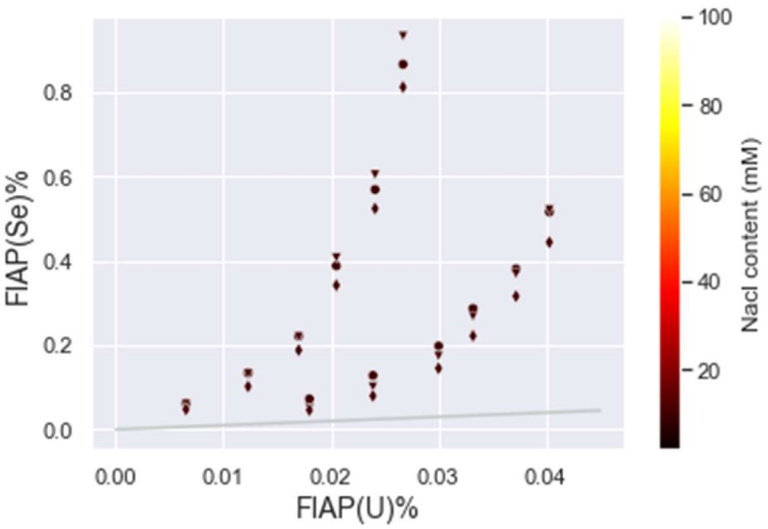

Fig A8.7 Scatterplot of Se release in relation to U release, where points have been categorized by colour depending on NaCl content and the grey line is a straight y = x line. Circles represent Se-79, triangles Se-80 and diamonds Se-82.

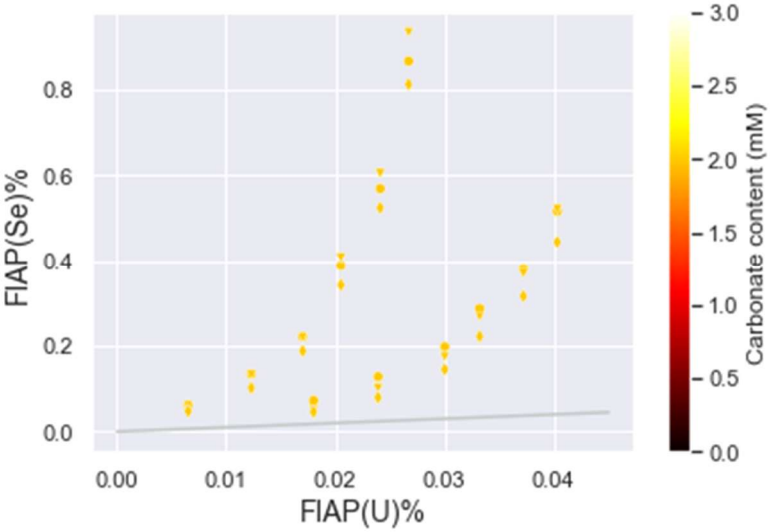

Fig A8.8 Scatterplot of Se release in relation to U release, where points have been categorized by colour depending on carbonate content and the grey line is a straight y = x line. Circles represent Se-79, triangles Se-80 and diamonds Se-82.

Carbon

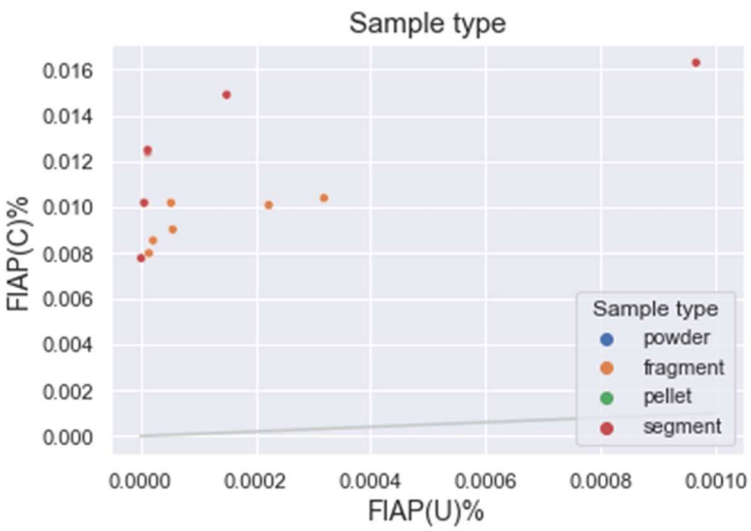

Fig A8.9 Scatterplot of Se release in relation to U release, where points have been categorized by colour depending on sample type and the grey line is a straight y = x line.

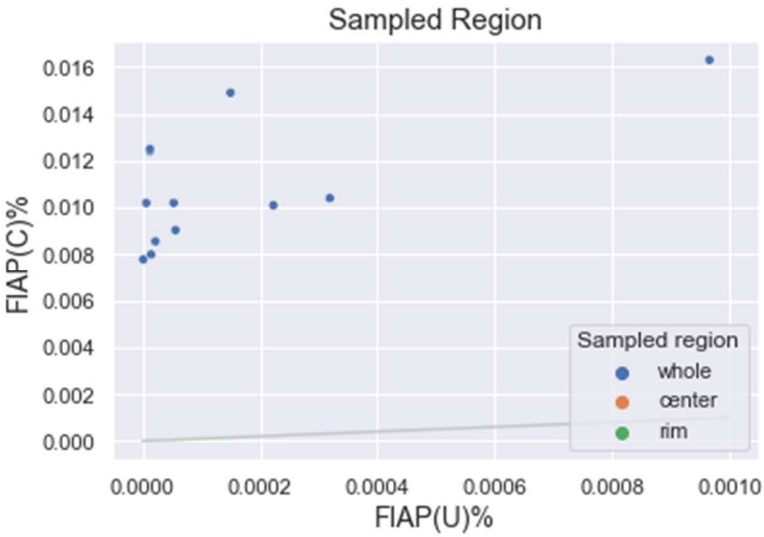

Fig A8.10 Scatterplot of Se release in relation to U release, where points have been categorized by colour depending on sampled region and the grey line is a straight y = x line.

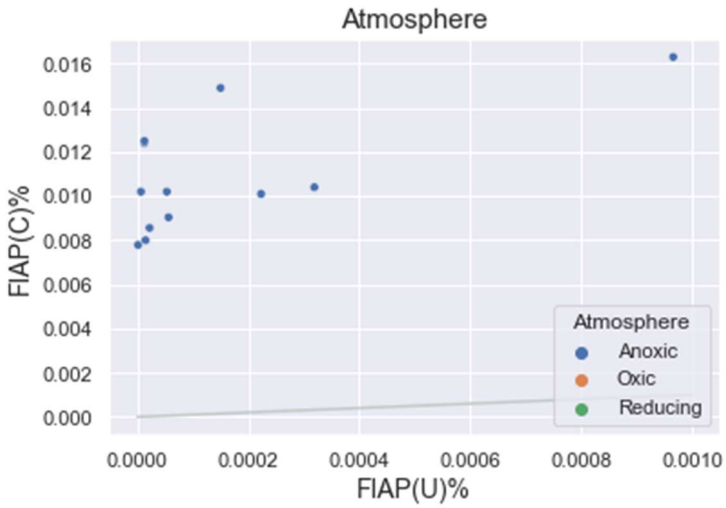

Fig A8.11 Scatterplot of Se release in relation to U release, where points have been categorized by colour depending on atmosphere and the grey line is a straight y = x line

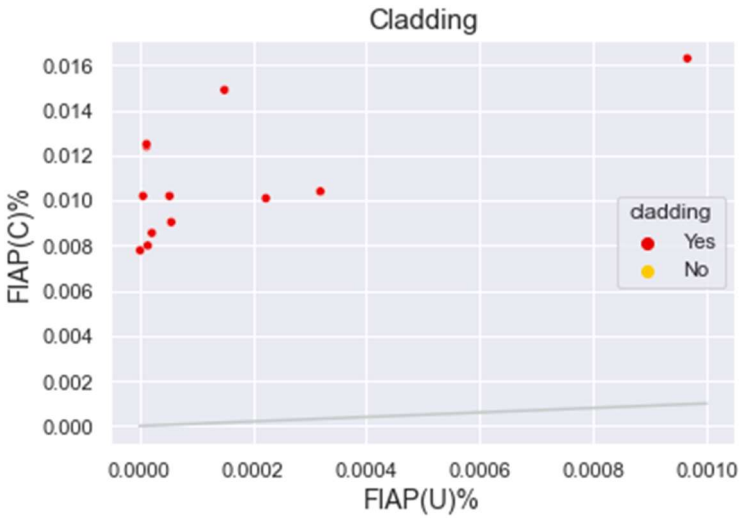

Fig A8.12 Scatterplot of Se release in relation to U release, where points have been categorized by colour depending on presence of cladding and the grey line is a straight y = x line.

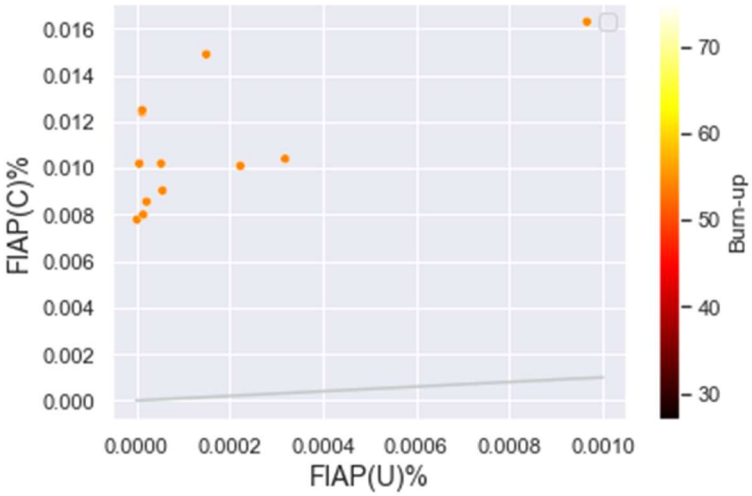

Fig A8.13 Scatterplot of Se release in relation to U release, where points have been categorized by colour depending on BU and the grey line is a straight y = x line.

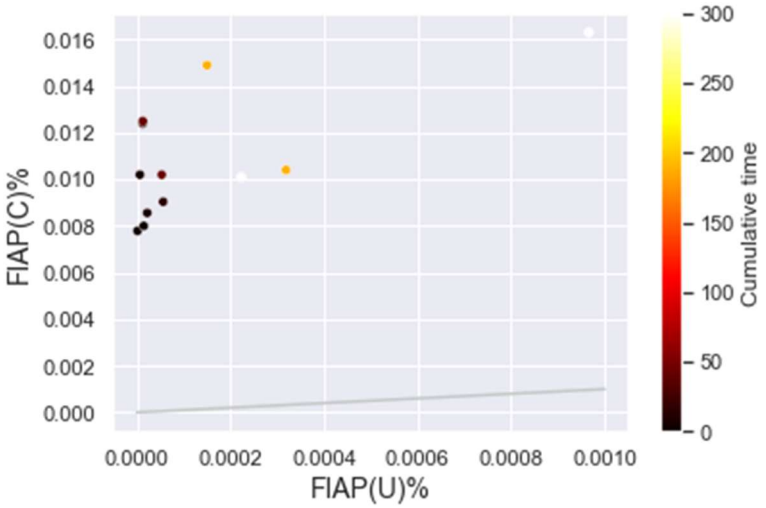

Fig A8.14 Scatterplot of Se release in relation to U release, where points have been categorized by colour depending on cumulative time and the grey line is a straight y = x line.

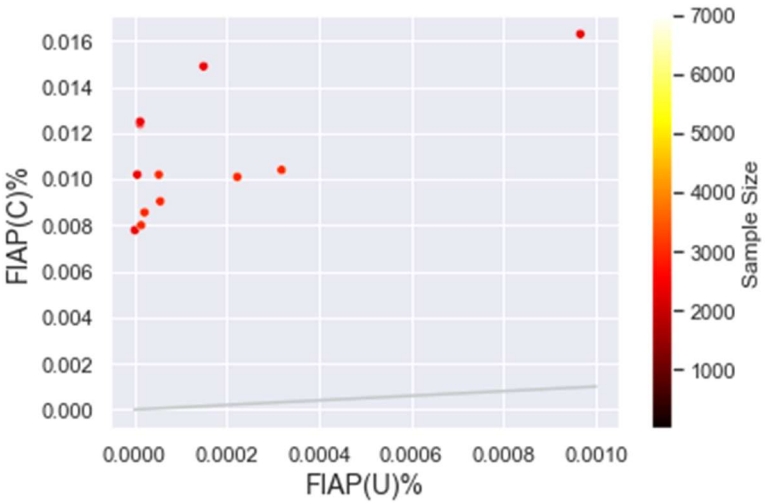

Fig A8.15 Scatterplot of Se release in relation to U release, where points have been categorized by colour depending on sample size and the grey line is a straight y = x line.

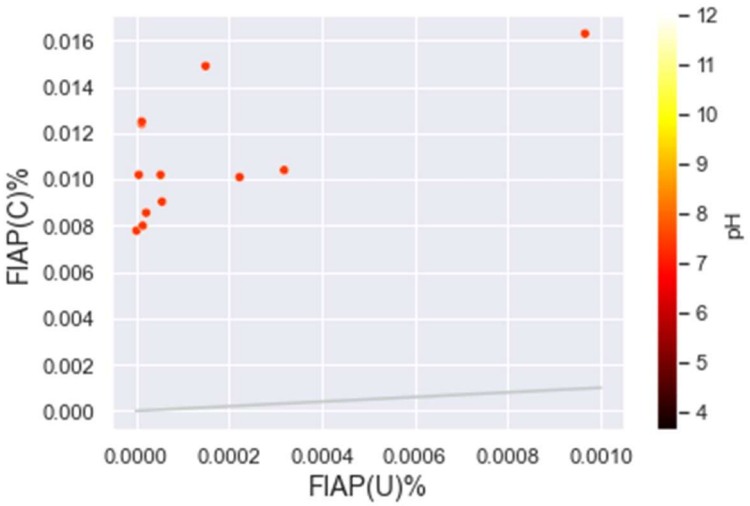

Fig A8.16 Scatterplot of Se release in relation to U release, where points have been categorized by colour depending on pH and the grey line is a straight y = x line.

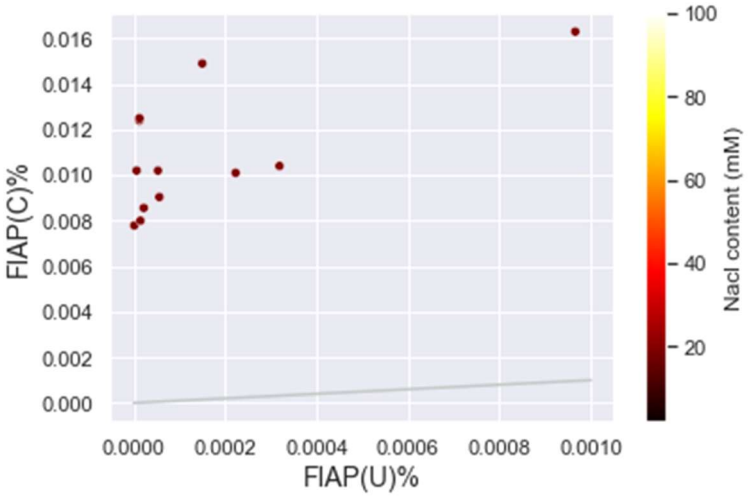

Fig A8.17 Scatterplot of Se release in relation to U release, where points have been categorized by colour depending on NaCl content and the grey line is a straight y = x line.

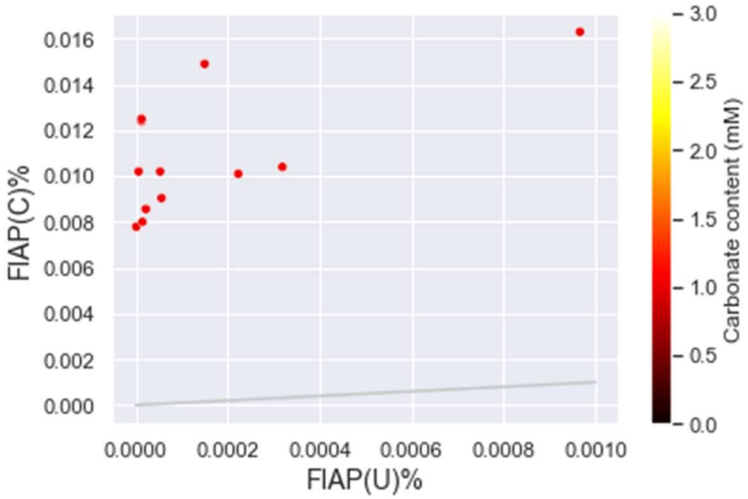

Fig A8.18 Scatterplot of Se release in relation to U release, where points have been categorized by colour depending on carbonate content and the grey line is a straight y = x line.